Stefan Payer, BSc.

ω-Transaminases for the Preparation of Optically Pure Xenovenine, an α-Chiral tert-Amine

MASTER'S THESIS

to achieve the university degree of

Master of Science

Master's degree programme: Chemistry

submitted to

Graz University of Technology

Supervisor

Univ.-Prof. Dipl.-Ing. Dr.techn. Wolfgang Kroutil

Dept. for Organic and Bioorganic Chemistry
Institute for Chemistry

University of Graz

Graz, December 2014

AFFIDAVIT

I declare that I have authored this thesis independently, that I have not used other than the declared sources/resources, and that I have explicitly indicated all material which has been quoted either literally or by content from the sources used. The text document uploaded to TUGRAZonline is identical to the present master's thesis dissertation.

4.12.2014
Date

Stefan Payer
Signature

Acknowledgments

This work wouldn't have been possible without the aid of these great people.

At first and foremost I want to announce my sincere gratitude to Wolfgang Kroutil, Joerg Schrittwieser and Barbara Grischek.

Thank you, Wolfgang, for providing me the opportunity to write this thesis and always being there for upcoming questions. Further, I highly appreciate both your suggestions and your support in applications for various scientific events. These will undoubtedly be an invaluable benefit for my scientific career.

Joerg, for being such a great, inspiring and patient teacher; thank you so much for sharing your vast knowledge and your sweets with me and becoming a good friend now. I was really enjoying our intermittent discussions and chats, which were of course not restricted to chemical topics.

Babsi, thanks a lot for introducing me to the world of molecular biology and microbiology and of course for the constantly good mood you are spreading.

Robert, thank you for your kind interest in my work and the valuable hints you gave me. I really appreciate all of them.

Horst, Desiree and Eduardo; I can't imagine better lab buddies than you guys!

Horst also deserves special thanks for his competent introduction to enzyme visualizing and - docking software, which resulted in some nice illustrations within this thesis. This graphics will truly support the readers understanding of the treated concepts.

Of course, I owe gratuity to the whole Elk Group with all its "old" and new members for providing such an enjoyable and dynamic working environment. It was (and will be) a great pleasure for me being a part of your community!

It should not be left unacknowledged that no NMR or HR-MS could have been recorded without the reliable and kind support of the group around Prof. Klaus Zangger and Dr. Kenneth Jensen, respectively.

Last but most importantly, I thank Carolin for her implicit love, incredible patience and helpful opinions in terms of design and construction of this work. With you at my side, everything perfectly works out!

Summary

Chemo-Enzymatic Synthesis of Xenovenine

Both enantiomers of the ant venom xenovenine (**1**) were successfully prepared in good yields by employing a chemo-enzymatic approach. Based on the recently reported chemo-enzymatic, stereoselective synthesis of isosolenopsin and dihydropinidine from diketones, the recent target molecule was accessed *via* transamination of an easily made triketone **7**. The free amine intermediate readily cyclized to the corresponding five-membered imine **4**, which was subsequently converted into the aromatic pyrrole derivative. The one-pot catalytic hydrogenation of the enantiomerically pure pyrrole resulted in the formation of the desired (5*Z*,8*E*) product diastereomer. By employing ω-transaminases with different stereoselectivity in the biocatalytic step, both (−)- and (+)-xenovenine **1** were easily accessed in only 4 steps and overall yields of 18 and 30% in optically pure form, respectively, starting from commercially available 2-heptylfuran **11**.
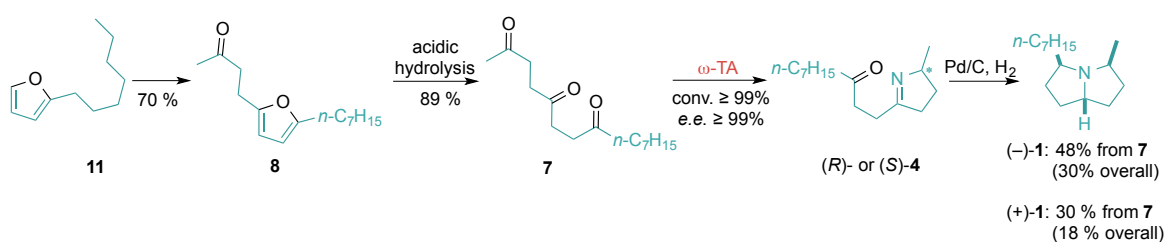
## *Novel "Smart Co-Substrates" for ω-transaminases*

An extensive search for novel smart co-substrates for enzymatic transaminations and an optimization of their reaction conditions has been conducted. In an initial screening, 1,2-diamines turned out being the most promising co-substrates in terms of conversion. The driving force by using these substances was expected to be the irreversible oxidative aromatization of the co-product dimer to a pyrazine derivative. The pH-optimum for these diamine co-substrates was found between 9 and 10 in an aqueous co-substrate buffer. Only 1,2-diaminopropane achieved good conversions and hence the emphasis was put on the optimization of reaction conditions for this compound. The examined additives and optimized parameters included substrate- and co-substrate concentration, oxidants with and without oxygen atmosphere, chelating metal ions and organic co-solvents. Throughout the optimization studies, very good to excellent *e.e.*'s were observed for (*R*)-selective enzymes whereas (*S*)-selective enzymes in almost all cases gave only moderate to poor *e.e.*'s. Finally the conversion of various substrates with 1,2-diaminopropane and 2-aminopropane as co-substrates was compared at optimal conditions. The new co-substrate achieved better e.e.'s but slightly lower conversions than 2-aminopropane. All in all, a proof of principle has been established for this class of smart co-substrates.

Zusammenfassung

Chemo-Enzymatische Totalsynthese von Xenovenin

Beide Enantiomere des Ameisengiftes Xenovenin (**1**) wurden durch Anwendung eines chemo-enzymatischen Syntheseweges in guten Gesamtausbeuten hergestellt. Basierend auf der kürzlich beschriebenen chemo-enzymatischen, stereoselektiven Synthese von Isosolenopsin und Dihydropinidin aus Diketonen, wurde das Zielmolekül **1** über eine enzymatische Transaminierung des einfach zugänglichen Triketons **7** synthetisiert. Das resultierende freie Amin bildete spontan das ringförmige Imin **4**, welches weiter in das entsprechende aromatische Pyrrol überführt wurde. Die folgende katalytische Hydrierung des enantiomerenreinen Pyrrols führte zum gewünschten (5*Z*,8*E*) Produktdiastereomer. Durch die Verwendung von ω-Transaminasen mit unterschiedlicher Stereoselektivität im biokatalytischen Schritt konnten, ausgehend von kommerziell erhältlichem 2-heptylfuran **11**, sowohl (−) als auch (+)-Xenovenin **1** in nur 4 Schritten und Gesamtausbeuten von 18 bzw. 30 % in optisch reiner Form (≥ 99% *e.e.*) hergestellt werden.
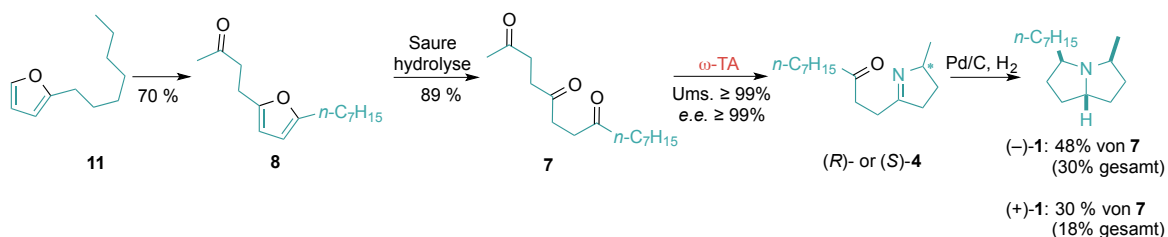
Neue "intelligente Co-Substrate" für ω-Transaminasen

Eine ausgedehnte Suche nach geeigneten Co-Substraten für die enzymatische Transaminierung, sowie eine Optimierung der Reaktionsbedingungen wurde durchgeführt. Im ersten Schritt stellten sich, in Bezug auf den Umsatz, 1,2-Diamine als vielversprechende Co-substrate heraus. Die erwartete Triebkraft beim Einsatz dieser Verbindungen lag in der irreversiblen Oxidation des Co-Produktdimers zu aromatischen Pyrazinderivaten. Das pH-Optimum für den Umsatz dieser Diamin Co-Substrate in wässrigem Co-Substrat Puffer lag zwischen 9 und 10. Da hier nur 1,2-Diaminopropan gute Umsätze zeigte, konzentrierten sich die folgenden Untersuchungen und Optimierungen auf diese Verbindung. Hierbei wurden Einflüsse von Substrat- und Co-Substrat Konzentration, Oxidationsmittel mit und ohne Sauerstoffatmosphäre, chelatierende Metallionen und Co-Lösungsmittel untersucht. (*R*)-selektive Enzyme gaben durchwegs perfekte *e.e.*s, der *e.e.* für (*S*)-selektive Enzyme war jedoch schlecht. Zum Schluss wurde der Umsatz von verschiedenen Substraten bei optimalen Bedingungen unter Einsatz von entweder 2-Aminopropan oder 1,2-Diaminopropan verglichen. Das neue Co-Substrat lieferte bessere *e.e*'s aber geringere Umsätze. Das zugrundeliegende Prinzip der Funktionsweise dieser Co-Substrate wurde bewiesen.

Table of Contents

1 Introduction

"... the use of biocatalysts should sit alongside more traditional methodologies in the forefront of chemists' minds when designing synthetic routes, providing shorter, greener and entirely new routes to target molecules."

Nicholas J. Turner *Nat Chem Biol* **2013**, *9*, 285-288.

1.1 Xenovenine

1.1.1 The Bicyclic Alkaloid Family

Pyrrolizidines (**1**), indolizidines (**2**) and quinolizidines (**3**) constitute the bicyclic core structures of a vast number of natural products. Being actually secondary metabolites of plants that serve as chemical defense against enemies, some higher organisms such as insects[1] and amphibians[2] are capable of sequestering these substances and in turn utilizing them for self-defense against predators.[3] Even bacterial and fungal sources are reported.[4] Figure 1.1 is just a small selection of examples to illustrate the structural richness of this compound class.

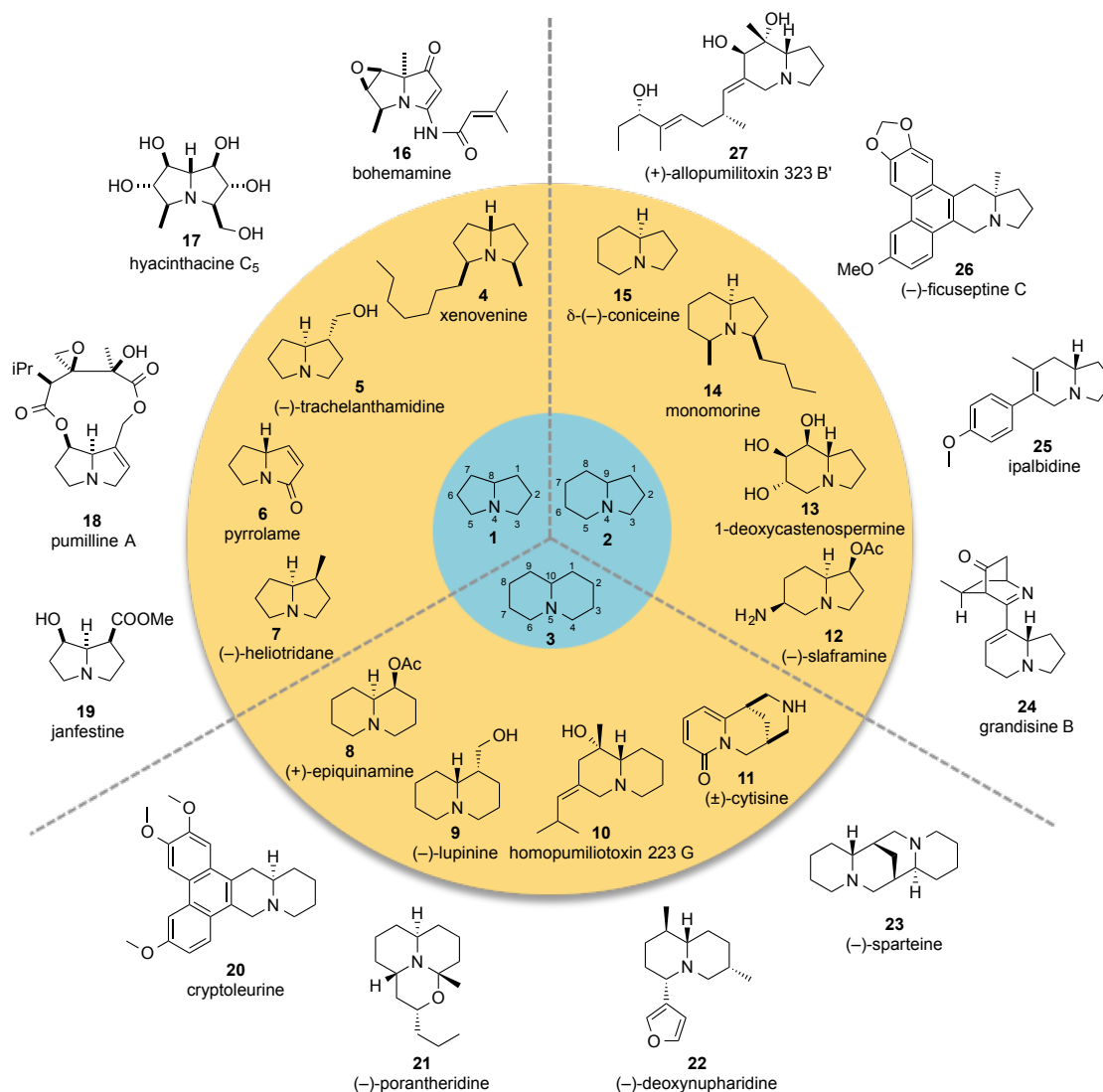**Figure 1.1** | Various simple and more complex pyrrolizidine, indolizidine and quinolizidine alkaloids from plant and animal sources.[5]

Considering their wide distribution in nature, it does not appear surprising that molecules bearing these motifs in their structure very often exhibit interesting biological activities. Their actions on organisms are as diverse as their structures, with effects ranging from

signaling pheromones[6] over enzyme inhibition (e.g. glycosidase inhibitors) to very effective poisons that interact with neuroreceptors. The liver degradation products of pyrrolizidines are even thought to cause cancer.[3, 5b, 7] Owing to these diverse biological activities, these alkaloids also constitute important drug targets for lowering blood pressure, pain relieve or tumor treatment.[3]

Pyrrolizidine alkaloids in particular are formally referred to as azabicyclo[3.3.0]octane derivatives. However, the more common nomenclature of pyrrolizidines consists of the relative configuration followed by the nominal mass of the compound, which is associated by a letter for example 223H for xenovenine.[8]

Many structurally distinct compounds of the pyrrolizidine subfamily were discovered and synthesized during the last four decades[5c, 7, 9], but nature derives them all from the amino acid arginine via the biosynthetic pathway depicted in Scheme 1.1. The first two steps essentially degrade arginine to 1,4-diaminobutane (putrescine) by decarboxylation of the α-amino acid and cleavage of urea from the ε-N-terminal end. Spermidine synthase catalyzes the N-alkylation to spermidine by a S-adenosyl methioninamine co-substrate, which is in turn derived from S-adenosyl methionine (SAM) by decarboxylation of the methionine moiety. This paves the way for homospermidine synthase, which first oxidises spermidine to the corresponding imine dehydrospermidine and second replaces the propanamine by a butanamine residue to end up with homospermidine. Notably, the latter step in eukaryotes differs from plants in a lysine residue and a eukaryotic initiation factor that are involved in the transfer of 4-aminobutylidene.[10] Homospermidine readily cyclizes to the 5-membered imine after oxidative deamination, which in turn, after a second oxidative deamination, undergoes an intramolecular MANNICH-reaction that furnishes the pyrrolizidine ring.[11] Reduction of the aldehyde leads to trachelanthamidine (**28**), the common precursor of pyrrolizidine alkaloids. The latter transformations are thought to occur in the plant's roots but for further modifications the more hydrophilic trachelanthamidine N-oxide is transported to upper parts of the plant.[10]
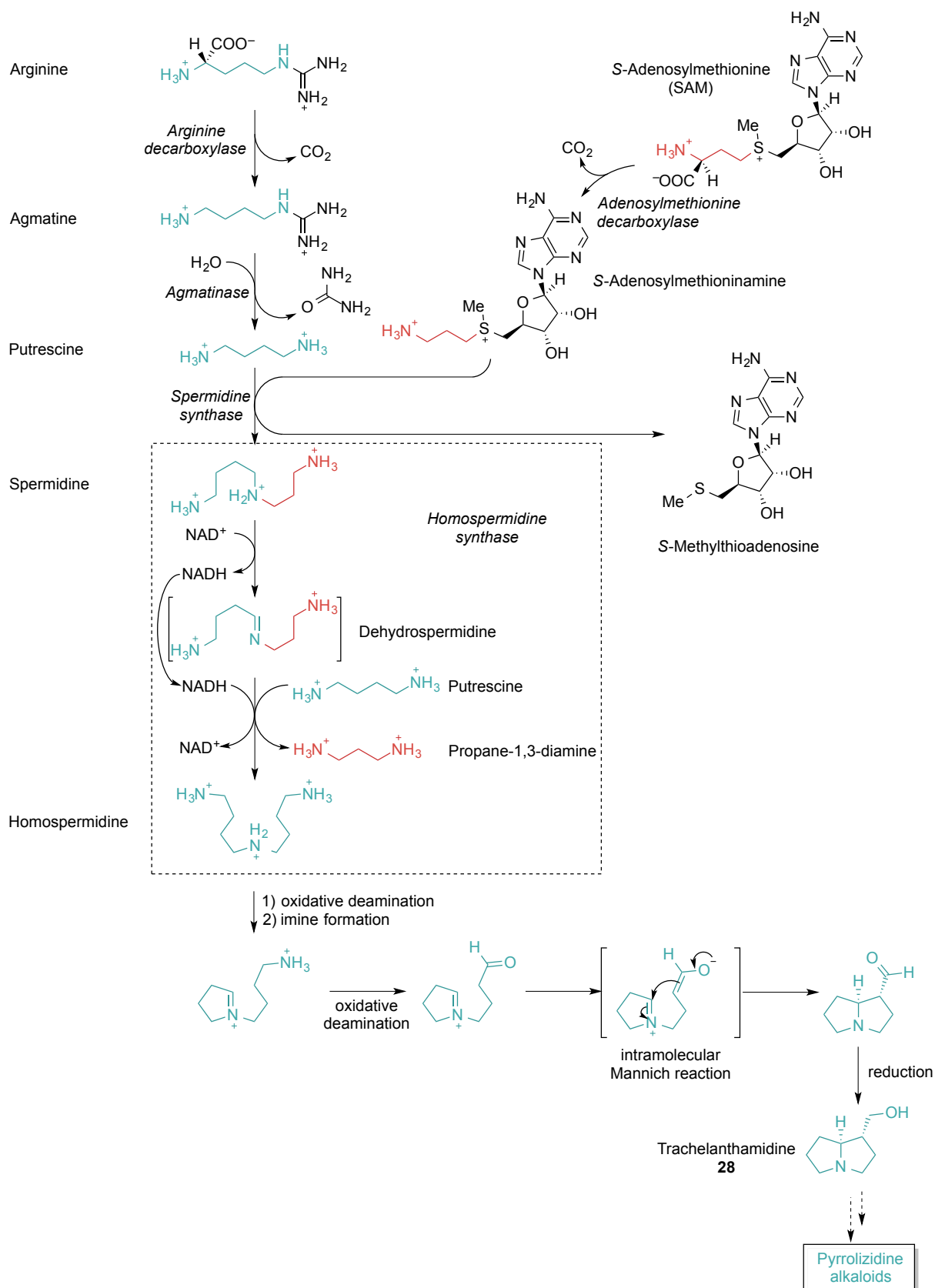
Scheme 1.1 | The plant biosynthetic pathway of pyrrolizidine alkaloids from arginine.

1.1.2 Discovery of Xenovenine and its Properties

Xenovenine (5Z,8E-223H) (5Z,8E-**4**) is, among a variety of other alkaloids, part of the venom of the ant species *Solenopsis tennesseensis*[12] (also more informally referred to as *Solenopsis xenovenenum*)[1] and was also isolated from the skin of both the Madagascar poison frog species *Mantella crocea*[2] and the bufonid toad *Melanophryniscus stelzneri*[13] (Figure 1.2 a–c). Out of the four possible diastereomers in Figure 1.3, the isomer with 5*Z*,8*E* relative stereochemistry was found to be the naturally occurring compound by means of GC-MS, IR and NMR spectroscopy.[12] The absolute configuration of the natural enantiomer, occurring both in ant venom and amphibian skin, was found 3*R*,5*S*,8*S* thus matching the (+)-rotatory isomer.[14]
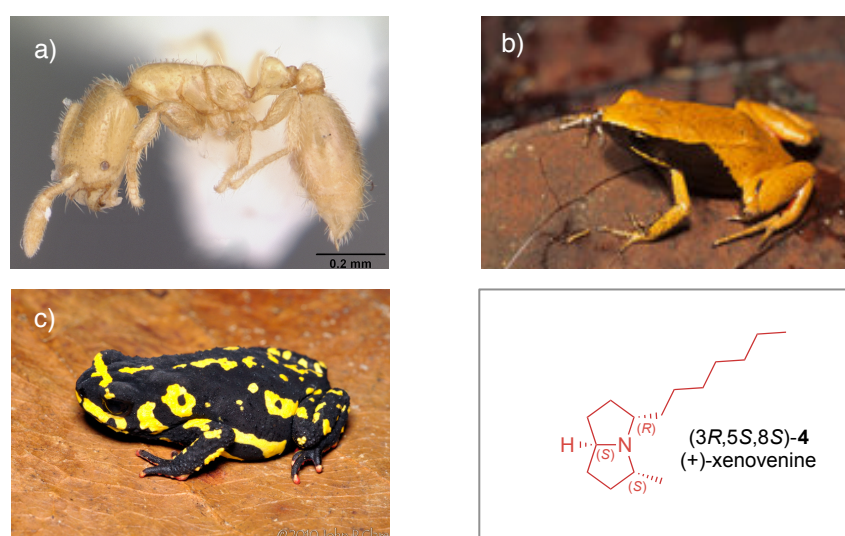
Figure 1.2 | Specimens of a) the ant *Solenopsis tennesseensis* (photo by April Nobile / from www.antweb.org. accessed 10 September 2014), b) the poison frog *Mantella crocea* (photo by Franco Andreone. Mantella crocea. The IUCN Red List of Threatened Species. Version 2014.2. www.iucnredlist.org downloaded on 10 September 2014.) and c) the bufonid toad *Melanophryniscus stelzneri* (© 2010 John P. Clare).
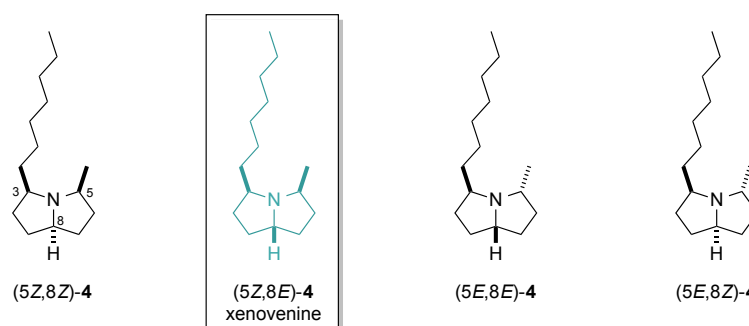
Figure 1.3 | The four possible diastereomers of alkaloid 223-H (xenovenine).

Depending on their substitution pattern, pyrrolizidine compounds adopt either a *cis-* or *trans-*conformation, which are in equilibrium with each other (Figure 1.4). Whereas 3,5-

---

[1] According to the e-mail correspondence with Mark Deyrup, entymologist at the Archbold Research Station,

disubstituted, hydroxylated derivatives from plant sources prefer the trans-conformation, [5c, 15] 3,5-(*Z*)-dialkylpyrrolizidines derived from insects such as xenovenine are mainly found in the less sterically strained *cis*-conformation.[12] Hence, the predominant conformation of each individual alkaloid derivative compromises minimal steric interactions and formation of intramolecular hydrogen bonds.
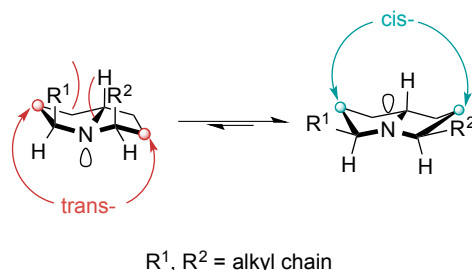

R^1, R^2 = alkyl chain

Figure 1.4 | Conformational equilibrium of 2,5-disubstituted pyrrolizidine alkaloids.

Recently, the remarkably high affinity of non-natural (−)-xenovenine to neuronal acetylcholin-receptors (nAChR) in *Torpedo californica* with an IC_{50} of 0.05 mM has been reported.[16] The IC_{50} is defined as the concentration of a substance at which half of the available receptors are inhibited.

1.1.3 Synthetic Efforts Towards Xenovenine

Since its first appearance in literature in 1980[12], xenovenine received notable attention among the synthetic chemist community. Even though being a relatively small molecule, the three stereocenters arranged around the bicyclic heterocycle core render this alkaloid a challenging target for asymmetric synthesis, with 16 literature-reported ones in up to now. Taking non-diastereoselective syntheses into account, there are a total of 19 synthetic routes published, featuring various cyclization approaches:

- (±)-xenovenine and diastereomers, not diastereoselective (3)[12, 17]
- (±)-xenovenine diastereoselective (2)[18]
- (+)-(3S,5R,8S)-xenovenine (natural isomer), enantioselective (11)[16, 19]
- (−)-(3R,5S,8R)-xenovenine (non-natural isomer), enantioselective (3)[19f, 20]

The key steps of xenovenine syntheses are subsequenly discussed in a retrosynthetic manner. The first synthesis conducted by the discoverers themselves features triketone **29** as key intermediate, which was prepared from methylvinylketone **29d**, acrolein diethylacetal **29e** and heptanal **29f** in two steps that both required the umpolung of an aldehyde. Reductive amination with ammoniumacetate and sodium cyanoborohydride gave *rac*-xenovenine (**4**) in 73 % *d.e.* and 14 % overall yield. The authors managed to separate the four diastereomers by preparative GC and thus could assign them a relative stereochemistry with NMR spectroscopy experiments.[12]

Interestingly, both the first and latest described synthesis use the same intermediate triketone **29**, yet the preparation of the latter is different in the recent report. Barthelme *et al.* chose the rather laborious way of providing **29** via methyl- and heptyl-GRIGNARD (**29a** and **29c**) addition to the protected double-WEINREB-amide **29b**. Reductive amination again gave racemic **4** in 5 % overall yield.[17b]

A third approach uses nitro-diketone **31** that was obtained from conjugate addition of an α-nitro carbanion **31a** to the α,β-unsaturated compound **31b**. Reduction with either palladium on charcoal and 10 atm hydrogen or borohydride reagents yielded the racemic *C*-8-epimer of **4** in 65 % *d.e.* or *rac*-**4** in 88 % *d.e.*, respectively.[17a]

Scheme 1.2 | Syntheses of racemic xenovenine, non-enantioselective.

Lathbury *et al.* utilized the LEWIS-acid catalyzed cyclization of an allenic oxime **30b** to the corresponding nitrone **30a**, which in turn stereoselectively added to methylvinylketone **29d** in a (3+2) fashion to give **30**. Catalytic reduction of **30** with H_2/$PdCl_2$ *via* the *in situ* generated imine furnished the bicyclic core with all stereocenters in place. Ultimately, the remaining hydroxyl-group was removed via oxidation, subsequent thioacetal-formation and catalytic reduction.[18a]

A diastereoselective synthesis from 2010 employed a Sc(III) catalyst for setting up the left moiety of the bicyclus starting from the aminodiene **32a**. Formally being a hydroamination, this step defined the correct relative stereochemistry in the 5 and 8-position in **32** with 98% *d.e.* Upon heating, the second cycle was closed in a stereoselective manner and catalytic reductive removal of the thiophene auxiliary yielded *rac*-**4**.[18b]

Not surprisingly, there are by far more syntheses of natural occurring (+)-xenovenine described than of its enantiomer (compare Scheme 1.3 and Scheme 1.4). The first was accomplished in 1983, three years after the molecule was discovered. In this sequence, the

first stereocenter was defined by a SHARPLESS asymmetric epoxidation of the allylic alcohol derivative **33a**. The chiral epoxide was then converted under inversion into the chiral amine with a MITSUNOBU reaction. Hydrolysis of the furan ring subsequently yielded the corresponding keto-hydroxyethyl-imine **33**. Substrate-controlled face-selective hydride transfer (**33**) set up the second stereocenter and imine-formation (or rather enamine formation) of the newly generated secondary pyrroline nitrogen with the δ-carbonyl group closed the bicycle. Under the former reaction conditions, the enamine was readily reduced and the enantiomerically pure alkaloid core was complete.[19a]

Scheme 1.3 | Enantioselective syntheses yielding (+)-xenovenine. [a]) Formal syntheses.

The most efficient enantioselective synthesis up to now came from Takahata *et al.* Starting from D-alanine **36b**, the authors prepared precursor **36a** whose double bond was subjected to a intramolecular amidomercuration to give the respective chiral pyrroline. A HORNER-WADSWORTH-EMMONS olefination among other minor transformations gave rise to the unsaturated ketone **36**, whose saturated derivative (**35**) was found to be a common intermediate in other syntheses. Catalytic hydrogenation of **36** yielded the target molecule in 21 % overall yield from **36a**.[19d]

Another remarkable synthesis by Arredondo *et al.* featured the chiral aminoalkene-allene **40** that underwent cyclization with Sm(III) catalysis to furnish the entire pyrrolizidine core in a single transformation. Chiral amine **40** was initially made in 20 % yield from the corresponding allene aldehyde, which was asymmetrically allylated by diallylzinc and a chiral LEWIS-acid catalyst. The amine was then introduced by a MITSUNOBU-reaction that demanded inversion of the stereocenter from the (*R*) to the desired (*S*) configuration. The allene aldehyde mentioned before was efficiently made from alkyne **40a** via addition of hexanal to the alkyne anion and subsequent elimination of the hydroxyl group.[19g]

The first enantioselective synthesis of non-natural (−)-xenovenine was conducted by Oppolzer and Cuny and required the camphor-derived 2-carbonylsultam in **44b** (Scheme 1.4) as chiral auxiliary in an asymmetric borohydride-reduction of the intermittent imine-*N*-oxide. The auxiliary was removed by hydrolysis and spontaneous decarboxylation (and could be recovered through flash chromatography) to give **44a** as single enantiomer. The substrate-controlled homoallylation of **44a** with the respective GRIGNARD-reagent and WACKER-oxidation of the olefin gave **44** in > 99% *d.e.* Catalytic reduction after deprotection and enamine formation gave (−)-xenovenine for the first time.[20a]
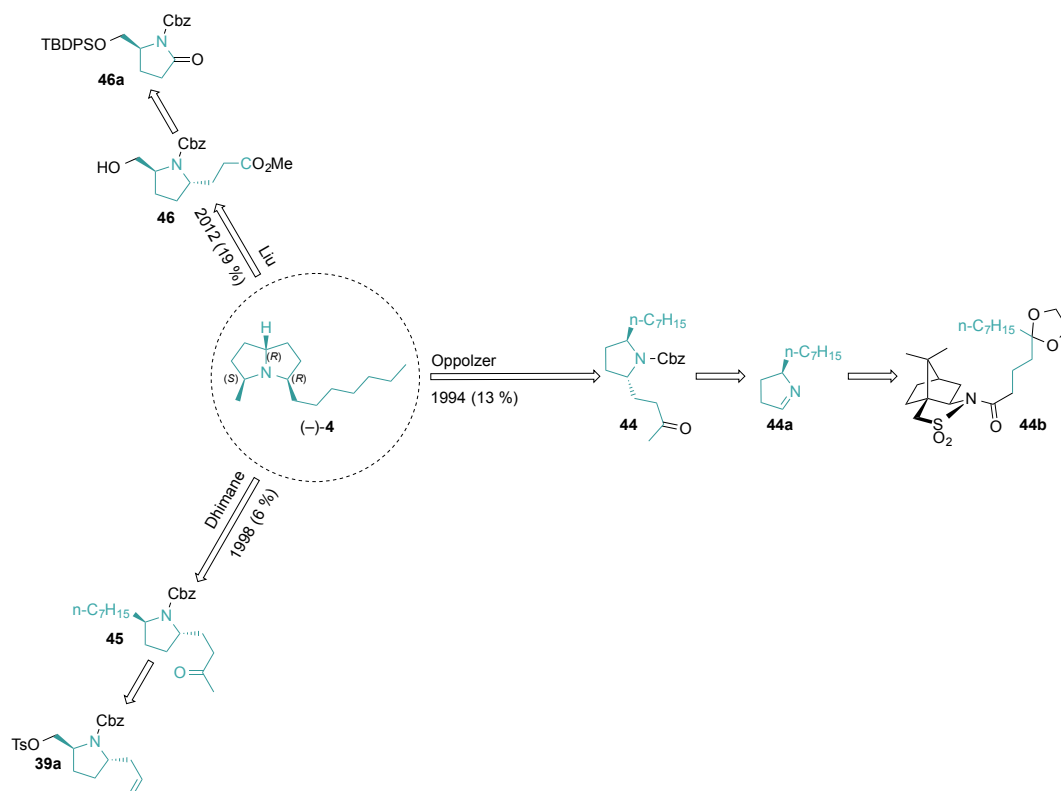
Scheme 1.4 | Enantioselective syntheses yielding (−)-xenovenine.

The other two (−)-selective syntheses merely rely on the chiral pool of starting materials and use substrate control for the establishment of the other two stereocenters.

Strictly speaking, none of these approaches is reasonably selective and gives satisfying yields at the same time. Even though being impressively creative, especially enantioselective sequences are characterized by a considerable, yet impressive, number of steps and thus only low to moderate overall yields. Up to now, there are no chemoenzymatic approaches known for making enantiomerically pure xenovenine.

1.2 Asymmetric Chemical Methods for the Preparation of Chiral Amines

The syntheses of enantiomerically pure xenovenine already imply that the preparation of chiral amines can be a formidable task. Indeed, the regio- and chemoselective preparation of secondary (2°) or tertiary (3°) α-chiral amines by conventional synthetic methods is not always straightforward and considerable effort has been dedicated to this transformation in recent years. An overview is given in Figure 1.5 where the most useful methods are highlighted in green. Among those is the Mitsunobu-reaction that converts an alcohol into a leaving group and replaces it by a nitrogen nucleophile under inversion of stereoconfiguration (a). Addition of carbanions to ketimines and aldimines (b) gives tertiary and secondary α-chiral amines, respectively. Furthermore, the asymmetric reduction of ketimines, enamines and *N*-acetylenamines or the reductive amination of prochiral ketones to the corresponding amines via an imine intermediate (c) constitute other ways for making amines.[21] Even though being extraordinarily atom-efficient, hydroaminations (d) and C–H insertions (e) are only rarely reported due to their unfavorable thermodynamics associated with substrate activation.[22]
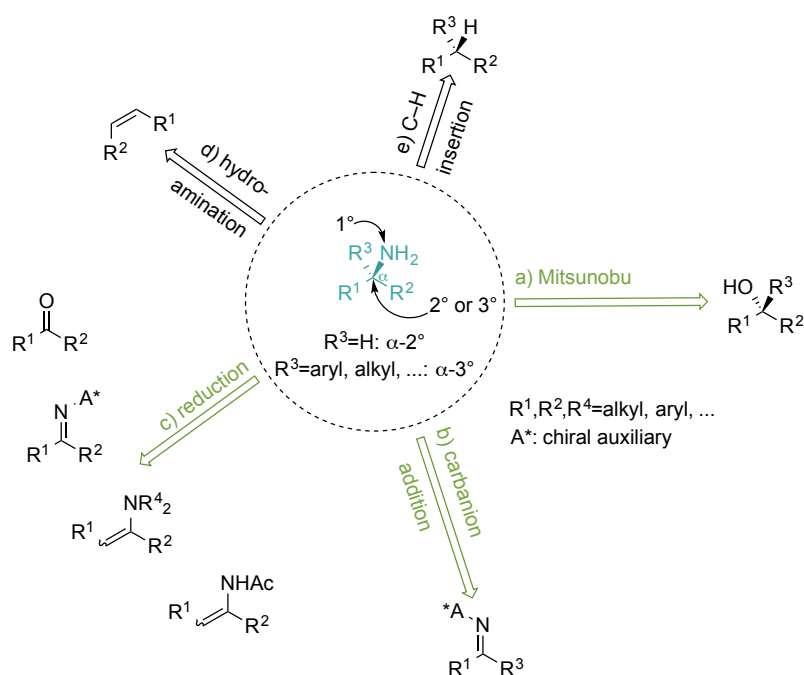
Figure 1.5 | "Chemical" approaches towards secondary and tertiary α-chiral primary amines. It depends on the case, whether they work with secondary and tertiary amines as well.

Virtually all of these methods either depend on a chiral organocatalyst or on a transition metal (mostly Pd, Ru and Ir) in complex with a chiral ligand to induce stereoselectivity. The only exception here is the Mitsunobu-reaction that just depends on the stereocenter of the substrate.

Figure 1.6 shows a summary of methods for chiral amine synthesis, which were employed in reported xenovenine syntheses. In the majority of cases, stereoselectivity happens in the catalytic *syn*-hydrogenation of prochiral, cyclic imines and enamines or the ring-forming reductive amination of ketones. Because the former two constitute tautomers, in many cases it depends on the pH whether the imine or the enamine gets reduced.
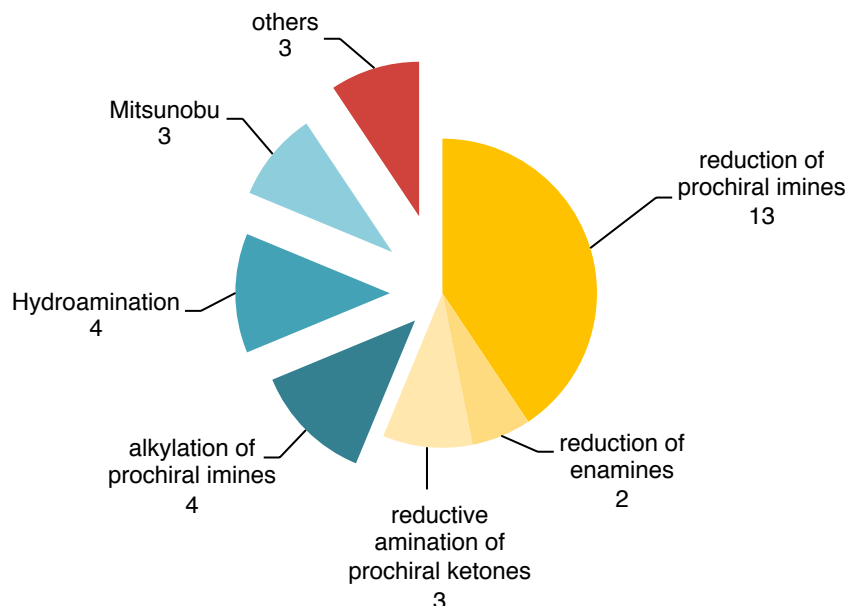
Figure 1.6 | Methods for the introduction of amino-functionalities employed in xenovenine syntheses: Hydroaminations including amidomercurations; others: radical cyclizations, cycloadditions, electrophilic addition of hydroxylamine.

These reduction steps mentioned above are often carried out as one of the final steps in a synthetic sequence, where an already present stereocenter enables for substrate diastereocontrol. Scheme 1.5 provides a rationale for explaining how the newly introduced stereocenter in the catalytic hydrogenation of a prochiral, cyclic imine is dictated by the orientation of the sterically demanding alkyl-chain.
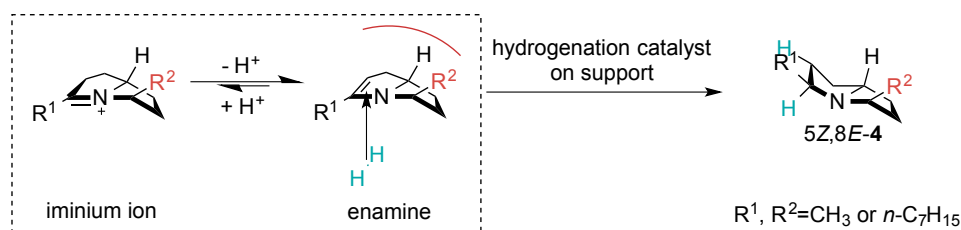
Scheme 1.5 | Catalytic hydrogenation of the bicyclic enamine in the last step of many xenovenine syntheses: Already present R^2 sterically shields one face of the enamine so that activated hydrogen from the catalyst surface is added in a way to give the 5*Z*,8*E*-diastereomer predominantly.

Actually, stereoselectivity in virtually all enantioselective syntheses of xenovenine more or less arises from a chiral starting material and/or, in the later steps, from substrate control whereas examples for chiral catalysts and auxiliaries are rare.

Subsequently, some of the approaches in Figure 1.5 will be discussed and examples of applications of making α-chiral primary amines are given to illustrate the chemical alternatives to ω-transaminases that are the subject of section 1.3.2.

Hydridic reduction of imines and derivatives thereof (such as oximes, hydrazines, acetamides, phosphoramides, sulfamides and many more) can be rendered asymmetric with the aid of chiral boron organocatalysts, which direct hydride delivery to one enantiotopic face of the prochiral imine by steric interactions as shown in Scheme 1.6 a.[23]

Tang *et al.* developed a chiral bidentate phosphane ligand, that, in Rh-catalyzed hydrogenations of acetyl-enamines, perfectly dictates the configuration of the newly formed stereocenter (Scheme 1.6 b).[24] Hydrolysis of the amide bond ultimately provides the primary amine.

In the improved second-generation manufacture process of the diabetes II drug sitagliptin, direct asymmetric reductive amination using ammonia as nitrogen source was used (Scheme 1.6 c), which is indeed a remarkable example. The chiral ruthenium catalyst carries out the asymmetric, catalytic reduction of the intermediate imine to the α-chiral, primary amine with almost perfect *e.e.* and excellent yield.[25] This metal-catalyzed process, which was by the way never used on industrial scale, and the better performing biocatalytic variant were both honored with the "Presidential Green Chemistry Award" issued by the US-EPA.
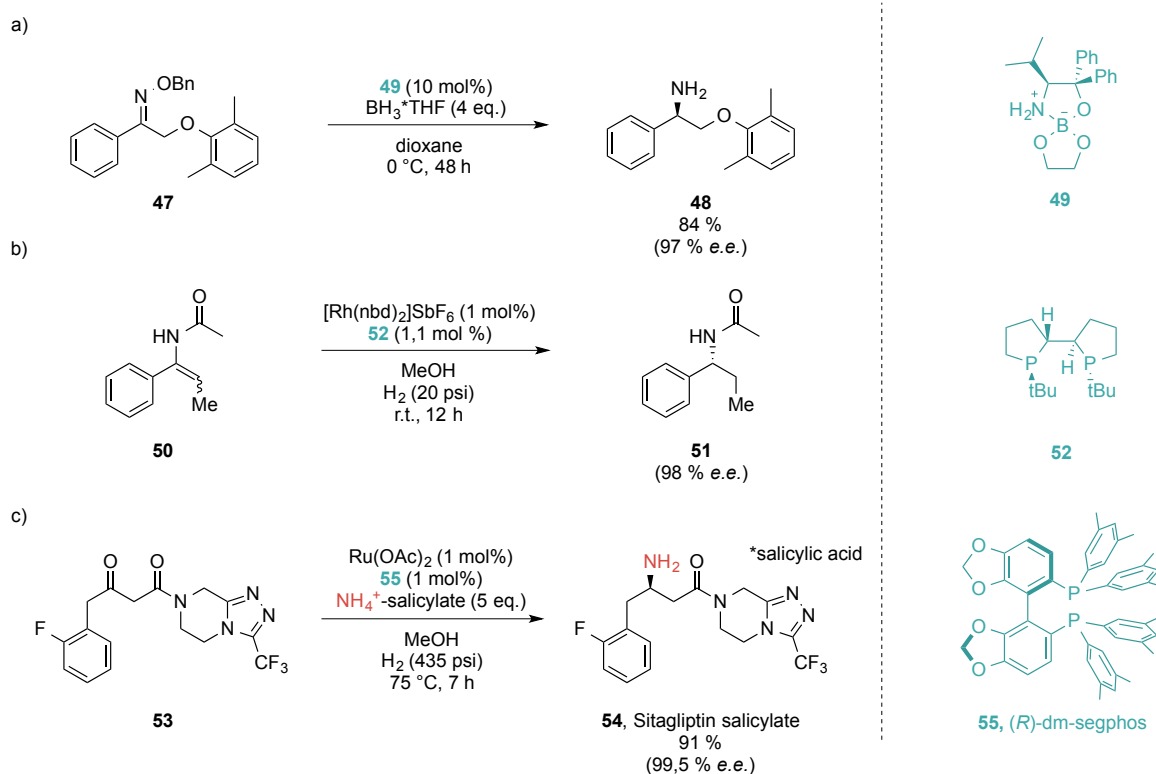
Scheme 1.6 | Examples of α-chiral primary amine syntheses. (a) asymmetric imine reduction, (b) asymmetric enamine reduction, (c) asymmetric reductive amination of a prochiral ketone.

The phosphane ligands used in the latter process (*e.g.* **55**) turned out as effective conveyors of stereochemical information. A set of structurally distinct ligands for countless applications has been developed, which can either be mono- or bidentate depending on the number of bonds to the center-atom (Figure 1.7). Among the most popular ones are BINOL-derived ligands, which posses axial chirality along the bond that connects the naphthalene subunits. The molecule thus adopts the shape of two twisted planes, which influence the steric interactions of prochiral substrates and the actual catalyst entity in favor of one single product enantiomer or diastereomer.[21]
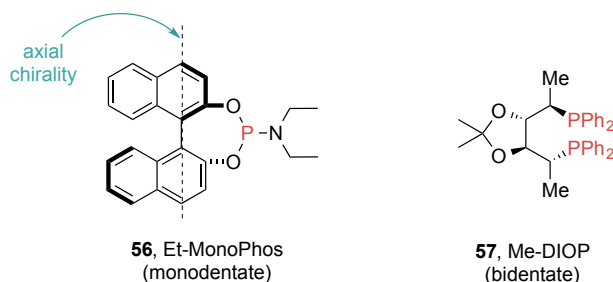
Figure 1.7 | Mono- and bidentate phosphane ligands for asymmetric aminations. Left: BINOL-derived ligand with axial chirality; right: tartrate-derived ligand.

Apart from chiral catalysts and ligands, removable chiral auxiliaries that are covalently bound to the imine substrate can be used to control stereoselectivity. In general, there are two possible binding positions (Scheme 6, a and b) for the introduction of these auxiliaries but the principle of stereoinduction through face shielding remains the same.[22] The lower sequence in Scheme 1.7 b shows the so-called ELLMAN-imine in action: a chiral sulfinylimine **64** that shields one diastereotopic face of the imine with a bulky t-butyl group that is easily removed after alkylation via acidic hydrolysis.[26]
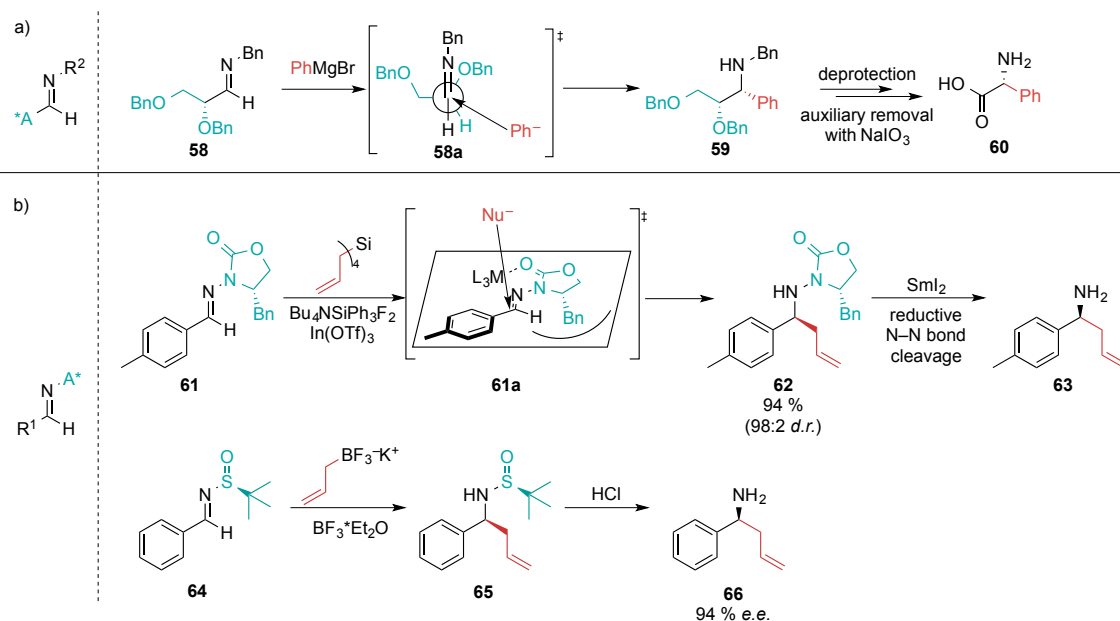
Scheme 1.7 | Asymmetric nucleophilic addition of non-stabilized carbanions to imines with chiral auxiliaries as inductors of stereochemistry.

Hydroaminations are the formal addition of nitrogen and hydrogen to multiple C–C bonds. Gong *et al.* used this transformation in combination with an acid-catalyzed isomerization and HANTZSCH-ester reduction in the asymmetric synthesis of tetrahydroquinoline **68** (Scheme 1.8 a). HANTZSCH-ester with chiral BRØNSTED acids, such as **70** and **69**, for asymmetric reductions have gained much attention in recent years, especially for the reduction of imines.[27] Scheme 1.8 b shows one of the rare amine syntheses that involve C–H activation. The process is catalyzed by ruthenium associated with the sterically demanding, tridentate chiral ligand **72** and gives both excellent yields and good *e.e.*'s.[28] The primary amine is liberated by hydrolysis of the cyclic sulfamic acid derivative **73**.
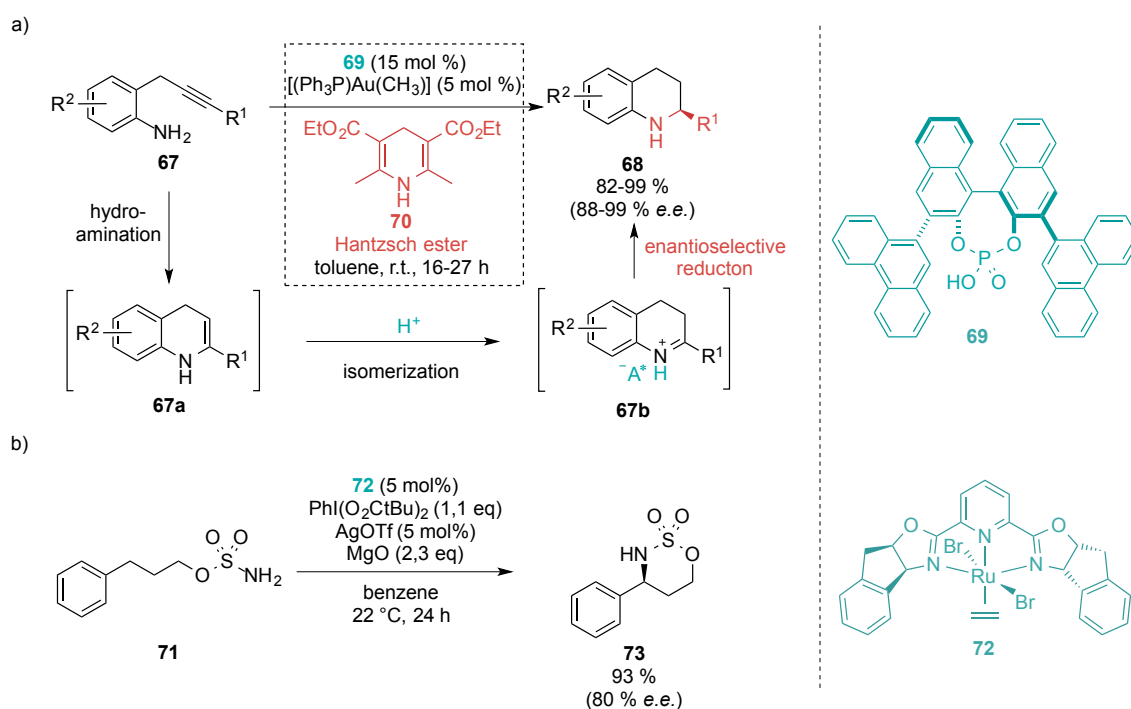
Scheme 1.8 | a) Gold-catalyzed hydroamination with subsequent asymmetric transfer-reduction of the imine with a HANTZSCH-ester and a chiral BRØNSTED acid. b) insertion of an amine into a C–H bond with a Ru-catalyst that bears a chiral, tridentate ligand for stereoinduction.

Scheme 1.6 and Scheme 1.8 exemplify only a few chiral amine syntheses; in fact there are countless methods of each transformation approach illustrated in Figure 1.5. However, the main point becomes clear: the majority of these techniques require structurally complex and expensive catalysts or auxiliaries, which hamper their availability and user-friendliness and lead to a low atom-efficiency. This is the point where enzymes join the game.

1.3 Enzymatic Methods for the Preparation of Chiral Amines

1.3.1 Enzymes and Catalysis

Enzymes are wonderful catalysts. Apart from their remarkable chemo-, regio- and stereoselectivity in biotransformations, they are able to speed up reactions by a factor of 10^8 to 10^{10} compared to the respective uncatalyzed reaction.[29] This is a performance far beyond that of chemical catalysts. Moreover and conveniently, enzymes work in aqueous media and at mild conditions such as 30 °C and around neutral pH values. However, this can turn into a drawback; for example, selectivity cannot be enhanced by simply lowering the temperature without losing the enzyme's activity. On the other hand, enzyme-catalyzed reactions sometimes work even better with organic solvents or other additives. Mild reaction conditions result from the fact that enzymes are catalysts originating from a living environment. In their natural roles they are part of enzymatic pathways, thus they are also required to be compatible with each other.[30] This opens manifold possibilities to use them in cascade biotransformations where multiple enzymes furnish complex products in a cascade reaction.[31]

The most striking feature and the reason why enzymes can be used for biotransformations in organic synthesis is called "substrate promiscuity".[32] This means that enzymes are not necessarily bound to their natural substrates but can also accept and convert a wide scope of substances in their active sites. However, this is not the case for their natural cofactors e.g. nicotinamide adenine dinucleotide (phosphate) [NAD(P)H] and adenosyltriphosphate (ATP) to name the most important, which must be available to the enzyme in order to carry out catalysis.[30]

Given the substrate promiscuity and the fact that there is enzyme-catalysis known for many organic reactions renders them incredibly valuable tools for organic synthesis.

1.3.2 Enzymatic Nitrogen-Swapping – General Features of ω-Transaminases

ω-Transaminases (ω-TA) or aminotransferases (E.C.2.6.1.X) are pyridoxal-5'-phosphate (PLP) dependent enzymes that are capable of transferring an amino group from a donor amine to a carbonyl group (amino acceptor) of a substrate molecule. For ω-transaminases in particular, at least one of the components does not need to be an α-amino acid or an α-keto acid.

The mechanism, which takes place in the enzyme active site, requires a flexible lysine residue that both acts as acid and base and in absence of an amine donor serves as a covalent linkage between the PLP cofactor and the enzyme (Scheme 1.9). If a proper amine donor molecule is added, it replaces lysine and liberates the cofactor, which, however, stays in the active site as it is still bound *via* non-covalent interactions (1).

The free lysine now abstracts the α-hydrogen of the co-substrate amine and the electrons are shifted into the pyridine ring (2). Upon their return, the proton from lysine is transferred back and ends up in the benzylic position. Thus, the overall transformation was a shift of the imine bond from PLP to the amine-donor (3). Now, hydrolysis of the imine gives the respective ketone of the former amine donor and pyridoxamine-5'-phosphate (PMP), which carries the amino function to be transferred (4). Next, the acceptor ketone comes along and forms a SCHIFF-base with PMP and the deprotonation/protonation mechanism takes place in reverse (5-7). In the final step, the covalent lysine-PLP imine bond is restored and the newly generated amine expelled from the active site (8).[30, 33]
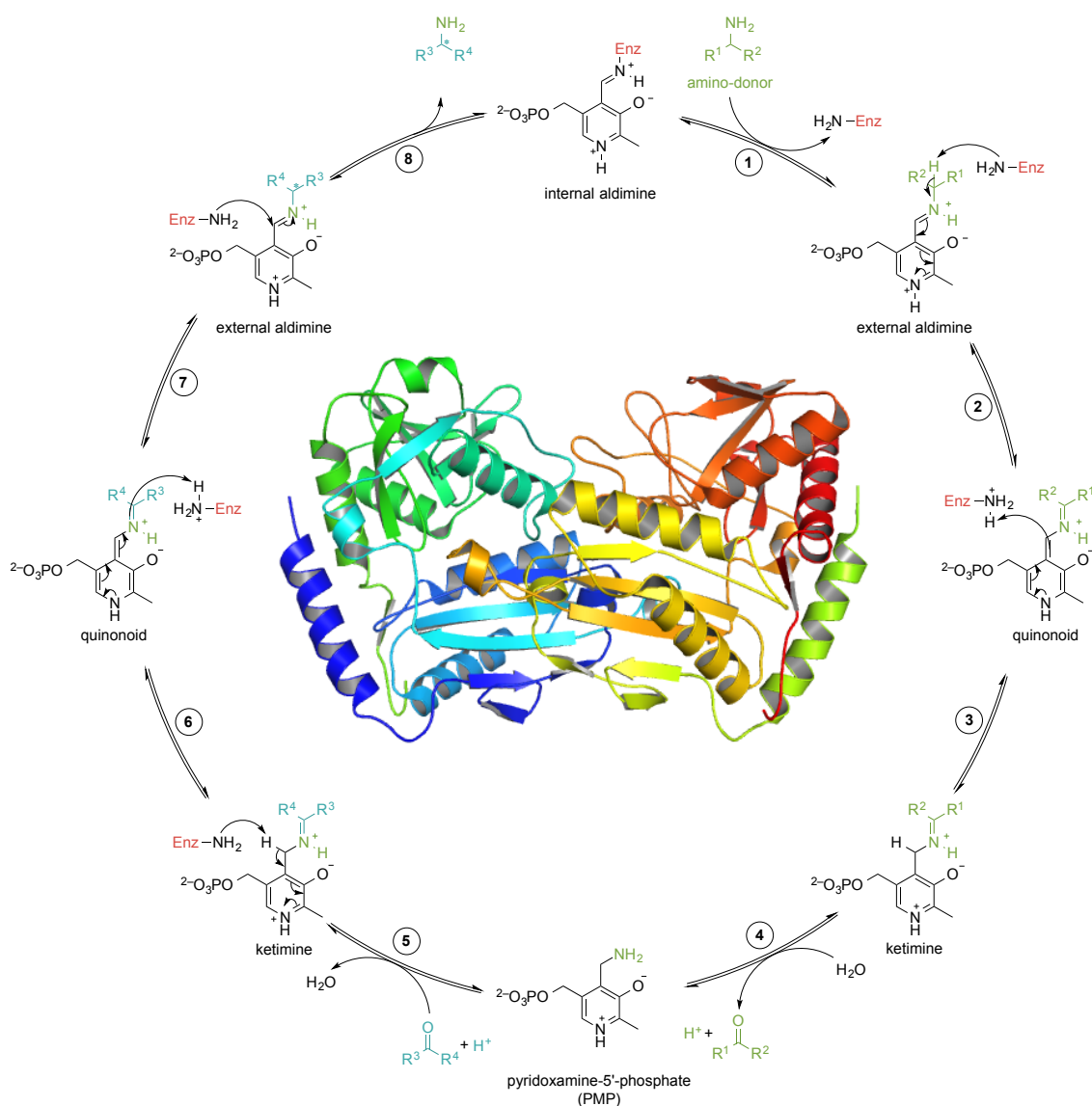
Scheme 1.9 | The mechanism of a PLP-dependent transamination taking place in an enzyme active site. Center: X-ray crystal structure of a (R)-selective ω-TA from *Aspergillus terreus*.[34]

The most striking advantage of transaminases is their excellent stereoselectivity exhibited in the amination of prochiral ketones. The prerequisites for this, however, are sterically distinct residues on the two sides of the ketone (as in **73** in Figure 1.8 a) enabling the enzyme to distinguish between the *Si* and *Re* face. Transaminases are considered very flexible entities featuring one small and one large pocket in proximity to their active site. The substrate arranges within this pockets by placing the larger substituent into the large pocket and *vice versa*. According to the inuced fit model, the Lys-residue, which is located on a highly flexible loop subunit, then approaches one enantiotopic face to carry out acid / base catalysis to yield one amine enantiomer preferentially as shown in Figure 1.8 c.
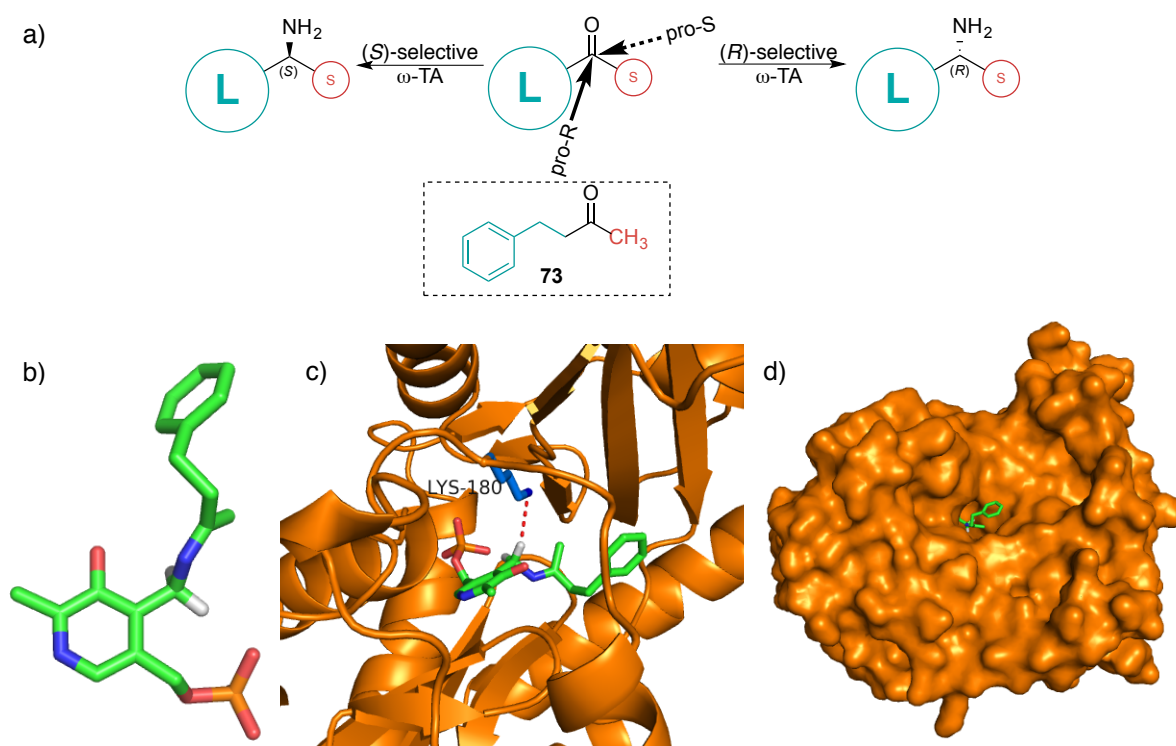
Figure 1.8 | (a) Enantiotopic face discrimination by enzymes; a sequence rule order of NH_2 > "L" (large) > "S" (small) is assumed. (b) A prochiral substrate (4-phenyl-2-butanone **73**)-PLP ketimine (atoms in green: C, white: H, blue: N, red: O, orange: P) (c) being deprotonated by Lys_{180} in the active site of an (*R*)-selective ω-TA from *Aspergillus terreus*[34] (step 6 in Scheme 1.9). (d) The substrate molecule arranges in the active site with the small residue ahead, which causes proton introduction to occur from the pro-(*R*) face preferentially.

Nature provides (S)- and, more rarely, (R)-selective ω-TA's in several organisms and recombinant expression of the proteins, in for example in E. coli hosts, provides access to amounts suitable for preparative-scale biotransformations. A selection of commonly used ω-TA's with the organisms they are derived from, is shown in Table 1.1.

Table 1.1 | Selection of ω-transaminases from various organisms and their displayed stereoselectivity.

Entry	Parent Organism	Selectivity	Ref.
1	*Bacillus megaterium*	(*S*)	[35]
2	*Arthrobacter citreus*	(*S*)	[36]
3	*Chromobacterium violaceum*	(*S*)	[37]
4	*Vibrio fluvialis*	(*S*)	[38]
5	*Arthrobacter sp.*	(*R*)	[39]
6	*Aspergillus terreus*	(*R*)	[39]
7	*Hyphomonas neptunium*	(*R*)	[39]
8	*Arthrobacter* round 11 mutant[a]	(*R*)	[39]

[a]mutant capable of accepting and converting more bulky substrates.[40]

Transaminases can be used in two modes for the preparation of α-chiral amines: the enantioselective (trans)amination of prochiral ketones and the kinetic resolution of racemic amines (Scheme 1.10 a and b, respectively), *via* deamination. In a kinetic resolution the maximum yield is limited to 50% since the enzyme converts only one enantiomer to the corresponding ketone. The other enantiomer remains untouched and accumulates during the course of the reaction. On the other hand, asymmetric amination of prochiral ketones results in a 100 % theoretical yield.[41] As indicated, the substrate scope for these enzymes is remarkably wide, and so is their application in asymmetric synthesis.

R^1, R^2 = H, alkyl, aryl, arylalkyl, alkene
$R^4 = R^5 = CH_3$: 2-aminopropane / acetone
$R^4 = COOH, R^5 = CH_3$: alanine / pyruvate
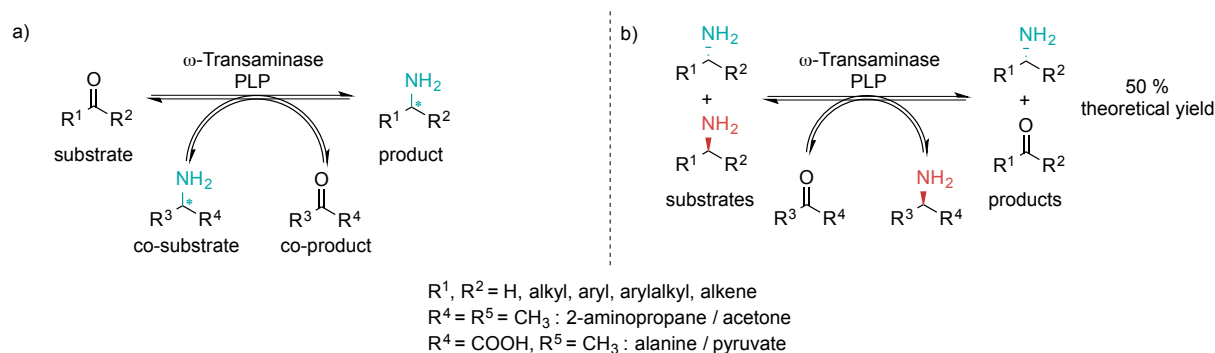
Scheme 1.10 | Preparation of α-chiral tertiary amines using ω-transaminases. Assumed sequence rule order: $R^1 > R^2$, $R^3 > R^4$, $NH_2 > R^{1-4}$

From a thermodynamic point of view, there is one major drawback to be considered in the amination of ketones. The conversion of a carbonyl group into an (actually energetically lower) amine group *via* transamination, requires the amine-donor being converted into its corresponding ketone. Thus, no overall change in energy is observed, but the overall equilibrium can be influenced by intramolecular intractions in co-substrates and co-products, *e.g.* hydrogen bonding or conjugation.

For example, the equilibrium constant between acetophenone and alanine was determined to $8.8 \cdot 10^{-4}$.[42] This essentially means that conversion of the ketone substrate will be incomplete unless one can overcome the problem of displacing the equilibrium to the *per se* thermodynamically unfavorable product-side. Hence, several techniques to accomplish that have been established.[43]

One approach chooses co-substrates that are converted to volatile co-products and thus can be removed from the equilibrium by simple evaporation. The most common of these co-substrates, also used in industry, is 2-aminopropane, which gives volatile acetone upon deamination (Scheme 1.11).[44] Stripping the reaction mixture with inert gas can accelerate the evaporation of acetone and thus supports equilibrium displacement to the product side in industrial biotransformations.[45]

R^1, R^2: H, alkyl, aryl, arylalkyl, alkene
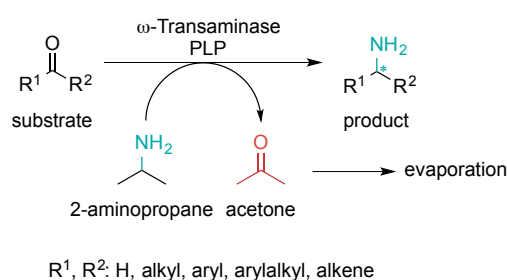
Scheme 1.11 | Equilibrium displacement by evaporation of co-product with 2-amino-propane as co-substrate.

The most effective, yet complicated methods involve the cascade-fashioned enzymatic degradation or recycling of co-products to achieve full conversion. Those cascades can be effectively operated in several ways that will be discussed subsequently.

Staying with 2-aminopropane as co-substrate there is another possibility for the removal of co-product acetone: NADH dependent yeast alcohol dehydrogenase (YADH) readily reduces it to 2-propanol, which cannot serve as substrate for the transaminase anymore (Scheme 1.12). Of course, the YADH must not reduce the substrate ketone to its corresponding alcohol. The reducing equivalents for the acetone reduction step are derived from formate salts to ultimately give water and carbon dioxide as inert co-products. [43, 44b]

R^1, R^2: H, alkyl, aryl, arylalkyl, alkene
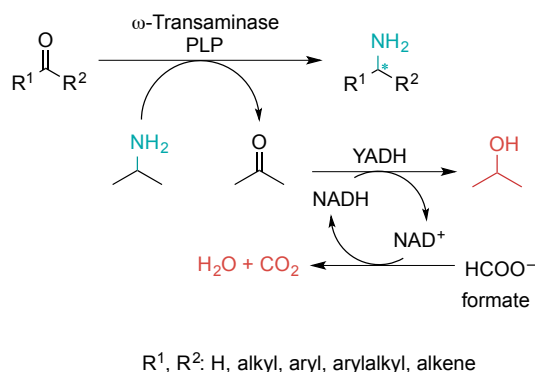
Scheme 1.12 | Equilibrium displacement by enzymatic reduction of the acetone co-product. YADH = yeast alcohol dehydrogenase.

Transamination of prochiral ketones employing the amino acid alanine as co-substrate are frequently used in cascade setups due to the variety of available enzymes that are able to effectively convert the co-product pyruvate. Among the most important ones are alanine dehydrogenase, lactate dehydrogenase, pyruvate decarboxylase and acetolactate synthetase. The latter three are used in general for irreversible degradation of pyruvate as shown in Scheme 1.13 a).[43, 46]
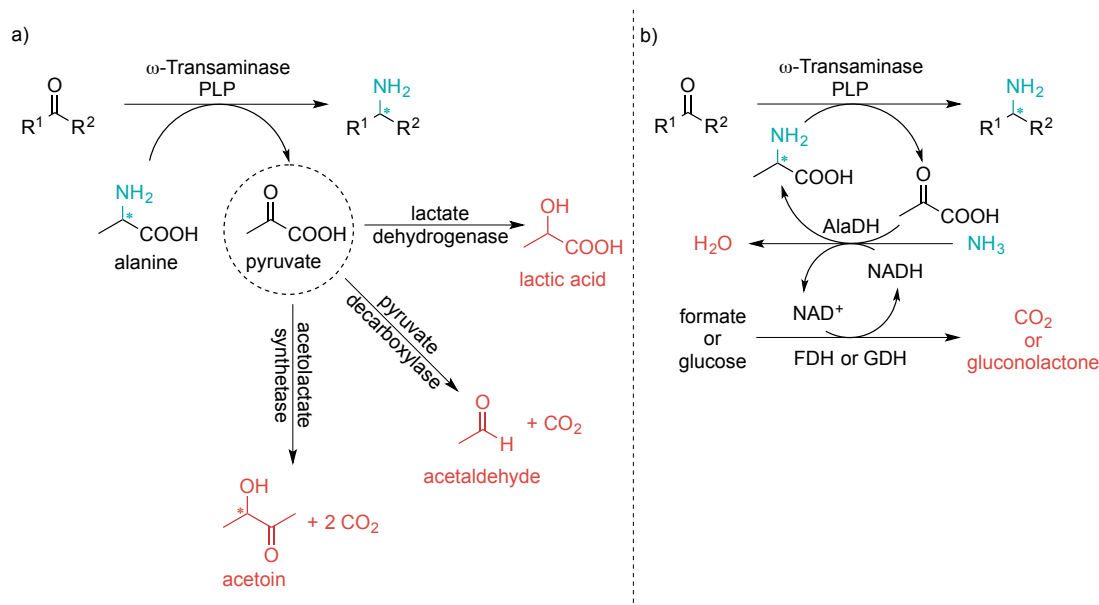

Scheme 1.13 │ Degradation (a) and recycling (b) of the co-product pyruvate by different enzyme coupled techniques. AlaDH = alanine dehydrogenase, FDH = formate dehydrogenase, GDH = glucose dehydrogenase.

A more elegant approach seeks to recycle the co-product by coupling its regenerative step with another irreversible biotransformation that degrades a cheap second co-substrate rather than the more valuable (chiral) amino acid. An example is the three-enzyme cascade for a transamination that uses alanine dehydrogenase in combination with formate dehydrogenase or glucose dehydrogenase for alanine recycling. Scheme 1.13 b shows the cascade setup with ammonium formate or glucose serving as source for reducing equivalents.[43] The implementation of such enzymatic cascades in whole-cell biocatalysts has now been explored, which would make them easier to use.[47]

Only recently, the emphasis of equilibrium displacement in enzyme catalyzed reactions was put on so-called "smart co-substrates".[48] This approach does not require additional enzymes for degradation and/or recycling nor volatile co-products but rather uses specially designed co-substrates with a built-in energy sink. Scheme 1.14 shows two examples where the co-product undergoes a spontaneous, irreversible follow-up reaction that drives the whole system towards complete substrate conversion. In the case of a), which was invented by Berglund *et al*.[49], re-aromatization of the ketone co-product after tautomerization constitutes a strong and effective driving force for the whole system.

A somewhat distinct approach by Green, Turner and O'Reilly[50] uses a benzylic 1,4-diamine that spontaneously forms a cyclic imine upon deamination, which irreversibly aromatizes to an isoindole (Scheme 1.14 b). The isoindole in turn can polymerize to intensively colored products, which were used as conversion indicators in high-throughput screenings for ω-transaminase activity.
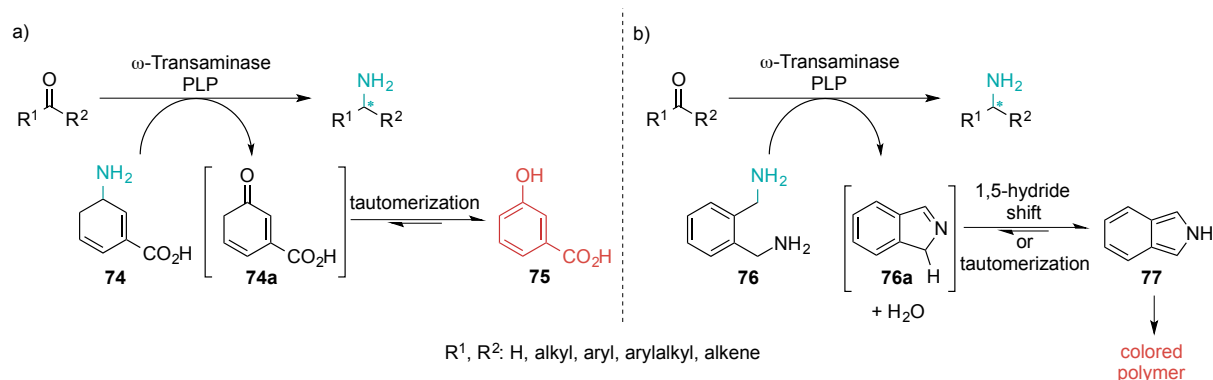
Scheme 1.14 | Equilibrium displacement in transaminase catalyzed reactions using "smart co-substrates".

While effective and creative, there are quite a few disadvantages associated with these methods. 2-Aminopropane is commonly used as co-substrate in industrial transaminations because it is cheap. However, high excesses are needed to drive the reactions to completion and the removal of acetone in these processes is not always easily achievable.[51]

On laboratory scale, enzyme cascades perform well, but they are prone to inhibition effects and/or side reactions of intermediates involved in the cascades. Moreover, the required recycling and degradation enzymes are expensive and strictly depend on (also expensive) co-factors that have to be supplied with the reaction medium.[52] This necessarily does not contribute to the simplicity of such systems.

When checking for the vendor prices of the above-presented smart co-substrates, one will quickly see that these compounds are not among the cheapest.[2] Thus it can be claimed here, that both chemically- and cost-efficient "smart co-substrates" for ω-transaminases have not been developed yet.

---

[2] On wednesday, Oct. 8th 2014, Sigma Aldrich offered the cheaper dihydrochloride of **76** for 19.4 € per g. The Co-substrate **74** was not even offered by any serious supplier at this time.

1.3.3 Other Ways of Making Chiral Amines with Enzyme Catalysis

Beside ω-transaminases, there are a few other enzymatic techniques for enantioselective introduction of primary and secondary amines[53] that will be mentioned only briefly here. In their 2014 review,[54]Kohls, Steffen-Munsberg and Höhne provide a good overview of that topic and show examples that illustrate nicely the enzymatic pendants to chemical aminations discussed before in Scheme 1.6 through Scheme 1.8.

a) reductive amination with ammonia as nitrogen-source

b) enzymatic hydroamination

c) enzymatic insertion of nitrogen into a C–H bond

d) asymmetric reduction of prochiral imines

e) enzymatic Pictet-Spengler reaction
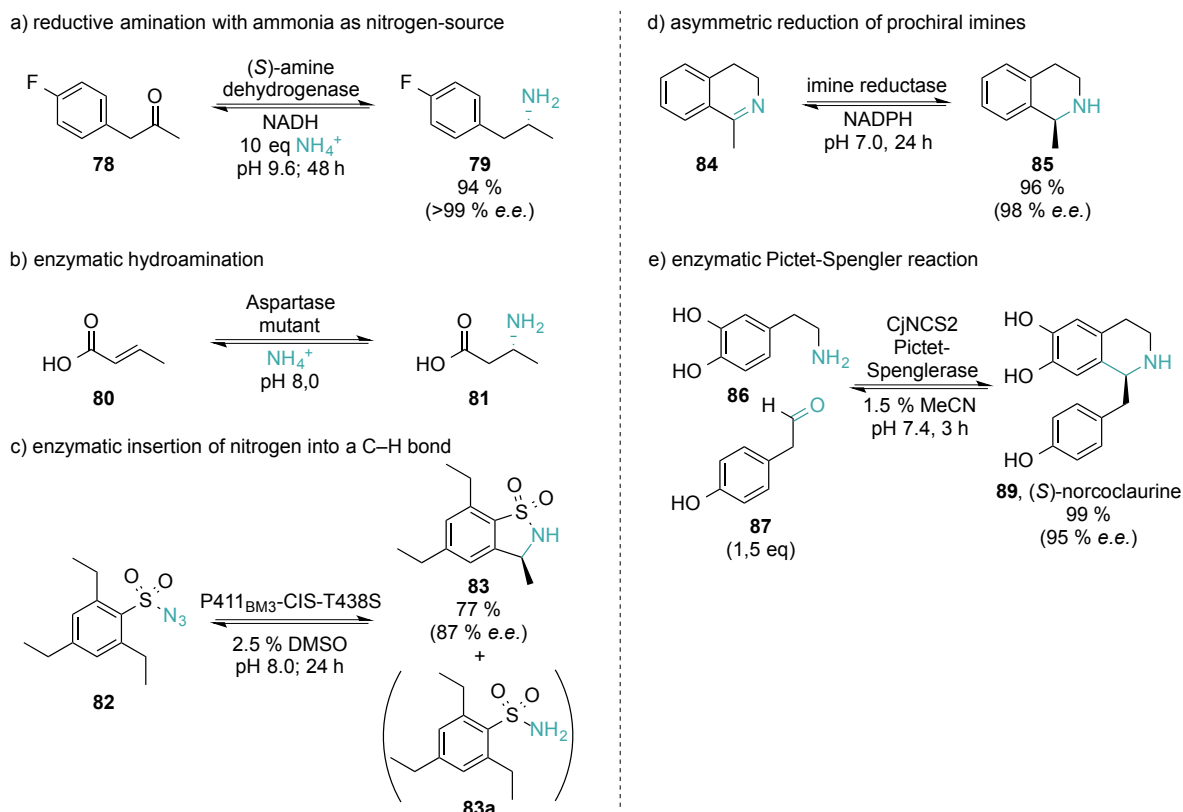
Scheme 1.15 | Enzymatic toolbox for primary (a-c) and secondary (d, e) chiral amine synthesis.[54-55]

1.4 Chemo-Enzymatic Applications in Alkaloid Synthesis

Transaminase-catalyzed, asymmetric aminations of carbonyl compounds have been firmly established in modern organic synthesis during the past years. Creative examples of their application demonstrated their perfect chemo-, regio- and stereoselectivity as well as a wide substrate scope and excellent yields under optimized conditions.[56] Recently, the power of chemo-enzymatic synthesis has been nicely demonstrated in the diastereo- and enantioselective preparation of isosolenopsin, an alkaloid from the ant *Solenopsis invicta*[57], and of dihydropinidine, both enantiomers of which are potent antifeedants of forest pests.[40, 58] The initial step in both of the synthetic sequences required formal reductive amination of solely the methyl ketone moiety (Scheme 1.16). This task was accomplished with quantitative conversions and a perfect regio-and enantioselectivity by ω-transaminases. The thus enzymatically introduced, first stereocenter then dictates the diastereoselectivity through steric shielding in the subsequent reduction step using either catalytic hydrogenation or LEWIS-acid assisted hydridic reduction. The LEWIS-acid is thought to cause a conformational change of the substrate, which in turn favors reduction of the anti-isomer.[59]
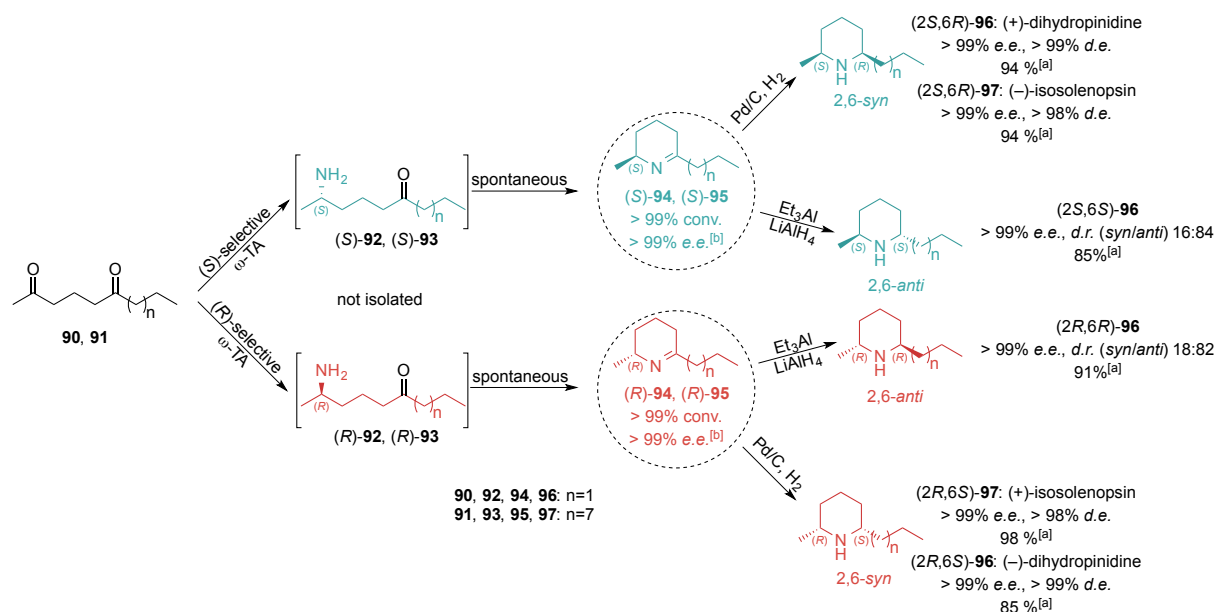
Scheme 1.16 | Chemo-enzymatic synthesis of both enantiomers of isosolenopsin[57] and dihydropinidine.[40] [a] yield over 2 steps as HCl salt. [b] conv. and *e.e.* for both cases.

Notably, some enzymes tolerate mild chemical reduction conditions and therefore can be employed in a one-pot fashion along with these reagents. O'Reilly and co-workers established a chemo-enzymatic, diastereo- and enantioselective route towards 2,5-disubstituted pyrrolidines involving a dynamic kinetic resolution with monoamine oxidases (MAOs).[31a] MAOs are enzymes capable of stereoselectively oxidizing α-chiral, benzylic amines to imines.

In the present case, their substrates were prepared from a 1,4-diketone that, like before, spontaneously cyclized to the respective chiral imine. The enantiomerically pure imines were then reduced non-selectively with ammonia-borane complex giving the two possible cis- and trans-diastereomers. The present MAO-D5, exhibiting selectivity for benzylic (*S*)-imines, oxidizes only one diastereomer back to the imine, which is in turn again reduced by borane. Repeating these cycles a couple of times leads to accumulation of one diastereomer with >99 % *d.e.* thereby constituting a deracemisation of the benzylic carbon center.
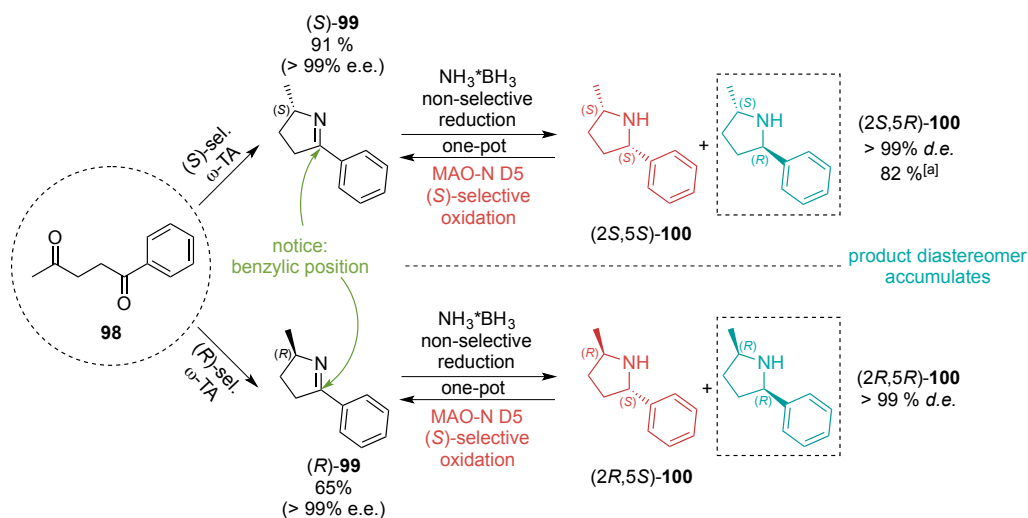
Scheme 1.17 | Chemo-enzymatic synthesis of enantio- and distereomerically pure 2,5-disubstituted pyrrolidines. [a] yield over 2 steps.

1.5 Aim of this Work

In the light of the recent advances in this field, it was of interest, whether the alkaloid xenovenine **4** can be prepared enantio- and diastereoselectively from triketone **29** by using an enantiodivergent chemo-enzymatic approach. We intended to introduce the first stereocenter with a ω-TA and use the surface process of a catalytic hydrogenation for setting up the relative stereochemistry in the remaining centers. Hence it was necessary to find optimal conditions for the transamination and explore different hydrogenation procedures.
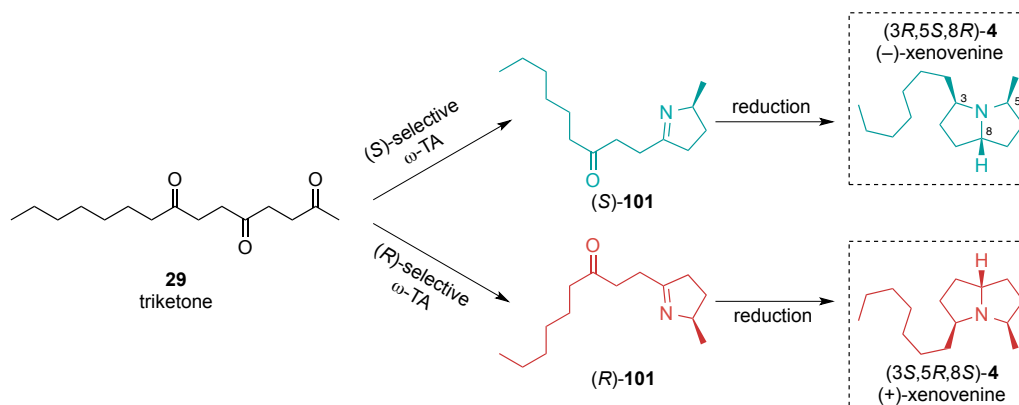
Scheme 1.18 | Chemo-enzymatic synthesis of (+)- and (–)-xenovenine from a triketone.

As mentioned in section 1.3.2, there is a requirement for a convenient, cheap and efficient method for the equilibrium displacement in transaminations in order to achieve complete conversion of the ketone substrate. The amination of 1,2-diketones revealed the reactivity of the resulting α-aminoketone towards dimerization and aromatization to the corresponding pyrazine. Thus, we intended to turn this process "upside-down" by employing 1,2-diamines and an array of other bifunctional molecules as "smart co-substrates" and using the follow-up reaction of the co-product as thermodynamic driving force for the biotransformation. Therefore, an extensive co-substrate screening with various ω-TAs, optimization of the reaction conditions, a proof of concept and the applicability to the enzymatic reductive amination of a set of ketone substrates is required.
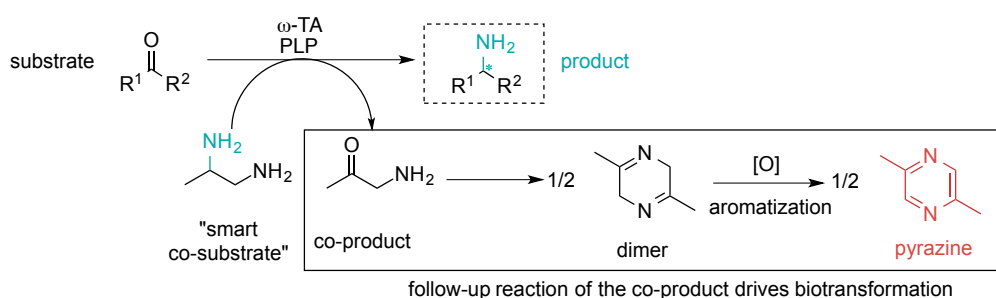
Scheme 1.19 | "Smart co-substrate" concept using 1,2-diamines for equilibrium displacement in transaminations.

2 Results and Discussion
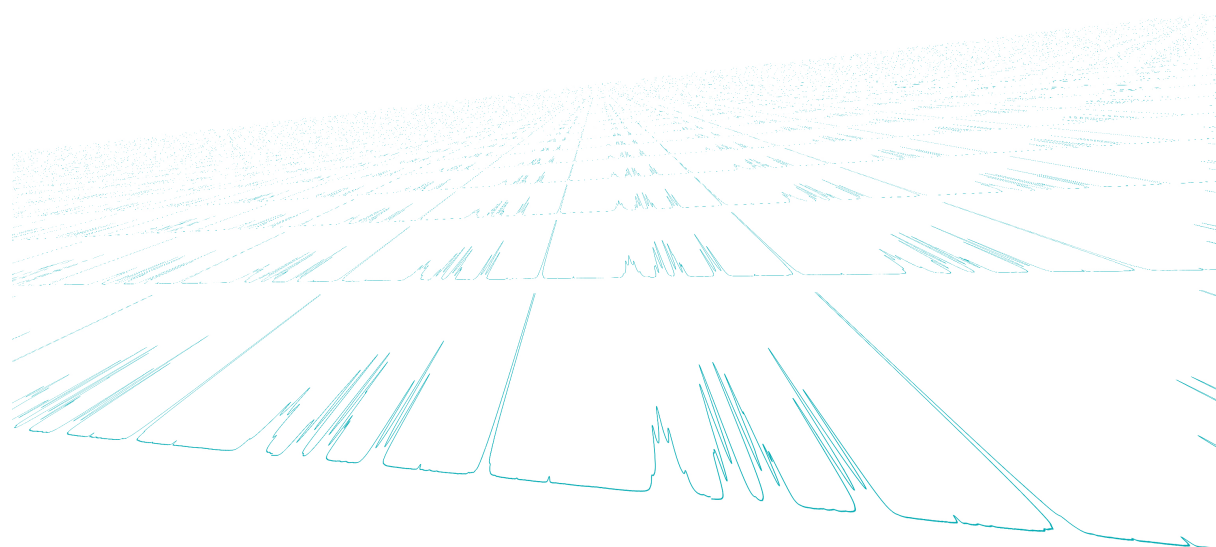
2.1 Chemo-Enzymatic Total Synthesis of Xenovenine

2.1.1 General Synthetic Approach

The chemo-enzymatic approach for the preparation of isosolenopsin[57] and dihydropinidine[40, 58] from diketones was expanded to xenovenine **1** from triketone **7**. Several
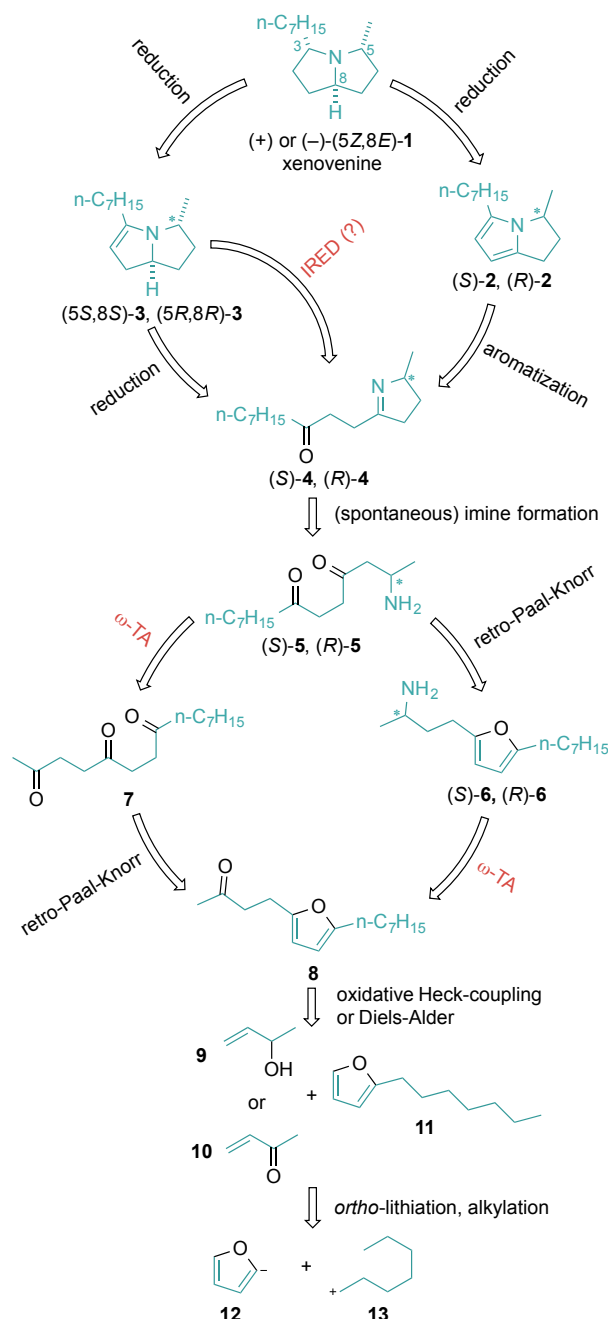
Scheme 2.1 | Retrosynthetic analysis of the target molecule xenovenine **1**.

options for achieving this task were considered here, as illustrated in Scheme 2.1. In a retrosynthetical approach, the pyrrolizidine core of the target molecule could be furnished by reduction of the respective unsaturated derivatives **2**, **3** or **4**. Imine **4** could be reduced directly[60] to give the intermediate enamine **3** after a second cyclization, which is subsequently hydrogenated to give xenovenine **1**. This last step was successfully applied in the majority of reported xenovenine syntheses (see previous section) and was thus considered a reasonable step. Alternatively, imine **4** may first be converted into the aromatic pyrrole derivative **2**, which was, however, expected to be somewhat more difficultly reduced under mild conditions[61] (*i.e.* at 1 - 2 atm. hydrogen). The origin of relative stereoselectivity in both these approaches was the pre-defined stereoconfiguration of the methyl group in position 5 of the chiral substrate. A third idea involved an enzymatic stereoselective reduction of imine **4** catalyzed by an IRED,[55, 62] which could have been implemented in a cascade together with a ω-transaminase to yield the enamine **3**. Due to lack of precedence it was uncertain

if the enzyme would accept the rather bulky substrate. Again, catalytic reduction of **3** was thought to selectively provide access to the target molecule **1** *via* substrate control. Investigation of the three mentioned pathways should especially address the achieved diastereoselectivity and overall yields.

The "hub-compound" imine **4** resulted from cyclization of keto-amine **5**, which was likely to proceed spontaneously if assuming similar (or even higher) reactivities as for 6-membered rings.[40] Since formation of 5-membered rings is favored according to BALDWIN's rules,[63] this step should proceed regioselectively to yield the 5-membered ring over the eight-membered one. Here, the chemo-enzymatic pathway forked once more. Imine **4** could be prepared from ketofuran **8** via retro-Paal-Knorr ring opening[64] followed by ω-TA catalyzed reductive aminaton of triketone **7** or *vice versa*.[19a] Ketofuran **8** was accessible via an oxidative HECK-coupling[65] of the furan ring of **11** and an allylic alcohol **9**, or simpler, by a DIELS-ALDER cycloaddition of **11** and methyl vinyl ketone **10** with subsequent rearrangement.[64b, 66] Alkylfuran **11** could be purchased from commercial sources or was easily prepared from furan **12** and a heptyl halogenide **13** by ortho-alkylation. Thus, starting from commercially available alkylfuran **11** both enantiomers of xenovenine could be accessed within 4 steps. This sequence would thus constitute the shortest enantioselective synthesis of this target up to now.

2.1.2 *Synthesis of Precursors, Substrates and Reference Substances*

For the initial studies, alkylfuran **11** was prepared freshly and in good yield from furan *via ortho*-lithiation by *n*-butyllithium and heptyl bromide. Later on, however, this substance was ordered from a commercial supplier and no differences in reactivity were observed between these two batches.
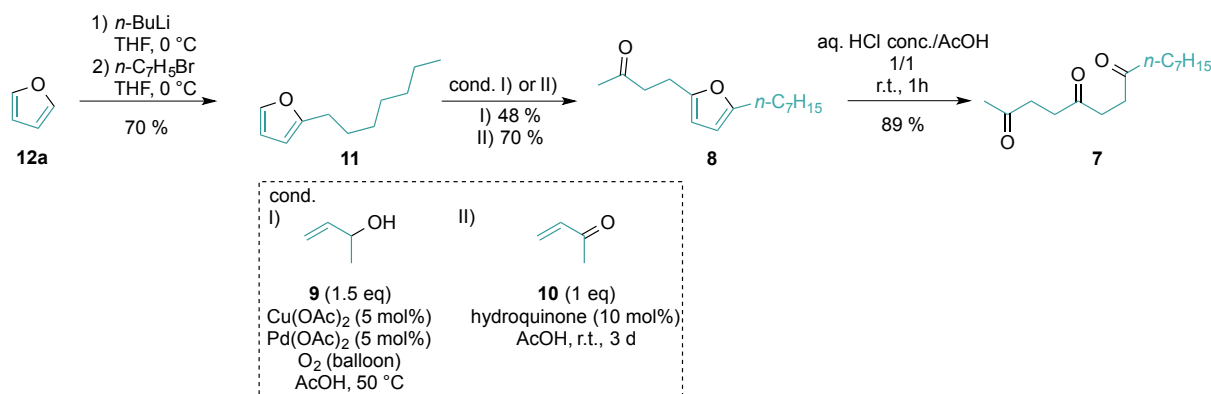
Scheme 2.2 │ Synthesis of substrates **7** and **8** with given reaction conditions and yields.

For the second transformation, two procedures were explored. The first essentially constitutes an oxidative, palladium-catalyzed HECK-coupling of the heteroaromatic furan **11** with an allylic alcohol **9**, which was already successfully employed in a similar alkylation of 2-methylfuran.[65] The palladium(II)-species is initially thought to undergo oxidative insertion into the α-C−H bond of furan (Scheme 2.3, 1) and a subsequent 1,2-insertion of the allylic alcohol double bond into the palladium−furan bond (2). The next step is a β-H elimination that results in the enol (3) with Pd(II) coordinated to the double bond.

Deuterium labeling experiments of the hydrogen atom in green (conducted by Huang *et al.*)[65] suggest a migratory re-insertion of Pd(II), which ends up attached to the adjacent α-hydroxy carbon (4). Another β-H elimination, now along the hydroxyl group, (5) ultimately leads to the ketone product, **8** in this case. Reductive elimination of acetic acid (5) expels palladium(0), which is re-oxidized to the catalytically active palladium(II) species by oxygen and copper(II) assistance to close the catalytic cycle (6).[65]
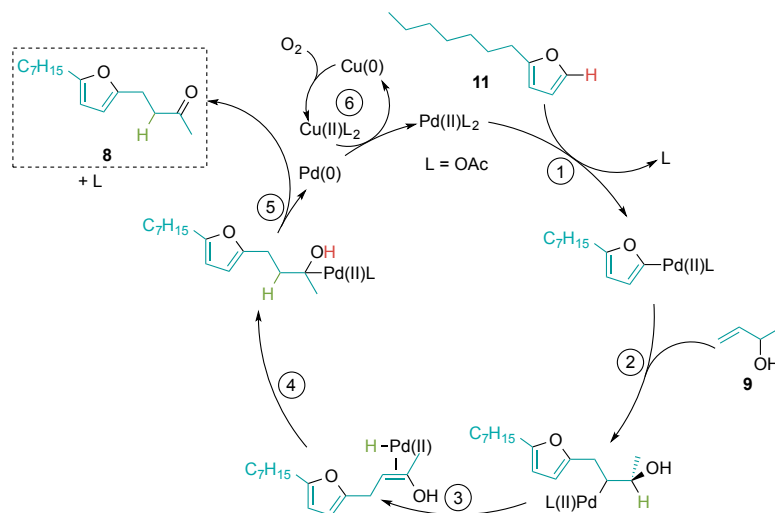
Scheme 2.3 | Proposed catalytic cycle for the oxidative HECK-coupling of aromatic heterocycles with allylic alcohols[65] applied to present substrates **11** and **9**.

However, for unknown reason, this reaction turned out not to be very reliable for the present substrate **11**, and due to side product formation only moderate yields were observed. 3 Å molecular sieve was added, since it avoids deactivation of Pd(0) through cluster formation.[67] A summary of all conducted experiments with the applied conditions is given in Table 2.1 below.

Table 2.1 | Oxidative HECK-coupling of alkylfuran **11** and but-1-en-3-ol **9** under various reaction conditions.

Entry	Scale	Catalyst / Additives	Temp. (°C)	Time (h)	% conv.[a]	**8** % GC-yield[b]
1[c]	50 mg	5 mol% Pd(OAc)$_2$	50	12	55	33
			50	48	68	47
2	50 mg	5 mol% Pd(OAc)$_2$, 5 mol% Cu(OAc)$_2$	25	12	69	35
			50	24	81	45
			50	72	100	65 (41)
3	1 g	5 mol% Pd(OAc)$_2$, 5 mol% Cu(OAc)$_2$	55	4	65	55
			55	20	94	79 (48)
4[e]	2 g	0.6 mol% Pd(OAc)$_2$, 2 mol% Cu(OAc)$_2$[d]	50	24	17	4
			50	48	94	40
			50	72	98	42 (15)
5[e]	25 mg	5 mol% Pd(OAc)$_2$, 5 mol% Cu(OAc)$_2$, 150 mg/mmol 3Å molsieve	25 (3.5 h) then 50 (14.5 h)	18	62	38
			50	23	70	32
6	25 mg	5 mol% Pd(OAc)$_2$, 5 mol% Cu(OAc)$_2$, 150 mg/mmol 3Å molsieve	60	4	44	25
			50	20	55.5	35.5
7	25 mg	5 mol% Pd(OAc)$_2$, 5 mol% Cu(OAc)$_2$	60	4	72	21
			50	20	84	36
8[f]	25 mg	5 mol% Pd(OAc)$_2$, 5 mol% Cu(OAc)$_2$	55	20	97	31

General conditions unless otherwise noted: 250 mM **11**, 1.5 eq **9**, 1 atm oxygen, AcOH.

[a] Conversion determined from GC-MS area ratios of educt **11** and formed products. Peak identification through reference substance retention time (educt **11**) and mass spectrum.
[b] GC-yield from GC-MS peak areas, percentage of **8** in reaction mixture. Isolated yields in % are given in parentheses where measured.
[c] Additional 0.5 eq of 1.2 eq allylic alcohol **9** added after 12 h.
[d] Additional 4.4 and 3 eq Pd(OAc)$_2$ and Cu(OAc)$_2$ added after 24 h, respectively.
[e] Bubbling oxygen through reaction mixture.
[f] 1000 rpm stirring speed to support oxygen uptake.

The major side product that was obtained from the reactions had the molecular mass corresponding to substance **8** minus two hydrogen atoms, but this was not further investigated.

Copper(II)acetate as co-catalyst enhanced conversion of **11** to **8**, whereas addition of molecular sieve did only lead to increased byproduct formation. The same effect was noted either when bubbling oxygen through the reaction mixture or at elevated temperatures. Due to these complications, an alternative method for providing **8** was sought for.

This second procedure was already described back in 1943 by Kurt Alder[64b] and recently by other authors[66] and scored with its simplicity. Alkylfuran **11** and methyl vinyl ketone **10** together with hydroquinone were mixed and stirred in acetic acid for three days after which the desired product **8** was obtained in good yields beside a brown oily polymer. The mechanism was not elucidated yet, but a plausible order of events, as depicted in Scheme 2.4,

might involve a DIELS-ALDER cycloaddition of the vinylic alkene (LUMO) to the inherent diene in alkylfuran **11** (HOMO). Only one regioisomer of the cycloadduct (**11a**) undergoes further reaction to **11b** whereas **11c** is a dead end intermediate. Abstraction of the bridgehead proton in **11a** (red in Scheme 2.4) displaces the electrons to the keto-group in the ene-moiety and thereby restores aromaticity of the furan ring and re-opens the bicycle. Tautomerization of the enol subsequently leads to ketone **8**.
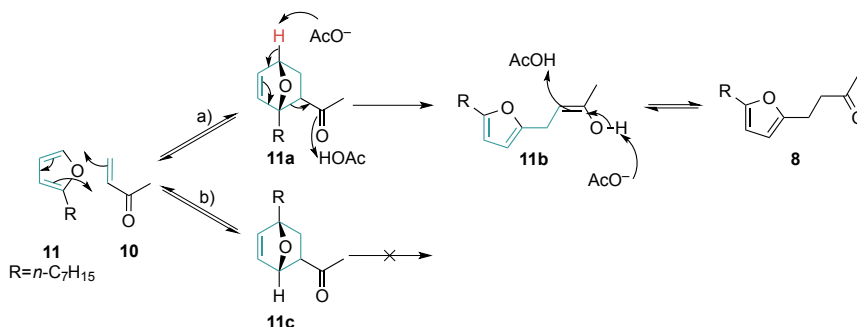
Scheme 2.4 | Plausible mechanism for the formation of **8** from **11** and **10** involving a DIELS-ALDER cycloaddition and subsequent deprotonation-induced opening of the bicycle.

This reaction was performed on an analytical and on a preparative scale with the results displayed in Table 2.2.

Table 2.2 | Synthesis of ketone **8** via DIELS-ALDER cycloaddition.

Entry	Scale	Temp. (°C)	Time	**8** g (% yield)[a]
1	20 mg	r.t.	4 d	n.i.[b]
2	2 g	r.t.	2 d	2.0 (70 %)

General conditions: 1.2 M 2-*n*-heptlyfuran **11**, 1 eq methylvinylketone **10**, 0.2 eq hydroquinone in AcOH (100 %), stirred at r.t. until full conversion of **11**.
[a] Yield after purification *via* column chromatography.
[b] n.i.: "not isolated", > 99 % conv. according to GC-MS.
See also Table 2.3 for a consecutive one-pot furan hydrolysis attempt.

Reductive amination of the keto-group in **8** yielded *rac*-**6**, which was used as reference substance for chiral and achiral GC analysis.
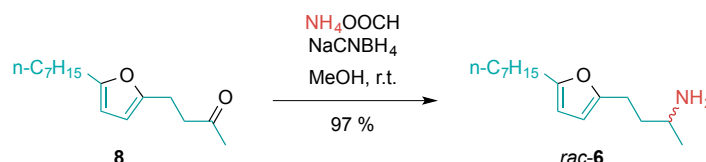
Scheme 2.5 | Non-stereoselective reductive amination of **11**.

With **8** and *rac*-**6** in hands, hydrolysis of the furan ring[68] was investigated. The lone pairs of the oxygen atom in the furan ring confer this heterocycle a high electron density hence making it more susceptible for electrophilic attack. In case of acidic hydrolysis, the electrophile is a proton that attacks in the β-position of oxygen (Scheme 2.6).

Water then acts as nucleophile and attacks the activated, positively charged oxonium-ion. The formal hemiacetal thus formed further degrades under acid catalysis to end up as 1,4-diketone. In fact, this mechanism corresponds to a reverse PAAL-KNORR synthesis of furans from diketones.[69]
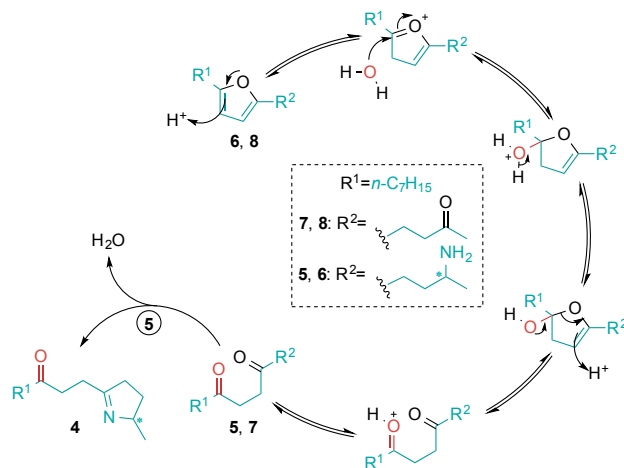
Scheme 2.6 | Acidic hydrolysis of furan derivatives according to a retro-PAAL-KNORR mechanism to give a 1,4-diketone.[70]

The reaction of **8** to **7** proceeded fast at room temperature with HCl (6 M) in AcOH. On a preparative scale, a maximum yield of 89 % of solid triketone **7** was obtained, which was further purified by recrystallization. Given the fact that there are three highly reactive keto-groups incorporated in **7** and no protecting groups were used, the obtained overall yields appeared satisfying.

Table 2.3 | Acidic hydrolysis of furan **8** under varying reaction conditions.

Entry	Scale (mg)	Temp. (°C)	Time (h)	7 [mg (% yield)]
1[a]	20	50	1	7 (31)
2	500	25	0.5	480 (89)
3	1 g	25	1.2	428 (39)[d]
4	850	25	1.5	420 (46)
5[b]	1 g	100[c]	0.5[c]	270 (18)[e]

General conditions unless otherwise stated: 200 mM **8**, 12 M HCl : AcOH=1:1.
[a] 85 mM substrate **8** concentration.
[b] One-pot attempt of transforming heptylfuran **11** into **7** via consecutive DIELS-ALDER-reaction and *in-situ* acidic hydrolysis of **8**. Conditions: 1.2 M **11** in AcOH, 1 eq methylvinylketone **10**, 0.05 eq hydroquinone, 130 °C, 4.25 h then 1.1 eq HClO$_4$.
[c] After HClO$_4$ addition.
[d] Yield from crude **8** after recrystallization from Et$_2$O.
[e] Yield over two steps from heptylfuran **11**.

Hydrolysis of racemic amine **6** actually yielded cyclic imine **4**, which was spontaneously generated from **5** during basic workup (left-hand bottom corner in Scheme 2.6). Notably, the reaction did not stop at this stage but proceeded further to the aromatic pyrrole **2**.

The result was a mixture of these two compounds **2** and **4**, whose composition was essentially governed by the workup conditions. By pouring the acidic reaction mixture into an ice-cooled, aqueous NaOH solution equimolar to the acid, highest ratios of imine **4** were obtained.

Again, the synthetic pathway forked into two sub-pathways in which the order of events, namely furan hydrolysis and biocatalytic reductive amination, were permutated. The establishment of the latter-mentioned biotransformation is the subject of the subsequent section.

2.1.3 *Biocatalytic Optimization Studies*

First, the biocatalytic reductive amination of ketofuran **8** was tested employing four (*S*)-selective and three (*R*)-selective ω-transaminases (see Table 2.10 in the smart co-substrate section) with alanine as co-substrate and various solvent systems. For recycling of the co-substrate pyruvate and thus equilibrium displacement, an alanine dehydrogenase (AlaDH)/ formate dehydrogenase (FDH) cascade was used.
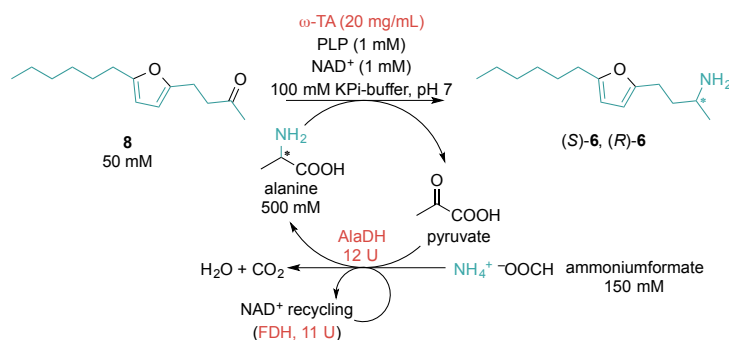
Scheme 2.7 | Biocatalytic transamination of **8** using an AlaDH/FDH pyruvate recycling system.

Table 2.4 | Biocatalytic transamination of **8** using an AlaDH/FDH system for pyruvate recycling.[a]

(S)-sel. ω-TAs	ArS		BM		CV		PF	
co-solvent	conv. (%)	e.e. (%)	conv. (%)	e.e. (%)	conv. (%)	e.e. (%)	conv. (%)	e.e. (%)
neat	6.1	5	17.8	32	9.2	94	12.7	84
5 v% DMF	10.4	12	11.0	52	6.1	91	7.0	87
5 v% DMSO	9.0	8	17.0	31	5.1	95	8.9	85
1 v% heptane	7.6	6	13.0	39	4.6	95	6.9	88
5 v% n-butanol	8.1	57	0.0	n.d.[b]	0.0	n.d.[b]	3.4	79

(R)-sel. ω-TAs	ArR		AT		HN	
co-solvent	conv. (%)	e.e. (%)	conv. (%)	e.e. (%)	conv. (%)	e.e. (%)
neat	24.0	>99	22.2	>99	16.4	>99
5 v% DMF	25.0	>99	12.5	>99	22.9	>99
5 v% DMSO	21.5	99	18.8	>99	25.7	>99
1 v% heptane	24.3	>99	10.5	>99	n.d.[c]	n.d.[c]
5 v% n-butanol	22.3	>99	< 1	n.d.[b]	< 1	n.d.[b]

[a] Conditions: substrate **8** (50 mM), lyophilized *E. coli* cells containing ω-TA (20 mg/mL), L- or D-alanine, resp. (500 mM), ammonium formate (150 mM), PLP (1 mM), NAD$^+$ (1 mM), AlaDH (solution, 12 U), FDH (lyophilisate, 11 U) in 1 mL 100 mM KPi-buffer pH 7.0; Co-solvent amount according to table; incubation for 24 h at 30 °C and 700 rpm.
Conversions were measured with GC-FID on a DB-1701 column.
The *E.e.* was measured after *N*-acetylation (2 eq Ac$_2$O and cat. DMAP for 2 h at 30 °C, 700 rpm) with GC-FID on a chiral DEX-CB column.
[b] No *e.e.* was determined because no detectable conversion took place.
[c] n.d.: "not determined".

The measured conversions revealed a better performance of (R)-selective ω-TAs over their (S)-selective counterparts with a maximum GC-yield of ca. 26 %. Some solvent effects could also be deduced from these results; for example *n*-butanol had inferior effects on conversion whereas the others showed only little and enzyme dependent effects compared to neat substrate. All (R)-selective enzymes exhibited moderate conversions and a perfect stereoselectivity displayed by *e.e.*'s beyond 99 %. In contrast, and although the substrate fulfilled the requirement for good stereoinduction by having a bulky and small residue on the two sides of the prochiral ketone, the *e.e.*'s and conversions obtained from biotransformations employing (S)-selective transaminases were not promising. Only the ω-TA from *Chromobacterium violaceum* (CV) achieved good *e.e.*'s but only at very low conversions.

Low *e.e.*'s were likely to result from inefficient equilibrium displacement that supported accumulation of stereochemical errors made by the enzyme when transforming product into substrate back and forth. In order to check for these effects, two (S)-selective transaminases

and three different enzyme cascades for equilibrium displacement (compare with Scheme 1.13) were employed and the *e.e.* measured after defined reaction times.
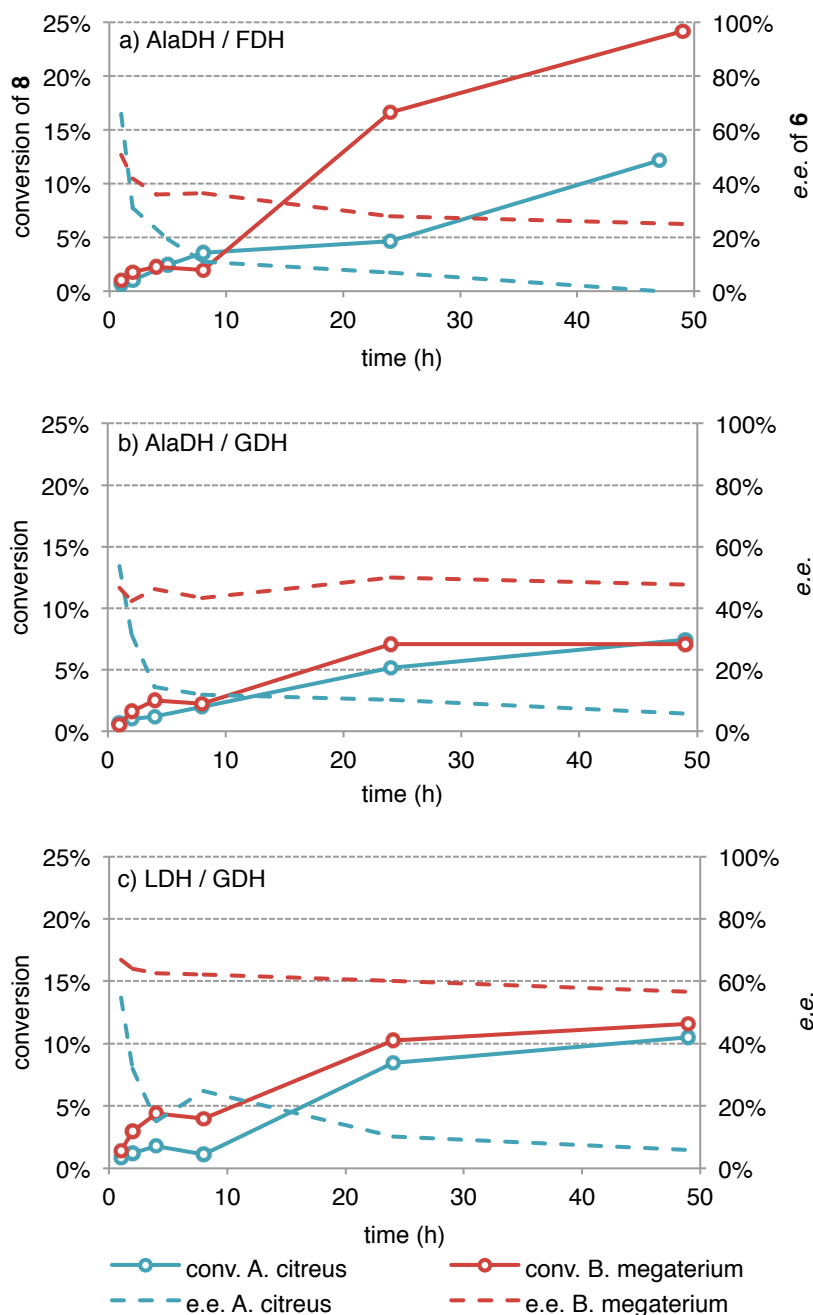
Figure 2.1 | Time-course of the biotransformation of **8** employing three different recycling or degradation cascades for equilibrium displacement.

Conditions: substrate **8** (50 mM), lyophilized *E. coli* cells containing ω-TA (20 mg/mL), L- or D-alanine, resp. (500 mM), PLP (1 mM), NAD⁺ (1 mM).
[a] ammonium formate (150 mM), AlaDH (solution) (12 U), FDH (lyophilisate) (11 U)
[b] ammonium formate (150 mM), glucose (100 mM), AlaDH (solution) (12 U), GDH (lyophilisate) (15 U)
[c] glucose (100 mM), LDH (lyophilisate) (90 U), GDH (lyophilisate) (15 U) in 1 mL 100 mM KPi-buffer pH 7.0; incubation at 30 °C and 700 rpm for 1, 2, 4, 8, 24 and 49 h (1 vial / time).

Time management required the 8 h samples to be run separately. Hence, due to imperfect reproducibility, a blip showed up at this point. For (a) and (b) the usage of a different AlaDH

stock with altered activity, which is probably a result of multiple thawing and freezing, resulted in values that did not exactly follow the overall trend. However, the latter can clearly be deduced from the obtained data sets.

The study revealed a drop in *e.e.* with ongoing reaction progress. The *B. megaterium* ω-transaminase showed a better performance in terms of conversion and *e.e.* compared to *A. citreus*. The data also suggested that no increase in conversion for system (b) and (c), which both contained GDH, can be detected after 24 h. It should be noted here, that if one of the recycling or degradation enzymes becomes inactive, the whole system stops. In other words: the cascade is only as resistant as its weakest component. Thus, it was concluded that, in terms of conversion, system (a) would be the best choice to concentrate on for further investigation. However, the poor *e.e*'s for substrate **8** implied to use triketone **7** as substrate for the formal reductive amination.
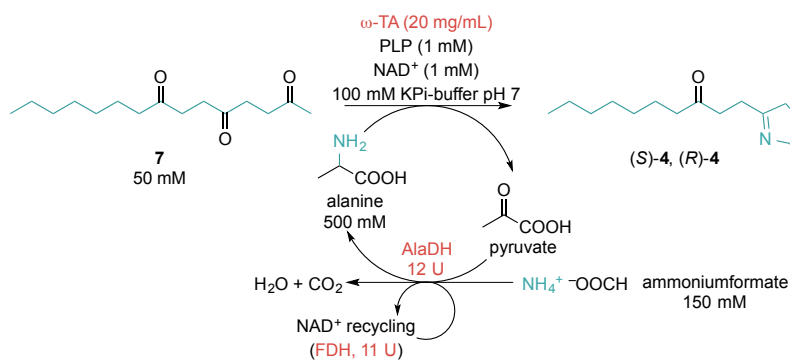
Scheme 2.8 | Biocatalytic transamination of **7** using an AlaDH/FDH pyruvate recycling system.

The biotransformation of triketone **7** featured a valuable advantage: a substrate-inherent driving force supporting the enzyme cascade in equilibrium displacement. Namely, the fast, spontaneous cyclization of the generated amine to the 5-membered imine removed the intermediate free amine from the equilibrium of the reductive amination. Since the cyclic imine did not serve as substrate for the enzyme anymore, the equilibrium could be drawn over to the product side.

Table 2.5 | Biocatalytic transamination of **7** using an AlaDH/FDH system for pyruvate recycling.[a]

(S)-sel. ω-TAs	ArS		BM		CV		PF	
co-solvent(s)	conv. (%)	e.e.[b] (%)	conv. (%)	e.e.[b] (%)	conv. (%)	e.e.[b] (%)	conv. (%)	e.e.[b] (%)
neat	4	>99	1	n.d.	8	68	8	54
5 v% DMF	6	>99	< 1	n.d.	3	70	6	55
5 v% DMSO	7	>99	< 1	n.d.	9	29	14	59
5 v% heptane	23	>99	3	>99	19	67	21	53
5 v% TBME	11	>99	< 1	n.d.	2	66	1	55
5 v% DMF + 20 v% heptane	63	>99	1	>99	7	68	9	52
5 v% DMSO + 20 v% heptane	42	>99	2	>99	13	67	16	55

(R)-sel. ω-TAs	ArR		AT		HN	
co-solvent(s)	conv. (%)	e.e.[b] (%)	conv. (%)	e.e.[b] (%)	conv. (%)	e.e.[b] (%)
neat	30	>99	3	>99	7	>99
5 v% DMF	36	>99	7	>99	19	>99
5 v% DMSO	49	>99	4	>99	12	>99
5 v% heptane	27	>99	6	>99	11	>99
5 v% TBME	8	>99	1	>99	8	>99
5 v% DMF + 20 v% heptane	61	>99	7	>99	26	>99
5 v% DMSO + 20 v% heptane	79	>99	6	>99	18	>99

[a] Conditions: lyophilized *E. coli* cells containing ω-TA (20 mg/mL), L- or D-alanine, resp. (500 mM), ammonium formate (150 mM), PLP (1 mM), NAD$^+$ (1 mM), AlaDH (solution, 12 U), FDH (lyophilisate, 11 U) in 1 mL 100 mM KPi-buffer pH 7.0; Co-solvent amount according to the table; substrate **7** (50 mM) added gravimetrically as solid, incubation for 24 h at 30 °C and 700 rpm.
Conversion was measured by GC-FID on a DB-1701 column.
[b] The *e.e.* was determined by GC-FID on a chiral phase (DEX-CB column) after aromatization to the corresponding chiral pyrrole derivative **2** in MeOH and 0.1 vol% AcOH for 30 min at 30 °C and 700 rpm.

The obtained results supported the assumption just made. This biotransformation worked better both in terms of conversion and *e.e.* and good initial results were obtained for both product enantiomers. Furthermore, it turned out that a combination of heptane and DMSO or DMF[57] as co-solvents reasonably enhanced conversion.

To further optimize conditions, the best performing ω-TAs, *i.e.* the (*R*)- and (*S*)-selective enzymes from *Arthrobacter*, were chosen and subjected to varying co-solvent composition ratios.
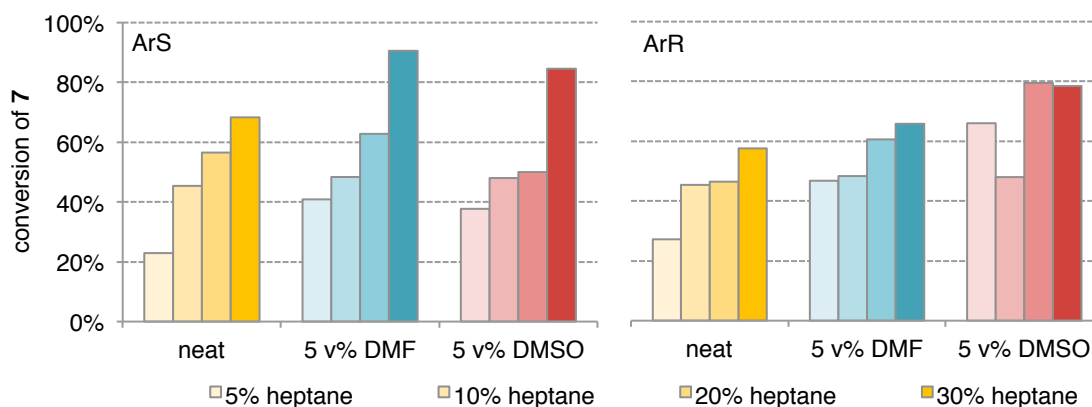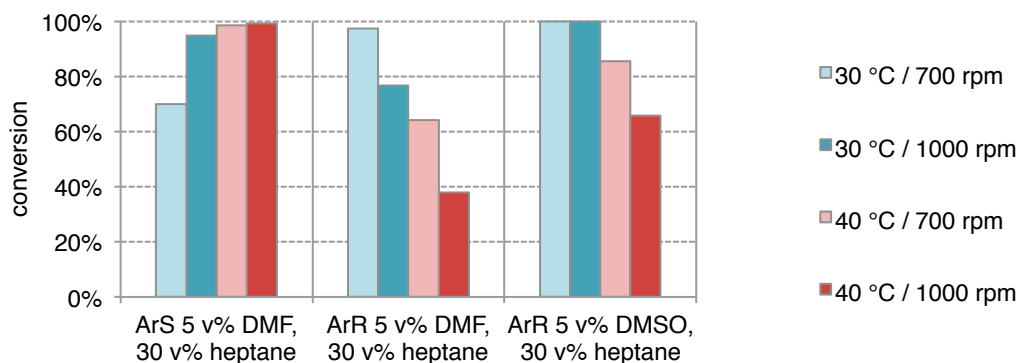

Figure 2.2 | Co-solvent optimization study for the biotransformation of **7** using an AlaDH/FDH system for co-product recycling.

Conditions: lyophilized cells containing ω-TA (20 mg/mL), L- or D-alanine, resp. (500 mM), ammonium formate (150 mM), PLP (1 mm), NAD$^+$ (1 mM), AlaDH (solution) (12 U), FDH (lyophilisate) (11 U) in 1 mL 100 mM KPi-buffer pH 7.0; rehydrated for 30 min at 30 °C and 700 rpm. triketone **7** (50 mM) added gravimetrically as solid, co-solvents added volumetrically, incubation for 24 h at 30 °C and 700 rpm.
Conversions measured with GC-FID on a DB-1701 column.
E.e.'s of pyrrole derivative **2** after derivatization with 1 vol% AcOH in 1 mL MeOH for 30 min at 30 °C and 700 rpm were determined with GC-FID on a chiral phase (DEX-CB column). *E.e.* ≥ 99 % in all cases.

The general trend revealed a positive effect of higher heptane loadings on conversion (bars from left to right within one colored group in Figure 2.2). Best results for both enzymes were achieved with 20 or 30 vol% heptane and 5 vol% DMF or DMSO as co-solvents, respectively. With the proper co-solvent composition found, the pH-dependency was tested at pH values 7.0, 8.0 and 9.0 in order to find the optimum.
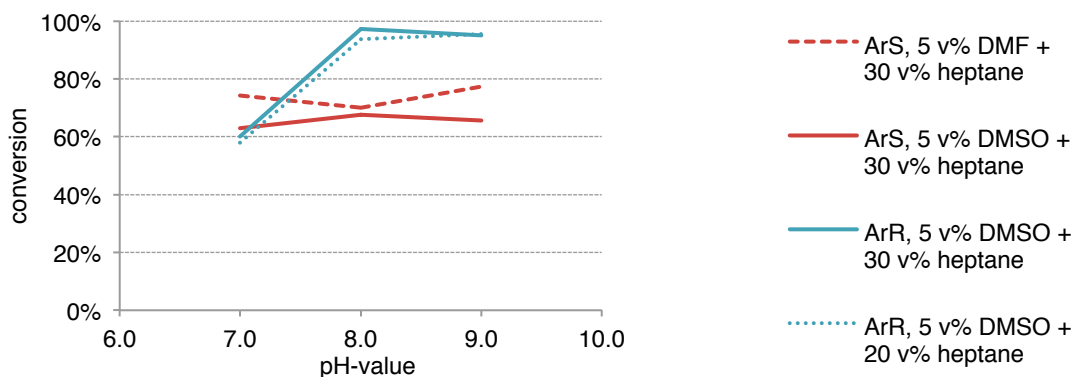
| pH optimization study for the biotransformation of **7** using an AlaDH/FDH system for co-product recycling.

Conditions: lyophilized cells containing ω-TA (20 mg/mL), L- or D-alanine, resp. (500 mM), ammoniumformate (150 mM), PLP (1 mM), NAD$^+$ (1 mM), AlaDH (solution) (12 U), FDH (lyophilisate) (11 U) in 1 mL 100 mM KPi-buffer pH 7.0, 8.0 and 9.0, respectively; rehydrated for 30 min at 30 °C and 700 rpm. 50 mM triketone **7** added gravimetrically as solid, co-solvents added volumetrically, incubation for 24 h at 30 °C and 700 rpm.
Conversions measured with GC-FID on a DB-1701 column.
E.e.'s of pyrrole derivative after derivatization with 1 vol% AcOH in 1 mL MeOH for 30 min at 30 °C and 700 rpm were determined with GC-FID on a chiral phase DEX-CB column. *E.e.* ≥ 99 % in all cases.

Figure 2.3 clearly shows a pH-optimum of 8.0 for the (*R*)-selective transaminase; an almost quantitative conversion of triketone **7** was achieved. For the (*S*)-selective enzyme, the pH optimum was around pH 8.0 too, although there was a plateau. For further optimization, a potassium phosphate buffer with pH 8.0 was chosen. Subsequently, the optimization of temperature and mixing speed was addressed.

| Temperature and mixing-speed optimization study for the biotransformation of **7** using an AlaDH/FDH system for co-product recycling.

Conditions: lyophilized cells containing ω-TA (20 mg/mL), L- or D-alanine, resp. (500 mM), ammoniumformate (150 mM), PLP (1 mM), NAD$^+$ (1 mM), AlaDH (solution) (12 U), FDH (lyophilisate) (11 U) in 1 mL 100 mM KPi-buffer pH 7.0, 8.0 and 9.0, respectively; rehydrated for 30 min at 30 °C and 700 rpm. 50 mM triketone **7** added volumetrically as stock in DMF or DMSO, co-solvents added volumetrically, incubation for 24 h at the denoted temperatures and mixing speeds.
Conversions measured with GC-FID on a DB-1701 column.
E.e. of pyrrole **4** (derivatization of **4** with 1 vol% AcOH in 1 mL MeOH for 30 min at 30 °C and 700 rpm) determined with GC-FID on a chiral phase (DEX-CB) column. *E.e.* ≥ 99 % in all cases.

The (*S*)-selective ω-TA from *A. citreus* quantitatively converted triketone **7** at 40 °C and 1000 rpm, whereas the (*R*)-selective transaminase preferred 30 °C to achieve full conversion. Elevated temperatures seemed reasonable, because the substrate did only dissolve completely in DMSO or DMF at >40 °C. At cooler conditions, the triketone precipitated from the aqueous medium and became unavailable for the enzyme.

Alternatively it was of interest, if the aforementioned solely transaminase-induced cyclization as driving force would be sufficient for displacing the equilibrium. Therefore, an experiment using only aqueous 2-aminopropane buffer was examined (Scheme 2.9).
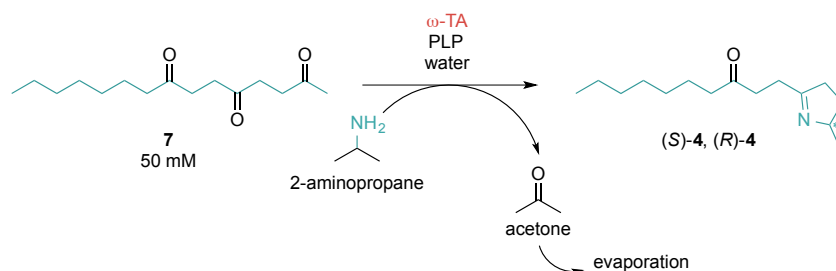
Scheme 2.9 | Biocatalytic transamination of **7** using 2-aminopropane as co-substrate in water.

Indeed, the biotransformation worked and quantitative turnover of **7** to **4** by employing a five-fold excess of co-substrate could be detected.

Table 2.6 | Biocatalytic transamination of **7** using 2-aminopropane as co-substrate and buffer-substance.

ω-TA	ArS		ArR	
2-aminopropane (mM) [eq.]	conv.[a] (%)	e.e.[b] (%)	conv.[a] (%)	e.e.[b] (%)
50 (1)	45	n.d.	23	n.d.
250 (5)	> 95	n.d.	> 95	n.d.

Conditions: lyophilized cells containing ω-TA (20 mg/mL), PLP (1 mM), in 1 mL 50 or 250 mM 2-aminopropane-buffer pH 10.0 (adjusted with 12 M HCl) in water, respectively; rehydrated for 30 min at 30 °C and 700 rpm. 50 mM triketone **7** added as DMSO-solution, 5 v% DMSO, 30 v% heptane. Incubation for 24 h at 30 °C and 700 rpm.
[a] Conversions measured with GC-MS on an HP-5 column.

With these parameters in hand, both enantiomerically pure imines (*S*)- and (*R*)-**4** could be made in a preparative 200 mg scale by using the AlaDH/FDH recycling system. The product was obtained with quantitative conversion according to GC-measurements as crude EtOAc-extract.

2.1.4 Investigations of Reduction Procedures

The last step in the synthesis of xenovenine required diastereoselective reduction of either the chiral imine **4** or the aromatic pyrrole derivative **2** with both options having their advantages and drawbacks that had to be considered. Imine **4** was readily reduced by hydrogen with Pd/C catalysis, but acid was necessary to achieve satisfying amounts of product **1**. Reduction using the mild reagent sodium cyanoborohydride achieved good conversion too, but with only poor diastereoselectivity.

Table 2.7 | Reduction of cyclic imine **4** employing various conditions and additives.
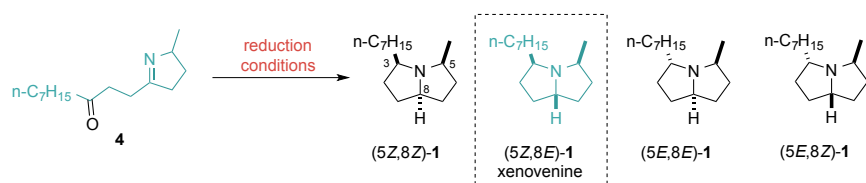
Scale (mg)	Conditions[a]	Additive	Conv.[b] (%)	1[c] (%)	1 d.r. (%)[d]			
					5Z,8Z	5Z,8E	5E,8E	5E,8Z
7	a, 20 h	–	77	43	3.8	95	< 1	1.2
7	b, 2 h	–	94	37	8.3	68	20	3.7
10	a, 14 h	0.5 vol% TFA	> 99	> 99	20	64	8	8
65[e]	a, 48 h	0.5 vol% TFA	(−): 93	89[f]	12	72	6	10
			(+): 96	79	14	71	5.5	9.5
6[e]	a, 26 h	0.1 eq (−)-CSA	(−): > 99	> 99	39	61	0	0
			(+): > 99	> 99	47	53	0	0

[a] Conditions a) 50 mM substrate, 10 w% Pd/C, 1 atm H_2, EtOAc, r.t.; b) 50 mM substrate, NaCNBH$_4$, MeOH, r.t., reaction time as indicated.
[b] Conversion determined *via* GC-MS peak areas.
[c] Determined *via* GC-MS areas. Percentage of xenovenine and its diastereomers in the product mixture, the major detected co-product was pyrrole **2** as result of aromatization beside partially reduced derivatives.
[d] Diastereomeric ratio of **1** determined from GC-MS peak areas.
[e] Run with both enantiomers separately, (+)-isomer results from (R)-**4**, (−)-isomer from (S)-**4**.
[f] Isolated yield of (−)-(5Z,8E)-**1** after separation of diastereomers with column-chromatography: 10 %

Stereoselective reduction of **4** by using imine reductases (IREDs) was attempted too, however without success. Imine reductases are NADP(H) dependent enzymes capable of stereoselectively reducing, preferably cyclic, imines. Kindly, Joerg Schrittwieser supplied some of these enzymes as either purified proteins or whole cell preparation, which were tested for their ability to accept and convert substrate **4**. The stereoselectivity as a result of substrate control was minimized, instead it should be determined by the enzyme's active site shape. Thus, *Z*- or *E*-**3** could be prepared selectively.

Table 2.8 | Attempted biocatalytic reduction of racemic, cyclic imine **4** to enamine **3** employing IREDs.
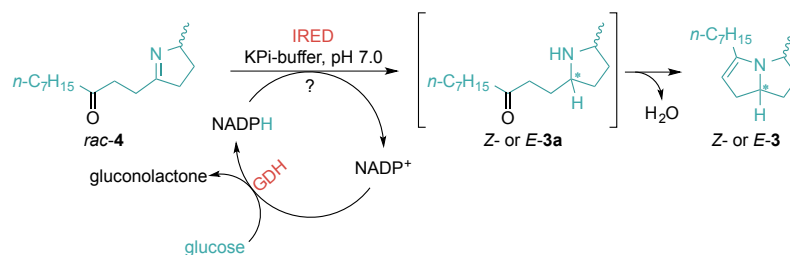
IRED (uniprot no.)		M4ZS15[b] (S)-selective	i8QLV7[a] pot. (R)-selective	Q1EQE0[b] (R)-selective
co-solvent (vol%)	**4**[c] (mM)	**3**[d] (%)	**3**[a] (%)	**3**[a] (%)
MeOH (5)	50	< 1	< 1	< 1
MeOH (5) + n-heptane (10)	10	< 1	< 1	< 1

General conditions: Glucose dehydrogenase (GDH, 1 mg/mL), glucose (100 mM), NADP$^+$ (1 mM) in 500 μL 100 mM KPi-buffer pH 7.0.
[a] Purified protein, 1 mg/mL.
[b] Whole cell pellet, 10 mg/mL
[c] Racemic substrate **4** added as MeOH stock-solution. Incubation for 24 h at 30 °C, 700 rpm.
[d] No reduced product **3a** or **3** could be detected with TLC and GC-MS on a HP-5 column, but considerable amounts of pyrrole **2** were observed.

Upon reduction of **4**, the generated secondary, cyclic imine **3a** might cyclize spontaneously under the biotransformation conditions to end up as bicyclic enamine **3**. Practically, the enzymatic reduction did not lead to any reduced derivative **3a** or **3**, but pyrrole **2** formation was observed instead. It has to be noted that these experiments were only preliminary studies and no emphasis has been put on extensive IRED and condition screenings yet.

Owing to its aromaticity, pyrrole **2** cannot serve as substrate for IREDs anymore and its emergence may be considered as a drawback here. This drawback, however, could turn into an advantage when comparing the 5-membered imine **4** with the somewhat more rigid bicyclic structure in **2** that could better facilitate substrate control by means of steric interactions with the reducing agent. Indeed, pyrrole **2** can be rapidly formed from **4** upon treatment with acid in a protic solvent (Scheme 2.10) and was thus accessible as substrate for testing it in reduction reactions.
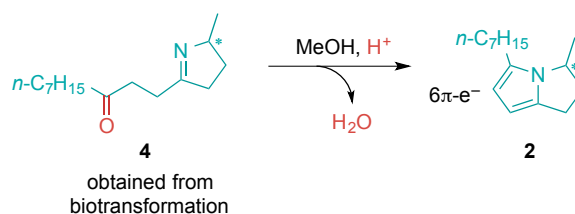
Scheme 2.10 | Cyclization of imine **4** to pyrrole **2** with gain of aromaticity as driving force.

Substrate control actually originated from the absolute stereoconfiguration of the methyl group, which restricted the access of the reducing agent to one of the two faces of the pyrrole.

Empirically, these circumstances supported the predominant yielding of xenovenine (5Z,8E)-**1** whereas formation of the other three possible diastereomers was suppressed. Enhancing the diastereoselectivity for the 5Z,8E-isomer by using strong and bulky acids as catalysts was also attempted.
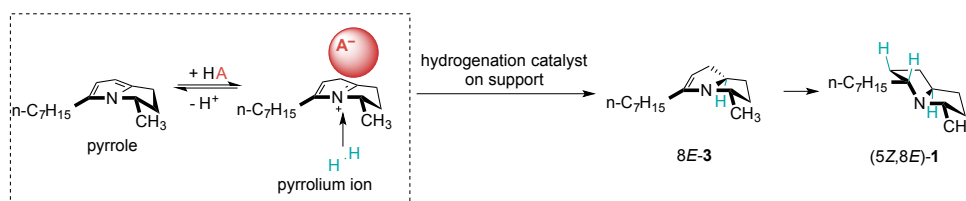
Scheme 2.11 | Rationale for explaining enhanced reduction diastereoselectivities in the presence of bulky acids.

The acid was thought to protonate the pyrrole, and its bulky anion to block the better accessible side, thus forcing hydrogen addition to happen *syn* to the methyl group. A summary of reaction outcomes under various conditions is tabulated below.

Table 2.9 | Reduction of pyrrole **2** employing various conditions and additives.
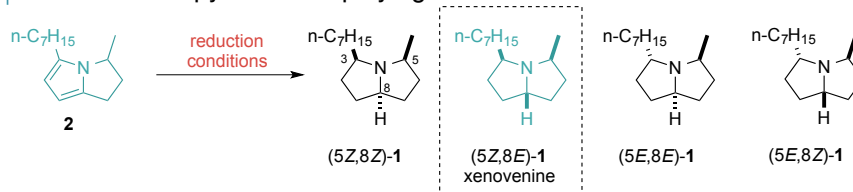
Entry	Scale (mg)	Reaction time	Additive	Conv.[b] (%)	1[b] (%)	1 d.r. (%)[c]			
						5Z,8Z	5Z,8E	5E,8E	5E,8Z
1	10	17 h	0.5 w% pivalic acid	0	0	–	–	–	–
2	10	17 h	0.5 w% benzoic acid	0	0	–	–	–	–
3	10	46 h	0.5 eq p-TsOH	95	79	< 1	72	4	23
4	10	29 h	0.5 eq (+)-CSA	82	85	< 1	79	< 1	21
5	5[d]	21 h	1 eq (+)-CSA	(+): 97 (–): 97	73 81	5 4	87 87	4 3	4 6
6	100[d]	40 h	0.5 eq (+)-CSA	(+): 96 (–): > 99	93[e] > 99[e]	4 8	84 57	6 19	6 17

General conditions unless otherwise stated: 50 mM substrate **2**, 10 w% Pd/C, 1 atm H₂, MeOH, r.t.

[a] Conversion determined *via* GC-MS peak areas.
[b] Determined *via* GC-MS areas. Percentage of xenovenine and its diastereomers in the product mixture. The major detectable side products were mono-hydrogenated derivatives of **2**, meaning the reduction was still incomplete.
[c] Diastereomeric ratio of **1** determined from GC-MS peak areas.
[d] Run with both enantiomers separately: (+)-isomer results from (R)-**2**, (–)-isomer from (S)-**2**.
[e] Performed on a preparative scale: isolated yield of (5Z,8E)-**1** over three steps (starting from triketone **7**) after separation of diastereomers *via* column chromatography: 48 % (–)-**1**; 30 % (+)-**1**.

A strong sulfonic acid was required since carboxylic acids are too weak to protonate the arene (entry 1 and 2). Comparing *p*-toluenesulfonic acid (*p*-TsOH) and the more sterical demanding (+)-camphorsulfonic acid (CSA), it turned out that the latter slightly enhances diastereoselectivity in favor of the 5*Z*,8*E* isomer. Interestingly, the *d.e.* of the (−)-enantiomer was considerably lower than of the (+)-enantiomer when adding (+)-CSA, hence giving rise to the assumption of match/mismatch effects. The amount of acid did also affect the reduction outcome where more acid increased the *d.e.* of the desired product isomer.

2.1.5 Summary

An enantioselective, chemo-enzymatic synthesis for both enantiomers of xenovenine has been established. The synthesis of the precursor triketone **7** was straightforward and followed conventional synthetic chemistry. An optimization of reaction conditions was conducted for the final biotransformation and hydrogenation steps, which led to preparatively useful yields. The thermodynamic driven product cyclization turned out to be crucial for quantitative conversion and excellent *e.e.* beside the presence of organic co-solvents DMSO and heptane and a slightly basic pH-value.

The hydrogenation of pyrrole **2** required acidic conditions to happen and bulky acid anions helped to control diastereoselectivity in favor of the desired product isomer.

With this synthetic pathway, sufficient amounts of (−)- and (+)-xenovenine were obtained for characterization in an overall yield of 30 and 17 % from commercially available alkylfuran **11**, respectively. Spectral data of both enantiomers matched the ones reported in literature and the enantiomeric purity of the products was ultimately confirmed by means of optical rotation.
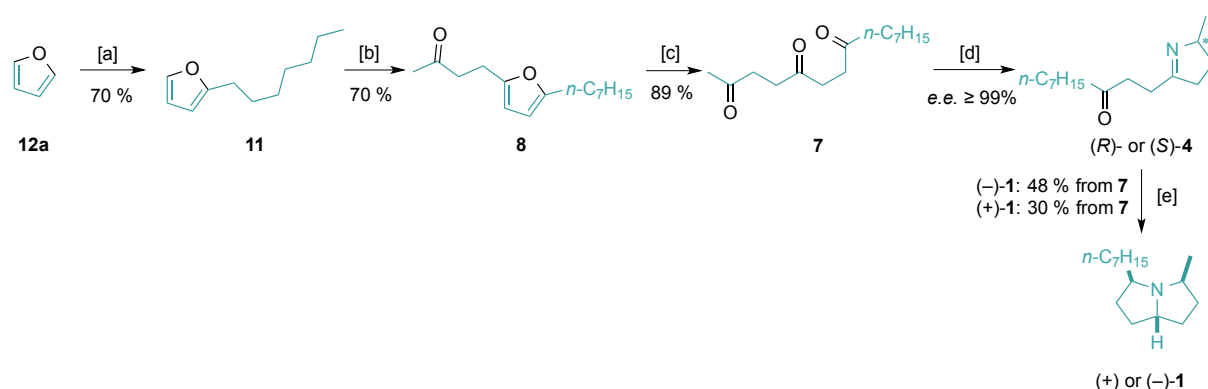
Scheme 2.12 | Chemo-enzymatic pathway towards both xenovenine enantiomers

Conditions: [a] 1) *n*-BuLi (1.05 eq), THF, 0 °C 2) *n*-C$_7$H$_5$Br (1 eq), THF, 0 °C; [b] methylvinylketone (1 eq), hydroquinone (10 mol%), AcOH, 21 °C, 3 d [c] aq. HCl conc./AcOH (1/1), r.t. 1 h [d] lyophilized cells containing ω-TA (20 mg/mL), substrate **7** (50 mM), alanine (500 mM), ammoniumformate (150 mM), PLP (1 mM), NAD$^+$ (1 mM), DMF or DMSO (5 v%), heptane (20 v%), FDH (11 U), AlaDH (12 U), 26 h, 35 °C, 290 rpm; [e] 1) AcOH (1 v%), MeOH, 2 h, 21 °C 2) (+)-CSA (0.5 eq), Pd/C (10 wt%) H$_2$ (1 atm), 40 h, 21 °C.

2.1.6 Outlook

Even though some final optimization in terms of imine or pyrrole hydrogenation is still required, the feasibility of the concept was proven herein. The emphasis in reduction will be on a more intense investigation of imine reductases and their application in cascades together with an ω-transaminase. Up to now, none of the examined IREDs was willing to accept the rather bulky substrate; a problem that could be circumvented by medium engineering and a more extended enzyme screening. Furthermore, if enantioselectivities of the cascade enzymes were independent from each other (*i.e.* if substrate control is overridden by the enzyme's enantioselectivity) the synthesis would be rendered remarkably flexible in terms of diastereoselectivity. A desired diastereomer could thus be prepared enantiomerically pure by choosing enzymes for the cascade exhibiting the proper enantioselectivity.

Additionally, we also intend to extend the chemo-enzymatic enantioselective approach to the structurally related indolizidine alkaloid monomorine I. This compound was also derived from ants where it plays a vital role as signaling pheromone.[6, 71] The precursor and ω-transaminase substrate would be a tridecane-2,6,9-trione in this case.

monomorine I

tridecane-2,6,9-trione
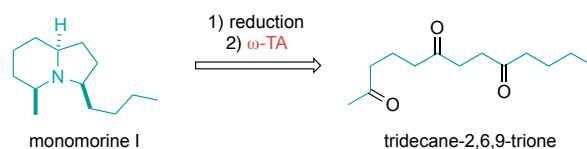
Scheme 2.13 | Retrosynthesis of monomorine I bearing in mind the chemo-enzymatic approach using enzymatic transamination and catalytic reduction or hydrogenation.

With the now established chemo-enzymatic pathway, the substituted bicyclic core structures of pyrrolizidines, indolizidines and quinolizidines should become easier accessible in an enantio- and diastereoselective fashion. As illustrated in Figure 1.1, the spectrum of possible bioactive target molecules including potential drugs is considerably wide. Hence, this approach would also provide an alternative and greener way towards these compounds on an industrial scale.

2.2 Novel "Smart Co-Substrates" for ω-Transaminases

2.2.1 Overview screening

The quest for novel, feasible ω-transaminase co-substrates was initiated by an extensive screening, which combined an array of either (S)- or (R)-selective ω-transaminases from different organisms and a selection of bi-functional molecules (Scheme 2.14, **15** through **25**). As model reaction, the thermodynamically neutral formal reductive amination of 4-phenyl-2-butanone **13** was chosen. Substrate **13** lacks a thermodynamic sink, such as a carbonyl group conjugated to a π-system, thus conversion is governed in this case predominantly by the thermodynamics of the follow-up reaction of the co-product.
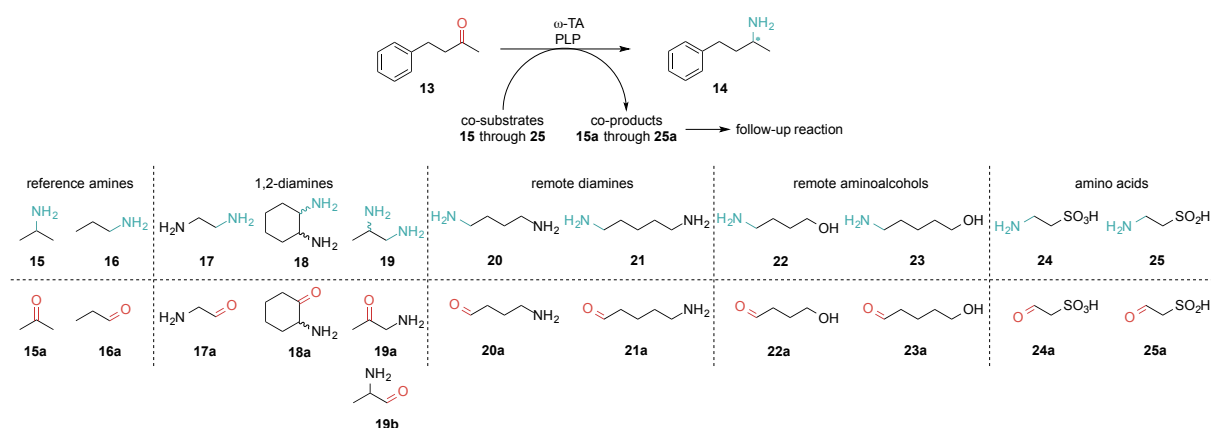
Scheme 2.14 │ Setup for the co-substrate overview screening involving formal reductive amination of 4-phenyl-2-butanone **13**.

The co-substrates were selected bearing in mind the tentative exothermic follow-up reactions, subsequently illustrated in Figure 2.5, including dimerization, aromatization, cyclization and decomposition processes. Importantly, these reactions were required to proceed spontaneously under the biotransformation conditions in order to withdraw co-product from the equilibrium and thus displace the equilibrium in support of the amine product formation.
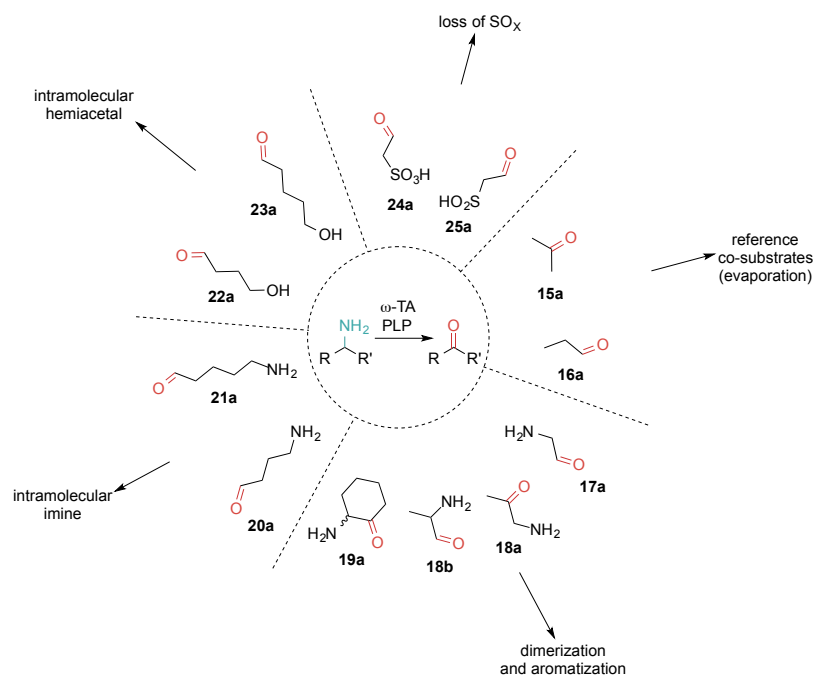
Figure 2.5 | Tentative follow-up reactions for co-products **15a** through **25a**.

The required ω-transaminases, which derive from various organisms, were heterologously expressed in *E. coli* hosts and applied as whole-cell catalysts. The substrate specificity and stereoselectivity of the majority of these enzymes have already been established and many examples for their usage can be found in literature[36, 41, 52-53] (see also Table 1.1 with references in the introduction part, especially for the establishment of stereoselectivity).

Table 2.10 | List of ω-transaminases used in this study (for a more detailed list see section 3).

Source Organism	Abbreviation	Selectivity
Bacillus megaterium	BM	(*S*)
Arthrobacter citreus	ArS	(*S*)
Chromobacterium violaceum	CV	(*S*)
Vibrio fluvialis	Vf	(*S*)
Pseudomonas flourescens	PF	(*S*)
Paracoccus denitrifcans	PD	(*S*)
Silicibacter pomeroyi	SP	(*S*)
Arthrobacter sp.	ArR	(*R*)
Arthrobacter sp. round 11 variant	ArRmut11	(*R*)
Aspergillus terreus	AT	(*R*)
Hyphomonas neptunium	HN	(*R*)
Ochrobactrum anthropii	OA	(*R*)
Neosartoria fischeri	NF	(*R*)
Gibberella zeae	GZ	(*R*)

For the sake of simplicity, only conversions were measured in the initial screening. An overview of conversions achieved is given in the following table.

Table 2.11 | Co-substrate/ω-transaminase overview screening: Conversion results.

Co-Substrate

ω-Transaminase	15	16	17	18	19	20	21	22	23	24	25
BM	27	2	2	2	13	2	0	4	4	0	2
ArS	28	3	13	5	28	10	17	2	3	0	0
CV	5	2	2	3	3	2	0	2	3	0	7
Vf	17	2	2	2	5	2	0	2	3	0	2
PF	3	0	0	3	0	0	0	2	3	0	0
SP	19	0	0	0	12	15	12	0	0	0	0
PD	0	0	0	0	0	0	0	0	0	0	0
ArR	17	0	5	3	31	8	15	0	3	0	0
ArRmut11	28	0	0	35	19	0	21	0	0	0	0
AT	23	2	5	4	20	9	11	0	3	0	4
HN	0	0	0	0	0	0	0	0	0	0	0
OA	0	0	0	0	0	0	0	0	0	0	0
NF	13	0	0	0	9	0	11	0	0	0	0
GZ	11	0	0	0	0	0	0	0	0	0	0

Conditions: lyophilized cells containing ω-TA (20 mg/mL), PLP (1 mM) in 1 mL 100 mM KPi-buffer pH 8.0, rehydrated for 1 h at 30 °C, 400 rpm; 50 mM substrate **13** and 50 mM (1 eq) co-substrate **15-25** for 72 h at 30 °C, 400 rpm.

Conversions were determined with GC-FID on a DB-1701 column, values given in %. The color intensity in the matrix correlates with the extent of conversion.

From these results, it was possible to gain an idea about how readily an amine-donor is accepted by the enzymes and if its usage would be advantageous compared to "conventional" co-substrates **15** and **16**. The highest conversion in this experiment was achieved with the *Arthrobacter* round 11 mutant and 1,2-diaminocyclohexane **18** as co-substrate – a comprehensible fact when considering that the mutant was designed for converting bulky substrates.[40] Furthermore, co-substrates **19** and **21** exhibited promising conversions that were close to, or even higher than with the benchmark amine donor isopropylamine **15**. The best performing enzyme/co-substrate pairs were chosen for the next steps towards optimization of the biotransformation. Namely, these were ArRmut11 with **18**; BM, ArS, SP, ArR, AT and NF with **19** and ArS and ArR with **21**.

2.2.2 Optimization of pH-Conditions

ω-Transaminases are known to exhibit their highest activity in asymmetric reductive aminations at slightly basic conditions.[57] Owing to their pK_a values around 9, primary and secondary amines display their highest nucleophilicity above this pH-value, where they are present in their non-protonated form. Recalling the PLP mechanism for ω-TA catalysis, a nucleophilic attack of the nitrogen atom at the PLP-enzyme iminium-linkage initiates the catalytic cycle and the migration of the amino-group from the PMP-entity also requires nucleophilic attack on the substrate carbonyl (see also Scheme 1.9).

In order to find the optimal pH-range in which limited denaturation of the enzyme and the nucleophilicity of the co-substrate amine sum up to give the highest conversion, a study with the selected enzyme/co-substrate pairs in the range of pH 6 to 11 with two different buffer systems was conducted.

Table 2.12 | pH variation study with a KPi-buffer system using co-substrate **21** (1,5-diaminopentane).

ω-TAs	ArS (S)-selective		ArR (R)-selective	
pH-value	conversion [%]	e.e. [%]	conversion [%]	e.e. %]
6.0	0	n.d.	0	n.d.
7.0	0	n.d.	0	n.d.
8.0	2	12	2	48
8.9	2	33	2	48
9.9	3	16	4	n.d.

Conditions: lyophilized cells containing ω-TA (20 mg/mL), PLP (1mM) in 1 mL 100 mM KPi-buffer and 50 mM co-substrate **21**, pH 6, 7, 8, 9 and 10 (adjusted with H_3PO_4 conc. or 1 M KOH) rehydrated for 45 min at 30 °C, 400 rpm; 50 mM substrate **13** for 72 h at 30 °C, 400 rpm.
Conversions were determined with GC-FID on a DB-1701 column.
The e.e. was measured with GC-FID on a chiral phase (DEX-CB column) after N-acetylation of **14** (2 eq Ac_2O, cat. DMAP, 2 h at 30 °C, 700 rpm, then + 500 μL Na_2CO_3 sat. for 1h)

Table 2.13 | pH variation study with a KPi-buffer system using co-substrate **18** (1,2-diaminocyclohexane).

ω-TA:	ArRmut11 (R)-selective	
pH-value	conversion [%]	e.e. [%]
6.1	13	n.d.
7.1	17	6
7.9	21	7
8.7	29	6
10.1	35	7

Conditions: lyophilized cells containing ω-TA (20 mg/mL), PLP (1mM) in 1 mL 100 mM KPi-buffer and 50 mM co-substrate **18**, pH 6, 7, 8, 9 and 10 (adjusted with H_3PO_4 conc. or 1 M KOH) rehydrated for 45 min at 30 °C, 400 rpm; 50 mM substrate **13** for 72 h at 30 °C, 400 rpm.
Conversions were determined with GC-FID on a DB-1701 column.
The e.e. was measured with GC-FID on a chiral phase (DEX-CB column) after N-acetylation of **14** (2 eq Ac_2O, cat. DMAP, 2 h at 30 °C, 700 rpm, then + 500 µL Na_2CO_3 sat. for 1 h)

Co-substrates **18** and **21** were accepted by the enzymes, but the initial conversions and e.e.'s were not promising. Therefore, these enzyme/co-substrate pairs were excluded from further investigations.
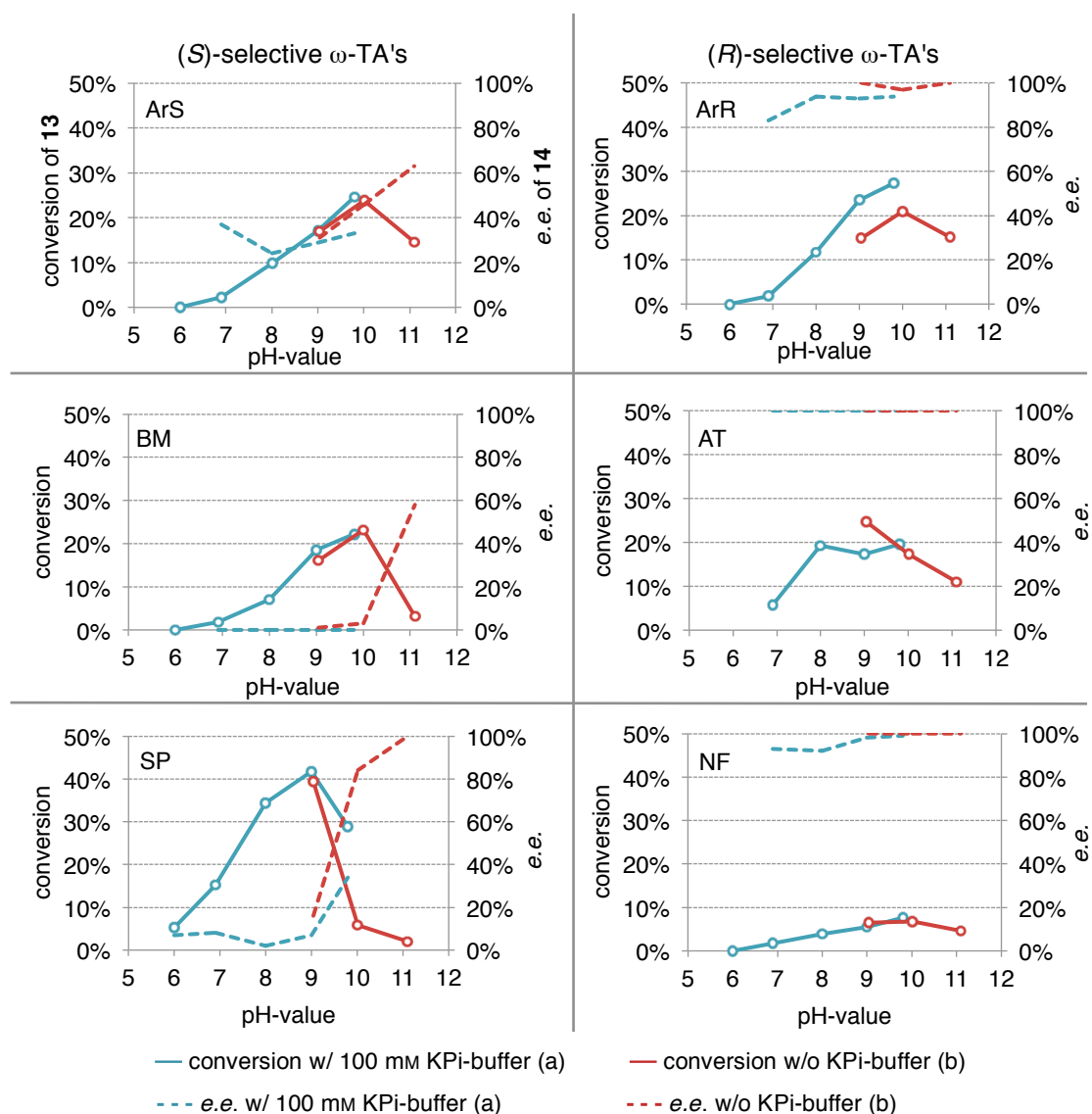
Figure 2.6 | pH variation study with two different buffer systems using co-substrate **19** (1,2-diaminopropane).

Conditions: lyophilized cells containing ω-TA (20 mg/mL), PLP (1 mM) in 1 mL (a) 100 mM KPi-buffer and 50 mM co-substrate **19**, pH 6.0, 7.0, 8.0, 9.0 and 10.0 (adjusted with H_3PO_4 conc. or 1 M KOH) (b) 50 mM **19** in H_2O, pH 9.0, 10.0 and 11.0 (adjusted with HCl conc.) rehydrated for 45 min at 30 °C, 400 rpm; 50 mM substrate **13** for 72 h at 30 °C, 400 rpm.
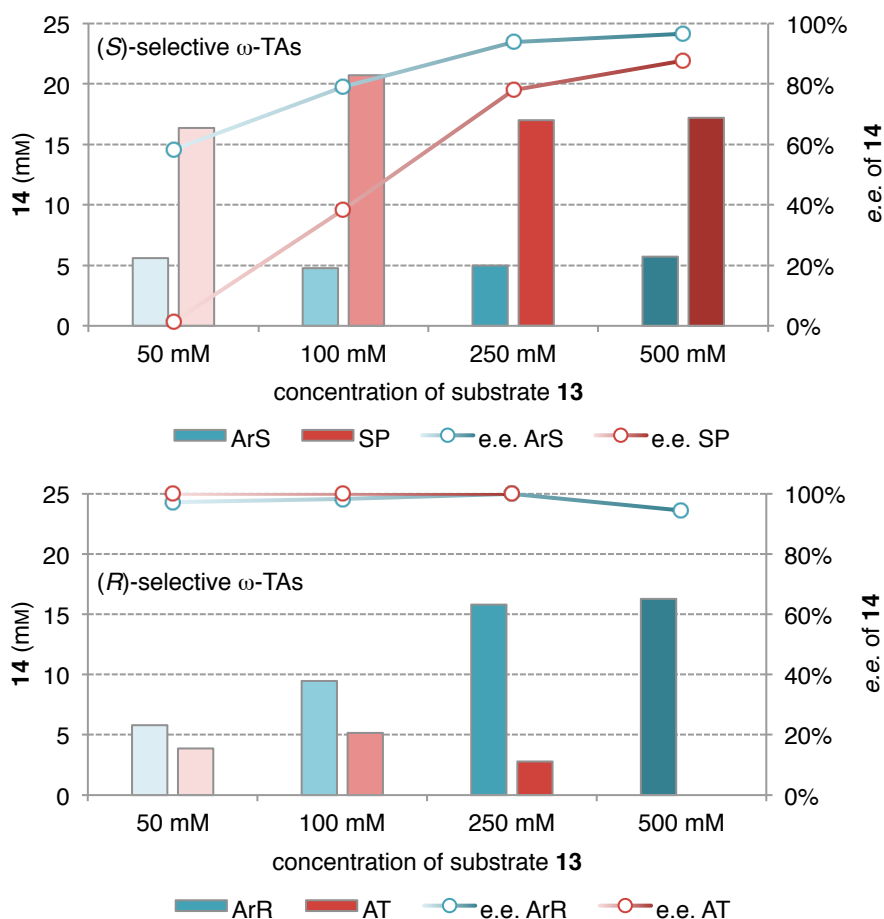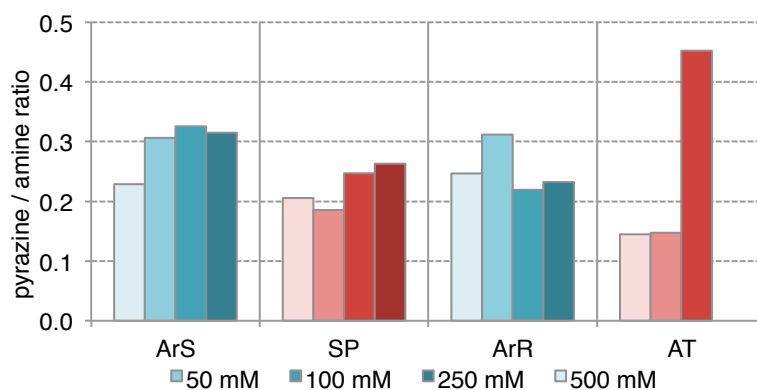Conversions were determined with GC-FID on a DB-1701 column.
The *e.e.* was measured with GC-FID on a chiral phase (DEX-CB column) after *N*-acetylation of **14** (2 eq Ac_2O, cat. DMAP, 2 h at 30 °C, 700 rpm, then + 500 μL Na_2CO_3 sat. for 1 h)

With co-substrate **19**, all enzymes achieved their highest conversions between pH 9 and 10 as proposed before, whilst disregarding their stereoselectivity. Importantly, the bell-shaped conversion trend was not altered dramatically within this pH-range when exchanging the KPi buffer for an aqueous co-substrate buffer (*i.e.* change from cond. a to b).

When assessing the enantiomeric excess, differences between (*S*)- and (*R*)-selective enzymes became striking. Whereas (*R*)-selective ω-TAs gave invariably good to excellent *e.e.*'s at all pH-values, the *e.e.*'s measured with (*S*)-ω-TAs showed a dependence on the extent of conversion. This can be clearly seen in the case of SP in Figure 2.6: at pH values below 9,

conversion increases with increasing pH but the *e.e.* remains constantly low. At more basic conditions (pH > 9), the conversion suddenly drops but the *e.e.* sharply increases. One should be aware that the *e.e*'s measured at low conversions, as it is sometimes the case here, could be incorrect due to overlap with other compounds at similar GC retention times. Nevertheless the main purpose of finding the enzymes' pH-optima was fulfilled and thus further optimization towards full conversion was addressed.

2.2.3 Investigation of the Follow-Up Reaction

Incomplete conversion of substrate **13** could be due to insufficient equilibrium displacement. If neglecting the thermodynamics of the follow-up reaction, the amounts of ketone substrate and amine product equilibrate and hence conversion stops at a certain extent. This threshold conversion value can be approximated with the equilibrium constant of the ketone and its respective amine. In the case of 4-phenyl-2-butanone (**13**) and its amine **14** the K_{eq} was reported as 0.74, which corresponds to an equilibrium conversion of 46 % if using 1 eq of *i*-propylamine as co-substrate.[44a]

Hence, this equilibrium does not solely depend on substrate and product concentration but also co-substrate and co-product concentration. Thus, removing either product or co-product, or using an excess of co-substrate both enhances conversion of the substrate. Removal of aminated product might pose a problem, but co-substrates can be carefully chosen so that their co-products undergo a spontaneous, exothermic follow-up reaction. Thereby the co-products are removed from the equilibrium and full conversion can be achieved. These substrates were termed "smart co-substrates"[48] and their exploration still advances.

In the present case, the 2-aminoketone (or -aldehyde) co-products **19a** and **19b** are able to form an intramolecular hydrogen bond, which contributes to the equilibrium displacement. Alternatively, the co-products could undergo a follow-up reaction involving dimerization and subsequent oxidative aromatization of the dimer to give a pyrazine derivative (Scheme 2.15). The gain of aromaticity should liberate energy sufficient for drawing over the biotransformation equilibrium to the product side.
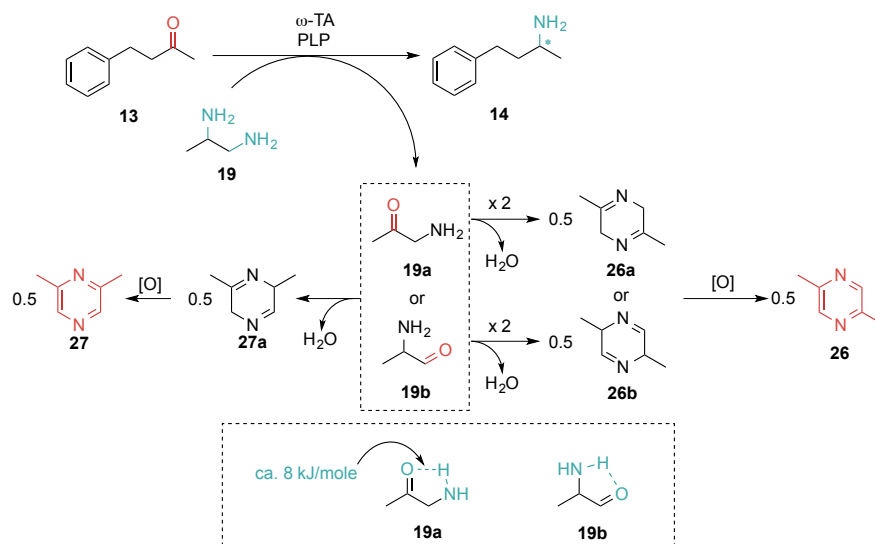
Scheme 2.15 │ Possible follow-up reactions for co-products **19a** and **19b**.

The rate of the follow-up reaction is influenced by the activation energy of the dimerization and the rate of pyrideine oxidation. Investigation of these parameters was addressed to find conditions at which the follow-up reaction was considerably faster than the biotransformation. This was necessary in order to avoid accumulation of stereochemical errors, possibly made by the enzyme in back and forth reactions at the equilibrium, which would lower the *e.e.*

As the reaction proceeded, the concentrations of the involved compounds changed. This means that, for example, the carbonyl group in co-products **19a** or **19b** initially was more likely to be nucleophilically attacked by a co-substrate diamine **19** since it was provided in excess. However, these reactions were likely reversible and as the reaction proceeded, the proportion of homo-dimerization reactions rose.

Hence it was of interest if enhancing the concentration of monomers, chelation or addition of co-solvents could speed up dimerization and thus avoiding an equilibrium state. Furthermore, oxidation of the dimers was tested at ambient conditions with atmospheric oxygen serving as oxidant, but supplementary oxidation agents and higher oxygen pressure were also checked for their feasibility in enhancing the reaction rate. Subsequently, the results of these studies, which were all carried out at the pH-optimum, are being discussed in detail.

2.2.3.1 Concentration Effects

The conducted concentration studies were all performed in the aqueous co-substrate buffer system with the pH adjusted with concentrated hydrochloric acid. This constituted a remarkably simple system and in view of suspected industrial applications, emphasis was put on the optimization of the biotransformation at these conditions.

Initially, the effect on conversion was tested at 50 mᴍ substrate **13** concentration with 1, 2 and 5 eq of co-substrate **19**. As mentioned before, an excess of co-substrate displaces the equilibrium to the product side and the obtained data confirmed this (Figure 2.7)
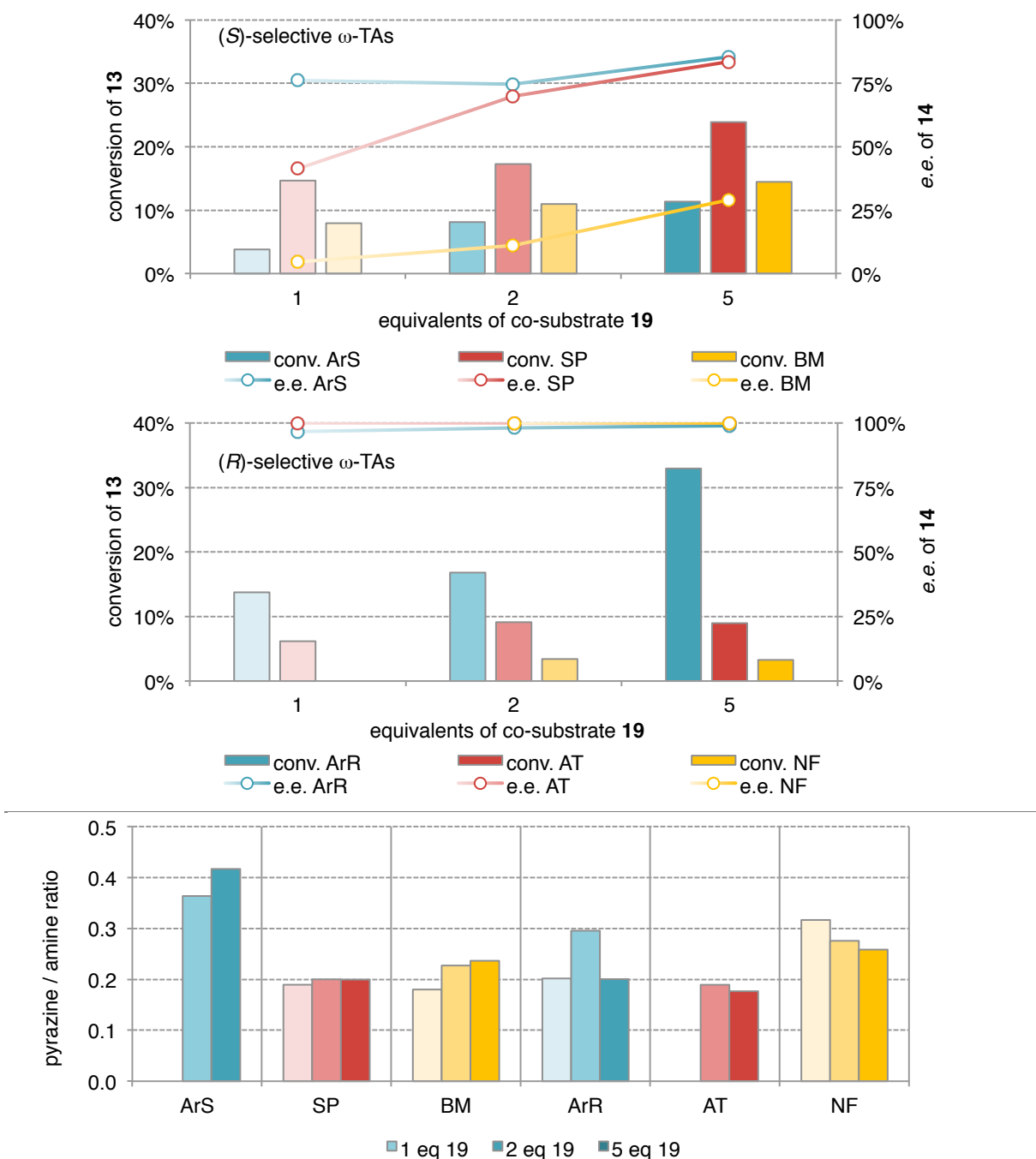
Figure 2.7 | Effect of co-substrate excess on conversion of **13**, product **14** *e.e.* and pyrazine **26** formation. The bars' color intensities correspond to concentration of **19**.

Conditions: lyophilized cells containing ω-TA (20 mg/mL), PLP (1 mᴍ) and 1, 2 or 5 eq co-substrate **19** in 1 mL 100 mᴍ KPi-buffer pH 9.5 (adjusted with H_3PO_4 conc.). Incubation with 50 mᴍ substrate **13** for 24 h at 30 °C, 700 rpm.
Conversions were determined with GC-FID on a DB-1701 column.
The *e.e.* was measured with GC-FID on a chiral phase (DEX-CB column) after *N*-acetylation of **14** (2 eq Ac_2O, cat. DMAP, 2 h at 30 °C, 700 rpm, then + 500 μL Na_2CO_3 sat. for 1 h)

Since neither co-products (**19a** and **19b**) nor dimers (**26a** and **26b**) could be detected by GC analysis, the concentration ratio of pyrazine **26** and product amine **14** was chosen as indicator for the follow-up reaction completeness. If all formed co-product molecules cyclize and aromatize, this ratio would be 0.5. In the current experiment this was never the case, however, ArS shows a satisfying ratio of 0.4 with 5 eq co-substrate.

In general, the observed substrate conversions increased with increasing co-substrate concentration (bars with same color) and also the *e.e.* of (*S*)-amines (from ArS, SP and BM) benefited from these conditions. All (*R*)-selective ω-TAs gave perfect *e.e.*'s throughout the measurements.

Next, the effect of increasing substrate concentration whilst maintaining one equivalent of co-substrate was tested. The concentration of biocatalyst was kept constant at 20 mg/mL. Due to varying substrate concentration, the reaction progress was henceforth measured in units of mM product formed.

Figure 2.8 | Effect of increasing substrate **13** concentration (corresponding to the bars' color intensities) with 1 eq co-substrate **19**.

Conditions: lyophilized cells containing ω-TA (20 mg/mL), PLP (1 mM) and 1 eq co-substrate **19** (i.e. 50, 100, 250 or 500 mM) in 1 mL water at pH 9 (AT, SP) or pH 10 (ArR, ArS) (adjusted with HCl conc.) rehydrated for 30 min at 30 °C, 700 rpm. Then incubation with 50, 100, 250 or 500 mM substrate **13** for 72 h at 30 °C, 700 rpm.
Quantification was done with GC-FID on a DB-1701 column.
The *e.e.* was measured with GC-FID on a chiral phase (DEX-CB column) after *N*-acetylation of **14** (2 eq Ac$_2$O, cat. DMAP, 2 h at 30 °C, 700 rpm, then + 500 μL Na$_2$CO$_3$ sat. for 1 h)

Whereas (*S*)-selective ArS and SP reached their maximum substrate loadings at 250 mM indicated by stagnating conversion, the activity of (*R*)-selective AT dropped above a substrate concentration of 100 mM. ArR on the other hand, performed best at highest substrate loadings of 500 mM. The initially (very) bad *e.e.*'s obtained from the (*S*)-selective ω-TA's ArS and SP considerably increased with substrate concentration.

After the maximum substrate loading was determined, the transaminases from ArR and SP, which displayed highest conversions at these conditions, were in turn employed at 250 mM substrate concentration with varying co-substrate concentration ranging from 1 to 10 equivalents.
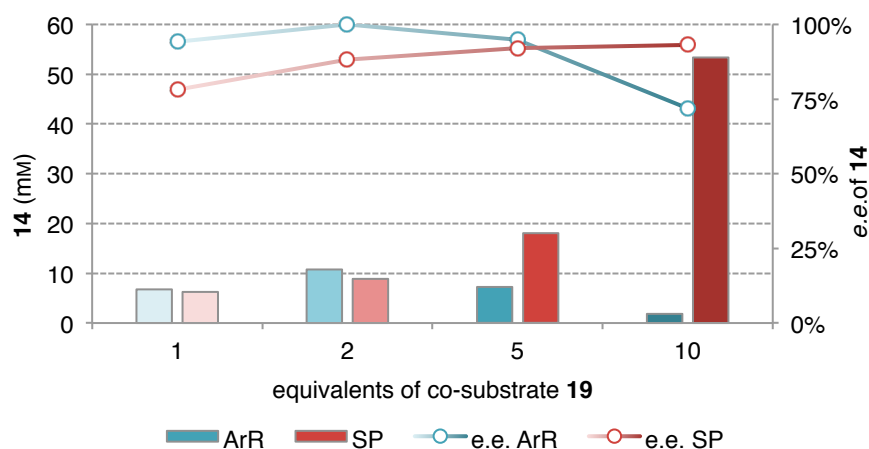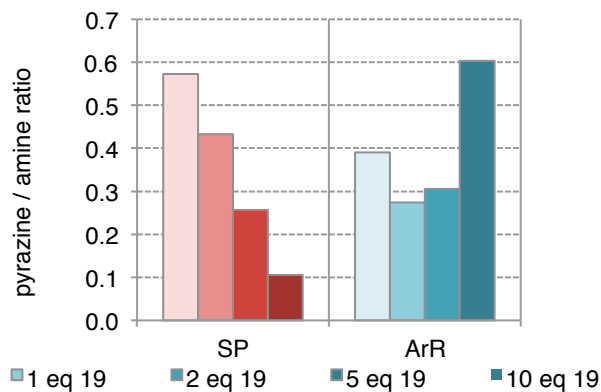
Figure 2.9 | Effect of increasing co-substrate **19** concentration (corresponding to the bars' color intensities) with constantly 250 mM substrate **13** concentration.

Conditions: lyophilized cells containing ω-TA (20 mg/mL), PLP (1 mM) and 1, 2, 5 or 10 eq co-substrate **19** (i.e. 250 mM, 500 mM, 1 M or 5 M) in 1 mL water at pH 9 (SP) or pH 10 (ArR) (adjusted with HCl conc.) rehydrated for 30 min at 30 °C, 700 rpm. Then incubation with 250 mM substrate **13** for 72 h at 30 °C, 650 rpm.
Quantification was done with GC-FID on a DB-1701 column.
The *e.e.* was measured with GC-FID on a chiral phase (DEX-CB column) after *N*-acetylation of **14** (2 eq Ac$_2$O, cat. DMAP, 2 h at 30 °C, 700 rpm, then + 500 μL Na$_2$CO$_3$ sat. for 1 h)

For the (*S*)-selective TA from SP, the trend towards higher product amounts with increasing co-substrate concentration resembles the one in the study with 50 mM substrate concentration. This enzyme from *S. pomeroyi* was found to be active even at 5 M co-substrate concentration! Also, the obtained product *e.e.* was considerably better than before. In contrast, ArR did not tolerate the high substrate and co-substrate loadings, which manifested itself in a drop of conversion and *e.e.* beyond 2 eq (i.e. 500 mM) of **19**. Pyrazine formation in both cases followed a trend reverse to conversion: selective pyrazine formation at low co-substrate concentrations and *vice versa*. At high co-substrate loadings, side reactions of the co-product with co-substrate, which did also displace equilibrium, may become dominant. Notably, the biotransformation suspensions obtained within these studies exhibited a yellow color whose increasing intensity seems to correlate with the extent of product formation. It was suspected that the origins of color were oligo- or polymers resulting from side reactions of co-product and co-substrate, however, this was not further investigated.

2.2.3.2 Chelating Metal Ions

Another approach to improve dimerization of the follow-up reaction involved the use of chelating metal ions with moderate LEWIS-acidity. The intended purpose of these additives was chelation and activation of the 2-amino-ketone **19a** (or aldehyde **19b**) co-products.
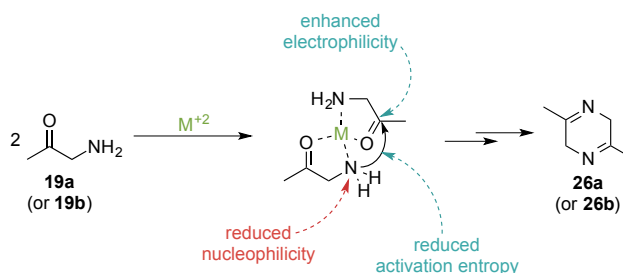
Figure 2.10 | Proposed effects of chelating metal ions on the dimerization.

When choosing metals possessing 4 coordination sites, chelation of two monomers through one metal-ion would bring together the two halves of the dihydropyrazine in close proximity, thereby lowering activation energy. Assuming the metal-monomer complex forms, the carbonyl group in **19a** or **b** is activated by the LEWIS-acidic character of the metal. In contrast, the same effect on the amino-group would considerably lower its nucleophilicity and thus the rate of dimerization. Hence the overall effect of such additives is a combination of beneficial and disadvantageous discrete actions on the monomer and had to be assessed empirically.

Table 2.14 | Effects of chelating, LEWIS-acidic metal-ions on the follow-up reaction.

ω-TAs:	ArS			SP			ArR			AT		
Additives	conv. (%)	*e.e.* (%)	p/a ratio	conv. (%)	*e.e.* (%)	p/a ratio	conv. (%)	*e.e.* (%)	p/a ratio	conv. (%)	*e.e.* (%)	p/a ratio
none	15	30	0.32	31	18	0.21	11	97	0.32	20	> 99	0.18
25 mM Mg^{2+}	15	53	0.21	50	5	0.15	15	97	0.16	22	> 99	0.13
25 mM Zn^{2+}	0	n.d.	n.d.	4	79	< 0.1	6	96	< 0.1	6	> 99	< 0.1

Conditions: lyophilized cells containing ω-TA (20 mg/mL), PLP (1 mM), 1 eq co-substrate **19** (50 mM) and 25 mM MgCl$_2$ or ZnCl$_2$ in 1 mL water at pH 9 (SP, AT) or pH 10 (ArS, ArR) (adjusted with HCl conc.) rehydratized for 30 min at 30 °C, 700 rpm. Then incubation with 50 mM substrate **13** for 72 h at 30 °C, 700 rpm. Quantification with GC-FID on a DB-1701 column.
The *e.e.* was measured with GC-FID on a chiral DEX-CB column after *N*-acetylation of **14** (2 eq Ac$_2$O, cat. DMAP, 2 h at 30 °C, 700 rpm, then + 500 μL Na$_2$CO$_3$ sat. for 1 h)

Supplementing the system with magnesium ions (25 mM as MgCl$_2$) enhanced conversion with SP by 20 % but this was associated with a very bad *e.e.* of only 5 %. This seemed to be an exception as no other enzyme showed this considerable increase in conversion. The *e.e.* with ArS could be improved to 53 % from 30 %.

Whereas the results for (*R*)-selective enzymes ArR and AT are not affected by Mg(II)-ions, the addition of zinc turned out to be inferior for conversion. For SP a good *e.e.* but very low conversion was measured with zinc, thus supporting the observation of a negative conversion and *e.e.* correlation.

2.2.3.3 Co-Solvents

Organic co-solvents have proved valuable additives in biotransformations, enhancing both conversion and *e.e.*[57] This can be due to solvent-induced alterations of the enzyme's structure and/or (co-)substrate solubility. An array of water miscible and non-miscible co-solvents with different polarities was examined.

Table 2.15 | Co-solvent effects on the biotransformation. The solvent's polarity increases from the top to the bottom.

ω-TAs:	ArS			SP			ArR			AT		
Co-Solvent (20 v%)	conv. (%)	*e.e.* (%)	p/a ratio	conv. (%)	*e.e.* (%)	p/a ratio	conv. (%)	*e.e.* (%)	p/a ratio	conv. (%)	*e.e.* (%)	p/a ratio
none	16	31	0.32	31	18	0.21	11	97	0.32	20	> 99	0.18
DME	11	73	0.26	27	35	0.17	11	95	0.15	3	> 99	< 0.1
DMF	11	90	0.26	15	74	0.19	0	> 99	n.d.	7	> 99	0.27
DMSO	20	65	0.21	43	16	0.15	24	96	0.21	20	> 99	0.2
Formamide	2	> 99	< 0.1	6	91	< 0.1	0	> 99	n.d.	n.d.	n.d.	n.d.
MeOH	9	84	0.22	21	69	0.11	6	> 99	0.26	13	> 99	0.16

Conditions: lyophilized cells containing ω-TA (20 mg/mL), PLP (1 mM), 1 eq co-substrate **19** (50 mM) in 1 mL water at pH 9 (SP, AT) or pH 10 (ArS, ArR) (adjusted with HCl conc.) rehydrated for 30 min at 30 °C, 700 rpm. Then incubation with 50 mM substrate **13** and 20 v% water-miscible co-solvent for 72 h at 30 °C, 700 rpm.
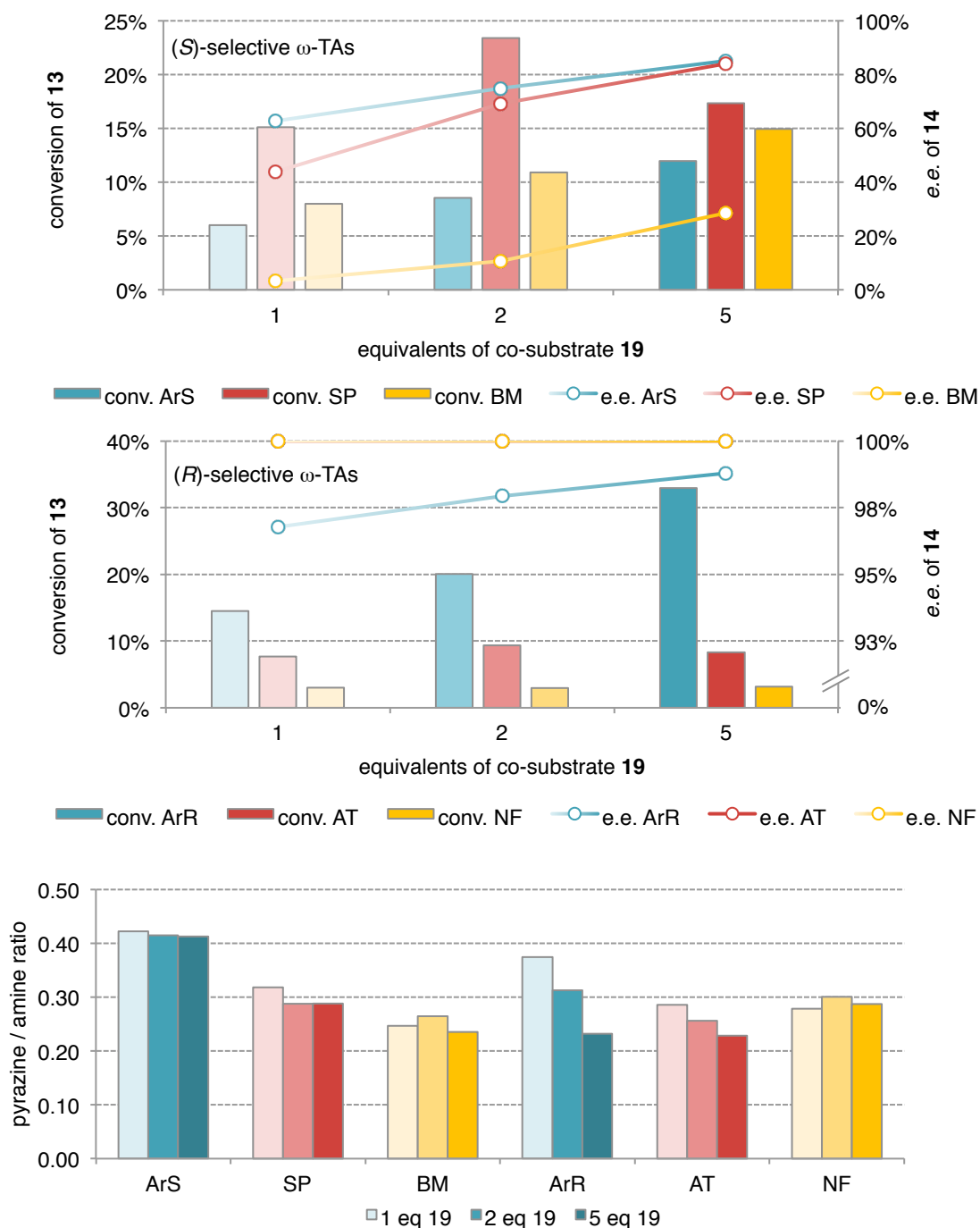Quantification with GC-FID on a DB-1701 column.
The *e.e.* was measured with GC-FID on a chiral phase (DEX-CB column) after *N*-acetylation of **14** (2 eq Ac$_2$O, cat. DMAP, 2 h at 30 °C, 700 rpm, then + 500 μL Na$_2$CO$_3$ sat. for 1 h)

Addition of water immiscible solvents (100 v% of toluene, MTBE or EtOAc) resulted in 0 % conversion. With DMSO, the highest conversions were achieved, however with very bad *e.e.*'s for (*S*)-selective enzymes. By plotting the *e.e.* against the conversion for all co-solvents, a negative correlation between these parameters emerges.
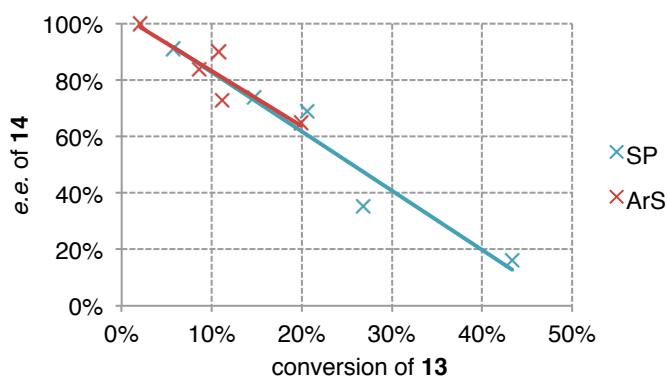
Figure 2.11 | Correlation of *e.e.* and conversion with (*S*)-selective ω-TAs.

2.2.3.4 Oxidation Agents

The second step in the follow-up reaction of co-products **19a** and **19b** after dimerization was the oxidation of the 2,4-dihydropyrazines **26a** and **26b**. The most obvious way to facilitate this step was the application of oxidation agents. For this purpose, a model reaction employing **19** as substrate and pyruvate as co-substrate as depicted in Scheme 2.16 was chosen. The driving force is partially provided by thermodynamically favored formation of alanine. This ensures that **19a** and/or **19b** are formed and can undergo the follow-up reaction, which then contributes to equilibrium displacement. The results should give information on oxidant effects on pyrazine formation and their compatibility to the enzymes.
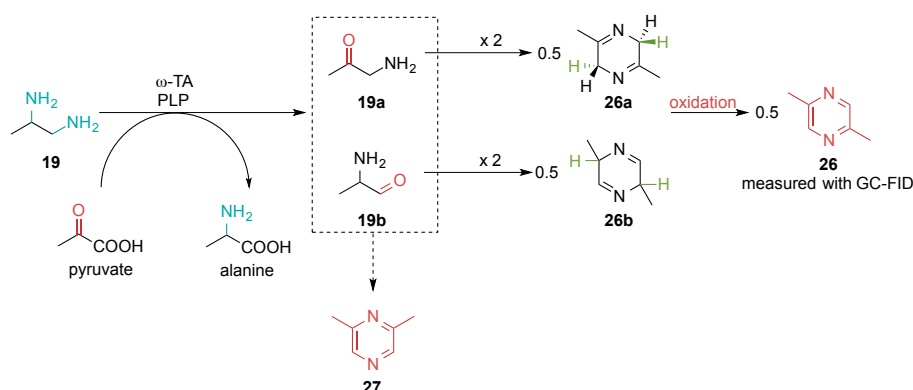
Scheme 2.16 │ Model reaction for examining the effect of oxidants on the pyrazine formation from **19**.

Regarding analysis of the reactions, only the aromatic compound **26** derived from homo-dimerization was considered. The other possible isomer **27**, which is the product of hetero-dimerization, was not detected.
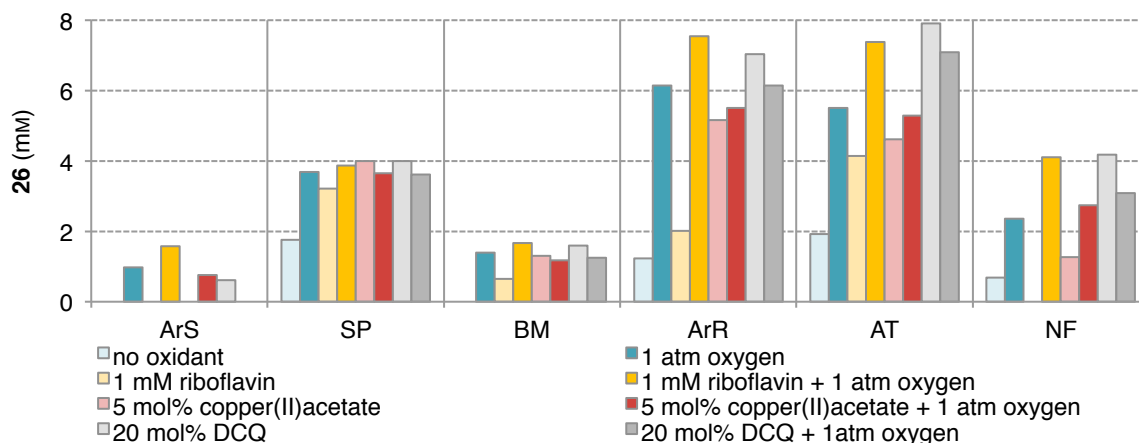
Figure 2.12 │ Effects of various oxidants with (full colored bars) and without (pale colored bars) oxygen-atmosphere on pyrazine **26** formation.

Conditions: lyophilized cells containing ω-TA (20 mg/mL), PLP (1 mM) and 50 mM Na-pyruvate in 1 mL 100 mM KPi-buffer pH 7 incubated with 50 mM substrate **19** at actual pH 9 for 72 h at 30 °C, 700 rpm with the oxidizing conditions denoted in the legend above. DCQ = 1,4-dichlorobenzoquinone.
Pyrazine quantification with GC-FID on a DB-1701 column.

The shade of the bars in Figure 2.12 correspond to the different oxidants applied and the color intensity implies whether the reactions were run with or without oxygen pressure. The results for each ω-TA are summarized within one group of bars. Comparing the light-blue bars on the left edge, which refer to reactions without any oxidant, with the other adjacent bars within one group, already suggests a positive effect of present oxidants on pyrazine formation. In other words, the additionally formed moles of pyrazine are derived from the effect of equilibrium displacement, which was in turn caused by the oxidant-enhanced follow-up reaction. Even the application of only 1 atm oxygen pressure enhanced the pyrazine concentration five-fold in some cases (compare light-blue and blue bars). In general, (R)-selective ω-TAs gave higher pyrazine levels than the (S)-selective ones, however, at none of the used conditions a full conversion of **19** to **26** (theoretically 25 mM) could be detected. There was no data acquired that would provide information about the extent of the intermediate biotransformation and dimerization.

Nonetheless the positive results in this study motivated to investigate the biotransformation of model substrate **13** under oxidative conditions (for the experimental setup see Scheme 2.14).
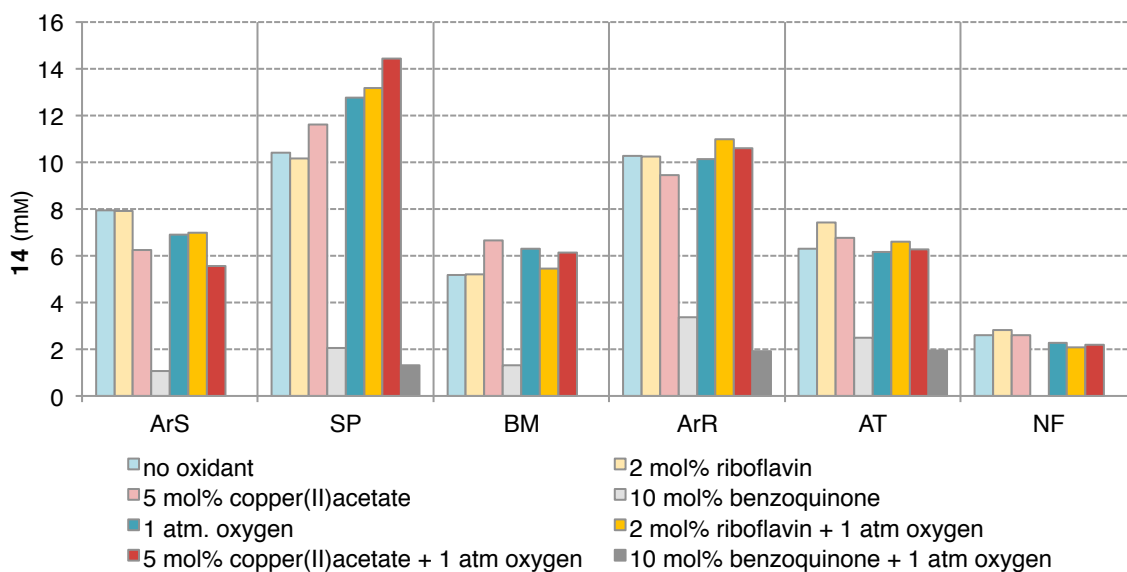
Figure 2.13 | Effects of various oxidants without (pale colored bars) and with (full colored bars) oxygen-atmosphere on amine **14** formation.

Conditions: lyophilized cells containing ω-TA (20 mg/mL), PLP (1 mM) and 1 eq co-substrate **19** (50 mM) in 1 mL 100 mM KPi-buffer pH 9.6 incubated with 50 mM substrate **13** for 72 h at 30 °C, 700 rpm with the oxidizing conditions denoted in the legend above. Quantification with GC-FID on a DB-1701 column.

The conversion values presented in Figure 2.13 should be considered with precaution because the reactions conducted with oxygen atmosphere were found to be prone to evaporation losses. By performing blank-samples, it was found that this effect was more pronounced on

substrate ketone **13** (31% recovery) than on its corresponding amine (90% recovery)[3]. Thus, the conversion was here interpreted in terms of mM of amine **14** formed and data comparisons were limited to values either with or without oxygen atmosphere (i.e. only within pale-colored *or* full-colored bar groups).

All in all, the effects of oxidants on the formation of amine **14** are only minimal. In the case of benzoquinone, which was used instead of 1,4-dichlorobenzoquinone in the former study, they were even inferior. Changes in *e.e.* and pyrazine / amine ratio with different oxidants are subsequently tabulated in Table 2.16, where an enhancement for both parameters was expected.

Table 2.16 | Effects of various oxidants with and without oxygen-atmosphere on the enantiomeric excess of product amine **14** and the pyrazine / amine ratio (p/a).

(S)-selective ω-TAs	ArS		SP		BM	
Additives	*e.e.* (%)	p/a ratio	*e.e.* (%)	p/a ratio	*e.e.* (%)	p/a ratio
no oxidant	30	0.32	29	0.22	< 1	0.16
2 mol% riboflavin	31	0.35	31	0.25	< 1	0.27
5 mol% copper(II)acetate	31	0.27	22	0.21	< 1	0.18
10 mol% benzoquinone	> 99	< 0.1	81	0.16	12	< 0.1
1 atm. oxygen	43	0.22	31	0.18	< 1	0.17
2 mol% riboflavin + 1 atm oxygen	42	0.23	29	0.22	< 1	0.21
5 mol% copper(II)acetate + 1 atm oxygen	43	0.19	n.d.	0.08	n.d.	0.17
10 mol% benzoquinone + 1 atm oxygen	85	< 0.1	86	< 0.1	> 99	n.d.

---

[3] From triplicate samples treated the same way as oxygen-atmosphere samples. Quantification with GC-FID on a DB-1701 column.

(R)-selective ω-TAs	ArR		AT		NF	
Additives	e.e. (%)	p/a ratio	e.e. (%)	p/a ratio	e.e. (%)	p/a ratio
no oxidant	93	0.28	98	0.30	98	0.32
2 mol% riboflavin	93	0.33	99	0.29	98	0.41
5 mol% copper(II)acetate	92	0.28	99	0.23	98	0.25
10 mol% benzoquinone	> 99	0.22	> 99	0.19	n.d.	n.d.
1 atm. oxygen	94	0.24	> 99	0.16	> 99	0.23
2 mol% riboflavin + 1 atm oxygen	95	0.27	99	0.22	> 99	0.34
5 mol% copper(II)acetate + 1 atm oxygen	94	0.21	99	0.15	> 99	0.25
10 mol% benzoquinone + 1 atm oxygen	> 99	0.17	> 99	< 0.1	n.d.	n.d.

Conditions: see Figure 2.13.
Quantification of amine **14** and pyrazine **26** with GC-FID on a DB-1701 column.
The *e.e.* was measured with GC-FID on a chiral phase (DEX-CB column) after *N*-acetylation of **14** (2 eq Ac_2O, cat. DMAP, 2 h at 30 °C, 700 rpm, then + 500 μL aq. Na_2CO_3 sat. for 1 h)

Again, it appeared that there is a correlation between conversion and *e.e.* for (*S*)-selective enzymes where a higher conversion is accompanied by lower *e.e.*'s and *vice versa* (compare Figure 2.13 and Table 2.16 and see also Figure 2.11). For example, with ArS the *e.e.* benefits from the addition of oxidants, especially from benzoquinone, but here the conversion is not feasible as mentioned before. Where applied, an oxygen atmosphere in some cases also seems to facilitate *e.e.* enhancement.

(*R*)-selective enzymes gave very good to excellent *e.e.*s in all cases, but a negative effect of oxygen on pyrazine formation indicated by lower p/a ratios was noted. However, a distortion of this parameter by evaporation losses cannot be excluded and thus should be subject to further evaluation.

2.2.3.5 Palladium on Charcoal

As an alternative to the aforementioned oxidation agents, the supplementation of catalytic amounts of palladium on activated charcoal (7 wt%) and its impact on the reaction was tested. Since metallic palladium exhibits an affinity towards molecular hydrogen, the intended action was the withdrawal of hydrogen from dimers **26a** and **26b** (green labelled hydrogens in Scheme 2.16) and thus oxidation to the pyrazine. The screening was conducted with 1, 2 or 5 equivalents of co-substrate.

Figure 2.14 | Effect of Pd/C on the follow-up reaction employing 1, 2 or 5 eq co-substrate **19**. The bar's color intensity correlates with the co-substrate concentration.

Conditions: lyophilized cells containing overexpressed ω-TA (20 mg/mL), PLP (1 mM) and 1,2 or 5 eq co-substrate **19** (50, 100 or 250 mM) in 1 mL 100 mM KPi-buffer pH 9.5 (adjusted with H_3PO_4 conc.). 7 wt% (of **13**) Pd/C, incubation with 50 mM substrate **13** for 24 h at 30 °C, 700 rpm.
Conversions were determined with GC-FID on a DB-1701 column.
The *e.e.* was measured with GC-FID on a chiral phase (DEX-CB column) after *N*-acetylation of **14** (2 eq Ac_2O, cat. DMAP, 2 h at 30 °C, 700 rpm, then + 500 μL Na_2CO_3 sat. for 1h)

Compared to the results in Figure 2.7 where no Pd/C was applied, no significant differences in any of the measured parameters emerged.

2.2.4 The e.e. Problem with (S)-Selective Enzymes

In order to assess whether the bad *e.e.*'s with (*S*)-selective ω-transaminases derive from an accumulation of stereochemical errors of the enzyme when the system reaches equilibrium or from a *per se* bad selectivity of the enzyme the following experiments were conducted.

The performance of the (*S*)-selective transaminase ArS was tested against an older cell preparation containing this enzyme using an AlaDH / FDH recycling system for equilibrium displacement. Perfect *e.e.*'s and good conversions were measured, indicating that the enzyme is enantioselective but the follow-up reaction with the 1,2-diamine substrate is too slow compared to the biotransformation. This justifies the conducted experiments to speed up the aforementioned follow-up reaction.

Table 2.17 | ArS performance test: comparison with other cell preparation.
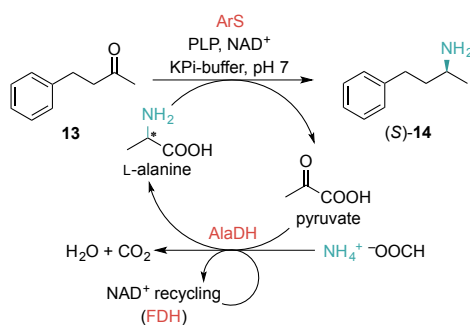
ω-TA	conv. (%)	*e.e.* (%)	recovery (%)
ArS current batch	67	96	> 99
ArS old batch	30	> 99	> 99

Conditions: lyophilized cells containing ω-TA (20 mg/mL), L-alanine (500 mM), ammonium formate (150 mM), PLP (1 mM), NAD$^+$ (1 mM), AlaDH (solution) (12 U), FDH (lyophilisate) (11 U) in 1 mL 100 mM KPi-buffer pH 7.0 rehydrated for 30 min at 30 °C and 700 rpm. 50 mM substrate **13** added volumetrically, incubation for 24 h at 30 °C, 700 rpm.
Conversions measured with GC-FID on a DB-1701 column.
The *e.e.* was measured with GC-FID on a chiral DEX-CB column after *N*-acetylation of **14** (2 eq Ac$_2$O, cat. DMAP, 2 h at 30 °C, 700 rpm, then + 500 μL Na$_2$CO$_3$ sat. for 1 h).

Furthermore, a possible racemization of enantiomerically pure amine **14** and MBA was tested at the biotransformation conditions used in the latter screenings. The effect of catalytical amounts of the corresponding ketones was also addressed here.

Table 2.18 | Suspected racemization of optically pure amines with 1,2-diaminopropane buffer conditions.

Conditions: lyophilized *E. coli* cells containing ω-TA (20 mg/mL), PLP (1 mM) in 1 mL 50 mM **19**-buffer pH 9.0 (adjusted with HCl conc.) rehydrated for 30 min at 30 °C and 700 rpm. 50 mM substrate (*R*)-**14** or (*S*)-MBA and, as indicated, 5 mol% **13** or acetophenone added volumetrically, incubation for 24 h at 30 °C, 700 rpm. The *e.e.* was measured with GC-FID on a chiral phase (DEX-CB column) after *N*-acetylation of **14** and MBA (2 eq Ac$_2$O, cat. DMAP, 2 h at 30 °C, 700 rpm, then + 500 μL Na$_2$CO$_3$ sat. for 1 h).

Amine	(*R*)-**14**		(*S*)-MBA	
Cat. ketone	without **13**	with 5 mol% **13**	without acetophenone	with 5 mol% acetophenone
e.e. (%)	98	92	> 99	> 99

The results give rise to the assumption that, under these conditions, a racemization of amine **14** takes place to some extent. However, this was only a single experiment and hence these results should be supported by further experiments.

2.2.5 Model Substrate Conversion Study

Finally, the conditions that gave the best results in terms of conversion and e.e. were applied to a set of structurally diverse substrates and the results were compared to a system employing iso-propylamine **15** as co-substrate. In addition, the reaction outcome after 5 hours and 3 days were measured to account for kinetic or thermodynamic effects, respectively. All experiments were conducted at the enzymes' pH-optimum (Table 2.19).

These conditions involved the usage of aqueous co-substrate buffer instead of potassium phosphate buffer. With this buffer, a moderate excess of 5 eq of co-substrate **19** was chosen in order to achieve reasonable conversion. Apart from these, no other additives were used since none of them turned out to be really effective and the system was kept as simple as possible.

Regarding the model substrates, a selection of established substrates for ω-transaminases was used. The emphasis was put on structurally diverse ketones and intra-molecularly stabilized co-products through hydrogen bonding (**30a** and **31a**) or cyclization (**32a**).

Table 2.19 | Substrate conversion comparison using two different co-substrates.

ω-TA co-substrate	SP 15		SP 19		ArR 15		ArR 19	
substrate	conv. (%)	e.e. (%)	conv. (%)	e.e. (%)	conv. (%)	e.e. (%)	conv. (%)	e.e. (%)
13	42	77	21	85	13	> 99	12	> 99
27	75	87	45	93	53	97	35	98
28	–	–	–	–	–	–	–	–
29	45	88	22	97	24	> 99	17	> 99
30	98	77	92	84	97	> 99	72	> 99
31	< 1	n.d.	< 1	n.d.	< 1	n.d.	< 1	n.d.
32	98	n.d.	31	n.d.	70	n.d.	5	n.d.

ω-TA co-substrate	SP 15		SP 19		ArR 15		ArR 19	
substrate	conv. (%)	e.e. (%)	conv. (%)	e.e. (%)	conv. (%)	e.e. (%)	conv. (%)	e.e. (%)
13	67	2	53	70	57	98	38	> 99
27	81	24	67	89	78	98	78	89
28	*93*	> 99	*> 99*	> 99	*78*	> 99	*65*	> 99
29	52	< 1	55	82	44	> 99	43	> 99
30	99	12	> 99	81	99	99	95	> 99
31	< 1	n.d.	< 1	n.d.	< 1	n.d.	< 1	n.d.
32	98	n.d.	37	n.d.	98	n.d.	5	n.d.

Upper table: 5 h reaction time; lower table: 72 h reaction time.

Conditions: lyophilized cells containing ω-TA (20 mg/mL), PLP (1 mM) in 500 μL of a 250 mM (5 eq) aqueous co-substrate **19** buffer pH 9 (SP) or pH 10 (ArR) (adjusted with HCl conc.) rehydrated for 30 min at 30 °C, 700 rpm. Incubation with 50 mM substrate **13**, **27-32** for 5 h or 72 h at 30 °C, 700 rpm.

Conversions were determined with GC-FID on a DB-1701 column, except for **32** where GC-MS was used additionally.

The e.e. was measured with GC-FID on a chiral phase (DEX-CB column) after N-acetylation of the amine (2 eq Ac$_2$O, cat. DMAP, 2 h at 30 °C, 700 rpm, then + 500 μL Na$_2$CO$_3$ sat. for 1 h).

The attempted conversion of the tetralin derivative **28** gave a mixture of undefined compounds, which hampered conversion measurement and *e.e.* determination. The conversions obtained for this substrate after 72 h were derived from peaks with very low areas, meaning an incomplete molar recovery due to side reactions (values in *italic*).

Substrate **31** exhibits a considerable volatility, which made its quantification (and therefore conversion measurement) difficult. No compound matching the GC-FID retention time of the amine could be detected.

32 in combination with the diamine co-substrate **19** yielded a large quantity of a pyrrole derivative as result of a PAAL-KNORR synthesis. Since a reference substrate of pyrroline **32a** was lacking, the conversion needed to be deduced from GC-FID and GC-MS spectra.

The most important difference regards the *e.e.*, which, for (*S*)-ω-TAs, is considerably better when using the diamine co-substrate instead of isopropylamine. This indeed indicates a restriction of the back-reaction with this system by equilibrium displacement, which limits the accumulation of stereochemical errors. The differences in conversions by using either co-substrate **15** or **19** were measurable but depend strongly on the nature of the substrate. The new smart co-substrate **19** can compete with the well-established isopropylamine in conversion of at least 2 substrates.

Nonetheless, the experiments with incomplete datasets should be repeated and the analytical methods improved in order to obtain more reliable results.

Racemic amines **27a**, **28a** and **30a**, which were required as reference substances, were synthesized in good yields within this work *via* reductive amination of **27**, **28** and **30** using ammonium formate and sodium cyano borohydride.

2.2.6 Summary

Eleven bi-functional co-substrates were tested towards their compatibility with 14 ω-transaminases derived from various organisms. Only three of these co-substrates could compete with the reference co-substrate isopropylamine in terms of conversion and were thus the subject of further investigation.

The pH-optimum was found between 9 and 10 for all enzyme/co-substrate pairings, whereby 1,2-diaminopropane showed the best conversion. The *e.e.* was excellent for (*R*)-selective, but bad to moderate for (*S*)-selective enzymes – an observation that persisted throughout all conducted experiments. Moreover, the reaction could be conducted in an aqueous co-substrate buffer at pH ≥ 9.0, thereby rendering the system more straightforward.

Attempts to improve dimerization by variation of co-substrate and substrate concentration was successful. An enhancement in both conversion and *e.e.* (for [S]-selective enzymes) could be detected if the concentration of either reaction partner was increased. On the other hand, supplementing chelating magnesium(II) ions had a positive effect on conversion or *e.e.* depending on the (*S*)-selective transaminases used.

Oxidation agents indeed enhanced the formation of pyrazine in a model reaction using 1,2-diaminoethane and pyruvate as substrates, but when returning to the transamination of 4-phenyl-2-butanone with these conditions, they failed. Neither improvement of conversion nor *e.e.* nor pyrazine formation could be observed. This was also the case for the addition of catalytic amounts of Pd/C.

Regarding organic co-solvents, only the addition of 5 vol% DMSO caused an increase in both conversion and *e.e.* for three out of four transaminases. Water immiscible solvents turned out to be inferior for conversion as no amine product could be observed for these samples.

Finally, the novel smart co-substrate system was tested by the formal reductive amination of various ketone substrates and compared with the results using isopropylamine as co-substrate. For this screening, the simplest conditions possible were applied, namely 50 mM substrate and aqueous co-substrate buffer with an optimal pH-value providing the system with 5 eq of amine donor. Whereas the conversion could compete with the reference co-substrate in only some instances, the *e.e.* for the examined (*S*)-selective enzyme was considerably enhanced. For the (*R*)-selective enzyme, isopropylamine gave better conversions but the *e.e* was perfect with both co-substrates.

2.2.7 Outlook

The co-substrate concept developed herein has the potential to displace the equilibrium to the product side. Nevertheless, extensive studies in terms of additives and reaction conditions did not achieve a quantitative conversion, meaning there is still room for improvement. Beside the 1,2-diaminopropane, other 1,2-diamines should be tested for their capability to serve as co-substrates (note: 1,2-diaminoethane did not work well in the initial screening).

Conducting the reaction in neat organic solvent such as TBME or ethyl acetate might also be considered. In order to gain more insight to the follow-up reaction, also a kinetic resolution of 2,3-diaminobutane could be performed.

The observed racemization of enantiomerically pure amine **14** gives rise to a more extensive investigation of this observation. The controlled racemization of amines would be of interest in, for example, dynamic kinetic resolutions of racemic amines or other desymmetrization techniques.

Finally, the promising results obtained herein pose a solid base for further studies on this "smart co-substrate" system, which indeed has the potential for industrial application.

3 Experimental
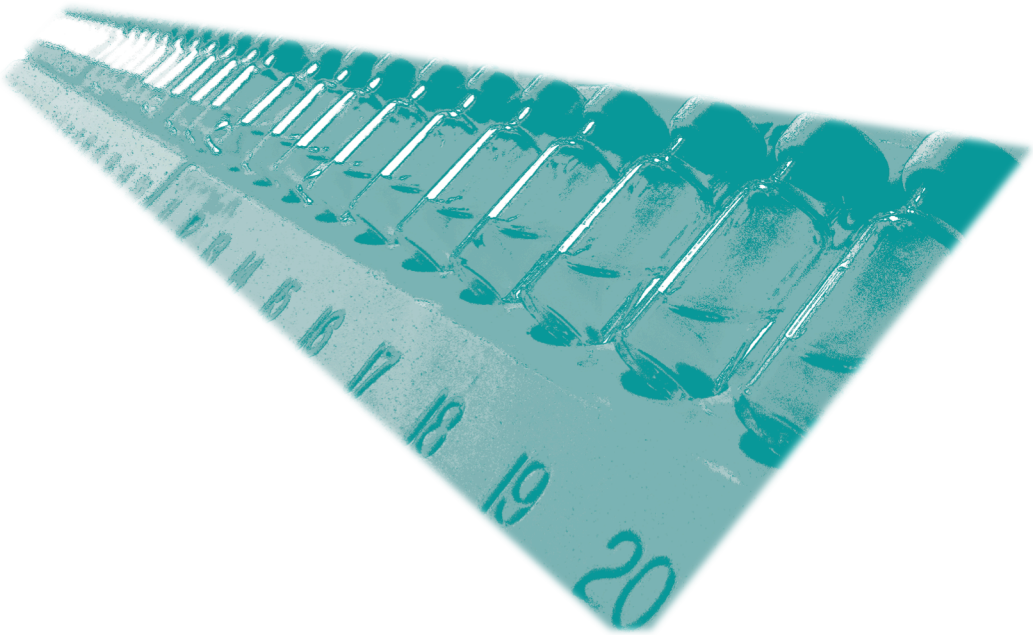
3.1 Materials

3.1.1 Compounds Used for the Chemo-Enzymatic Synthesis of Xenovenine

No.	Substance	Purity (%)	Supplier	Lot No.	Unit Size
12a	Furan	≥ 99.0	Fluka	1325101	50 mL
13	1-Bromoheptane	99	Sigma Aldrich	MKBG1477	100 mL
–	*n*-Butyllithium	2.5 M in hexanes	Sigma Aldrich	SHBD4553V	25 mL
–	THF[a]	99	VWR	n.a.	2.5 L
11	2-*n*-heptylfuran	98	Alfa Aesar	10157934	10 g
9	3-Buten-2-ol	97	Sigma Aldrich	MKAA3214	5 g
–	Palladium(II)acetate	99	Lancaster	FA001461	2 g
–	Acetic acid	100	VWR	10C290524	2.5 L
–	Copper(II)acetate	98	Sigma Aldrich	STBB7235V	25 g
–	Molecular sieve UOP 3Å	powder	Fluka	1336967	250 g
10	3-Buten-2-one	99	Sigma Aldrich	STBC2018V	100 mL
–	Hydroquinone	n.a.	BASF	n.a.	25 g
–	Ammonium formate	≥ 98	Riedel de Haën	72000	500 g
–	Sodium cyanoborohydride	95	Sigma Aldrich	SHBD3096	10 g
–	Methanol	≥ 99	Roth	483207422	1 L
–	Acetic anhydride	≥ 99	Sigma Aldrich	BCBF5751V	1 L
–	4-(Dimethylamino)pyridine (DMAP)	> 99	Sigma Aldrich	n.a.	50 g
–	Hydrochloric acid	35	VWR	12B020511	2.5 L
–	Palladium on activated charcoal	10 % Pd basis	Sigma Aldrich	BCBM4564V	10 g
–	Trifluoroacetic acid (TFA)	≥ 98	Fluka	81690	25 mL
–	Pivalic acid	99	Sigma Aldrich	SHBC6571V	5 mL
–	Benzoic acid	≥ 99.5	Fluka	1382368	50 g
–	*p*-Toluenesulfonic acid (*p*-TsOH) monohydrate	97	Alfa Aesar	D02W017	50 g
–	(1*R*)-(–)-Camphor-10-sulfonic acid [(–)-CSA]	≥ 98	Alfa Aesar	10176892	25 g
–	(1*S*)-(+)-Camphor-10-sulfonic acid [(+)-CSA]	99	EGA Chemie	n.a.	100 g
–	Triethylamine	≥ 99	Sigma Aldrich	STBD4118V	1 L
–	Chloroform-*d*	99.8 at-% D	ARMAR Chemicals	1098	100 mL
–	Silica gel 60 (0.04 - 0.063)	n.a.	Merck	TA1860785335	5 kg

[a] Freshly distilled from potassium/benzophenone.

3.1.2 Compounds, "Smart Co-Substrates" and Reference Materials

No.	Substance	Purity (%)	Supplier	Lot No.	Unit Size
–	*n*-Dodecane	≥ 99	Sigma Aldrich	08022BI-101	100 mL
13	4-Phenyl-2-butanone	98	Sigma Aldrich	S39821-017	250 mL
rac-**14**	1-Methyl-3-phenylpropylamine	98	Sigma Aldrich	55008319	25 g
15	*i*-Propylamine	≥ 99.5	Sigma Aldrich	BCBJ0566V	25 mL
16	*n*-Propylamine	98	Sigma Aldrich	S37865-237	250 mL
17	1,2-Diaminoethane	"for synthesis"	Merck	8148774	1 L
18	1,2-Diaminocyclohexane (mixture of *cis* and *trans*)	99 %	Sigma Aldrich	MKBN4417V	50 mL
19	1,2-Diaminopropane	≥ 99	Fluka	11108261	100 mL
		99	Sigma Aldrich	MKBH4474V	500 g
20	1,4-Diaminobutane	≥ 99	Fluka	1198498	10 mL
21	1,5-Diaminopentane (Cadaverine)	95	Sigma Aldrich	BCBB5182V	5 g
22	4-Amino-1-butanol	98	Sigma Aldrich	STBD5458V	5 g
23	5-Amino-1-pentanol	95	Sigma Aldrich	BCBD6087V	10 g
24	Taurine	≥ 99	Sigma Aldrich	BCBJ5897V	25 g
25	Hypotaurine	≥ 98	Sigma Aldrich	SLBF2197V	100 mg
26	2,5-Dimethylpyrazine	≥ 98	Sigma Aldrich	MKBG8106V	10 g
27	4-Methoxyphenylacetone[a]	≥ 97	Sigma Aldrich	S28569V	10 g
28	7-Methoxy-2-tetraline[a]	n.a.	BASF SE	n.a.	25 g
29	2-Octanone	98	Sigma Aldrich	BO0610BO	25 mL
29a	2-Octylamine	99	Sigma Aldrich	S24013-427	10 g
30	1-Phenoxypropan-2-one[a]	97	Sigma Aldrich	STBB0282V	5 g
31	Methoxyacetone	95	Sigma Aldrich	MKBK2015V	1 g
31a	1-Methoxy-2-propylamine	95	Sigma Aldrich	01611AHV	5 g
32	2,5-Hexanedione	97	Lancaster	10060525	25 g

[a]   The corresponding *rac*-amines were prepared within this work.

3.1.3 Compounds and Co-Solvents Used for Biocatalytic Screenings in Both Projects

Substance	Purity (%)	Supplier	Lot No.	Unit Size
Pyridoxal-5'-phosphate	97	Sigma Aldrich	1340567	25 g
Nicotinamide adenine dinucleotide (NAD$^+$)	n.a.	BASF	n.a.	25 g
Nicotinamide adenine dinucleotide phosphate (NADP$^+$)	99	Codexis	H71750.06	5 g
Potassium phosphate monobasic	> 99	Sigma Aldrich	SZBD0710V	1 kg
Potassium phosphate dibasic	≥ 99	Merck	AM0419304417	1 kg
Sodium pyruvate	≥ 99	Sigma Aldrich	SLBC6057V	25 g
L-Alanine	≥ 99.5	Fluka	0001440397	25 g
D-Alanine	≥ 98	Sigma Aldrich	SLBG243V	25 g
D-(+)-Glucose	≥ 99.5	Sigma Aldrich	071M01452V	5 kg
n-Heptane	99	Sigma Aldrich	MKBF6327V	1 L
Dimethylformamide (DMF)	≥ 99.8	Roth	29045510	1 L
Dimethyl sulfoxide (DMSO)	≥ 99.9	Sigma Aldrich	25296PMV	1 L
t-Butyl methyl ether (TBME)	≥ 99.5	Roth	473206781	1 L
n-Butanol	99.7	VWR	11I260500	1 L
L-Alanine dehydrogenase from *B. subtilis*[a]	733 U/mL	Elk group	n.a.	500 μL
Formate dehydrogenase	4.2 U/mg	evocatal	11230-E0595.01	20 g
Glucose dehydrogenase	12 U/mg (NADP) 7 U/mg (NAD)	DSM	n.a.	50 g
Lactate dehydrogenase	429 U/mg	Jülich	n.a.	20 g

[a] Purified enzyme.[39]

3.1.4 Reagents Used for Cell Cultivation

Substance	Purity (%)	Supplier	Lot No.	Unit Size
Tryptone, bacteriological	n.a.	Oxoid	n.a.	500 g
Yeast extract	n.a.	Oxoid	n.a.	500 g
Sodium chloride	≥ 99.8	Roth	n.a.	1 kg
Agar, bacteriological	n.a.	Oxoid	n.a.	500 g
Ampicillin Na-salt	≥ 99	Roth	272184049	100 g
Anhydrotetracyclin (AHT)	n.a.	IBA	04010135	50 mg
Isopropyl β-D-1-thiogalactoside (IPTG)	n.a.	peqlab	13411043	25 g
Competent BL21 (DE3) *E. coli* cells	n.a.	Invitrogen	multiple	25 μL
Competent BL21 (DE3) *E. coli* cells (T1 phage resistant)	n.a.	New England Biolabs	multiple	25 μL
Plasmids harboring ω-TA gene	n.a.	Elk Group	n.a.	n.a.

3.1.5 ω-Transaminases

Source Organism	Abbreviation	Selectivity	pEG No.	FCC No.	Activity[c]
Bacillus megaterium[a]	BM	(*S*)	31	362	0.15
Arthrobacter citreus[a]	ArS	(*S*)	29	366	1.20
Chromobacterium violaceum	CV	(*S*)	20	261	3.32
Vibrio fluvialis[a]	Vf	(*S*)	27	378	4.80
Pseudomonas fluorescens	PF	(*S*)	148	469	1.36
Paracoccus denitrificans[b]	PD	(*S*)	24	282	1.09
Silicibacter pomeroyi	SP	(*S*)	205	533	4.35
Arthrobacter sp.	ArR	(*R*)	23	316	0.96
Arthrobacter sp. round 11 variant[a]	ArRmut11	(*R*)	90	415	0.05
Aspergillus terreus[a]	AT	(*R*)	97	461	2.84
Hyphomonas neptunium[a]	HN	(*R*)	98	462	0.11
Ochrobactrum anthropii	OA	(*R*)	204	532	0.03
Neosartoria fischeri	NF	(*R*)	203	531	0.79
Gibberella zeae	GZ	(*R*)	202	530	1.44

[a] Proteins possessing a HisTag for purification with Ni-affinity chromatography.
[b] Protein possessing a *Strep*Tag for purification with *Strep*-Tactin affinity chromatography.
[c] Activity in U per mg lyophilized *E. coli* cells containing the ω-transaminase. Conditions: 100 mM 1-phenylethylamine, pyruvate (100 mM), pH 7, 30 °C. See also section 3.2.2.

3.2 Procedures

3.2.1 Plasmid Transformation and Heterologous Expression of ω-Transaminases

The plasmids (with respective pEG numbers) harboring the genes encoding the ω-transaminases were transformed into competent BL21(DE3) *E. coli* cells according to the following procedure.

Competent *E. coli* cells and the plasmid solution were thawed on ice. Then, the cell suspension (100 μL of self-made competent cells or 20 μL of commercial competent cells) was carefully mixed with 5 μL plasmid solution (ca. 50 ng plasmid) and kept on ice for 30 min. For negative control, only cell suspension was used. The mixture was heat treated at 42 °C for 10 sec and immediately cooled down on ice for 5 min. After 250 μL SOC recovery medium was added, the vial was incubated for 1 h at 37 °C and 300 rpm. 1 x 100 μL and 1 x 200 μL of liquid cell suspension was then plated on LB-agar plates containing 100 μg/mL ampicillin for selection. The colonies were grown overnight at 37 °C.

A single colony was picked, transferred aseptically to 15 mL LB-medium containing 100 μg/mL ampicillin and incubated overnight at 30 °C and 120 rpm. 3 x 330 mL of sterile LB-medium containing 100 μg/mL ampicillin were then inoculated with 3.3 mL of the over-night culture each and shaken at 30 °C and 120 rpm. When the OD600 reached 0.5, the expression was induced by adding either IPTG (0.5 mM final concentration for CV, ArR, ArRmut11, SP, GZ, NF, OA, AT, NF, HN) or AHT (0.2 mg/L final concentration for BM, ArS, Vf, PD) and incubation at 20 °C and 120 rpm. The cells were harvested after 12 h by centrifugation for 15 min at 5000 rpm and 4 °C. After washing with a few mL of 100 mM KPi-buffer pH 7.0, the cells were freeze-dried overnight and the obtained lyophilisate was stored at 4 °C.

3.2.2 Activity Tests
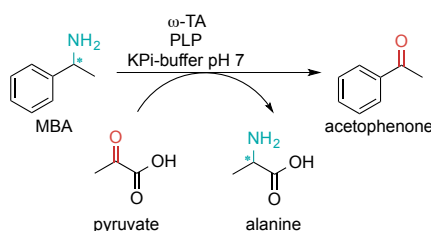
The tests were carried out in an EPPENDORF orbital thermoshaker.

Lyophilized *E. coli* cells (5.0 or 10.0 mg, depending on the expected activity) containing the ω-transaminase were provided in 2.0 mL reaction vials and rehydrated for 30 min at 30 °C, 700 rpm in 1.00 mL of a stock solution containing 1 mM PLP and 100 mM sodium pyruvate in 100 mM KPi-buffer pH 7.0. Then, (+)- or (−)-1-phenylethylamine (depending on the enzyme's selectivity, 13 μL, 100 mM) was added and vortexed to start the reaction. The reaction was stopped after exactly 1, 2 or 3 min (1 sample for each time) by addition of 10 M NaOH (200 μL) and the mixture was extracted with EtOAc (2 x 500 μL).

The combined organic extracts were dried with $MgSO_4$ and subjected to GC-FID analysis. The conversion was deduced from ketone and amine peak areas.

The corresponding activity was subsequently assessed by plotting the conversion against the reaction time and determining the slope. This value was divided through the applied cell mass to obtain the specific activity.

3.2.3 General Procedure for Analytical Biotransformations Employing ω-Transaminases

Variants of the following general procedures and conditions were used as stated in table and figure footnotes throughout section 2. All reactions were carried out in EPPENDORF orbital thermoshakers and 2.0 mL SARSTEDT reaction vessels.

Representative Procedure With AlaDH / FDH Recycling Cascades

Lyophilized *E. coli* cells (20 mg) containing the ω-transaminase, formate dehydrogenase (5 mg, 11 U) and alanine dehydrogenase (15 μL, 12 U) were rehydrated for 30 min at 30 °C, 700 rpm in 1.0 mL of a 100 mM KPi buffer pH 7.0 containing 1 mM PLP, 1 mM NAD^+, 150 mM ammonium formate and 500 mM D- or L-alanine (depending on the enzyme's selectivity). Then, the substrate (50 mM) was added to the cell suspension and the mixture was incubated for 24 h at 30 °C, 700 rpm, horizontally.

The reaction was stopped by the addition of 10 M NaOH (200 μL) and extracted with EtOAc (2 x 500 μL) containing 10.0 mM *n*-dodecane as internal standard. The combined organic extracts were dried with $MgSO_4$ and subjected to GC-FID analysis.

Representative Procedures for Biotransformations Employing Diamine **19** as Smart Co-substrate

Biotransformations with KPi-buffer:

Lyophilized *E. coli* cells (20 mg) containing the ω-transaminase were rehydrated for 30 min at 30 °C, 700 rpm in KPi buffer (1.0 mL, 100 mM pH 7.0) containing 1 mM PLP and 1, 2 or 5 eq 1,2-diaminopropane **19** (adjusted to pH 9 with H_3PO_4 conc.). Then, the substrate (50 mM) was added to the cell suspension and the mixture was incubated for 24 h at 30 °C, 700 rpm, horizontally.

The reaction was stopped by the addition of 10 M NaOH (200 μL) and extracted with EtOAc (2 x 500 μL) containing 10.0 mM *n*-dodecane as internal standard. The combined organic extracts were dried with $MgSO_4$ and subjected to GC-FID analysis.

Biotransformations without KPi-buffer:

Lyophilized *E. coli* cells (20 mg) containing the ω-transaminase were rehydrated for 30 min at 30 °C, 700 rpm in 1,2-diaminopropane buffer (1.0 mL, 50 mM, pH 9.0 or 10.0 adjusted with aq. HCl conc.) containing 1 mM PLP. Then, the substrate (50 mM) was added to the cell suspension and the mixture was incubated for 72 h at 30 °C, 700 rpm horizontally.

The reaction was stopped by the addition of 10 M NaOH (200 μL) and extracted with EtOAc (2 x 500 μL) containing 10.0 mM *n*-dodecane as internal standard. The combined organic extracts were dried with $MgSO_4$ and subjected to GC-FID analysis.

3.2.4 Total Synthesis of (+)- and (–)-Xenovenine

All starting materials were obtained from commercial suppliers and used as received, unless stated otherwise. Where indicated, reactions were carried out with standard SCHLENK techniques under argon atmosphere in oven-dried (120 °C) glassware. THF required for anhydrous reactions was distilled freshly from potassium/benzophenone. AcOH and MeOH were dried over 3 Å molecular sieve for at least 48 h prior to use. Solvents were dried and purified by conventional methods prior to use. Preparative chromatographic separations were performed by column chromatography on MERCK silica gel 60 (0.063–0.200 mm). Solvents for flash chromatography (petroleum ether/ethyl acetate) were distilled before use. Petroleum ether refers to a fraction with a boiling point between 40–60 °C. TLC was carried out with pre-coated aluminium sheets (TLC Silica gel 60 F_{254}, MERCK) with detection by UV (254 nm) and/or by staining with anisaldehyde solution [*p*-anisaldehyde (1.00 g), conc. H_2SO_4 (2.00 mL), EtOH (100 mL)], cerium molybdenum solution [phosphomolybdic acid (25 g), Ce(SO₄)2·H2O (10 g), conc. H_2SO_4 (60 mL), H_2O (940 mL)] or ninhydrin solution [ninhydrin (1.5 g) and AcOH (3 mL) in 100 mL *n*-butanol]. Melting points were determined on a GALLENKAMP melting point device. Optical rotation was measured at 20 °C on a PERKIN–ELMER Polarimeter 341 against the sodium D-line. GC-MS spectra were recorded with an AGILENT 7890A GC-system, equipped with an AGILENT 5975C mass selective detector and a HP-5 MS column (30 m x 0.25 mm x 0.25 μm) using helium as carrier gas (flow = 0.5 mL/min). HR-MS data was obtained on a THERMO-SCIENTIFIC Q-Exactive system using APCI in full scan mode (m/z : 90–1000); 5 mg/mL (in MeOH or *i*-PrOH) samples were diluted 40 times with acetonitrile and 25 μL were injected into a 100 μL/min flow of acetonitrile. ¹H and ¹³C NMR spectra were recorded at 20 °C on a BRUKER Avance 300 NMR unit; chemical shifts are given in ppm relative to Me_4Si (¹H: Me_4Si = 0.0 ppm) or relative to the resonance of the solvent (¹H: $CDCl_3$ = 7.26 ppm; ¹³C: $CDCl_3$ = 77.0 ppm).

2-*n*-Heptylfuran **11**
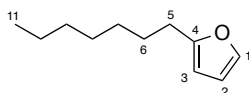
The reaction was carried out under argon inert atmosphere and standard Schlenk conditions.

Furan **12a** (2.0 g, 29.4 mmol) was dissolved in dry THF (40 mL) and cooled to 0 °C. A 2.5 M *n*-butyllithium solution in hexane (12.3 mL, 30.8 mmol, 1.05 eq) was added dropwise through a septum to the cooled, stirred furan solution. After 4 h, bromoheptane (4.6 mL, 29.4 mmol, 1.0 eq) was added dropwise at 0 °C and the mixture was stirred at 21 °C overnight. Product formation was monitored with TLC (petroleum ether/ethyl acetate=9/1). The reaction was quenched with aq. sat. NH_4Cl solution (20 mL) and extracted with ethyl acetate (3 x 30 mL). After washing the combined organic phases with brine (50 mL) and drying over Na_2SO_4 the solvent was evaporated and the brown, oily residue was subjected to flash chromatography (petroleum ether/ethyl acetate 9:1). Heptylfuran **11** was obtained as yellowish oil in 70.2 % yield (3.43 g) after drying *in vacuo*. Spectral data from ^{1}H-NMR matched the one found in literature.[72] R_f (PE/EtOAc 9:1)=0.91. ^{1}H NMR (300 MHz, CDCl$_3$) δ_H [ppm] 7.37 − 7.27 (m, 1H, C^{1}H), 6.40 − 6.20 (m, 1H, C^{2}H), 6.10 − 5.88 (m, 1H, C^{3}H), 2.62 (t, J = 7.6 Hz, 2H, C^{5}H$_2$), 1.76 − 1.45 (m, 2H, C^{6}H$_2$), 1.44 − 1.10 (m, 8H, 4 x C$^{7\text{-}10}$H$_2$), 0.89 (t, J = 6.6 Hz, 3H, C^{11}H$_3$). ^{13}C NMR (75 MHz, CDCl$_3$) δ_C [ppm] 156.8 (C^4), 140.7 (C^1), 110.1 (C^2), 104.6 (C^3), 31.9 (C^5), 29.3, 29.2, 28.2, 28.1, 22.8 (C$^{6\text{-}10}$, alkyl chain), 14.2 (C^{11}). GC-MS (EI+, 70 eV): t_R = 5.34 min; m/z (%) = 166 [M$^+$] (16), 151 (< 1), 137 (3), 123 [C$_8$H$_{11}$O$^+$] (8), 109 [C$_7$H$_9$O$^+$] (8), 95 [C$_6$H$_7$O$^+$] (19), 81 [C$_5$H$_5$O$^+$] (100), 67 (6), 53 (13), 41 (9), 32 (36).

¹H-NMR of **11**
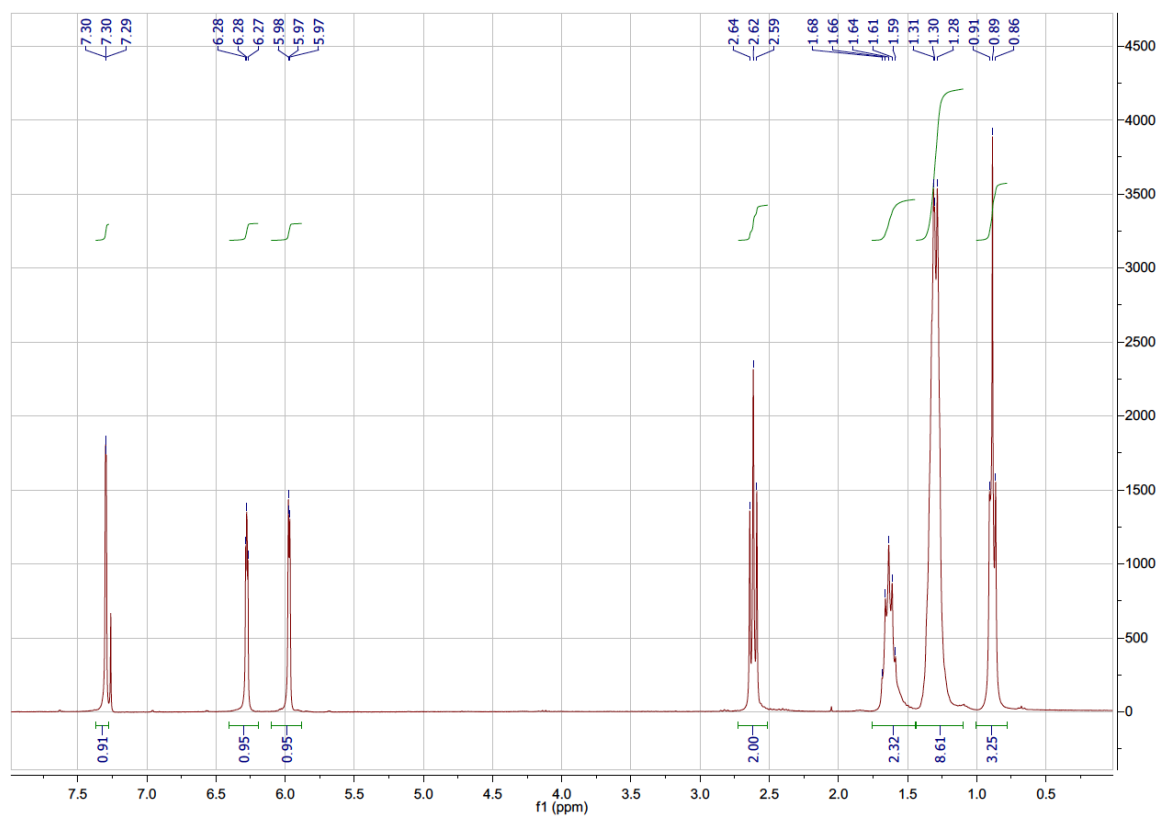
¹³C-NMR of **11**
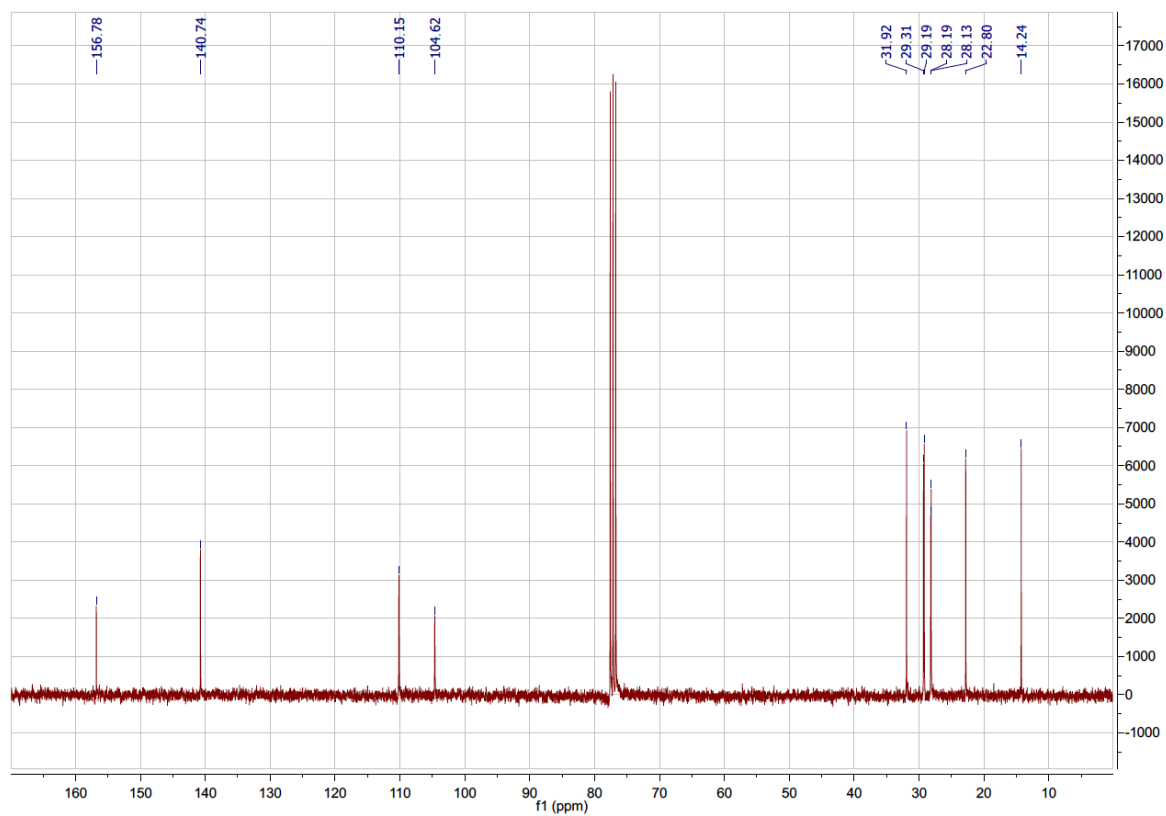
4-(5-Heptylfuran-2-yl)-butan-2-one 8
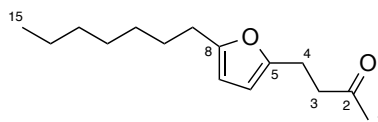
Via oxidative HECK-coupling:

The reaction was carried out under argon inert atmosphere and standard SCHLENK conditions. Palladium(II)acetate (67.5 mg, 300 µmol, 5 mol%) and copper(II)acetate (54.6 mg, 300 µmol, 5 mol%) were weighed into an inert reaction vessel and dissolved in AcOH (24 mL). Heptylfuran **11** (1.0 g, 6.0 mmol) and allylic alcohol **9** (782 µL, 9.0 mmol, 1.5 eq) were added to the greenish suspension and a balloon filled with oxygen was attached *via* a septum to the vessel. The reaction was stirred at 55 °C under oxygen atmosphere for 20 h after which an almost full conversion of **11** was detected with GC-MS and TLC. The reaction was stopped by addition of aq. sat. $NaHCO_3$ solution (100 mL) and shaken until gas evolution deceased. The neutral aqueous phase was then extracted with EtOAc (3 x 50 mL), the organic phases were combined, filtered through a small pad of celite and dried over Na_2SO_4. After evaporation of the solvent, the resulting brown oil was purified using flash column chromatography (petroleum ether/ethyl acetate=20/1) to yield 684 mg of **8** as pale yellow oil (48 %) after drying *in vacuo*. Analytical data see below.

Via DIELS-ALDER cycloaddition:

Heptylfuran **11** (2.00 g, 12.03 mmol) and *p*-dihydroxybenzene (132.5 mg, 1.2 mmol, 10 mol%) were dissolved in AcOH conc. (10 mL), and 3-buten-2-one **10** (976 µL, 12.03 mmol, 1 eq) was added. The mixture was stirred for 48 h at 21 °C after which TLC and GC-MS confirmed quantitative conversion of **11**. The reaction was quenched by adding aq. $NaHCO_3$ sat. solution (100 mL) and vigorous stirring until gas evolution deceased. The neutral aqueous phases were extracted with EtOAc (3 x 50 mL), the combined organic phases were dried over Na_2SO_4 and evaporated under reduced pressure. The resulting dark-brown oil was subjected to flash column chromatography (petroleum ether/ethyl acetate=9/1) to yield 2.0 g of **8** as yellowish oil (70 %) after drying *in vacuo*. R_f (PE/EtOAc 9:1) = 0.48. ^1H NMR (300 MHz, CDCl$_3$) δ_H [ppm] 5.84 (dd, J = 8.5, 3.0 Hz, 2H, C^6H and C^7H, aromatic), 2.81 (qd, J = 8.4, 1.7 Hz, 4H, C^4H_2 and C^5H_2), 2.54 (t, J = 7.6 Hz, 2H, C^9H_2), 2.16 (s, 3H, C^1H_3), 1.59 (p, J = 7.2 Hz, 2H, $C^{10}H_2$), 1.42 – 1.16 (m, 8H, $C^{11-14}H_2$), 0.88 (t, J = 6.7 Hz, 3H, $C^{15}H_3$). ^{13}C NMR (75 MHz, CDCl$_3$) δ_C [ppm] 207.7 (C=O), 155.3, 152.5 (C^5, C^8), 105.6, 105.1 (C^6, C^7), 42.0 (C^3), 31.9, 30.1, 29.3, 29.2, 28.2, 28.1, 22.8, 22.5 (C^1, C^9-C^{14}), 14.2 (C^{15}). GC-MS (EI+, 70 eV): t_R = 11.62 min; m/z (%) = 236 [M$^+$] (31), 221 (2), 207 (< 1), 193 [$C_{13}H_{21}O^+$] or [$C_{12}H_{17}O_2^+$] (14), 179 [$C_{12}H_{19}O^+$] or [$C_{11}H_{15}O_2^+$] (36), 164 (1), 151 [$C_9H_{11}O_2^+$] (100), 135 (3), 122 (4), 107 (16), 95 (11), 81 (17), 67 (3), 55 (7), 43 (24), 32 (< 1). HR-MS: m/z = 237.1852 [MH$^+$] (calcd.: 237.1849).

¹H-NMR of **8**
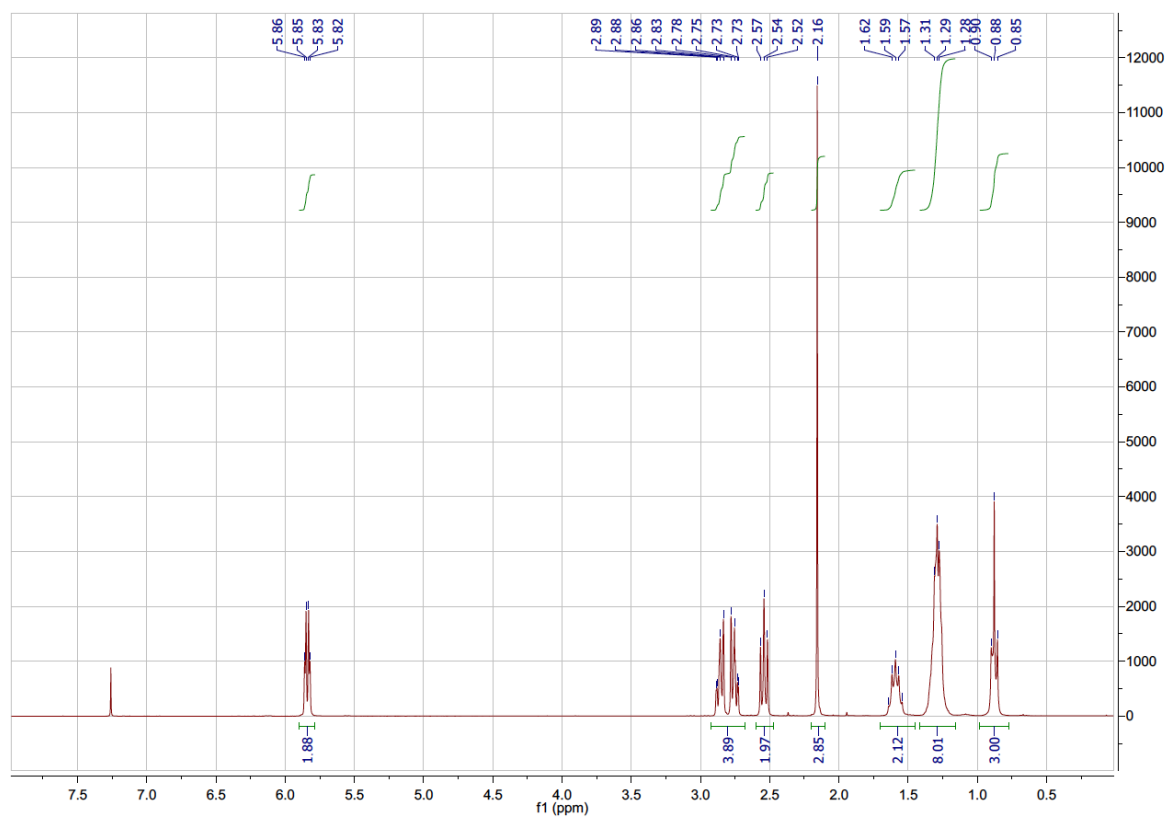
¹³C-NMR of **8**
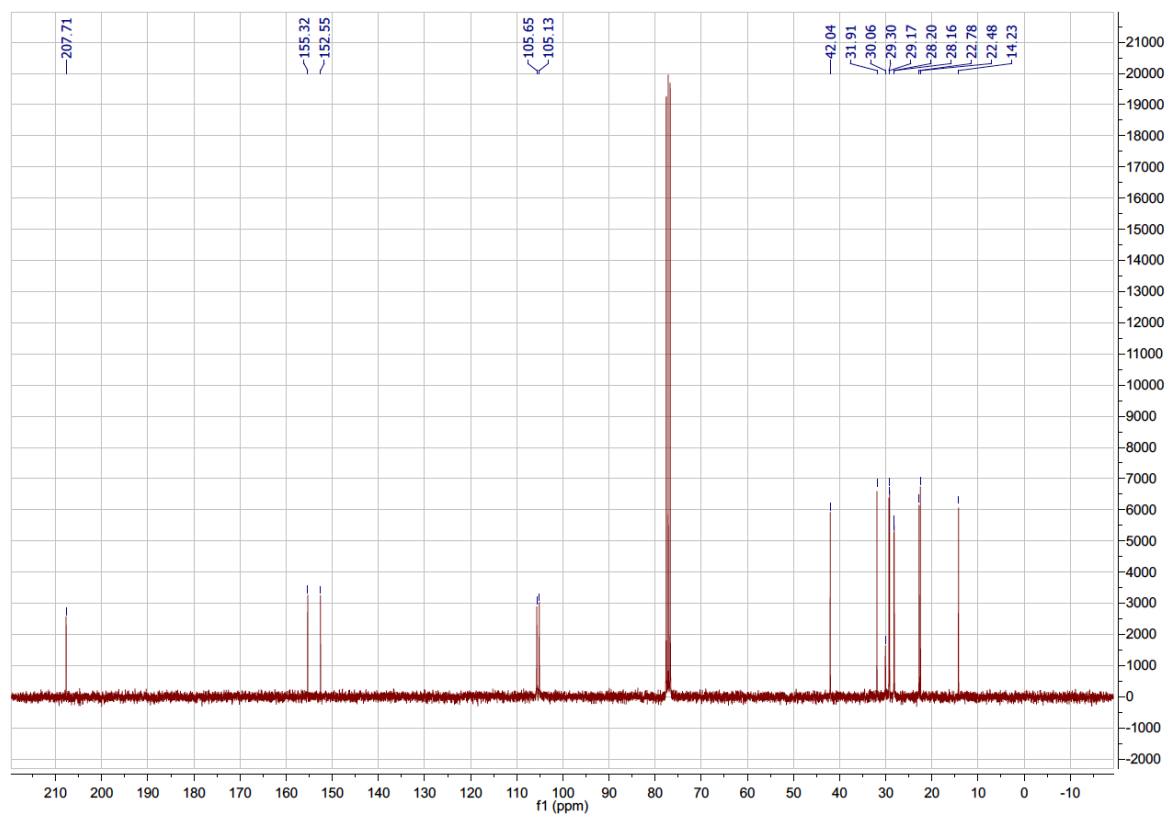
# HR-MS of **8**

Xenovenine10 #70-90 RT: 0.41-0.50 AV: 4 NL: 4.50E9
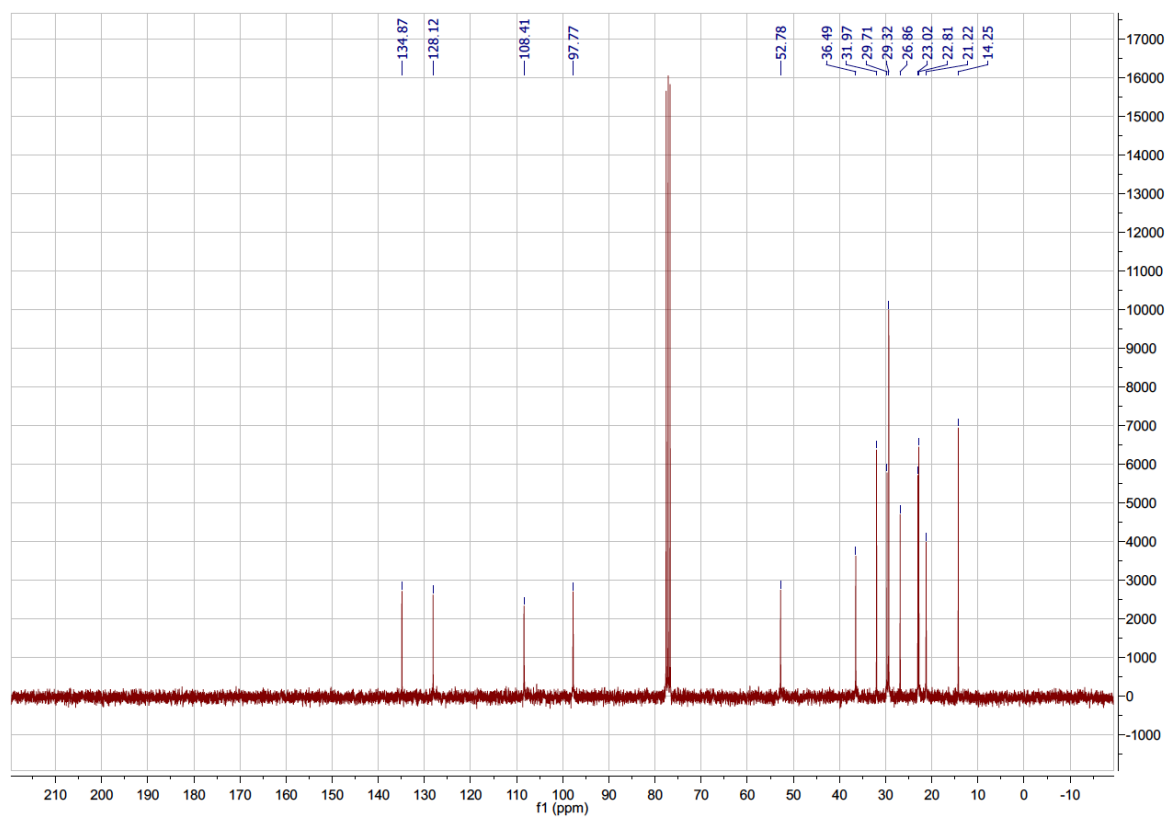T: FTMS + p APCI corona Full ms [90.00-1100.00]
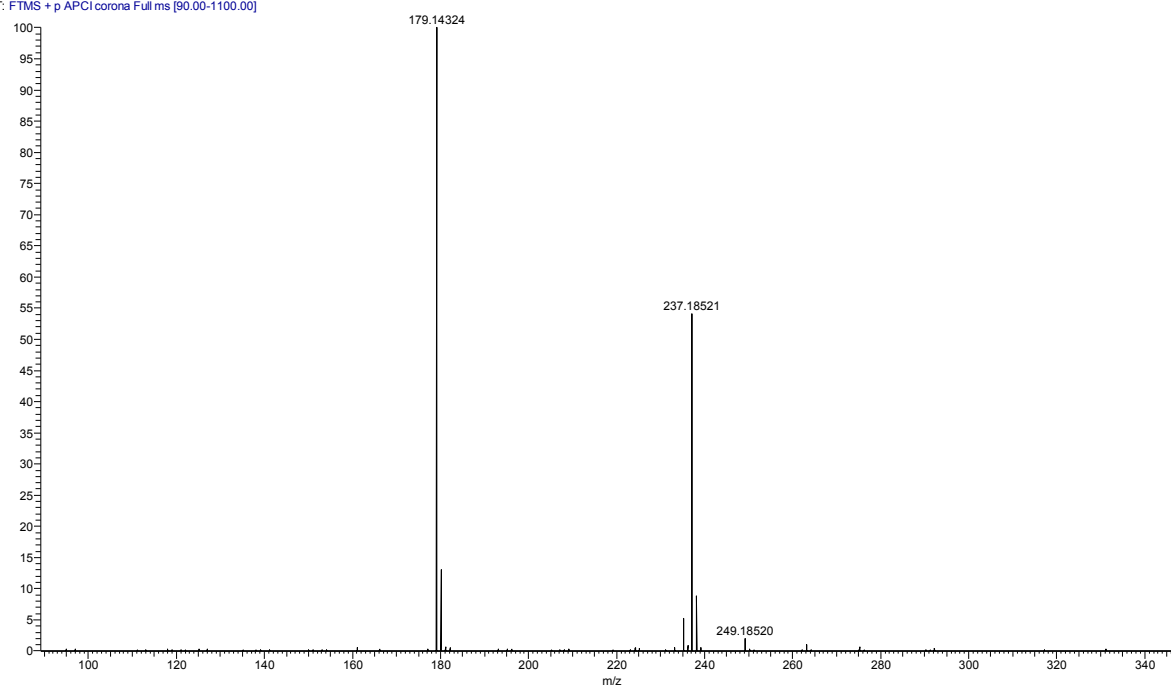
Pentadecane-2,5,8-trione 7
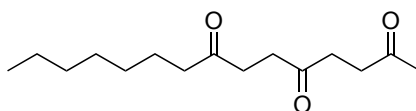
Ketofuran **8** (via DIELS-ALDER; 500 mg, 2.12 mmol) was dissolved in 12 M HCl/conc. AcOH=1/1 (11 mL) and stirred at 21 °C for 35 min. The red-brown reaction mixture was diluted with H_2O (20 mL) upon which a white solid precipitated. The suspension was extracted with ethyl acetate (3 x 30 mL) after adjusting the pH to 7.0 with 10 M NaOH (11 mL). The combined organic extracts were washed with sat. aq. $NaHCO_3$ solution (30 mL) to neutralize remaining acid and then dried over $MgSO_4$. Evaporation under reduced pressure gave 480 mg of **7** as greyish solid (89 %) after drying *in vacuo*. If necessary, the product was recrystallized from diethyl ether (5 mL) at 4 °C overnight. The spectral data from ¹H-NMR matches those found in literature.[12] R_f (PE/TEA/EtOH 90:7:3) = 0.28. Mp: 76 − 77 °C; lit.[12]: mp: 77 °C. ¹H NMR (300 MHz, CDCl$_3$) δ_H [ppm] 2.81 − 2.57 (m, 8H, $C^{3,4,6,7}H_2$), 2.41 (t, J = 7.5 Hz, 2H, C^9H_2), 2.16 (s, 3H, C^1H_3), 1.66 − 1.42 (m, 2H, $C^{10}H_2$), 1.25 (s, 8H, $C^{11-14}H_2$ alkyl chain), 0.85 (t, J = 6.7 Hz, 3H, $C^{15}H_3$). ¹³C NMR (75 MHz, CDCl$_3$) δ_C [ppm] 209.8, 208.1, 207.3 ($C^{2,5,8}$=O), 42.8 (C^9), 37.0, 36.1, 36.08, 36.0 ($C^{3,4,6,7}$), 31.6 , 29.9, 29.1, 29.0, 23.8, 22.6 (C^1, C^{10-13}), 14.1 (C^{14}). GC-MS (EI+, 70 eV): t_R = 14.05 min; m/z (%) = 254 [M^+] (4), 236 (3), 211 [$C_{13}H_{23}O_2^+$] (4), 196 (< 1), 183 [$C_{11}H_{19}O_2^+$] (4), 170 [$C_9H_{14}O_3^+$] (30), 152 (39), 141 (< 1), 127 [$C_7H_{11}O_2^+$] (100), 112 (11), 99 [$C_7H_{15}^+$] (42), 82 (9), 71 [$C_4H_7O^+$] (12), 57 (35), 43 [$C_2H_3O^+$] (38). HR-MS: m/z = 255.1955 [MH^+] (calcd.: 255.1955).

¹H-NMR of **7**
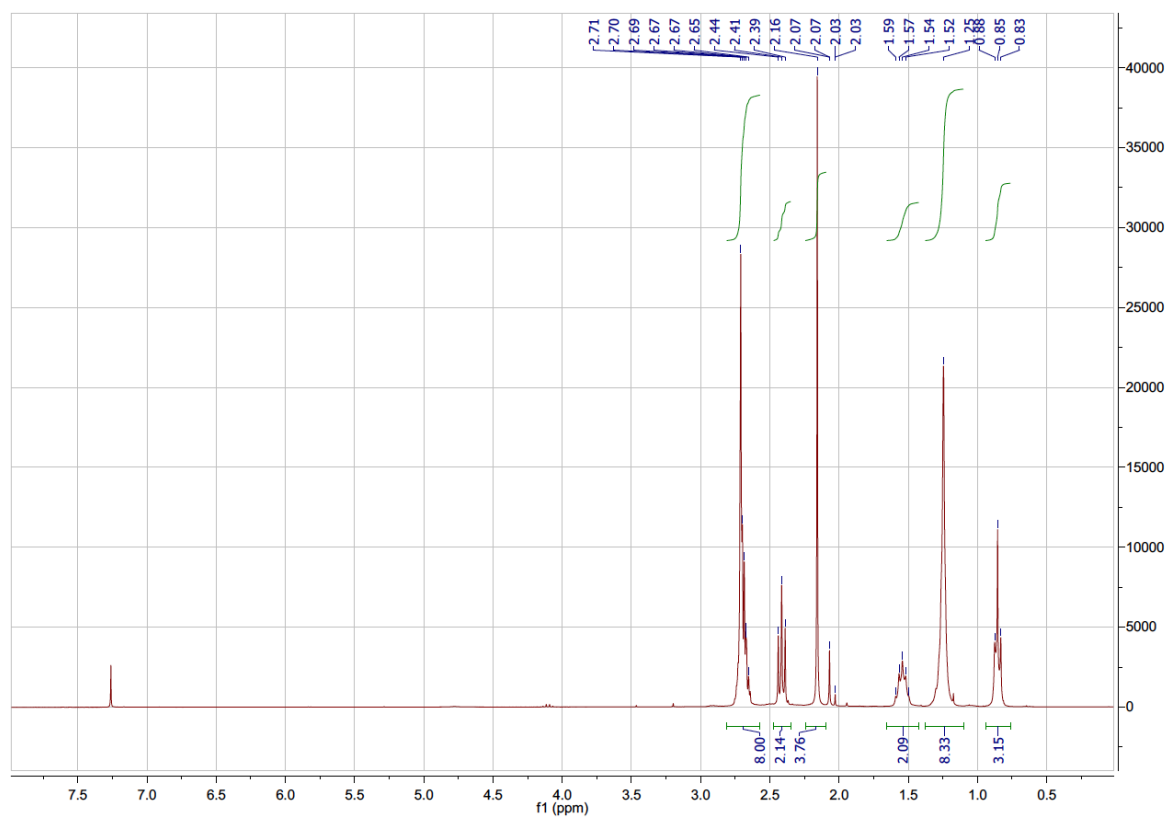
¹³C-NMR of **7**
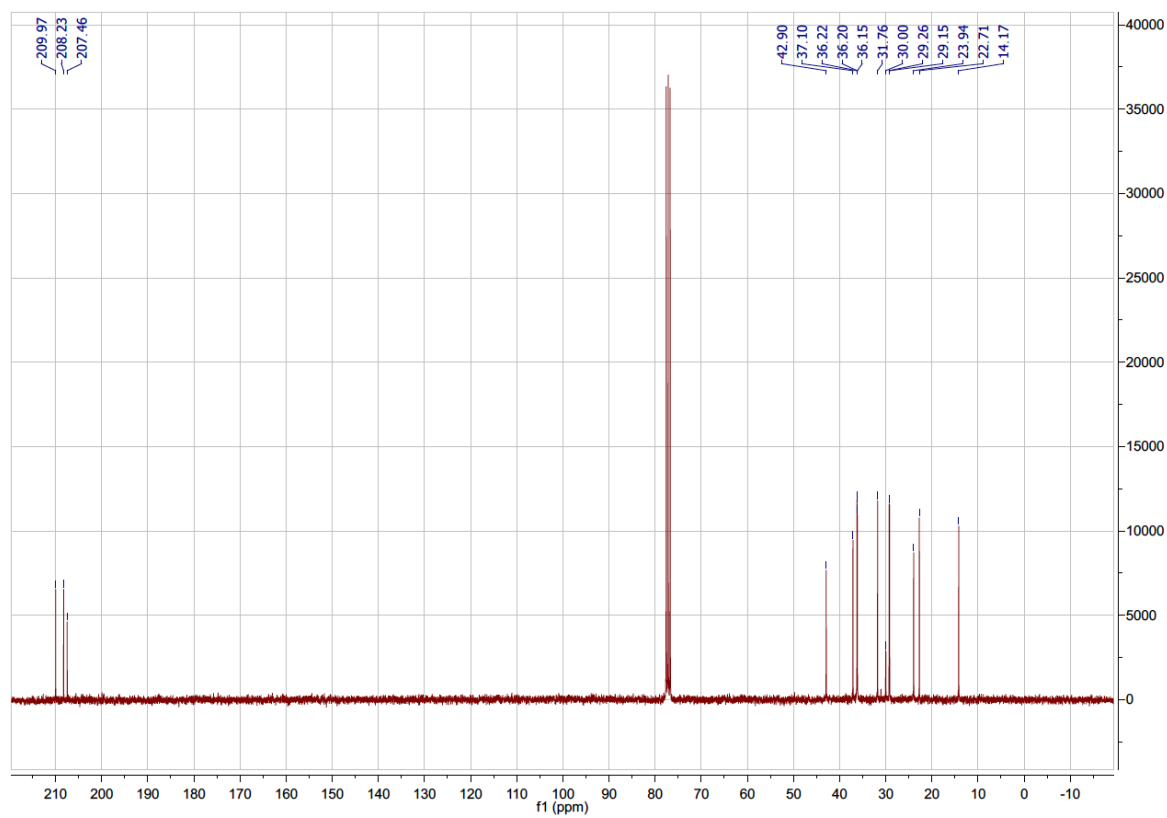
HR-MS of **7**

Xenovenine2 #73 RT: 0.39 AV: 1 NL: 7.93E9
T: FTMS + p APCI corona Full ms [90.00-1100.00]
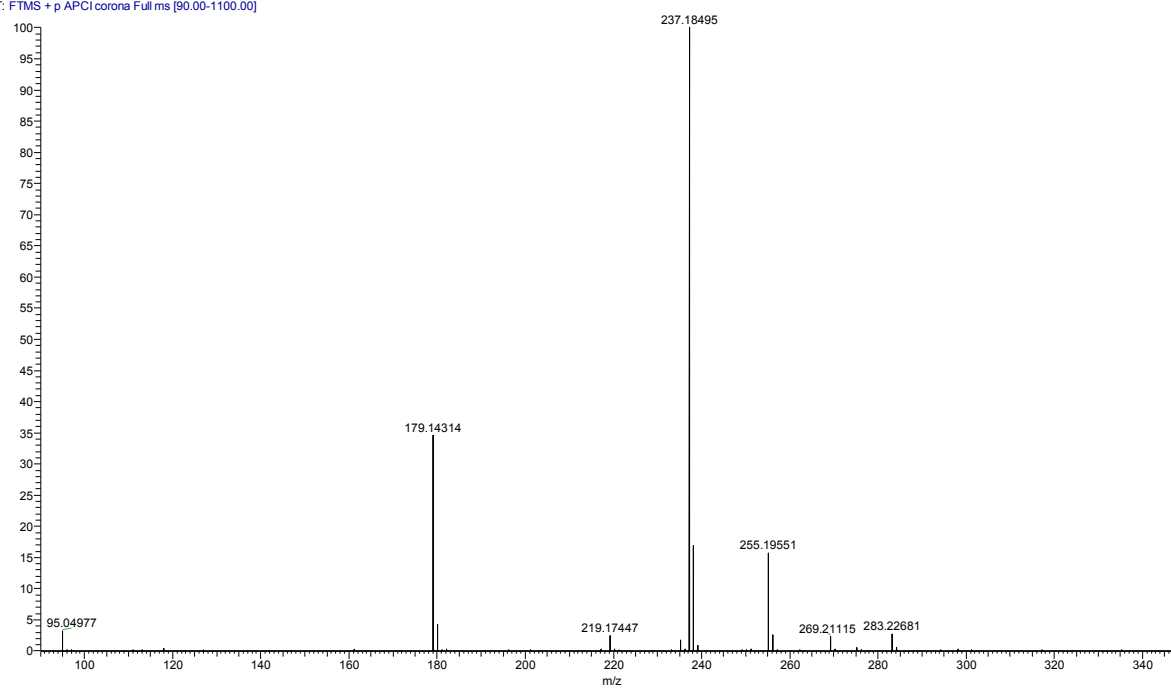
1-(2-methyl-3,4-dihydro-2*H*-pyrrol-5-yl)decan-3-one **4**
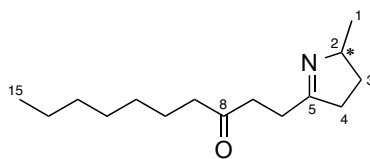
The preparative biotransformation was carried out in 50 mL SARSTEDT-tubes in a VWR benchtop incubator. Concentrations and volume% given in parentheses refer to the final concentration during the biotransformation. The procedure describes the setup of two reactions with different transaminases, using a common cofactor stock solution.

Ammonium formate (151.5 mg, 2.8 mmol; 150 mM), NAD^+ (21 mg, 32 μmol; 1 mM) and PLP (8.4 mg, 34 μmol; 1 mM) were dissolved in 100 mM KPi buffer pH 8.0 (32 mL). Then, L-alanine and D-alanine (713 mg, 8.0 mmol; 500 mM), respectively, was dissolved in the buffer/cofactor solution (16 mL) in separate tubes. Lyophilized *E. coli* cells (315 mg each) containing the ω-transaminase ArS (378 U) and ArR (189 U) were suspended in the L-alanine and D-alanine solution, respectively. After addition of AlaDH-solution (236 μL; 173 U) and FDH-whole cells (79 mg; 190 U) to each tube, the cells were rehydrated for 30 min at 30 °C, 120 rpm. Triketone **7** (200 mg, 0.78 mmol; 50 mM) was dissolved in DMF (800 μL; 5 v%) at 50 °C and added to the tube containing ArS together with *n*-heptane (4.8 mL; 30 v%). Similarly, triketone **7** (200 mg) was dissolved in DMSO (800 μL; 5 v%) at 50 °C and added to the tube containing ArR together with *n*-heptane (4.8 mL; 30 v%). The tubes were incubated for 26 h at 35 °C, 290 rpm after which TLC and GC-MS confirmed quantitative turnover of **7**. The reaction mixtures were extracted with 1 x 5 mL and 2 x 10 mL EtOAc each and 3 g NaCl each were added for better phase separation upon intermittent centrifugation for 10 min at 4000 rpm. The combined organic extracts from each reaction were dried over Na_2SO_4 and stored as yellowish EtOAc solutions (35 mL, 5.13 mg/mL (*S*)-**4**, 3.96 mg/mL (*R*)-**4**) at 4 °C. R_f (PE/TEA/EtOH 90:7:3) = 0.5. ^1H NMR (300 MHz, $CDCl_3$) δ_H [ppm] 4.00 (dd, *J* = 13.9, 6.9 Hz, 1H, C^2H), 2.89 − 2.68 (m, 2H, C^7H_2), 2.62 − 2.35 (m, 6H, C^6H_2, C^4H_2, C^9H_2), 2.15 − 1.94 (m, 1H, C^3H^a), 1.57 (dd, *J* = 14.3, 7.2 Hz, 2H, $C^{10}H_2$), 1.44 − 0.90 (m, 12H, C^3H^b, $C^{11-14}H_2$, C^1H_3), 0.86 (t, *J* = 6.6 Hz, 3H, $C^{15}H_3$). ^{13}C NMR (300 MHz, $CDCl_3$) δ_C [ppm] 210.5 (C=O), 175.9 (C=N), 67.7 (C^2), 43.0, 39.0, 38.4 (C^9, C^7, C^4), 31.8 (C^{11-14}), 30.7 (C^3), 29.3, 29.2 (C^{11-14}), 27.2 (C^6), 24.0 (C^{10}), 22.7 (C^{11-14}), 22.1 (C^1), 14.2 (C^{15}). GC-MS (EI+, 70 eV): t_R = 12.20 min; *m/z* (%) = 237 [M^+] (3), 222 (2), 208 (5), 194 (4), 180 (3) 166 [$C_{10}H_{16}NO^+$] (26), 153 (12), 138 [$C_8H_{16}O^+$] (100), 124 (7), 110 [$C_7H_{12}N^+$] (70), 96 [$C_6H_{10}N^+$] (19), 82 (11), 69 (4), 55 (12), 41.1 (14), 30.1 (< 1). HR-MS: *m/z* = 238.2167 [(*S*)-MH$^+$], 238.2166 [(*R*)-MH$^+$] (calcd.: 238.2165).

¹H of crude (*S*)-**4** from biotransformation:
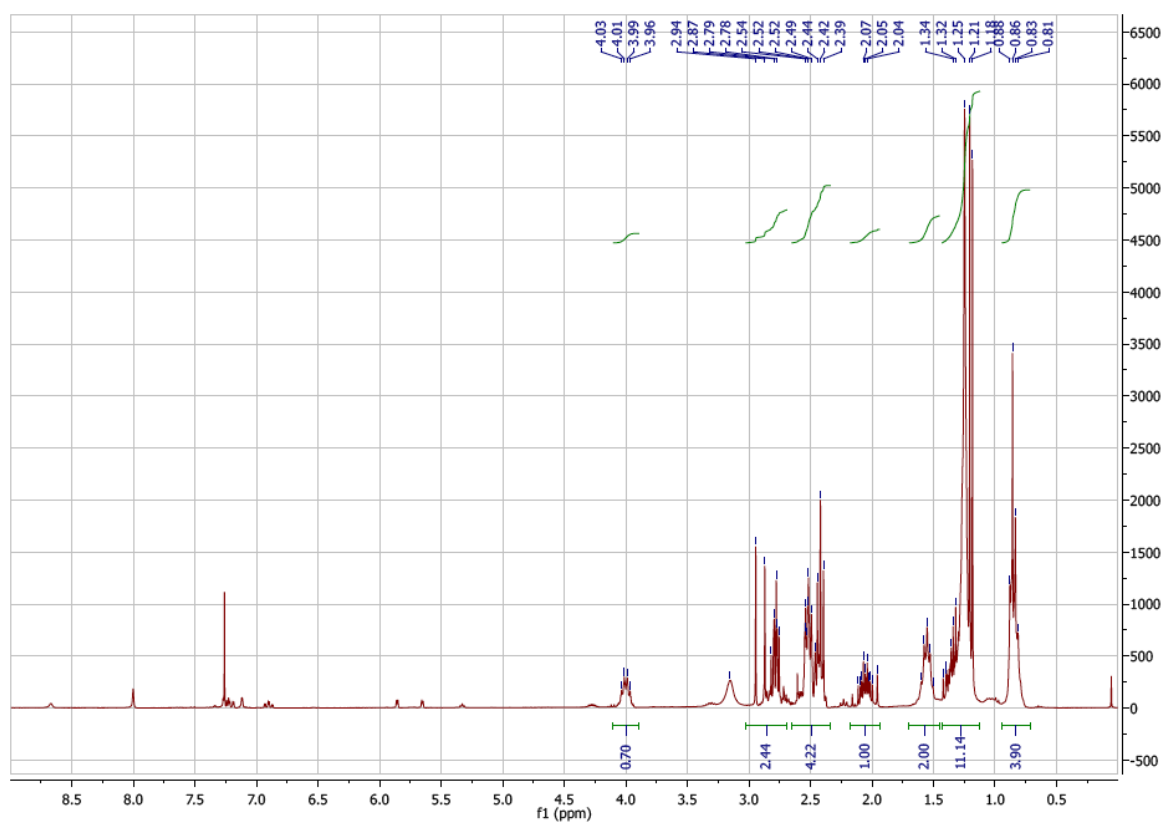
¹³C of crude (*S*)-**4** from biotransformation:
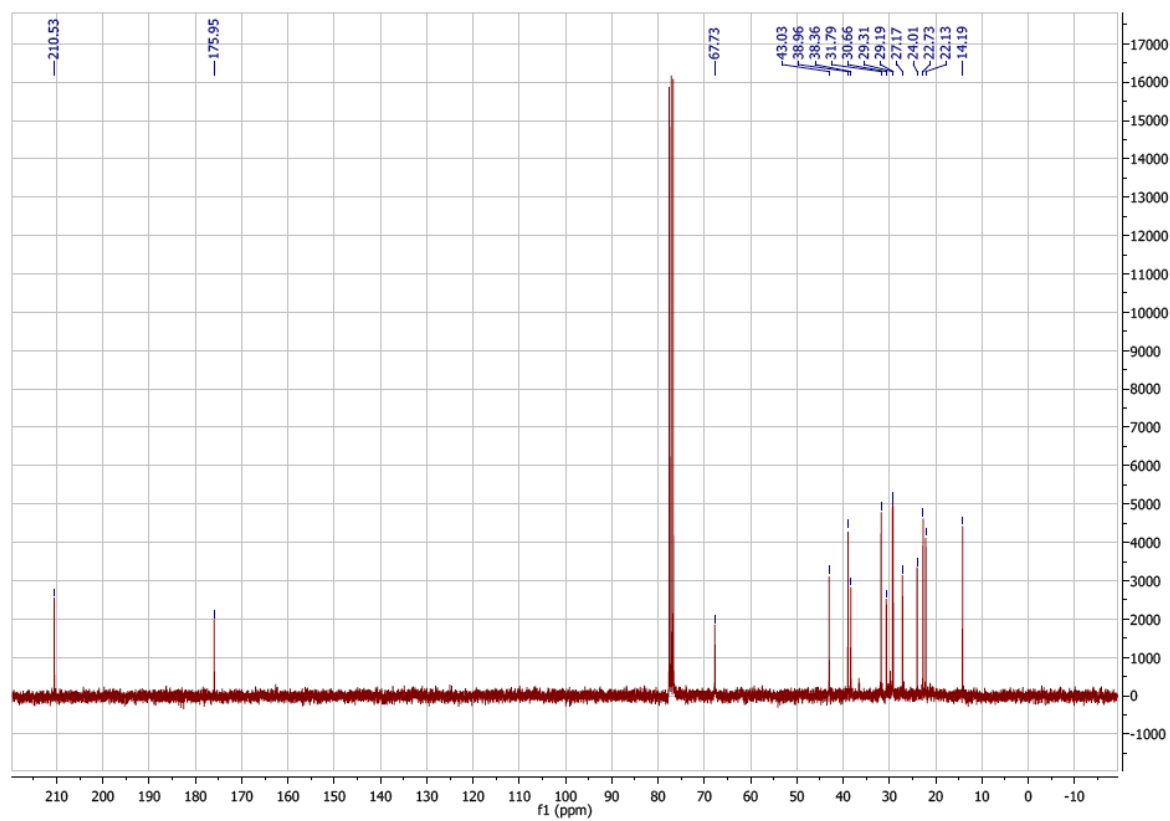
HR-MS of (*S*)-**4**:

Xenovenine20 #54-92 RT: 0.36-0.51 AV: 6 NL: 9.89E9
T: FTMS + p APCI corona Full ms [90.00-1100.00]
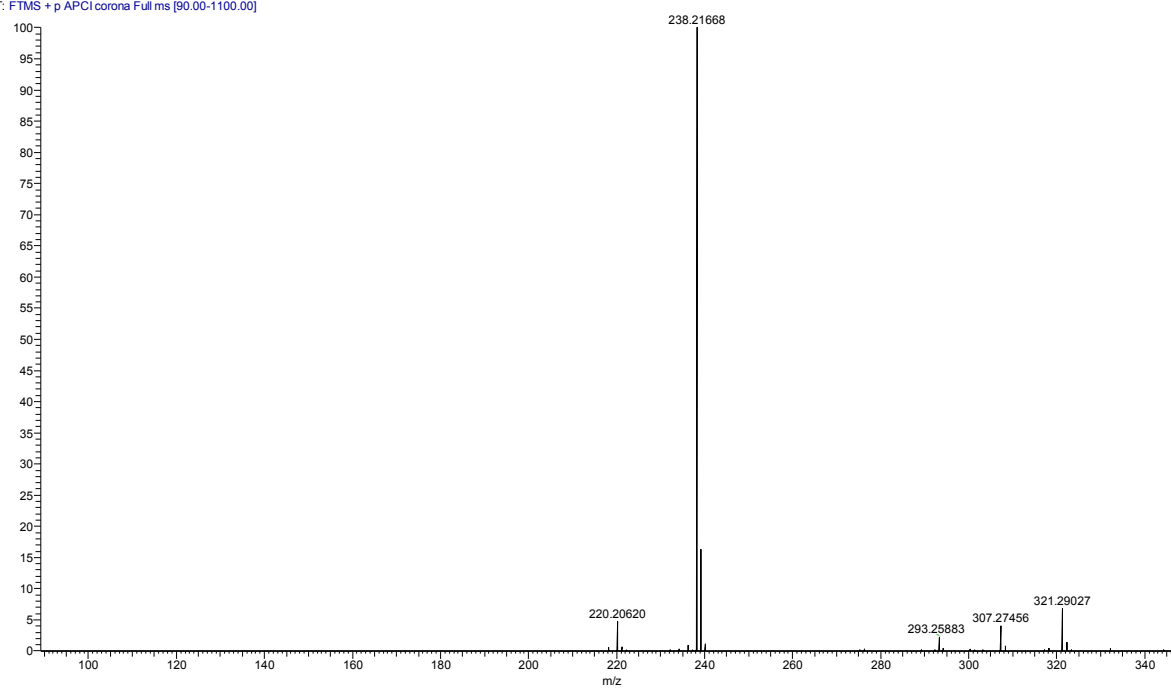
HR-MS of (*R*)-**4**:

Xenovenine24 #60-101 RT: 0.38-0.57 AV: 7 NL: 1.13E10
T: FTMS + p APCI corona Full ms [90.00-1100.00]
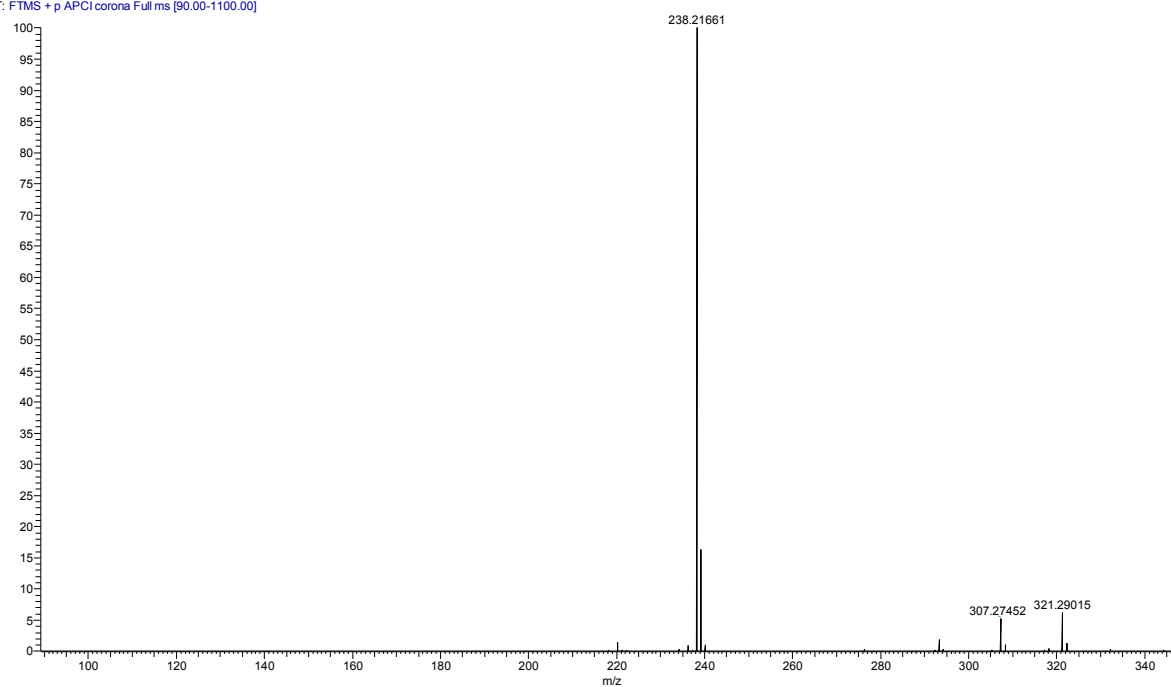
5-heptyl-3-methyl-2,3-dihydro-1*H*-pyrrolizine **2**
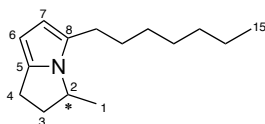
Solutions of 30 mM (*S*)- or (*R*)-**4** in EtOAc (9 mL) obtained from biotransformations were evaporated and re-dissolved in 9 mL MeOH each. Then, AcOH conc. (10 µL) was added and the samples were shaken for 30 min at 30°C, 700 rpm in a VWR benchtop incubator. When the reaction was completed as confirmed by GC-MS, the solvent was removed and the residues were subjected to flash column chromatography (petrol ether/TEA/ethyl acetate = 98.5/0.5/1). 27.3 mg of (*R*)-**2** and 22.3 mg of (*S*)-**2** (46 and 38 % yield from **4**, respectively) were obtained as colorless oils. R_f (PE/TEA/EtOH 90:7:3) = 0.78. ^{1}H NMR (300 MHz, CDCl$_3$) δ_H [ppm] 5.89 (d, J = 3.1 Hz, 1H, C^{7}H), 5.69 (d, J = 3.1 Hz, 1H, C^{6}H), 4.31 (dqd, J = 12.9, 6.4, 3.4 Hz, 1H, C^{2}H), 2.96 − 2.82 (m, 1H), 2.81 − 2.61 (m, 3H, C^{3}H^a, C^{4}H$_2$), 2.61 − 2.51 (m, 2H, C^{9}H$_2$), 2.15 − 2.01 (m, 1H, C^{3}H^b), 1.73 − 1.57 (m, 2H, C^{10}H$_2$), 1.34 (dd, J = 12.8, 7.0 Hz, 11H, C$^{11\text{-}14}$H$_2$, C^{1}H$_3$), 0.90 (t, J = 6.7 Hz, 3H, C^{15}H$_3$). ^{13}C NMR (75 MHz, CDCl$_3$) δ_C [ppm] 134.9 (C$_q^8$), 128.1 (C$_q^5$), 108.4 (C^7), 97.8 (C^6), 52.8 (C^3), 36.5, 32.0, 29.7, 29.3, 26.9, 23.0, 22.8 (C^4, C$^{9\text{-}14}$), 21.2 (C^1), 14.3 (C^{15}). GC-MS (EI+, 70 eV): t_R = 11.60 min; m/z (%) = 219 [M$^+$] (17), 204 [C$_{14}$H$_{22}$N$^+$] (< 1), 190 [C$_{13}$H$_{20}$N$^+$] (< 1), 176 [C$_{12}$H$_{18}$N$^+$] (< 1), 162 [C$_{11}$H$_{16}$N$^+$] (< 1), 148 [C$_{10}$H$_{14}$N$^+$] (3), 134 [C$_9$H$_{12}$N$^+$] (100), 118 (4), 106 (3), 93 (6), 77 (1), 65 (< 1), 55 (< 1), 41 (< 1). HR-MS: m/z = 220.2062 [(*S*)-MH$^+$], 220.2062 [(*R*)-MH$^+$] (calcd.: 220.2060).

¹H-NMR of (*R*)-**2**
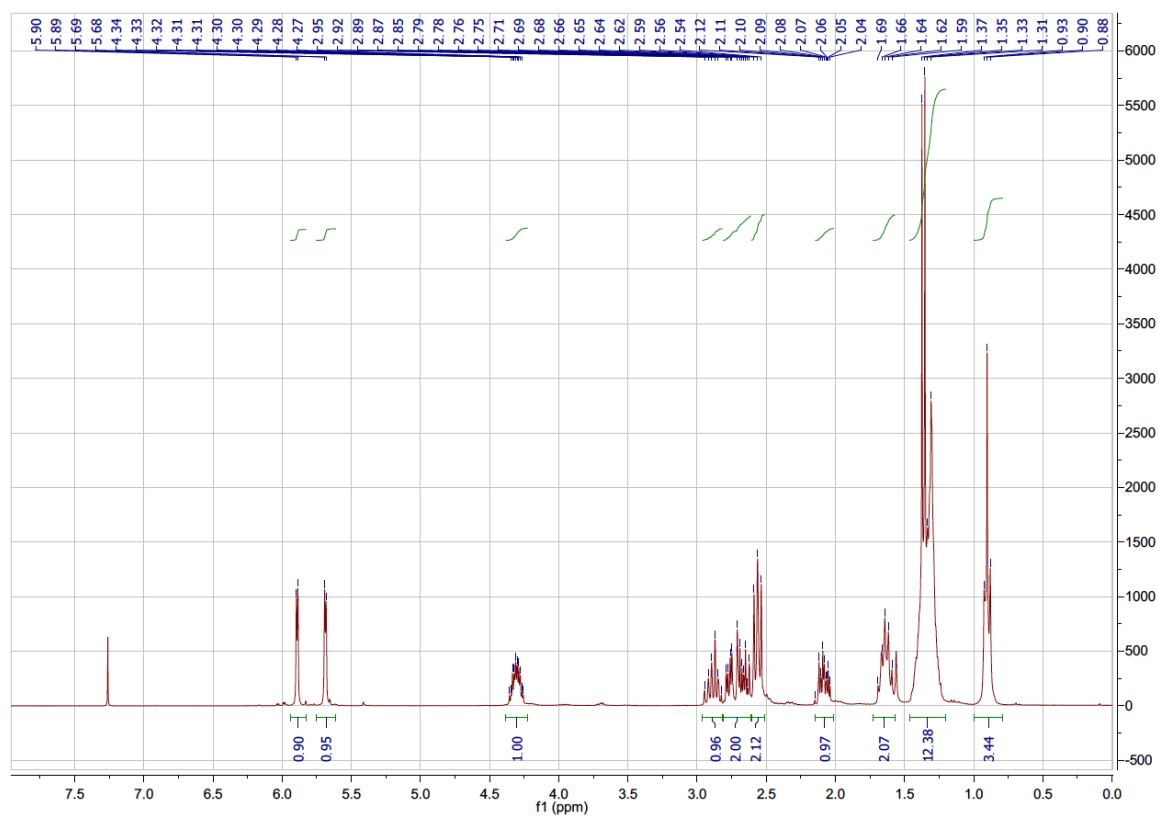
¹H-NMR of (*S*)-**2**
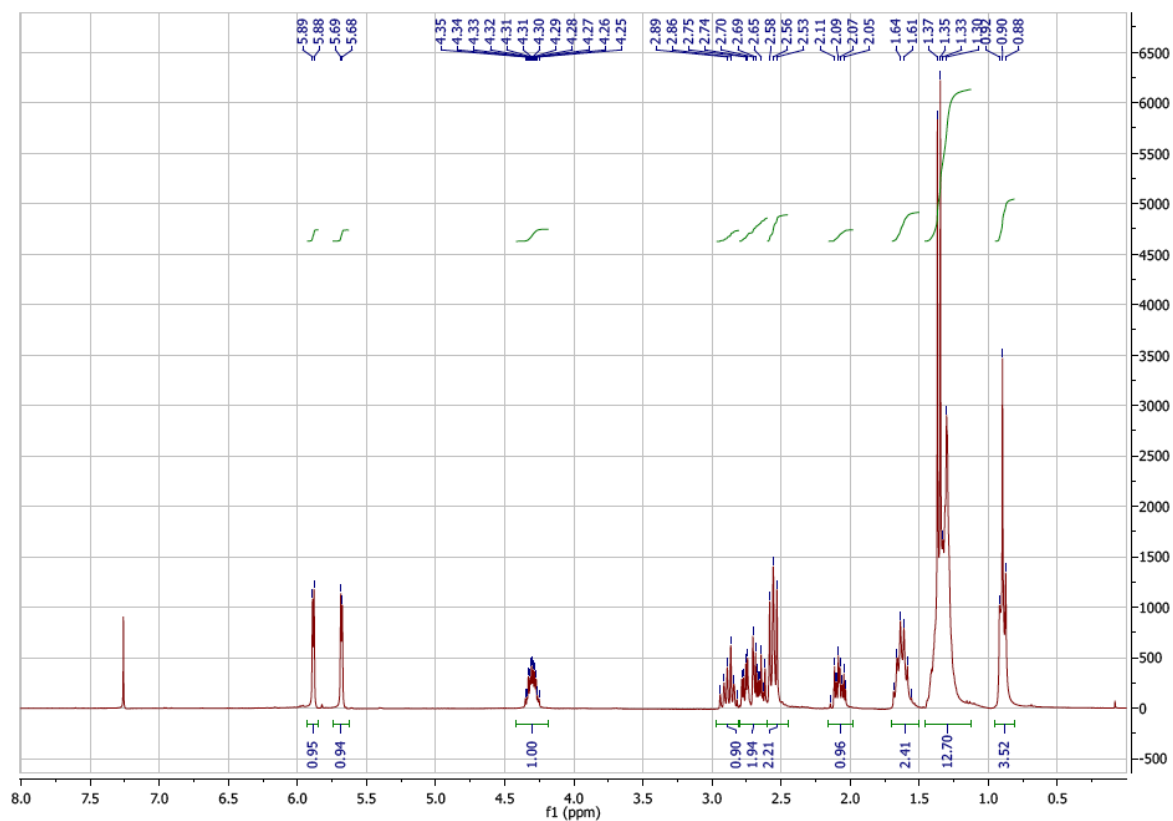
¹³C NMR of (*R*)-**2**

DEPT-45 of (*R*)-**2**

CH₃, CH₂, CH
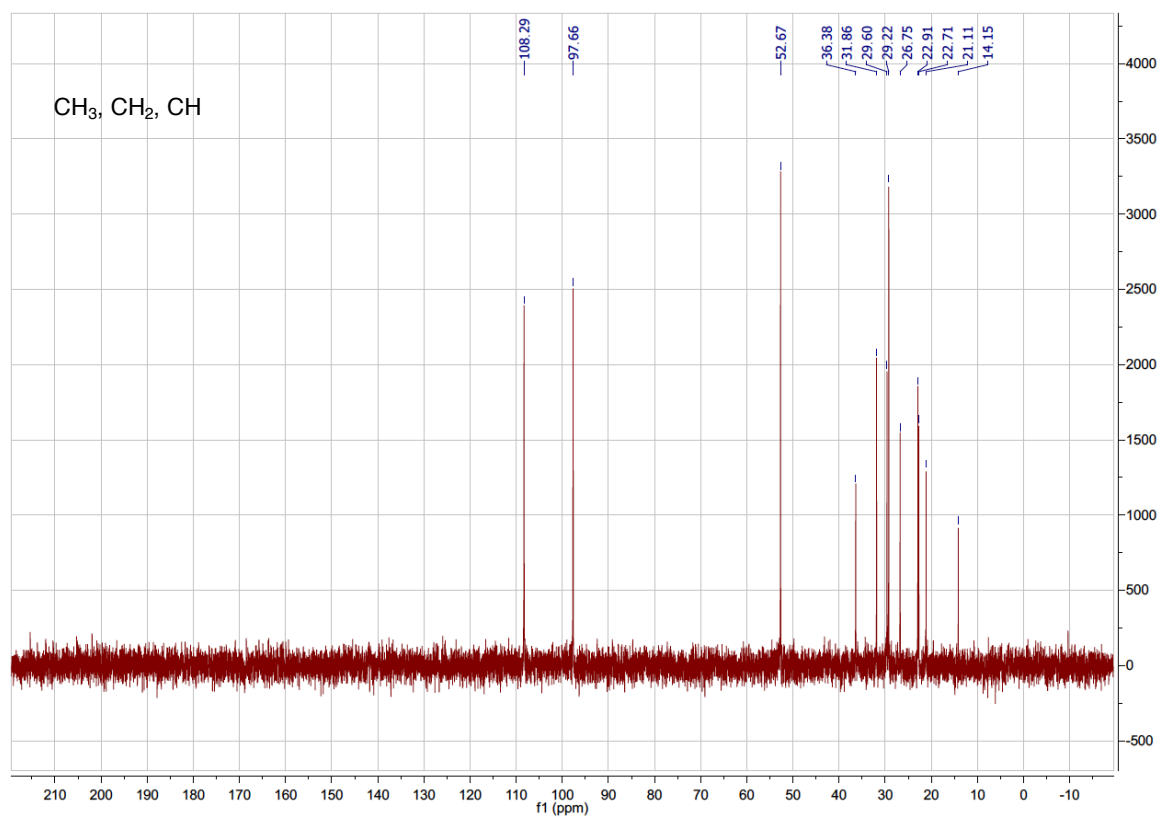
DEPT-135 of (*R*)-**2**
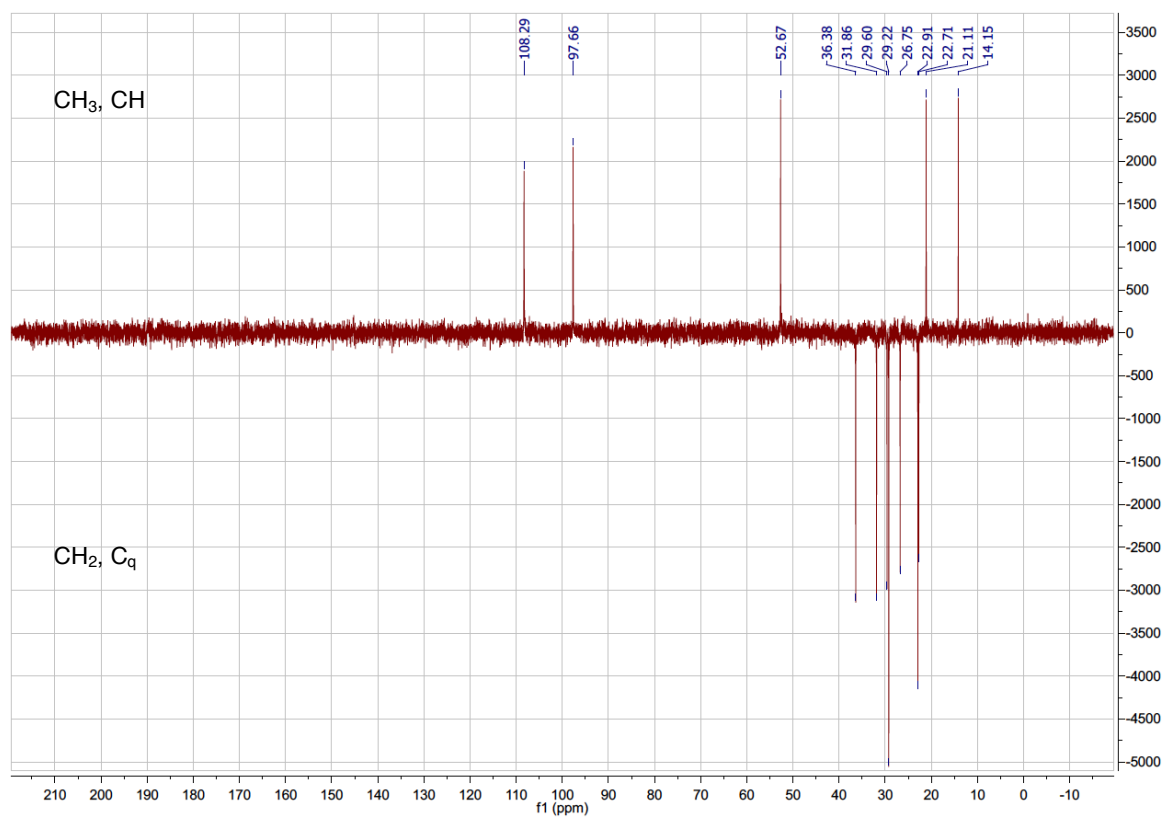
HSQC of (*R*)-**2**
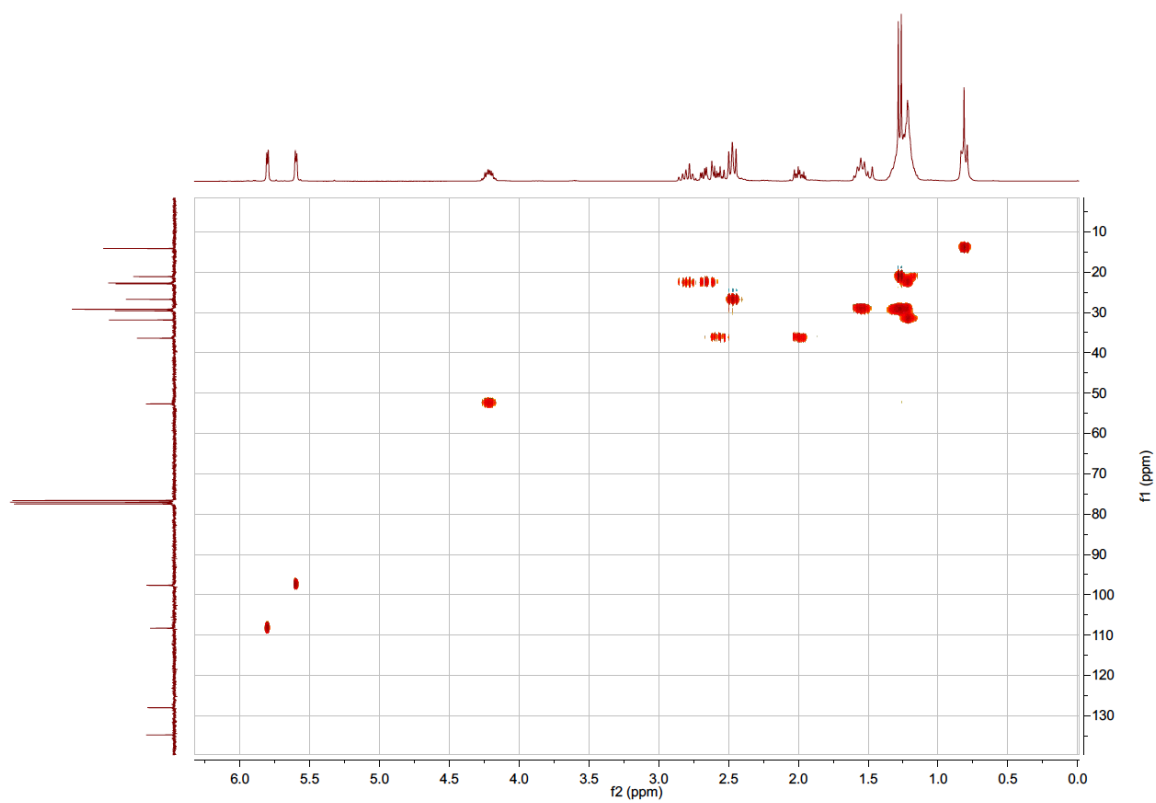
COSY of (*R*)-**2**
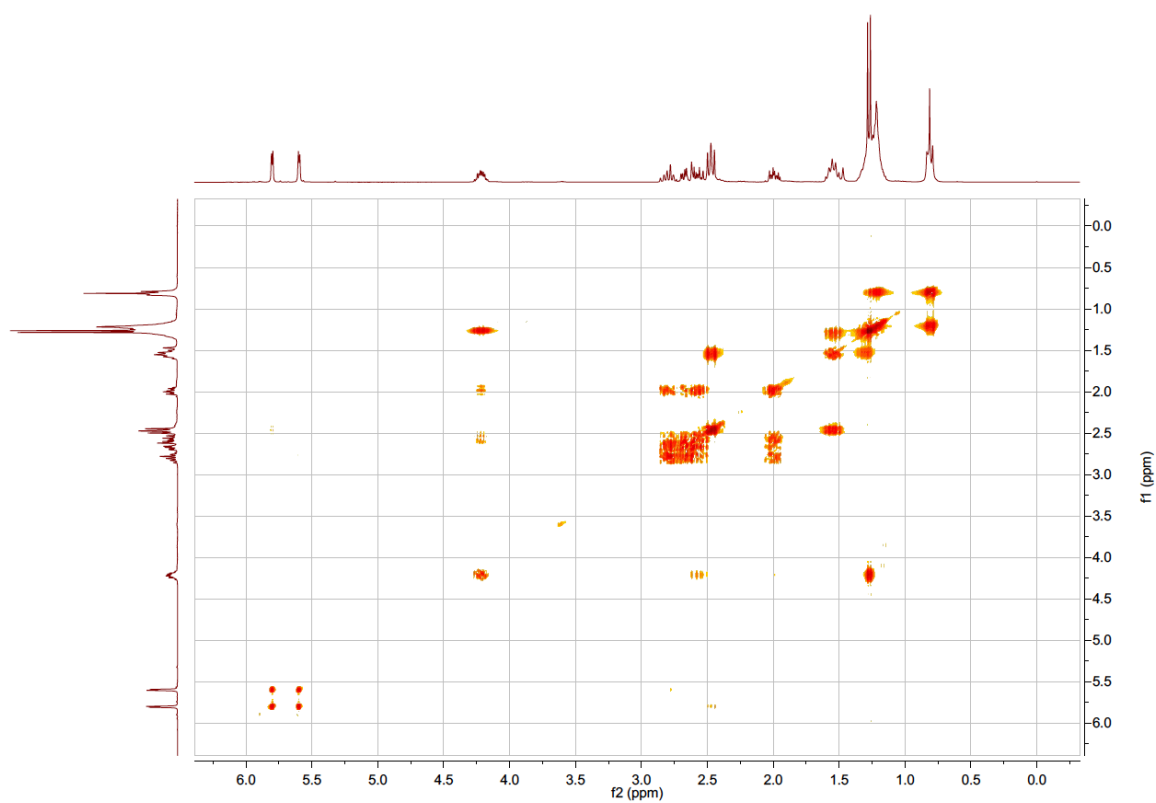
HR-MS of (*R*)-**2**

Xenovenine22 #60-90   RT: 0.37-0.50   AV: 5   NL: 6.23E9
T: FTMS + p APCI corona Full ms [90.00-1100.00]
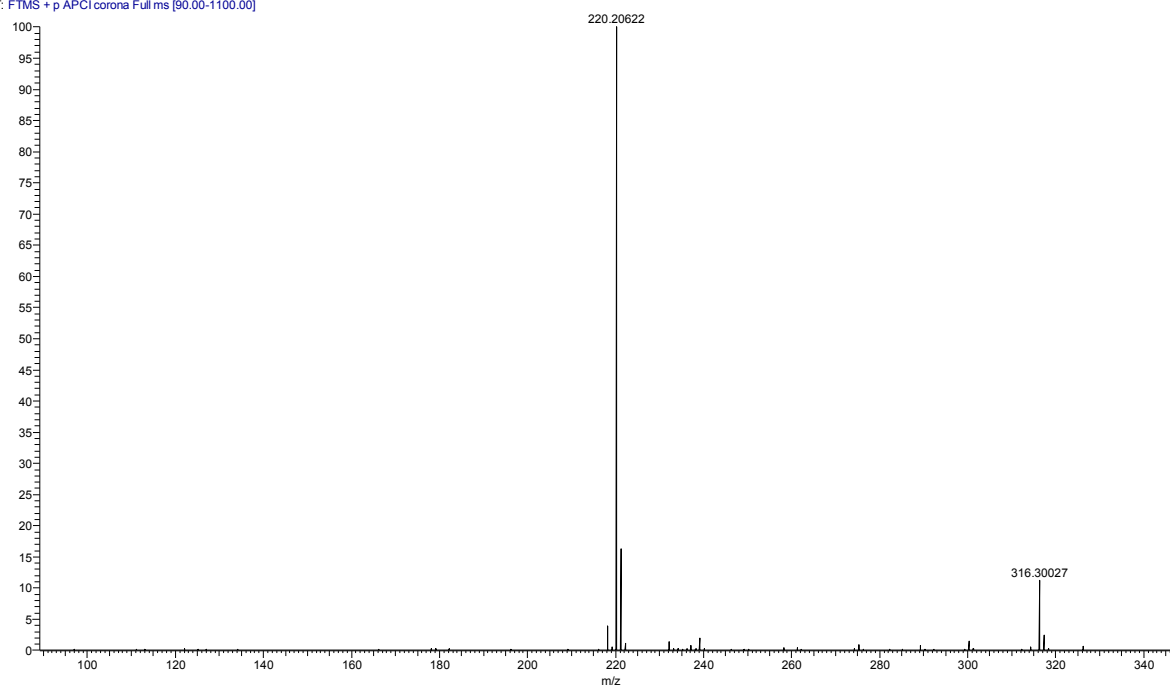
HR-MS of (*S*)-**2**
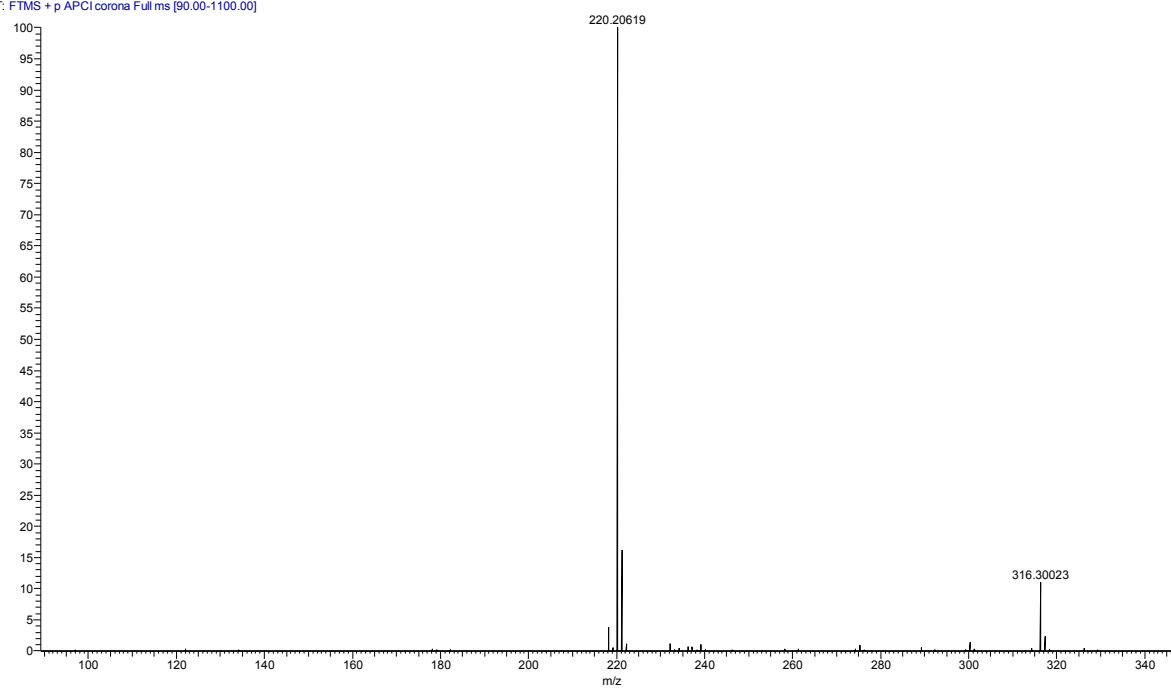
(−)-(3*R*,5*S*,8*R*)-3-heptyl-5-methylpyrrolizidine (−)-(5*Z*,8*E*)-**1**[4]
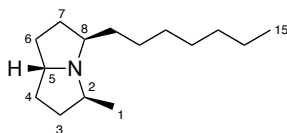
(*S*)-Imine **4** (118 mg, 0.5 mmol; 23 mL of a 5.13 mg/mL EtOAc solution from biotransformation evaporated under reduced pressure) was dissolved in MeOH (10 mL; final conc. of **4**: 50 mM). AcOH (10 μL, 1 vol%) was added and the mixture was stirred for 2 h at 21 °C until TLC (PE/TEA/EtOH 90:7:3) confirmed quantitative turnover to pyrrolizine **2**. (+)-CSA (53 mg, 0.26 mmol, 0.5 eq) and Pd/C (12 mg, 10 wt%) were suspended in MeOH (200 μL) and added to the stirred solution. The reaction vessel with the hydrogenation mixture was then subjected to three cycles of evacuation and backfilling with hydrogen from a balloon. The mixture was stirred under 1 atm hydrogen for 40 h at 21 °C after which GC-MS confirmed quantitative turnover of **2**. The black suspension was filtered through a pad of celite (1.5 cm x ø 2 cm). The pad was washed with MeOH (3 x 4 mL) and the collected yellow filtrate was evaporated under reduced pressure. The residue was taken up in sat. aq. Na_2CO_3 solution (10 mL) and extracted with EtOAc (3 x 10 mL). The combined organic extracts were dried over Na_2SO_4 and evaporated under reduced pressure to yield 130 mg of crude (−)-(5*Z*,8*E*)-**1** with a *d.r.* of 57:19:17:8 (see also Table 2.9). The product was purified by flash column chromatography with a BIOTAGE ISOLERA flash chromatograph on a BIOTAGE SNAP ultra 10 g silica gel column, which was conditioned with 80 mL PE/TEA 95:5. The product diastereomer (3*R*,5*S*,8*R*) eluted as second compound with the following gradient: PE/EtOAc 99:1 (2 CV), PE 99 to PE 80 (20 CV), PE 80 to PE 45 (7 CV), UV online detection at λ=245 nm and 135 nm. 54 mg of pure (−)-(5*Z*,8*E*)-**1** (48 % from **4**). The spectral data matches the one found in literature.[20a] R_f (PE/EtOAc on a plate deactivated with PE/TEA 95:5) = 0.46. ^{1}H NMR (300 MHz, $CDCl_3$) δ_H [ppm] 3.65 (p, *J* = 6.7 Hz, 1H, C^5H), 2.79 (dq, *J* = 12.4, 6.2 Hz, 1H, C^2H), 2.62 (dd, *J* = 12.4, 6.7 Hz, 1H, C^8H), 1.99 − 1.93 (m, 4H, C^3H^a, C^4H^a, C^6H^a, C^7H^a), 1.66 − 1.16 (m, 16H, C^3H^b, C^4H^b, C^6H^b, C^7H^b, $C^{9-14}H_2$), 1.12 (d, *J* = 6.4 Hz, 3H, C^1H_3), 0.86 (t, *J* = 6.7 Hz, 3H, $C^{15}H_3$). ^{13}C NMR (75 MHz, $CDCl_3$) δ_C [ppm] 66.8 (C^8), 65.1 (C^5), 61.8 (C^2), 37.3, 34.6, 32.6, 32.3 ($C^{3,4,6,7}$), 32.0, 31.9, 30.0, 29.5, 27.4, 22.8 (C^{9-14}), 22.1 (C^1), 14.2 (C^{15}). GC-MS (EI+, 70 eV): t_R = 10.26 min; *m/z* (%) = 223 [M^+] (4), 208 [$C_{14}H_{26}N^+$] (6), 194 (3), 180 (3), 166 (1), 152 (1), 138 (1), 124 [$C_8H_{14}N^+$] (100), 110 (3), 97 (2), 81 (4), 68 (3), 55 (3), 41 (4), 30 (< 1). HR-MS: m/z = 224.2373 [MH^+] (calcd.: 224.2373). Optical rotation: $[\alpha]_D^{20}$ = −12.0 (c 2.7, $CHCl_3$); literature value5[20a]: $[\alpha]_D^{20}$ = −11.6 (c 0.6, $CHCl_3$,).

---

[4] Note: the numbering in the drawn molecule is only for NMR-signal assignment and does not correspond to the numbering in the molecule's name.

[5] The first reported optical rotation by Takahata in 1992 was found to have the wrong sign, *i.e.* + instead of −.

¹H of (−)-xenovenine
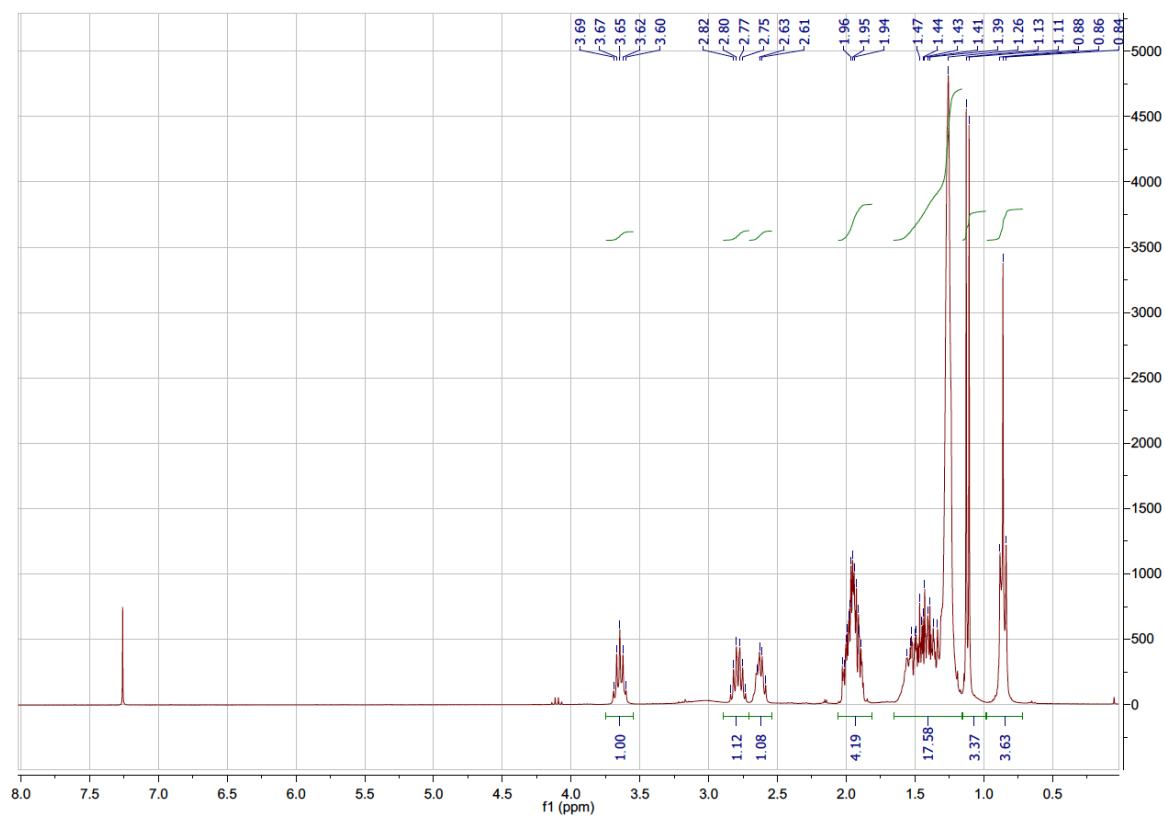
¹³C of (−)-xenovenine
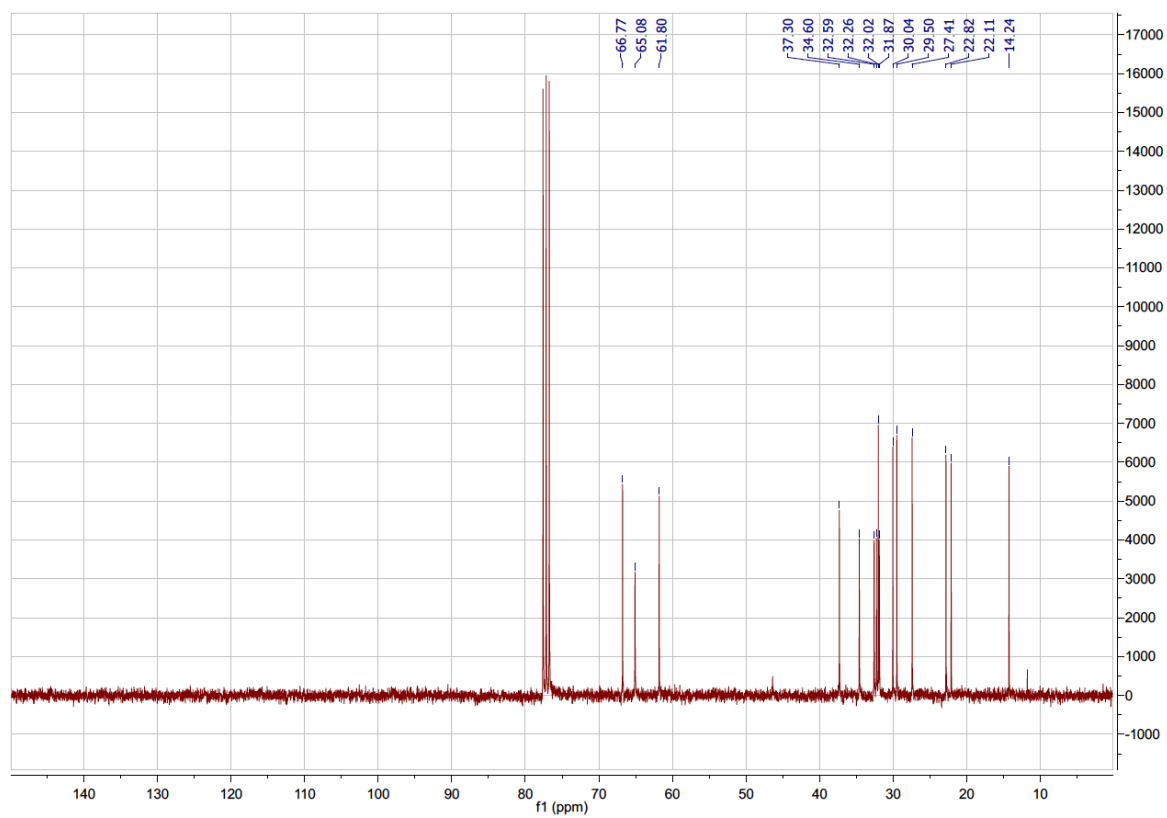
COSY of (−)-xenovenine
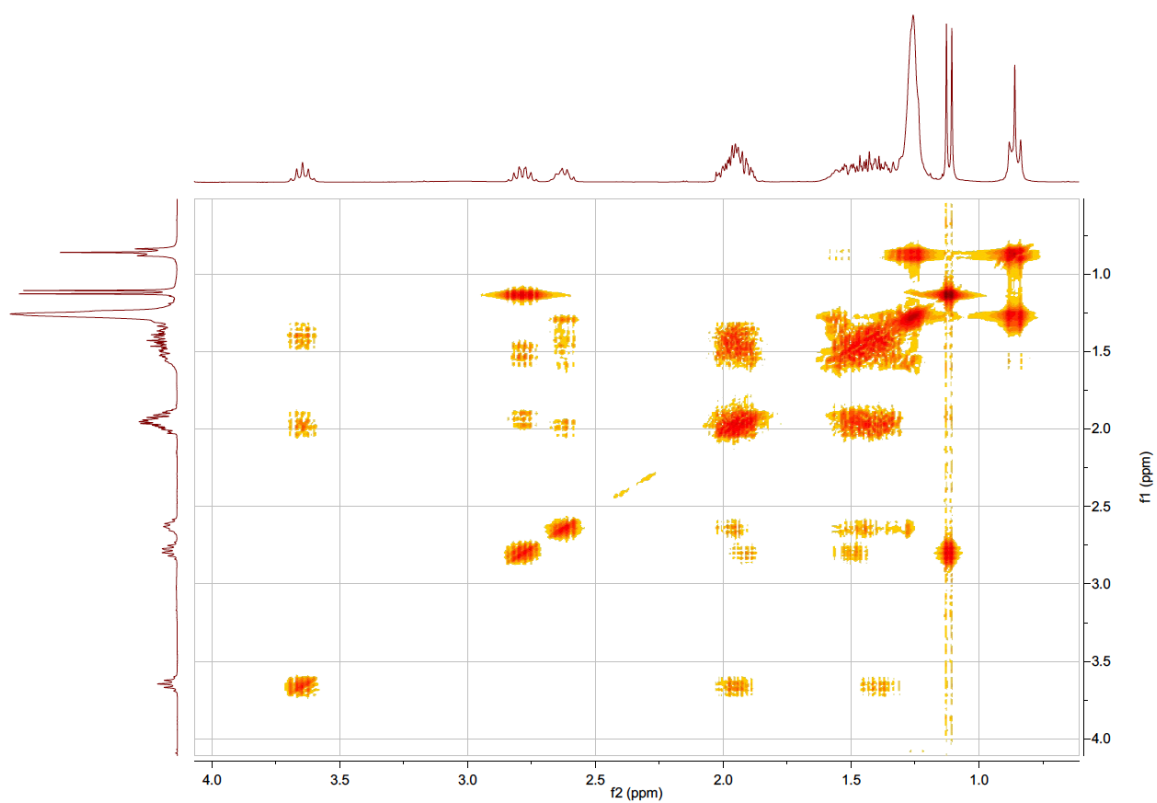
HSQC of (−)-xenovenine
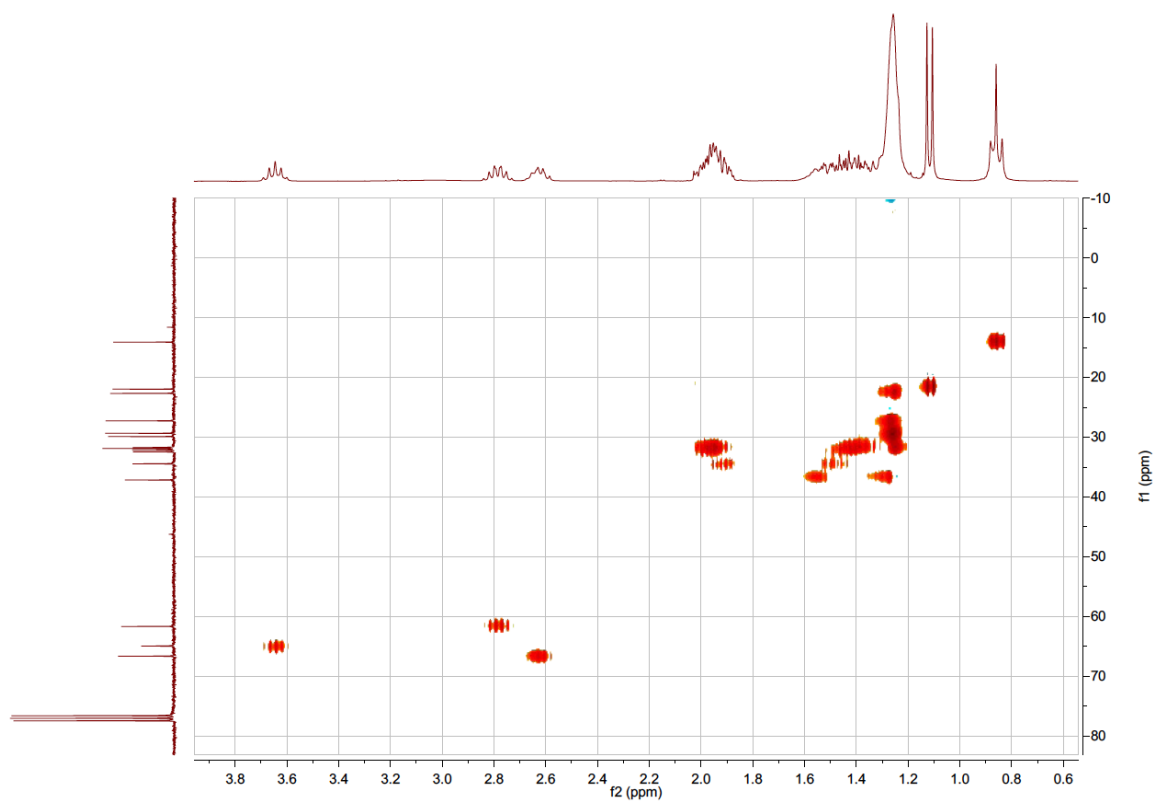
HR-MS of (−)-xenovenine

Xenovenine6 #175-186 RT: 0.95-0.99 AV: 2 NL: 7.22E9
T: FTMS + p APCI corona Full ms [90.00-1100.00]
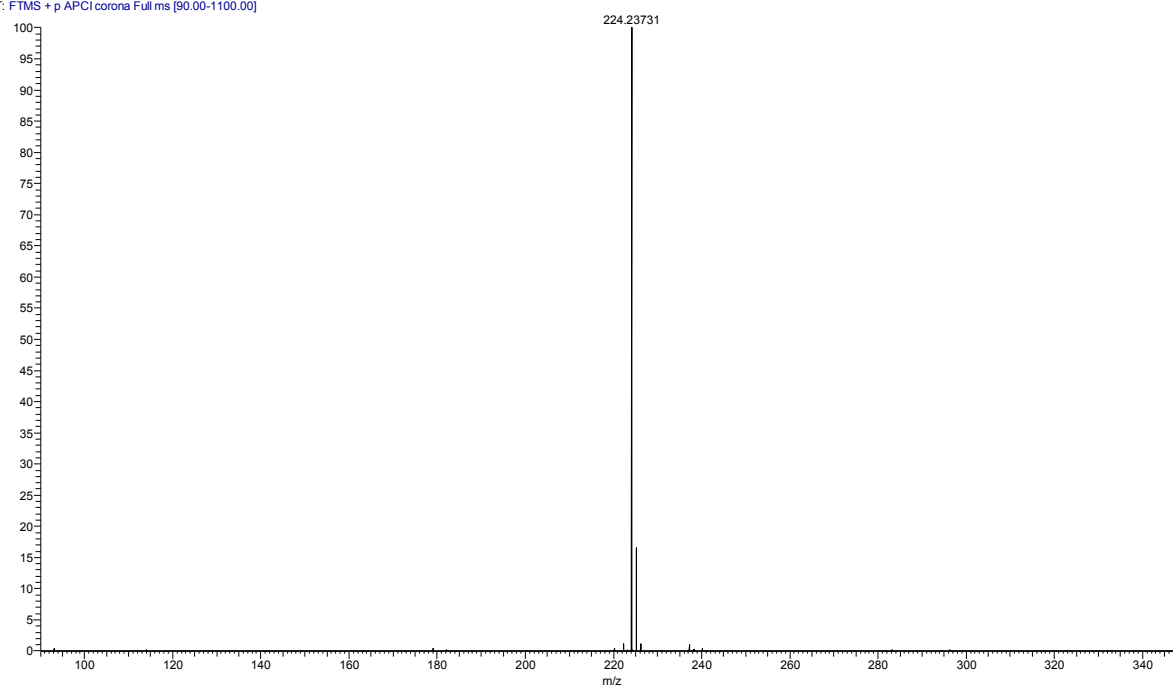
(+)-(3*S*,5*R*,8*S*)-3-heptyl-5-methylpyrrolizidine (+)-(5*Z*,8*E*)-**1**[6]
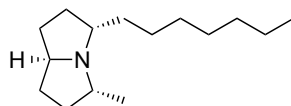
(*R*)-Imine **4** (91 mg, 0.38 mmol; 23 mL of a 3.96 mg/mL EtOAc solution from biotransformation evaporated under reduced pressure) was dissolved in MeOH (8.3 mL; final conc. of **4**: 50 mM). AcOH (10 µL, 1 vol%) was added and the mixture was stirred for 2 h at 21 °C until TLC (PE/TEA/EtOH 90:7:3) confirmed quantitative turnover to pyrrolizine **2**. (+)-CSA (44 mg, 0.2 mmol, 0.5 eq) and Pd/C (9 mg, 10 wt%) were suspended in MeOH (200 µL) and added to the stirred solution. The reaction vessel with the hydrogenation mixture was then subjected to three cycles of evacuation and backfilling with hydrogen from a balloon. The mixture was stirred under 1 atm hydrogen for 40 h at 21 °C after which GC-MS confirmed quantitative turnover of **2**. The black suspension was filtered through a pad of celite (1.5 cm x ø 2 cm). The pad was washed with MeOH (3 x 4 mL) and the collected yellow filtrate was evaporated under reduced pressure. The residue was taken up in sat. aq. Na_2CO_3 solution (10 mL) and extracted with EtOAc (3 x 10 mL). The combined organic extracts were dried over Na_2SO_4 and evaporated under reduced pressure to yield 80 mg of crude (+)-(5*Z*,8*E*)-**1** with a *d.r.* of 84:6:6:4 (see also Table 2.9). The product was purified by flash column chromatography with a BIOTAGE ISOLERA flash chromatograph on a BIOTAGE SNAP ultra 10 g silica gel column, which was conditioned with 80 mL PE/TEA 95:5. The product diastereomer eluted as second compound with the following gradient: PE/EtOAc 99:1 (2 CV), PE 99 to PE 80 (20 CV), PE 80 to PE 45 (7 CV), UV online detection at λ=245 nm and 135 nm. 26 mg of pure (+)-(5*Z*,8*E*)-**1** (30 % from **4**). The spectral data matches the ones found in literature.[19c] R_f (PE/EtOAc on a plate deactivated with PE/TEA 95:5) = 0.46. ^{1}H NMR (300 MHz, $CDCl_3$) δ_H [ppm] 3.65 (p, *J* = 6.7 Hz, 1H, C^{5}H), 2.79 (dq, *J* = 12.4, 6.2 Hz, 1H, C^{2}H), 2.62 (dd, *J* = 12.4, 6.7 Hz, 1H, C^{8}H), 1.99 – 1.93 (m, 4H, C^{3}H^a, C^{4}H^a, C^{6}H^a, C^{7}H^a), 1.66 – 1.16 (m, 16H, C^{3}H^b, C^{4}H^b, C^{6}H^b, C^{7}H^b, C$^{9-14}$H$_2$), 1.12 (d, *J* = 6.4 Hz, 3H, C^{1}H$_3$), 0.86 (t, *J* = 6.7 Hz, 3H, C^{15}H$_3$). ^{13}C NMR (75 MHz, $CDCl_3$) δ_C [ppm] 66.8 (C^8), 65.1 (C^5), 61.8 (C^2), 37.3, 34.6, 32.6, 32.3 (C^{3,4,6,7}), 32.0, 31.9, 30.0, 29.5, 27.4, 22.8 (C$^{9-14}$), 22.1 (C^1), 14.2 (C^{15}). GC-MS (EI+, 70 eV): t_R = 10.26 min; *m/z* (%) = 223 [M$^+$] (4), 208 [C$_{14}$H$_{26}$N$^+$] (6), 194 (3), 180 (3), 166 (1), 152 (1), 138 (1), 124 [C$_8$H$_{14}$N$^+$] (100), 110 (3), 97 (2), 81 (4), 68 (3), 55 (3), 41 (4), 30 (< 1). HR-MS: *m/z* = 224.2375 [MH$^+$] (calcd.: 224.2373). Optical rotation: $[\alpha]_D^{20}$ = +11.7 (c 0.25, $CHCl_3$); lit.[19g]: $[\alpha]_D^{23}$ = +10.9 (c 0.72, $CHCl_3$,).

---

[6] See footnote 4 on p. 96.

¹H-NMR of (+)-xenovenine
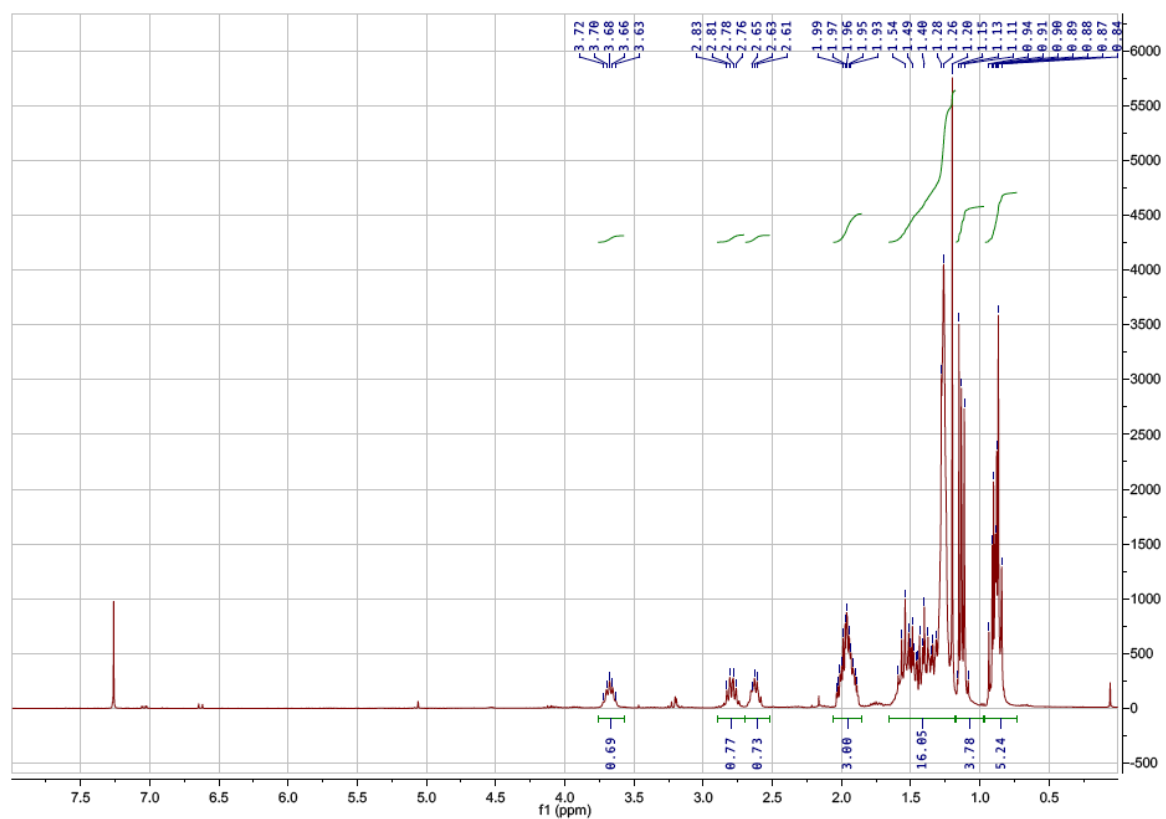
HR-MS of (+)-xenovenine

Xenovenine26 #134-181 RT: 0.77-0.99 AV: 8 NL: 5.30E9
T: FTMS + p APCI corona Full ms [90.00-1100.00]
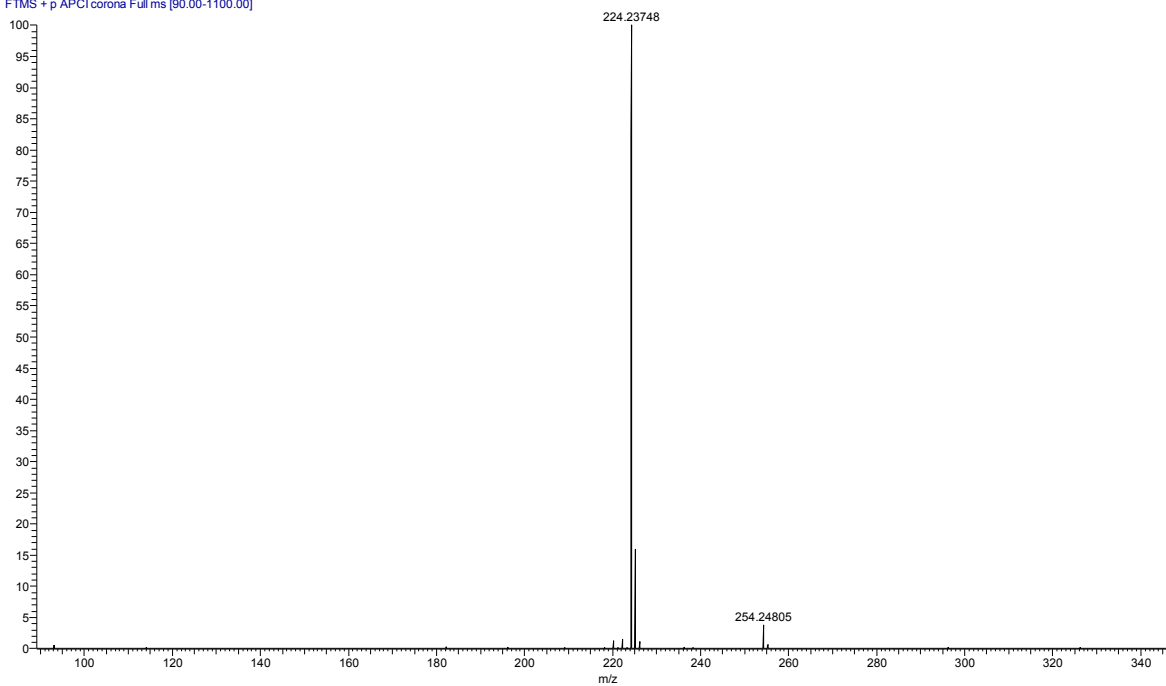
3.3 Analytical Methods

3.3.1 Syntheses of Reference Materials Used in the Chemo-Enzymatic Synthesis of Xenovenine.

rac-4-(5-Heptylfuran-2-yl)-butan-2-amine rac-**6**.
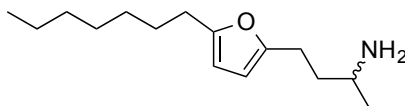
The reaction was carried out under argon inert atmosphere and standard-SCHLENK conditions.

Ketofuran **8** (100 mg, 423 μmol) was dissolved in MeOH (2.2 mL), and ammonium formate (267 mg, 4.23 mmol, 10 eq) was added. After stirring at 21 °C for 3.5 h, sodium cyanoborohydride (16 mg, 253.8 μmol, 0.6 eq) was added and the mixture was kept stirring at 21 °C for 3 h. TLC and GC-MS confirmed quantitative turnover of ketone **8** after that time and the reaction was stopped by addition of 6 M HCl (130 μL, 3 eq based on NaCNBH$_3$). The solvent was evaporated to yield a suspension of a colorless solid, which was taken up in water (4 mL) and basified (pH 12-13) with 10 M NaOH. Extraction of the aqueous phase with EtOAc (3 x 4 mL), drying of the combined organic phases and solvent evaporation under reduced pressure yielded 97.3 mg of rac-amine **6** (97 %) after drying in vacuo. R_f (PE/TEA/EtOH 90:7:3) = 0.13. ^{1}H NMR (300 MHz, CDCl$_3$) δ_H [ppm] 5.84 (dd, J = 8.2, 2.8 Hz, 2H, C^{6,7}H), 2.94 (h, J = 6.4 Hz, 1H, C^{2}H), 2.63 (t, J = 7.6 Hz, 2H, C$^{4/9}$H$_2$), 2.55 (t, J = 7.6 Hz, 2H, C$^{4/9}$H$_2$) , 2.22 (bs, 2H, NH$_2$), 1.81 – 1.42 (m, 4H, C^{3,10}H$_2$), 1.42 – 1.16 (m, 8H, C$^{11-14}$H$_2$), 1.09 (d, J = 6.4 Hz, 3H, C^{1}H$_3$), 0.87 (t, J = 6.7 Hz, 3H, C^{15}H$_3$). ^{13}C NMR (75 MHz, CDCl$_3$) δ_C [ppm] 155.1, 153.8 (C$_q^{5,8}$), 105.3, 105.0 (C^{6,7}), 46.6 (C^2), 38.1 (C^3), 31.9, 29.3, 29.2, 28.3, 28.2, 25.1, 23.6 (C$^{4,9-14}$), 22.8 (C^1), 14.2 (C^{15}). GC-MS (EI+, 70 eV): t_R = 11.58 min; m/z (%) = 237 [M$^+$] (15), 220 [C$_{15}$H$_{24}$O$^+$] (40), 205 (10), 193 [C$_{13}$H$_{21}$O$^+$] (< 1), 179 [C$_{12}$H$_{19}$O$^+$] (6), 166 (< 1), 149 (< 1), 135 [C$_9$H$_{11}$O$^+$] (100), 121 (5), 107 (12), 94 (6), 79 (5), 69 (5), 57 (11), 44 [C$_2$H$_6$N$^+$] (10), 30 (< 1). HR-MS: m/z = 238.2167 [MH$^+$] (calcd.: 238.2165).

¹H-NMR of *rac*-**6**
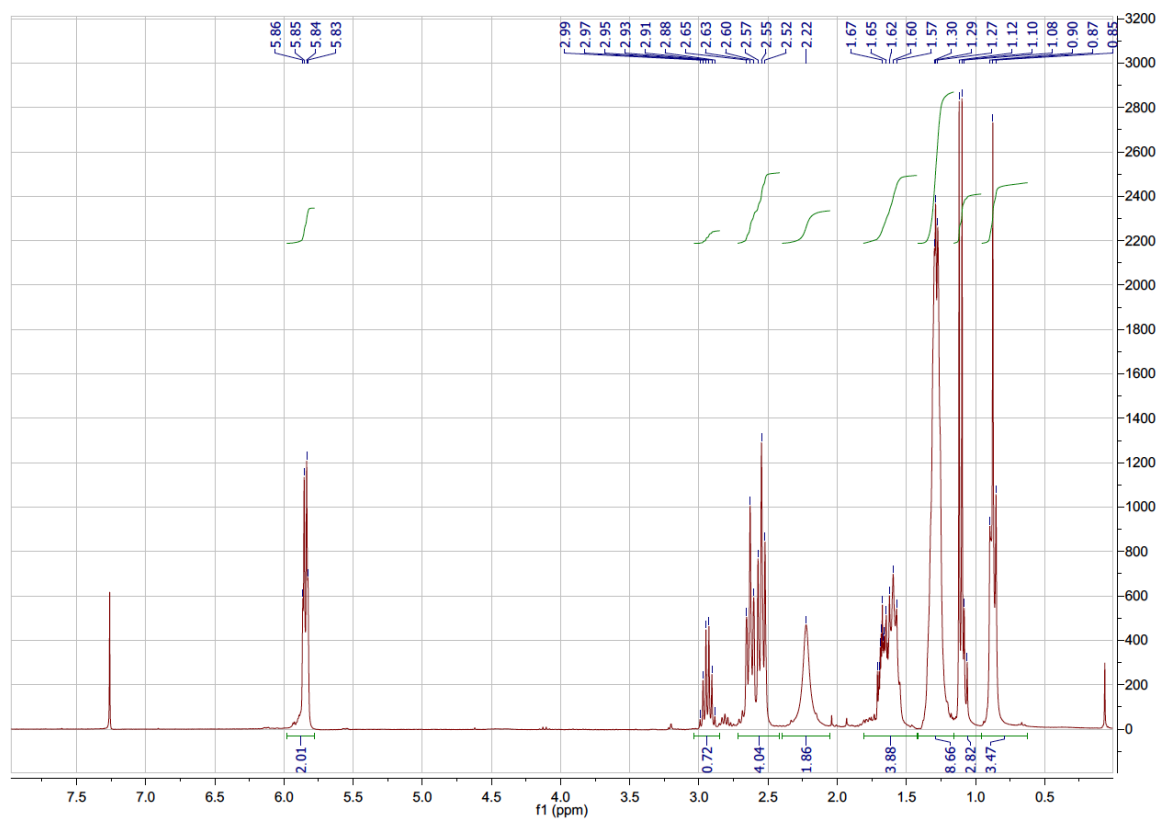
¹³C-NMR of *rac*-**6**
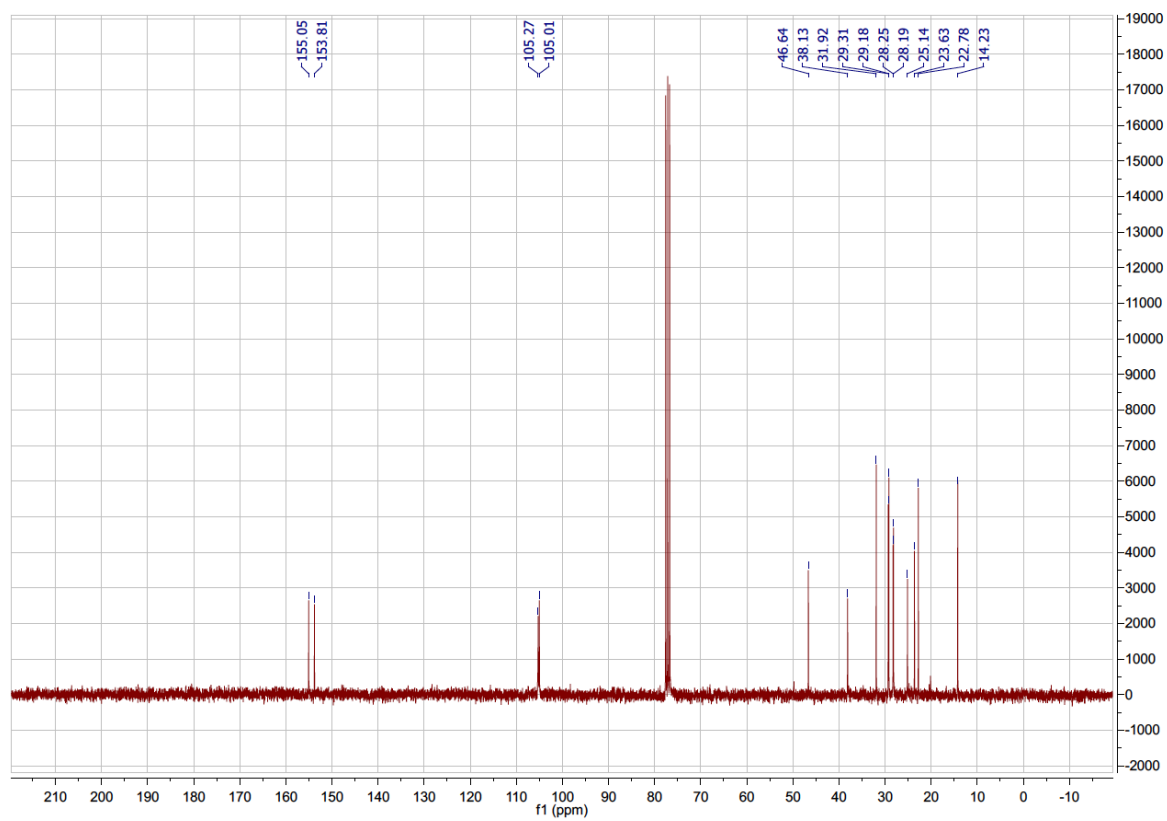
HR-MS of *rac*-**6**

Xenovenine12 #143-202   RT: 0.80-1.08   AV: 10   NL: 8.33E9
T: FTMS + p APCI corona Full ms [90.00-1100.00]
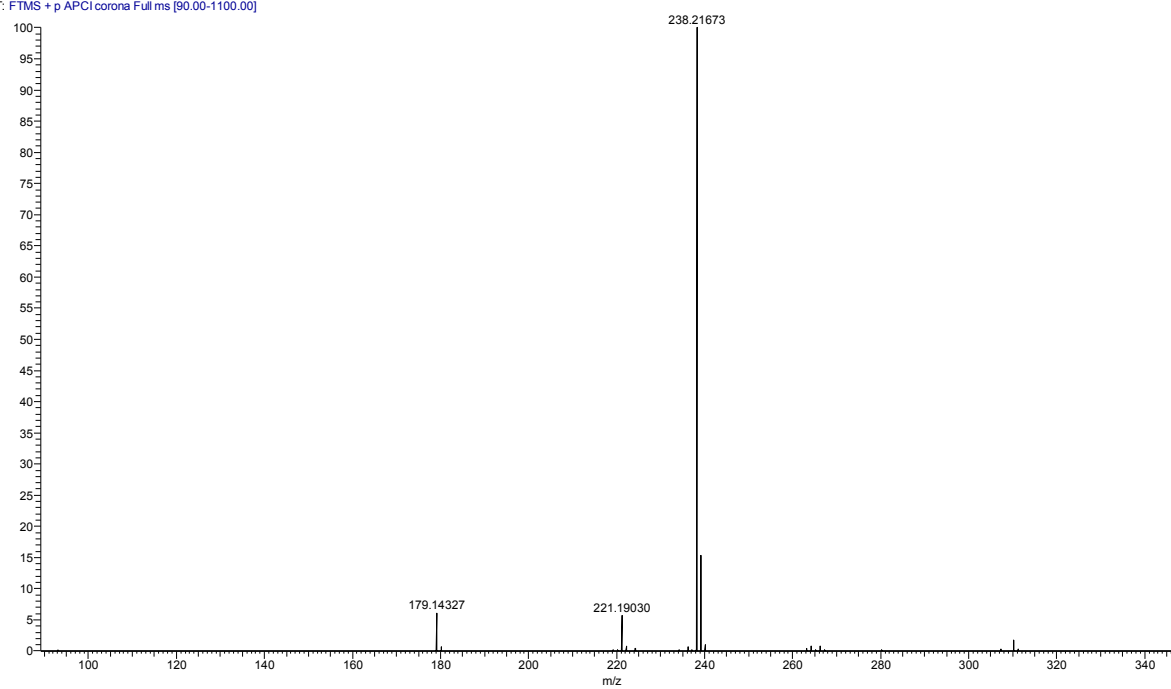
rac-1-(2-Methyl-3,4-dihydro-2*H*-pyrrol-5-yl)decan-3-one *rac*-**4**
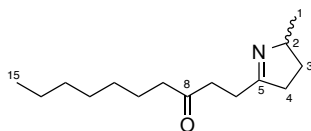
rac-Furanamine **6** (20 mg, 84 μmol) was dissolved in a mixture of AcOH (1 mL) and 12 M HCl (500 μL) and stirred for 2 h at 60 °C. Upon full conversion of **6** (confirmed GC-MS) the reaction was quenched by pouring into ice-cooled 10 M NaOH (1.2 mL, pH of resulting mixture ca. 10), and the product was extracted with EtOAc (3 x 1 mL). After drying over MgSO$_4$, solvent removal under reduced pressure and drying *in vacuo*, 16 mg of *rac*-imine **4** (80 %) were obtained without further purification. R_f (PE/TEA/EtOH 90:7:3) = 0.5. ^{1}H NMR (300 MHz, CDCl$_3$) δ_H [ppm] 4.00 (dd, J = 13.9, 6.9 Hz, 1H, C^{2}H), 2.89 – 2.68 (m, 2H, C^{7}H$_2$), 2.62 – 2.35 (m, 6H, C^{6}H$_2$, C^{4}H$_2$, C^{9}H$_2$), 2.15 – 1.94 (m, 1H, C^{3}H^a), 1.57 (dd, J = 14.3, 7.2 Hz, 2H, C^{10}H$_2$), 1.44 – 0.90 (m, 12H, C^{3}H^b, C$^{11\text{-}14}$H$_2$, C^{1}H$_3$), 0.86 (t, J = 6.6 Hz, 3H, C^{15}H$_3$). ^{13}C NMR (300 MHz, CDCl$_3$) δ_C [ppm] 210.5 (C$_q^8$=O), 175.9 (C$_q^5$=N), 67.7 (C^2), 43.0 (C^9), 39.0 (C^7), 38.4 (C^4), 31.8 (C$^{11\text{-}14}$), 30.7 (C^3), 29.3, 29.2 (C$^{11\text{-}14}$), 27.2 (C^6), 24.0 (C^{10}), 22.7 (C$^{11\text{-}14}$), 22.1 (C^1), 14.2 (C^{15}). GC-MS (EI+, 70 eV): t_R = 12.20 min; m/z (%) = 237 [M$^+$] (3), 222 (2), 208 (5), 194 (4), 180 (3) 166 [C$_{10}$H$_{16}$NO$^+$] (26), 153 (12), 138 [C$_8$H$_{16}$O$^+$] (100), 124 (7), 110 [C$_7$H$_{12}$N$^+$] (70), 96 [C$_6$H$_{10}$N$^+$] (19), 82 (11), 69 (4), 55 (12), 41.1 (14), 30.1 (< 1). HR-MS: m/z = 238.2167 [*rac*-MH$^+$] (calcd. 238.2165).

^{1}H-NMR of *rac*-**4**
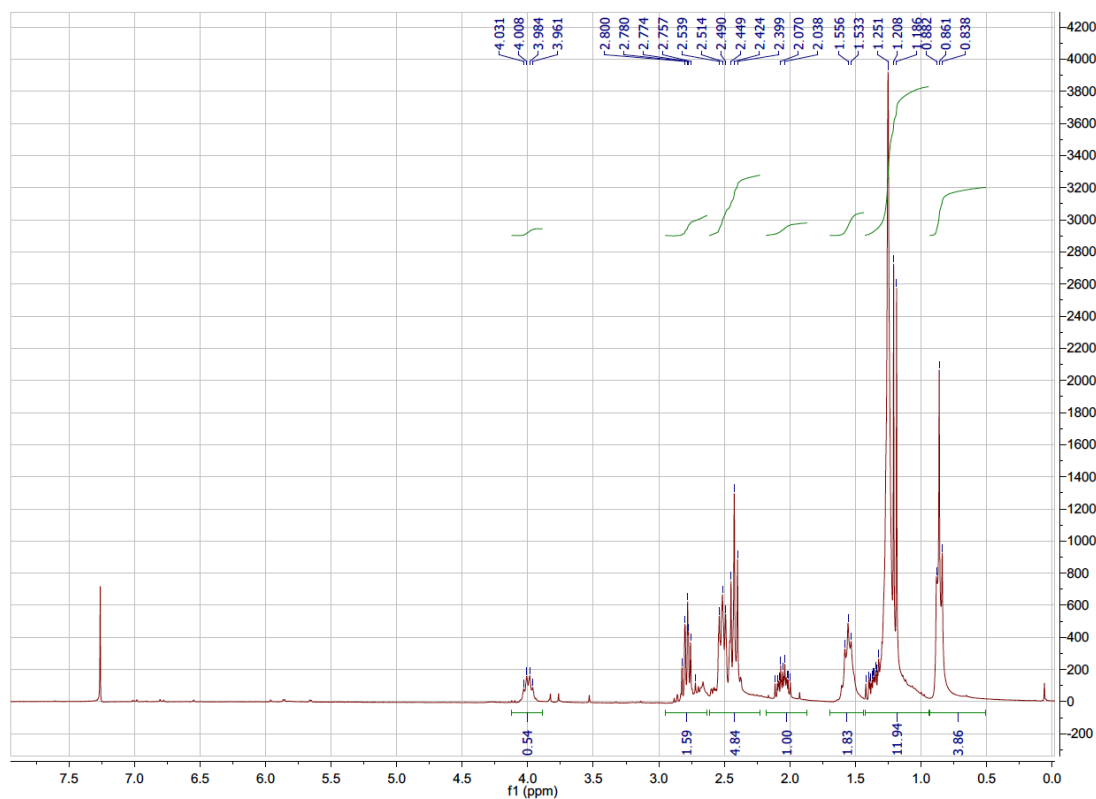
¹³C of *rac*-**4**
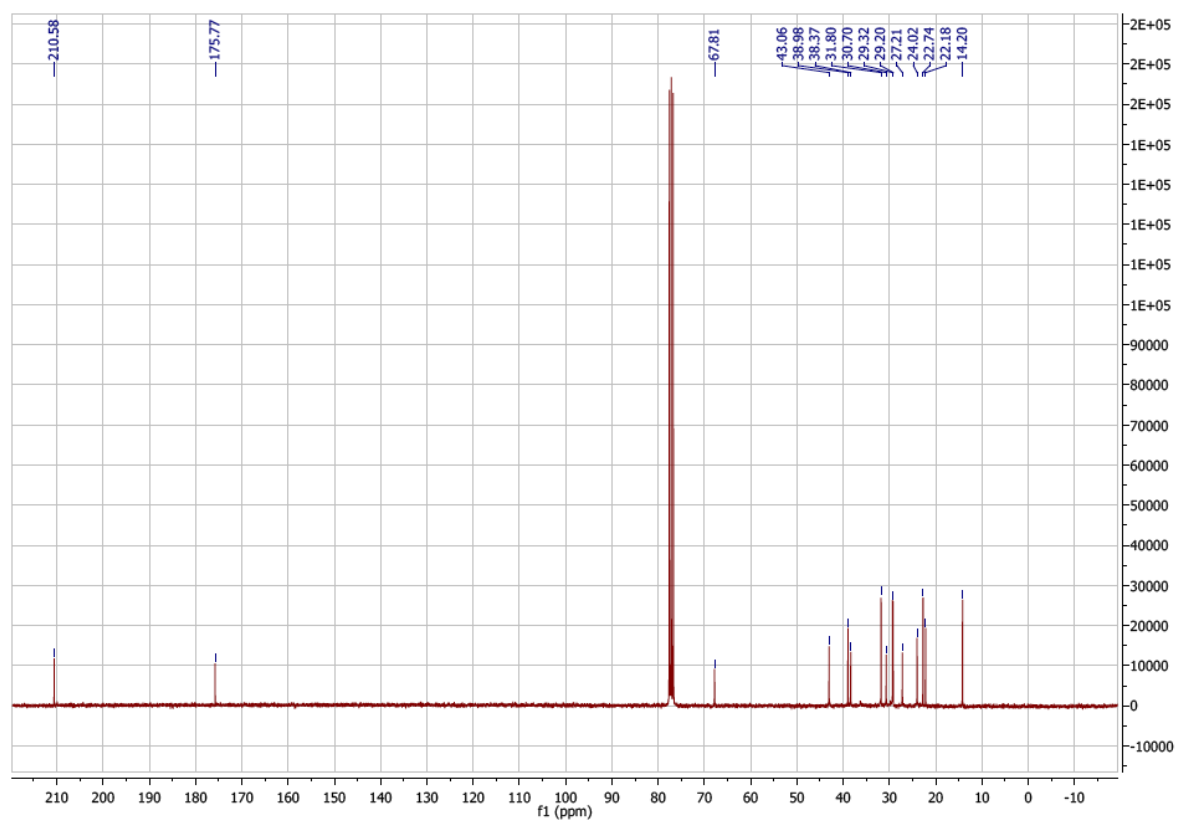
COSY of *rac*-**4**
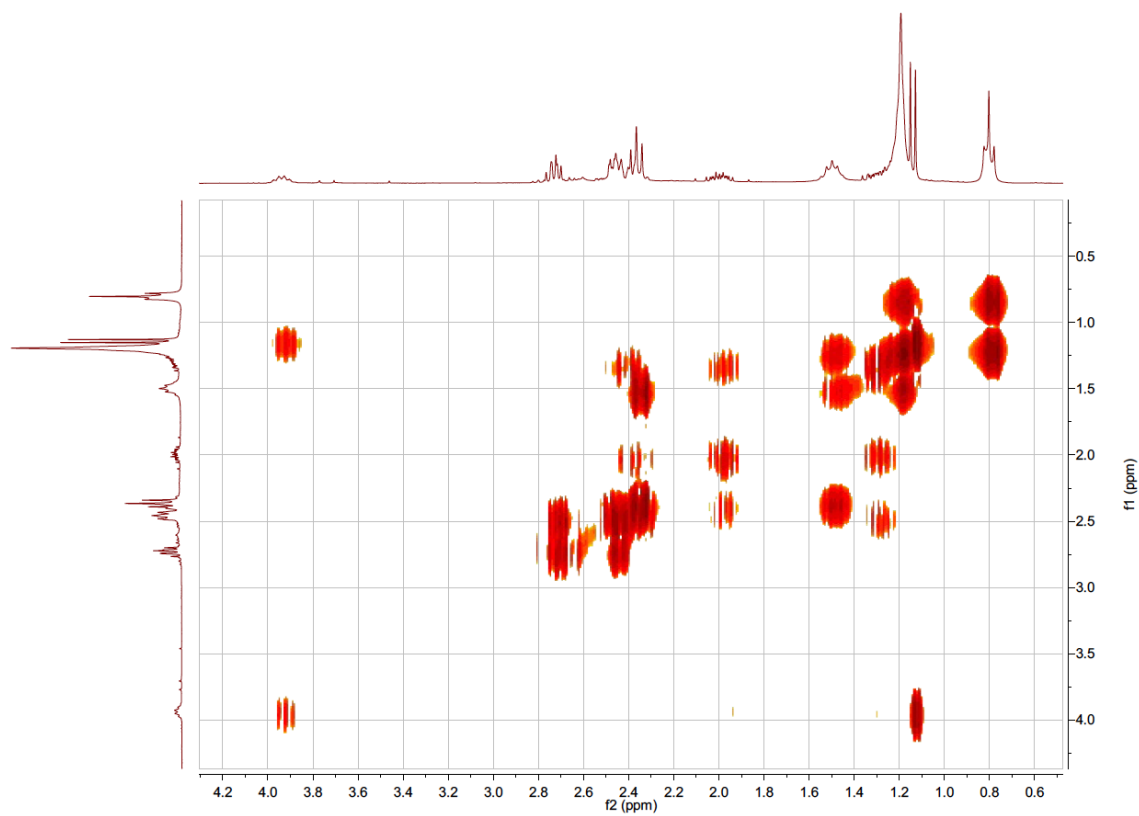
HSQC of *rac*-**4**
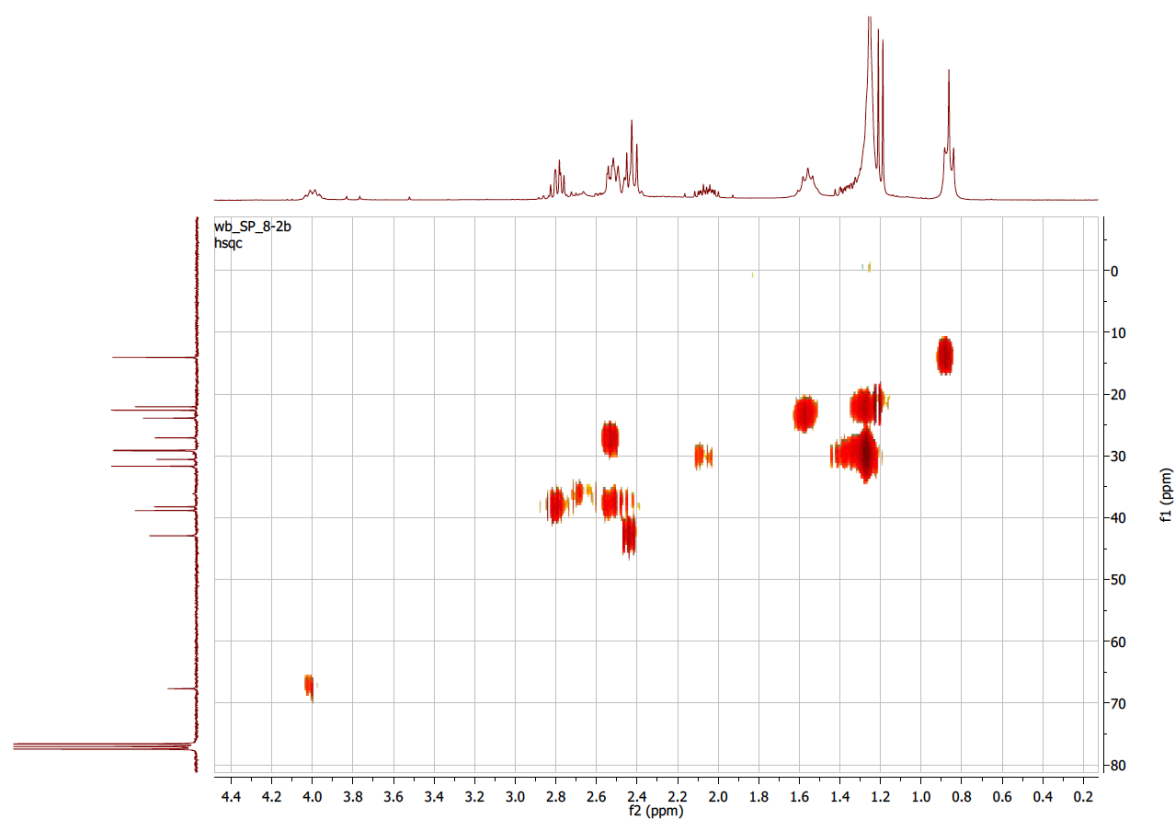
HR-MS of *rac*-**4**

Xenovenine16 #53-93 RT: 0.35-0.50 AV: 6 NL: 2.64E9
T: FTMS + p APCI corona Full ms [90.00-1100.00]
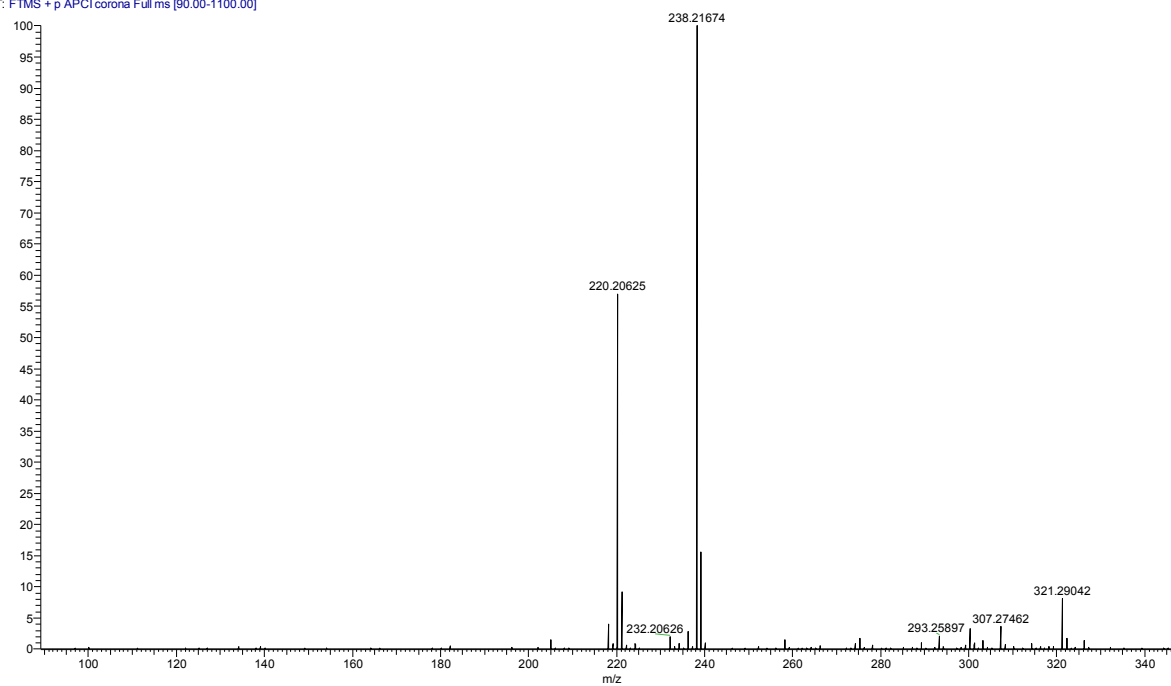
rac-5-Heptyl-3-methyl-2,3-dihydro-1*H*-pyrrolizine *rac*-**2**
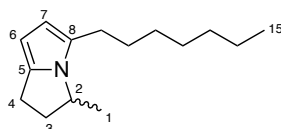
Racemic imine **4** (5 mg) was dissolved in MeOH (1 mL; final conc. of **4**: 21 mM) and AcOH (10 μL) was added. The mixture was shaken in an EPPENDORF orbital shaker at 21 °C for 1 h, after which GC-MS and TLC confirmed quantitative conversion to pyrrole **2**. Since this compound was only required for analytical purposes, it was evaporated in an air stream, re-dissolved in EtOAc (1 mL) and injected to GC as such. R_f (PE/TEA/EtOH 90:7:3) = 0.78. ^{1}H NMR (300 MHz, CDCl$_3$) δ_H [ppm] 5.89 (d, J = 3.1 Hz, 1H, C^{7}H), 5.69 (d, J = 3.1 Hz, 1H, C^{6}H), 4.31 (dqd, J = 12.9, 6.4, 3.4 Hz, 1H, C^{2}H), 2.96 – 2.82 (m, 1H), 2.81 – 2.61 (m, 3H, C^{3}H^a, C^{4}H$_2$), 2.61 – 2.51 (m, 2H, C^{9}H$_2$), 2.15 – 2.01 (m, 1H, C^{3}H^b), 1.73 – 1.57 (m, 2H, C^{10}H$_2$), 1.34 (m, 11H, C$^{11-14}$H$_2$, C^{1}H$_3$), 0.90 (t, J = 6.7 Hz, 3H, C^{15}H$_3$). ^{13}C NMR (75 MHz, CDCl$_3$) δ_C [ppm] 134.9 (C$_q$^{8}), 128.1 (C$_q$^{5}), 108.4 (C^7), 97.8 (C^6), 52.8 (C^3), 36.5, 32.0, 29.7, 29.3, 26.9, 23.0, 22.8 (C^4, C$^{9-14}$), 21.2 (C^1), 14.3 (C^{15}). GC-MS (EI+, 70 eV): t_R = 11.60 min; m/z (%) = 219 [M$^+$] (17), 204 [C$_{14}$H$_{22}$N$^+$] (< 1), 190 [C$_{13}$H$_{20}$N$^+$] (< 1), 176 [C$_{12}$H$_{18}$N$^+$] (< 1), 162 [C$_{11}$H$_{16}$N$^+$] (< 1), 148 [C$_{10}$H$_{14}$N$^+$] (3), 134 [C$_9$H$_{12}$N$^+$] (100), 118 (4), 106 (3), 93 (6), 77 (1), 65 (< 1), 55 (< 1), 41 (< 1). HR-MS: m/z = 220.2063 [*rac*-MH$^+$] (calcd.: 220.2060).

^{1}H-NMR of *rac*-**2**
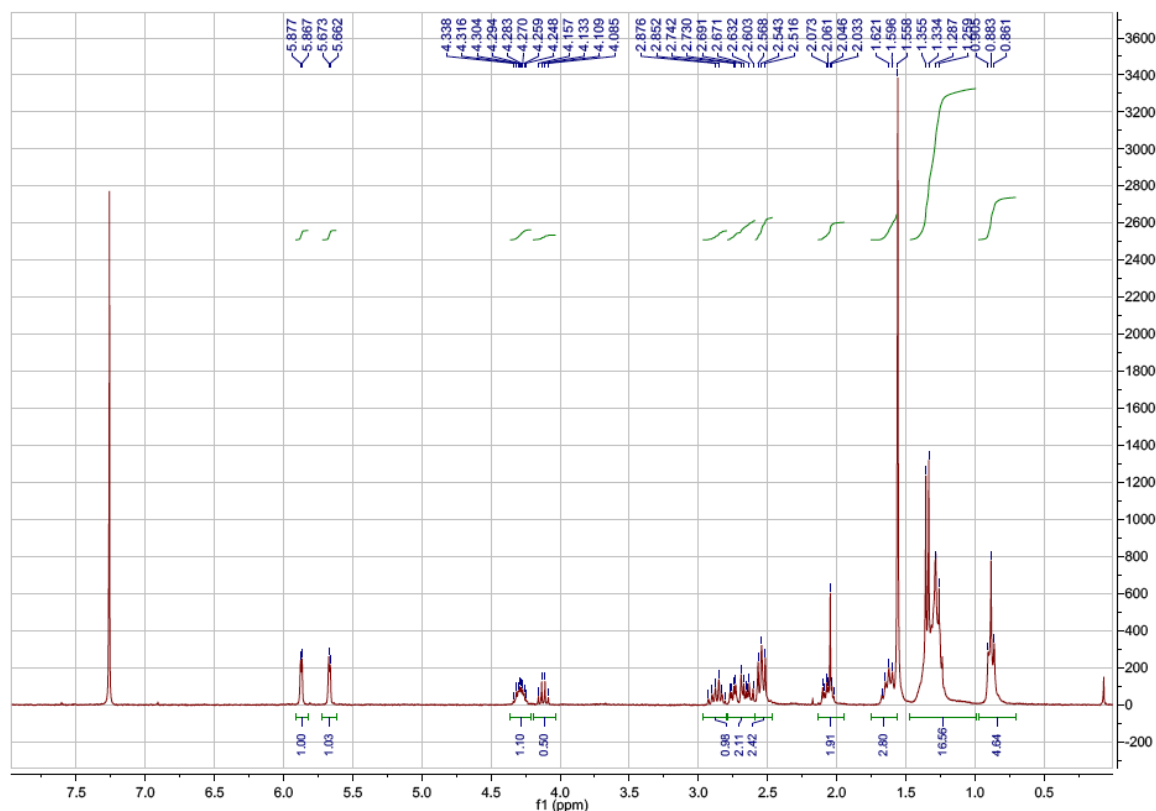
HR-MS of *rac*-**2**
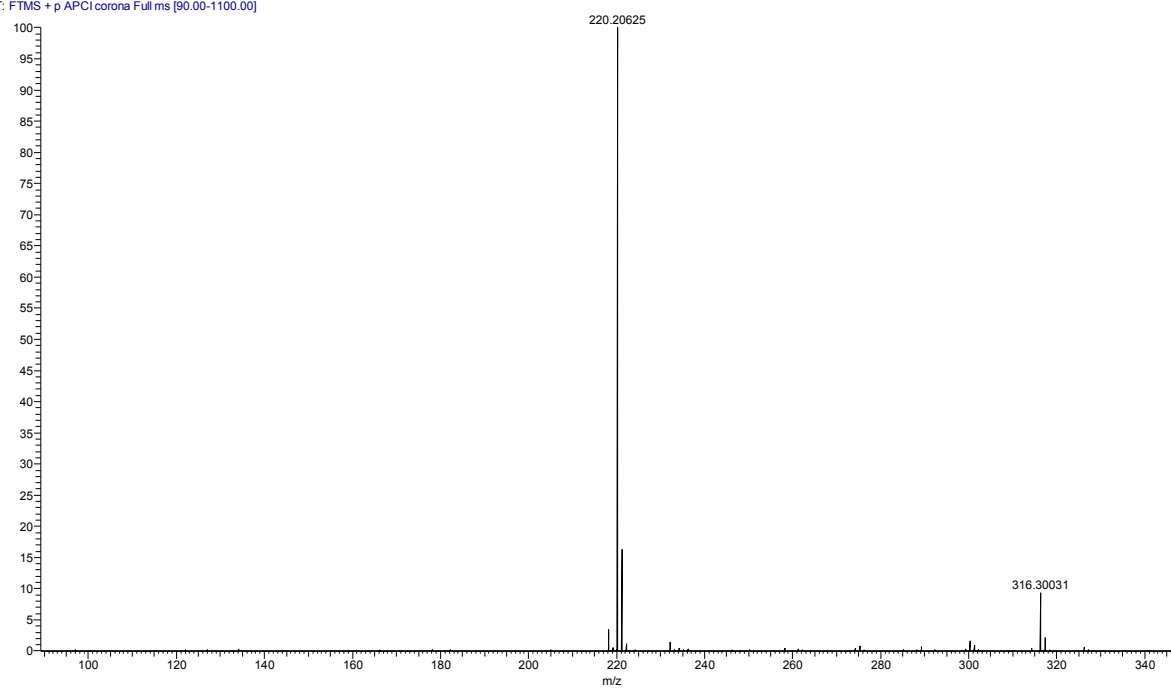
3.3.2 Syntheses of Reference Materials Used in the Screening of Novel Smart Co-Substrates.

rac-1-(4-Methoxyphenyl)ethan-1-amine *rac*-**27a**
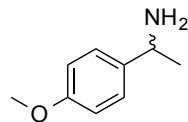
1-(4-Methoxyphenyl)ethan-1-one **27** (100 mg, 609 µmol) was dissolved in MeOH (5.0 mL). Ammonium formate (384.02 mg, 10 eq, 6.09 mmol) was added and the solution was stirred for 30 min at 21 °C. Then, sodium cyanoborohydride (23.0 mg, 0.6 eq, 365 µmol) was added and the mixture was kept stirring for 3 h after which TLC showed quantitative conversion of **27**. The reaction was quenched by adding 6 M HCl (1 mL) and evaporated under reduced pressure to give a colorless solid residue. This residue was taken up in H_2O (10 mL) and acidified to pH 3-4 with 6 M HCl. The aqueous phase was washed with EtOAc (10 mL) and basified to pH 9-10 with 10 M NaOH. The basic aqueous phase was extracted with EtOAc (3 x 10 mL) and the combined organic phases were dried over $MgSO_4$. After evaporation of the solvent under reduced pressure and drying *in vacuo*, 72 mg of the amine **27a** were obtained as colorless oil (71 %). If necessary, the amine was purified by flash column chromatography in a PASTEUR pipette packed to the half with silica gel in 1 mL PE/EtOAc 3:1. After applying the crude sample, impurities were eluted with 3 – 4 mL PE/EtOAc 3:1, the product amine was eluted with PE/TBME/NH_4OH 80:18:2. R_f (PE/EtOAc 3:1) = 0.19. GC-MS (EI+, 70 eV): t_R = 8.00 min; m/z (%) = 150.0 [M+] (2), 134, 122 [$C_7H_8NO^+$] or [$C_8H_{10}O^+$] (43), 115 (< 1), 107 (4), 91 (5), 78 (7), 65 (3), 58 (< 1), 51 (3), 44 [$C_2H_6N^+$] (100), 36 (3).

rac-7-Methoxy-1,2,3,4-tetrahydronaphthalen-2-amine *rac*-**28a**
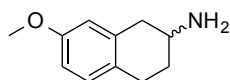
7-Methoxy-3,4-dihydronaphthalen-2(1*H*)-one **28** (100 mg, 567 µmol) was dissolved in MeOH (5.0 mL). Ammonium formate (358 mg, 10 eq, 5.67 mmol) was added and the solution was stirred for 30 min at 21 °C. Then, sodium cyanoborohydride (21.4 mg, 0.6 eq, 340 µmol) was added and the mixture was kept stirring for 3 h after which TLC showed quantitative conversion of **28** (difficult to monitor since both educt and product obviously decompose on silica gel). The reaction was quenched by adding 6 M HCl (1 mL) and evaporated under reduced pressure to give a colorless solid residue. This residue was taken up in H_2O (10 mL) and acidified to pH 3-4 with 6 M HCl. The aqueous phase was washed with EtOAc (10 mL) and basified to pH 9-10 with 10 M NaOH. The basic aqueous phase was extracted with EtOAc (3 x 10 mL) and the combined organic phases were dried over $MgSO_4$. After evaporation of the solvent under reduced pressure and drying *in vacuo*, 49 mg of the

amine **28a** were obtained as yellowish oil (49 %). If necessary, the amine was purified by flash column chromatography as described for **27a** above. R_f (PE/EtOAc 3:1) = 0.13. GC-MS (EI+, 70 eV): t_R = 10.97 min; m/z (%) = 177 [M$^+$] (30), 160 [C$_{11}$H$_{12}$O$^+$] (100), 145 [C$_{10}$H$_9$O$^+$] (24), 134 [C$_9$H$_{10}$O$^+$] (60), 115 (10), 104 (10), 91 (18), 77 (7), 65 (7), 51 (4), 36 (4).

rac-1-Phenoxypropan-2-amine *rac*-**30a**
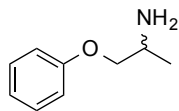
1-Phenoxypropan-2-one **30** (100 mg, 666 µmol) was dissolved in MeOH (5.0 mL). Ammonium formate (419.9 mg, 10 eq, 6.66 mmol) was added and the solution was stirred for 30 min at 21 °C Then, sodium cyanoborohydride (25.11 mg, 0.6 eq, 400 µmol) was added and the mixture was kept stirring for 3 h after which TLC showed quantitative conversion of **30**. The reaction was quenched by adding 6 M HCl (1 mL) and evaporated under reduced pressure to give a colorless solid residue. This residue was taken up in H$_2$O (10 mL) and acidified to pH 3-4 with 6 M HCl. The aqueous phase was washed with EtOAc (10 mL) and basified to pH 9-10 with 10 M NaOH. The basic aqueous phase was extracted with EtOAc (3 x 10 mL) and the combined organic phases were dried over MgSO$_4$. After evaporation of the solvent under reduced pressure and drying *in vacuo*, 81 mg of the amine **30a** were obtained as colorless oil (80 %). If necessary, the amine was purified by flash column chromatography as described for **27a** above. R_f (PE/EtOAc 3:1) = 0.27. GC-MS (EI+, 70 eV): t_R = 6.41 min; m/z (%) = 151 [M$^+$] (3), 134 (< 1), 119 (1), 108 (4), 94, 77 [C$_6$H$_5$$^+$] (10), 65 (4), 58 [C$_3H_8N^+$] (9), 51 (6), 44 [C$_2H_6N^+$] (100), 39 (5), 30 (3).

3.3.3 GC-FID Methods

GC-FID was used throughout all screenings for the determination of conversion and *e.e.*
For the smart co-substrate study, a calibration for all substrate ketones and product amines as well as 2,5-dimethylpyrazine was done, using *n*-dodecane as external standard. Calibration was performed in the range of 0.5 to 50 mM with standard concentrations 0.5, 2, 5, 20 and 50 mM. Standard preparation and dilution was carried out on a scale with 0.1 mg accuracy. The conversion for calibrated compounds was derived from their measured concentrations according to the following equation.

$$c = \frac{A_P}{A_P + A_E} \cdot 100\,\%$$

c .... conversion, in %.

$A_{E,P}$ .... area or concentration (mM) of educt or product peak in chromatogram.

The enantiomeric excess (*e.e.*) was solely derived from GC-FID areas of the peaks assigned to the derivatized enantiomers according to the formula below. (For detailed derivatization procedures please refer to table and figure footnotes in section 2)

$$e.e. = \frac{|A_R - A_S|}{A_R + A_S} \cdot 100\,\%$$

e.e. .... enantiomeric excess, in %

A_R .... area of (*R*)-enantiomer peak in chromatogram

A_S .... area of (*S*)-enantiomer peak in chromatogram

Achiral GC-Methods used within this work

Method	A
Column	DB-1701: J&W 122-0732, 30 m x 250 *μm* x 0.25 *μm* (no. 7)
Temperature Program	120 °C (0 min) –[10 °C/min]– 180 °C (0 min) –[60 °C/min]– 280 °C (2 min)
Carrier Gas Flow	H_2, 1.5 mL/min const.
Split Ratio	50:1
Injector Temperature	220 °C

Method	B
Column	DB-1701: J&W 122-0732, 30 m x 250 *μm* x 0.25 *μm* (no. 7)
Temperature Program	80 °C (0 min) –[10 °C/min]– 180 °C (0 min) –[60 °C/min]– 280 °C (5 min)
Carrier Gas Flow	H_2, 1.5 mL/min const.
Split Ratio	50:1
Injector Temperature	250 °C

Method	C
Column	DB-1701: J&W 122-0732, 30 m x 250 μm x 0.25 μm (no. 7)
Temperature Program	80 °C (1 min) –[10 °C/min]– 240 °C (10 min) –[40 °C/min]– 280 °C (2 min)
Carrier Gas Pressure	H$_2$, 1 bar const.
Split Ratio	50:1
Injector Temperature	250 °C

Method	D
Column	DB-1701: J&W 122-0732, 30 m x 250 μm x 0.25 μm (no. 7)
Temperature Program	50 °C (6.5 min) –[10 °C/min]– 100 °C (5 min)
Carrier Gas Pressure	H$_2$, 1 bar const.
Split Ratio	50:1
Injector Temperature	250 °C

Method	E
Column	DB-1701: J&W 122-0732, 30 m x 250 μm x 0.25 μm (no. 7)
Temperature Program	80 °C (0 min) –[10 °C/min]– 100 °C (0 min) –[60 °C/min]– 150 °C (2 min)
Carrier Gas Flow	H$_2$, 1.5 mL/min const.
Split Ratio	50:1
Injector Temperature	250 °C

Chiral GC-Methods used within this work.

Method	A*
Column	DEX-CB Varian CP7503, 25 m x 320 μm x 0.25 μm
Temperature Program	100 °C (2 min) –[1 °C/min]– 130 °C (5 min) –[10 °C/min]– 170 °C (1 min)
Carrier Gas Flow	H$_2$, 1.7 mL/min const.
Split Ratio	50:1
Injector Temperature	200 °C

Method	B*
Column	DEX-CB Varian CP7503, 25 m x 320 μm x 0.25 μm (27)
Temperature Program	100 °C (0 min) –[10 °C/min]– 170 °C (30 min)
Flow	H$_2$, 1.7 mL/min const.
Split Ratio	50:1
Injector Temperature	200 °C

Method	C*
Column	DEX-CB Varian CP7503, 25 m x 320 μm x 0.25 μm (27)
Temperature Program	100 °C (2 min) –[1 °C/min]– 130 °C (5 min) –[10 °C/min]– 170 °C (10 min)
Carrier Gas Flow	H$_2$, 1.7 mL/min const.
Split Ratio	50:1
Injector Temperature	200 °C

Method	D*
Column	DEX-CB Varian CP7503, 25 m x 320 μm x 0.25 μm
Temperature Program	100 °C (2 min) –[2 °C/min]– 130 °C (5 min) –[10 °C/min]– 180 °C (15 min)
Carrier Gas Flow	H$_2$, 1.7 mL/min const.
Split Ratio	50:1
Injector Temperature	200 °C

Method	E*
Column	DEX-CB Varian CP7503, 25 m x 320 μm x 0.25 μm
Temperature Program	60 °C (2 min) –[5 °C/min]– 100 °C (2 min) –[10 °C/min]– 160 °C (0 min)
Carrier Gas Flow	H$_2$, 1.7 mL/min const.
Split Ratio	50:1
Injector Temperature	250 °C

On the subsequent pages, achiral and chiral example chromatograms (left hand- and right hand columns, respectively) of all performed biotransformations are shown. The retention times are given for each compound involved.

Biotransformation of 4-(5-heptylfuran-2-yl)-butan-2-one **8**

Method	A
Column	DB-1701: J&W 122-0732, 30 m x 250 μm x 0.25 μm (no. 7)
Temperature Program	120 °C (0 min) –[10 °C/min]– 180 °C (0 min) –[60 °C/min]– 280 °C (2 min)
Carrier Gas Flow	H$_2$, 1.5 mL/min const.
Split Ratio	50:1
Injector Temperature	220 °C

Method	
Column	DEX-CB Varian CP7503, 25 m x 320 μm x 0.25 μm (27)
Temperature Program	100 °C (0 min) –[10 °C/min]– 170 °C (30 min)
Carrier Gas Flow	H$_2$, 1.7 mL/min const.
Split Ratio	50:1
Injector Temperature	200 °C

Compound	8	6	(*S*)-6	(*R*)-6
Method	A		B*	
t_R (min)	11.34	11.13	26.7	27.3

Biotransformation of **8**
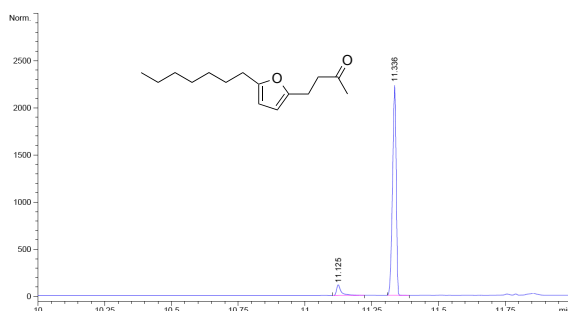
Reference **6**
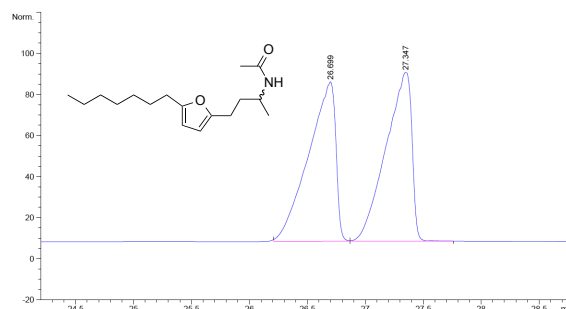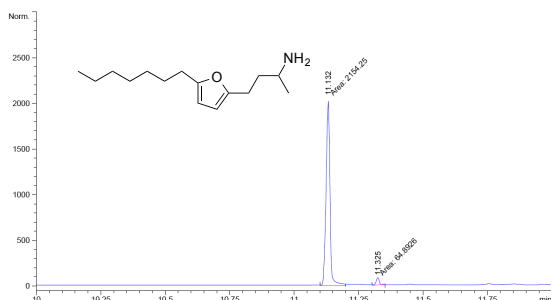
rac-N-acetyl-**6**
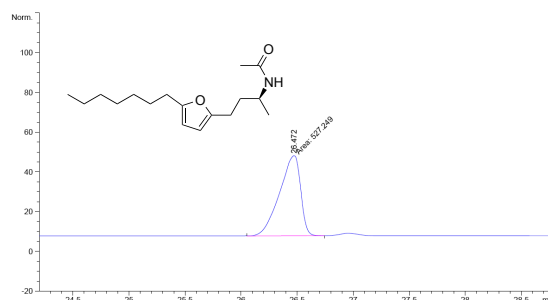
(*S*)-*N*-acetyl-**6**

(*R*)-*N*-acetyl-**6**
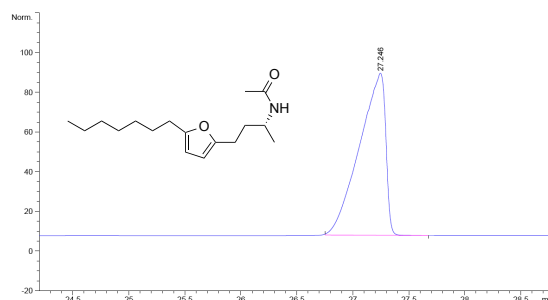
Derivatization of samples dissolved in EtOAc: 2 eq Ac$_2$O and 10 mol% DMAP for 30 min at 30 °C, 700 rpm (orbital shaker). Then add 200 µL Na$_2$CO$_3$, vortex, withdraw organic phase and dry with MgSO$_4$. (see also table and figure footnotes in section 2)

Biotransformation of pentadecane-2,5,8-trione 7

Method	B
Column	DB-1701: J&W 122-0732, 30 m x 250 μm x 0.25 μm (no. 7)
Temperature Program	80 °C (0 min) –[10 °C/min]– 180 °C (0 min) –[60 °C/min]– 280 °C (5 min)
Carrier Gas Flow	H_2, 1.5 mL/min const.
Split Ratio	50:1
Injector Temperature	250 °C

Method	B*
Column	DEX-CB Varian CP7503, 25 m x 320 μm x 0.25 μm (27)
Temperature Program	100 °C (0 min) –[10 °C/min]– 170 °C (30 min)
Carrier Gas Flow	H_2, 1.7 mL/min const.
Split Ratio	50:1
Injector Temperature	200 °C

Compound	7	4	(S)-6	(R)-6
Method	B		B*	
t_R (min)	12.37	11.52	10.0	9.9

Biotransformation of 7
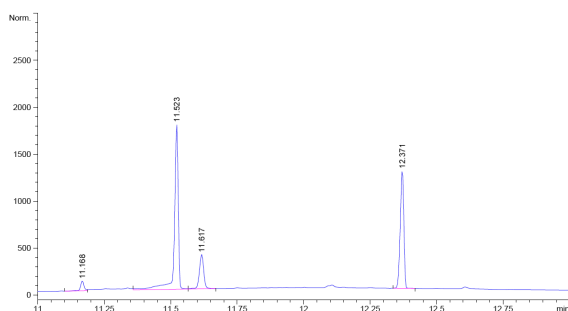
rac-2
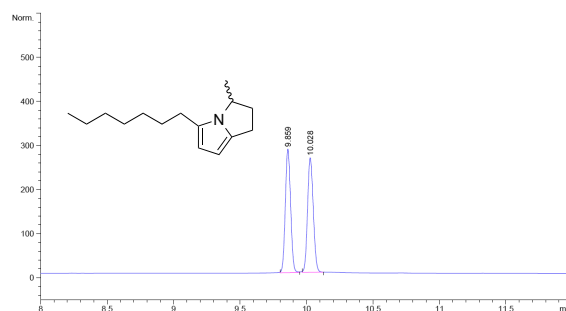
Reference 7
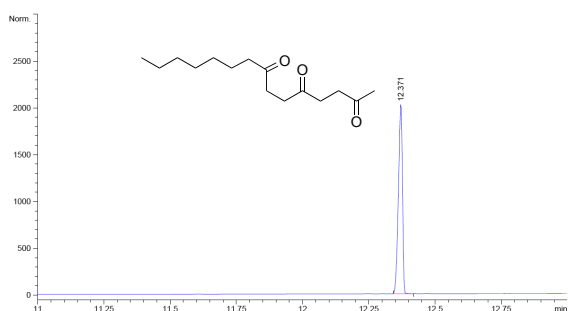
(R)-2
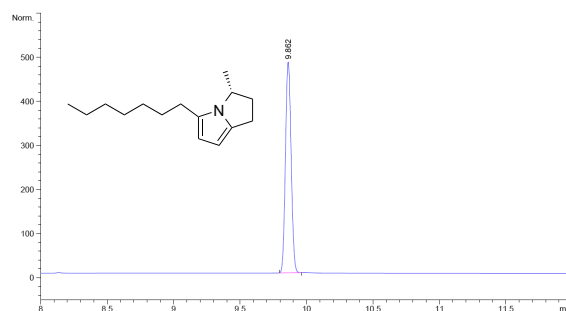
Reference 4

(S)-2
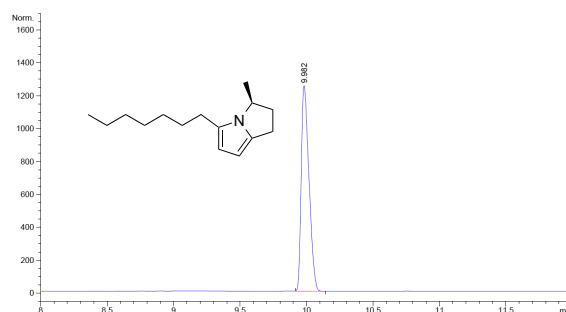
(Derivatization see footnote of table 2.5)

Biotransformation of 4-Phenyl-2-butanone **13**

Method	A
Column	DB-1701: J&W 122-0732, 30 m x 250 μm x 0.25 μm (no. 7)
Temperature Program	120 °C (0 min) –[10 °C/min]– 180 °C (0 min) –[60 °C/min]– 280 °C (2 min)
Carrier Gas Flow	H_2, 1.5 mL/min const.
Split Ratio	50:1
Injector Temperature	220 °C

Method	A*
Column	DEX-CB Varian CP7503, 25 m x 320 μm x 0.25 μm
Temperature Program	100 °C (2 min) –[1 °C/min]– 130 °C (5 min) –[10 °C/min]– 170 °C (1 min)
Carrier Gas Flow	H_2, 1.7 mL/min const.
Split Ratio	50:1
Injector Temperature	200 °C

Compound	26	n-$C_{12}H_{26}$	14	13	(S)-14	(R)-14
Method	A				A*	
t_R (min)	1.64	2.45	3.63	4.00	39.8	40.2

Biotransformation of **13**
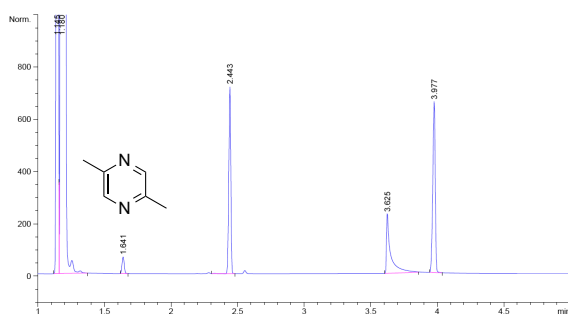
rac-N-acetyl-**14**
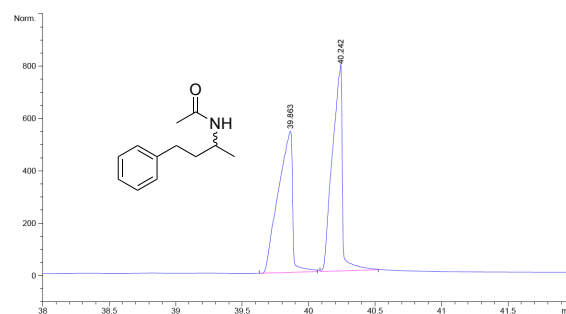
References **13** and **14** with I.S. n-$C_{12}H_{26}$
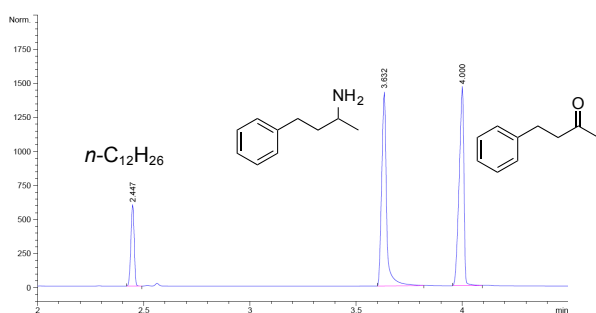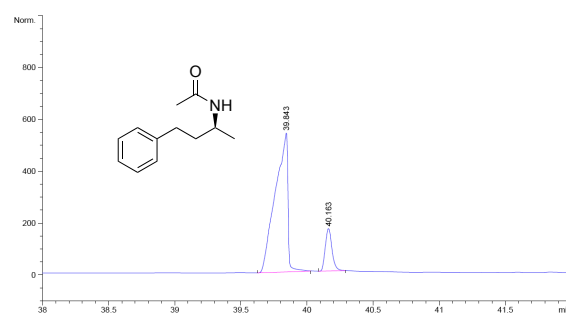
(S)-N-acetyl-**14**

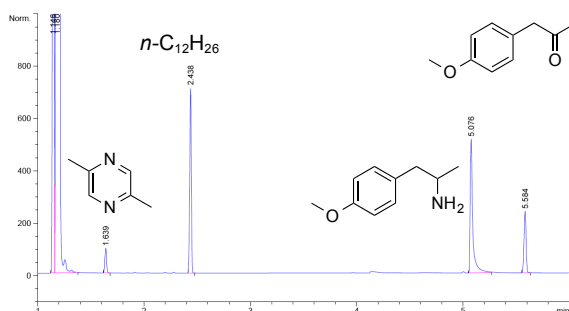Derivatization see p. 115.

(R)-N-acetyl-**14**
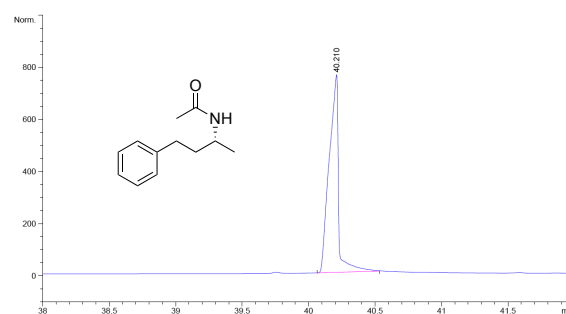
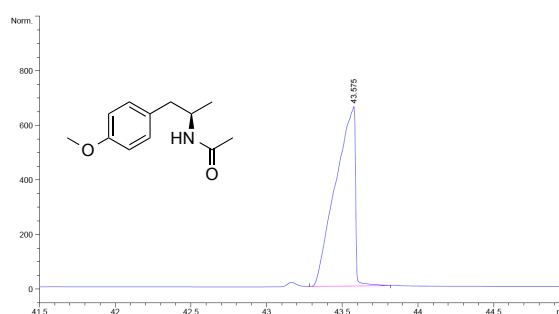## Biotransformation of 1-(4-methoxyphenyl)propan-2-one **27**

Method	A
Column	DB-1701: J&W 122-0732, 30 m x 250 μm x 0.25 μm (no. 7)
Temperature Program	120 °C (0 min) –[10 °C/min]– 180 °C (0 min) –[60 °C/min]– 280 °C (2 min)
Carrier Gas Flow	H_2, 1.5 mL/min const.
Split Ratio	50:1
Injector Temperature	220 °C

Method	A*
Column	DEX-CB Varian CP7503, 25 m x 320 μm x 0.25 μm
Temperature Program	100 °C (2 min) –[1 °C/min]– 130 °C (5 min) –[10 °C/min]– 170 °C (1 min)
Carrier Gas Flow	H_2, 1.7 mL/min const.
Split Ratio	50:1
Injector Temperature	200 °C

Compound	26	$n\text{-}C_{12}H_{26}$	27a	27	(S)-27a	(R)-27a
Method	A				A*	
t_R (min)	1.64	2.44	5.08	5.58	43.26	43.57

Biotransformation of **27**
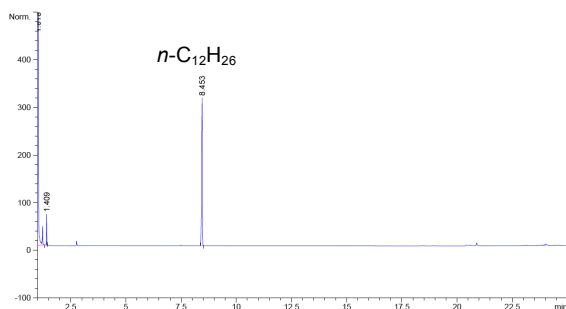

For derivatization see p. 115.

rac-N-acetyl-**27a**
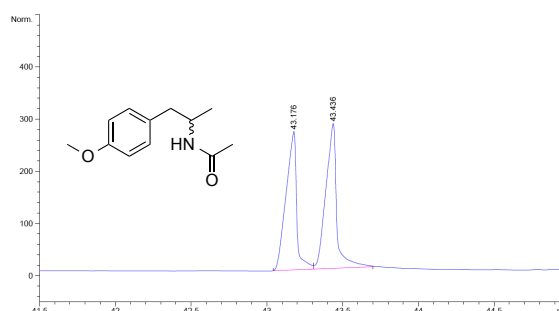
(*S*)-*N*-acetyl-**27a**
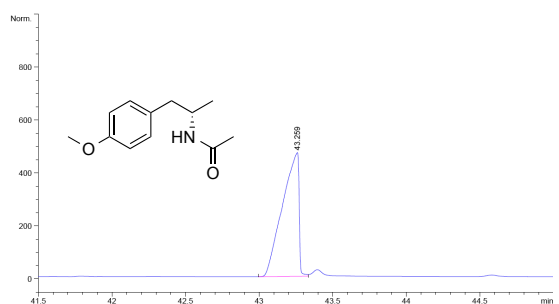
(*R*)-*N*-acetyl-**27a**

Biotransformation of 7-methoxy-3,4-dihydronaphthalen-2(1H)-one 28

Method	C
Column	DB-1701: J&W 122-0732, 30 m x 250 μm x 0.25 μm (no. 7)
Temperature Program	80 °C (1 min) –[10 °C/min]– 240 °C (10 min) –[40 °C/min]– 280 °C (2 min)
Carrier Gas Pressure	H$_2$, 1 bar const.
Split Ratio	50:1
Injector Temperature	250 °C

Method	D*
Column	DEX-CB Varian CP7503, 25 m x 320 μm x 0.25 μm
Temperature Program	100 °C (2 min) –[2 °C/min]– 130 °C (5 min) –[10 °C/min]– 180 °C (15 min)
Carrier Gas Flow	H$_2$, 1.7 mL/min const.
Split Ratio	50:1
Injector Temperature	200 °C

Compound	26	n-C$_{12}$H$_{26}$	28a	28	(S)-28a	(R)-28a
Method			C			D*
t_R (min)	n.d.	8.5	n.d.	n.d.	37.2	37.7

biotransformation of **28**

Note: no ketone or amine could be observed in the biotransformation.
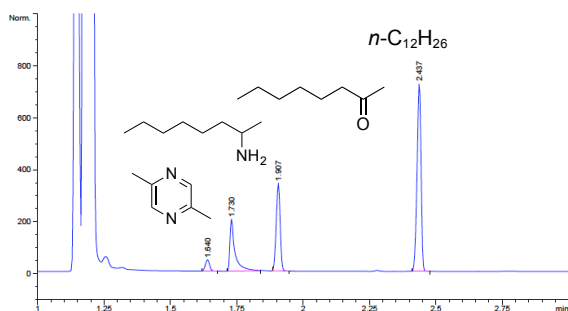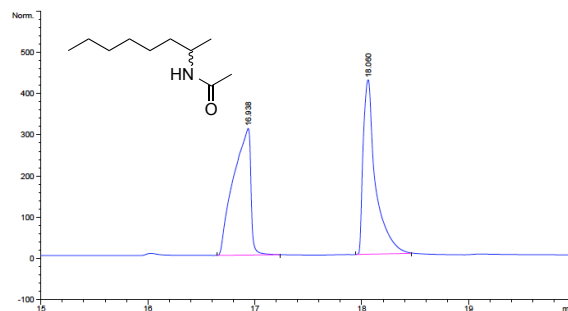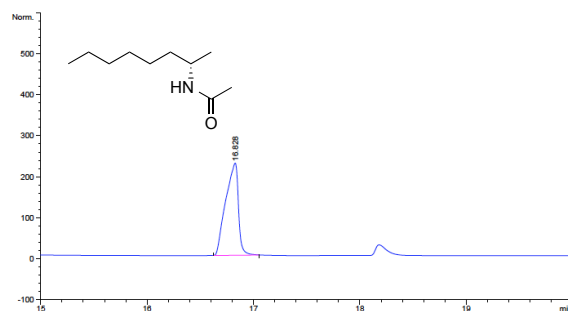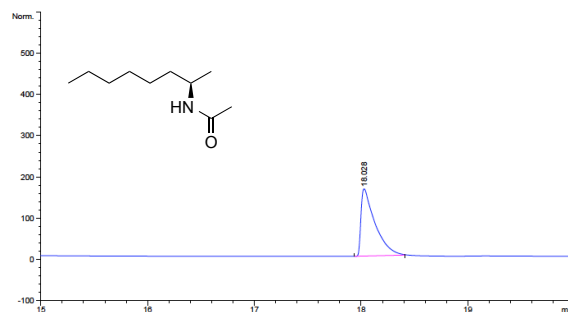
For derivatization see p. 115.

rac-N-acetylated **28a**
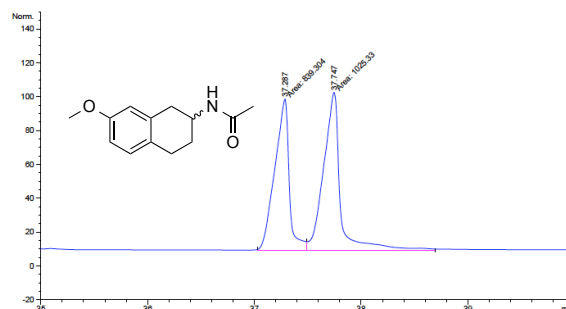
(S)-N-acetylated **28a**
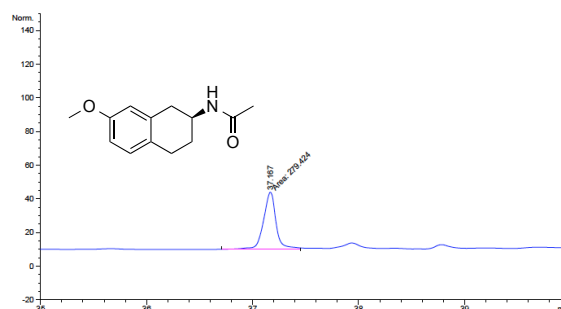
(R)-N-acetylated **28a**
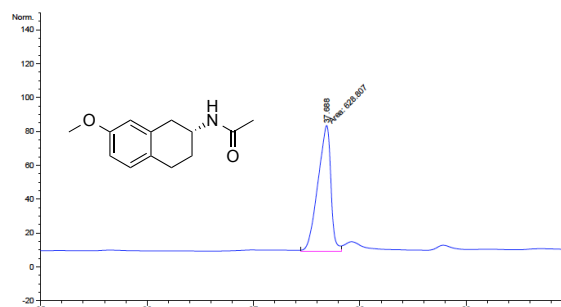
Biotransformation of octan-2-one **29**

Method	A
Column	DB-1701: J&W 122-0732, 30 m x 250 μm x 0.25 μm (no. 7)
Temperature Program	120 °C (0 min) –[10 °C/min]– 180 °C (0 min) –[60 °C/min]– 280 °C (2 min)
Carrier Gas Flow	H_2, 1.5 mL/min const.
Split Ratio	50:1
Injector Temperature	220 °C

Method	A*
Column	DEX-CB Varian CP7503, 25 m x 320 μm x 0.25 μm
Temperature Program	100 °C (2 min) –[1 °C/min]– 130 °C (5 min) –[10 °C/min]– 170 °C (1 min)
Carrier Gas Flow	H_2, 1.7 mL/min const.
Split Ratio	50:1
Injector Temperature	200 °C

Compound	26	29a	29	$n\text{-}C_{12}H_{26}$	(S)-29a	(R)-29a
Method	A				A*	
t_R (min)	1.64	1.73	1.91	2.44	16.83	18.03

Biotransformation of **29**

rac-N-acetylated **29a**

For derivatization see p. 115.

(S)-N-acetylated **29a**

(R)-N-acetylated **29a**

Biotransformation of 1-phenoxypropan-2-one **30**

Method	A
Column	DB-1701: J&W 122-0732, 30 m x 250 μm x 0.25 μm (no. 7)
Temperature Program	120 °C (0 min) –[10 °C/min]– 180 °C (0 min) –[60 °C/min]– 280 °C (2 min)
Carrier Gas Flow	H_2, 1.5 mL/min const.
Split Ratio	50:1
Injector Temperature	220 °C

Method	C*
Column	DEX-CB Varian CP7503, 25 m x 320 μm x 0.25 μm (27)
Temperature Program	100 °C (2 min) –[1 °C/min]– 130 °C (5 min) –[10 °C/min]– 170 °C (10 min)
Carrier Gas Flow	H_2, 1.7 mL/min const.
Split Ratio	50:1
Injector Temperature	200 °C

Compound	26	n-$C_{12}H_{26}$	30a	30	(S)-30a	(R)-30a
Method	A				C*	
t_R (min)	1.64	2.44	3.75	3.81	39.66	40.29

Biotransformation of **30**
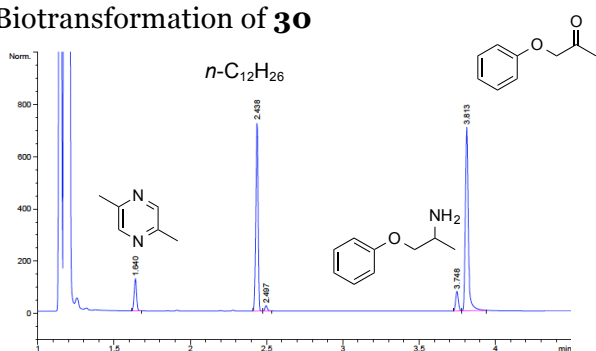
rac-N-acetylated **30a**
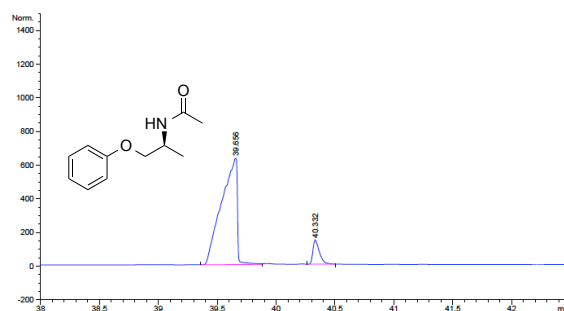
For derivatization see p. 115.

(S)-N-acetylated **30a**

(R)-N-acetylated **30a**
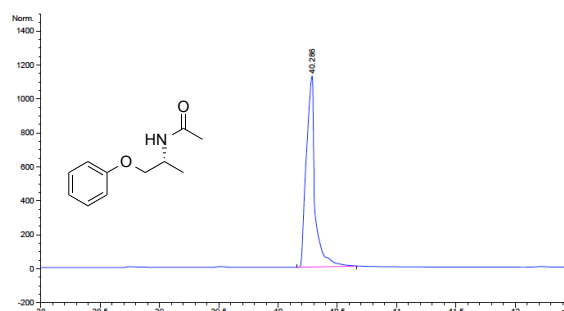
Biotransformation of 1-methoxpropan-2-one **31**

Method	D
Column	DB-1701: J&W 122-0732, 30 m x 250 μm x 0.25 μm (no. 7)
Temperature Program	50 °C (6.5 min) –[10 °C/min]– 100 °C (5 min)
Carrier Gas Pressure	H_2, 1 bar const.
Split Ratio	50:1
Injector Temperature	250 °C

Method	E*
Column	DEX-CB Varian CP7503, 25 m x 320 μm x 0.25 μm
Temperature Program	60 °C (2 min) –[5 °C/min]– 100 °C (2 min) –[10 °C/min]– 160 °C (0 min)
Carrier Gas Flow	H_2, 1.7 mL/min const.
Split Ratio	50:1
Injector Temperature	250 °C

Compound	26	n-$C_{12}H_{26}$	31a	31	(S)-31a	(R)-31a
Method			D			E*
t_R (min)	n.d.	13.07	11.42	2.05	10.65	12.01

Biotransformation of **31**
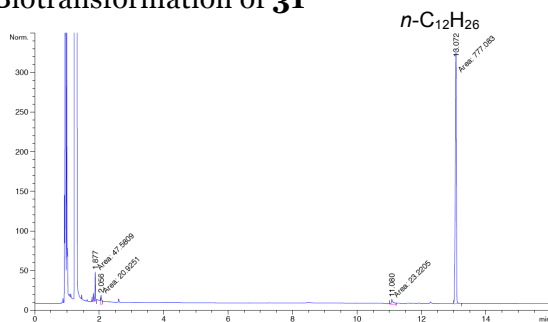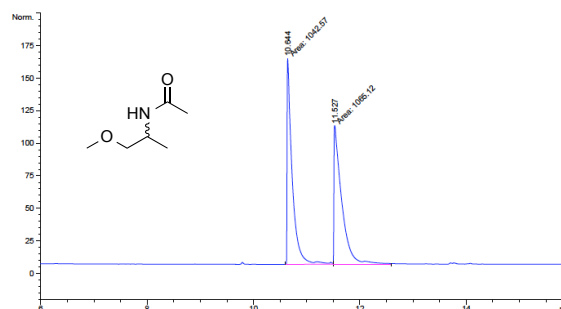
Calibration
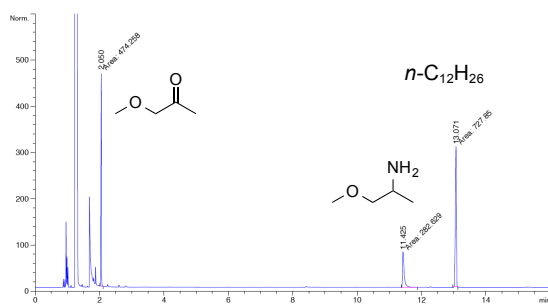
Note: very small peak areas likely due to substrate volatility.

For derivatization see p. 115.

rac-N-acetylated **31a**
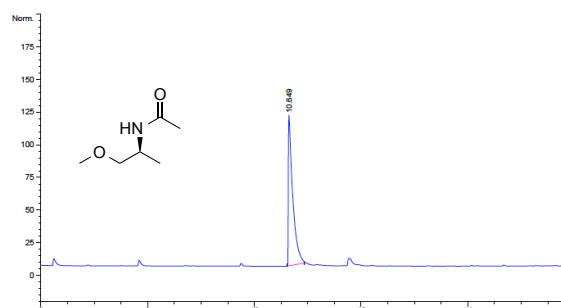
(S)-N-acetylated **31a**

(R)-N-acetylated **31a**
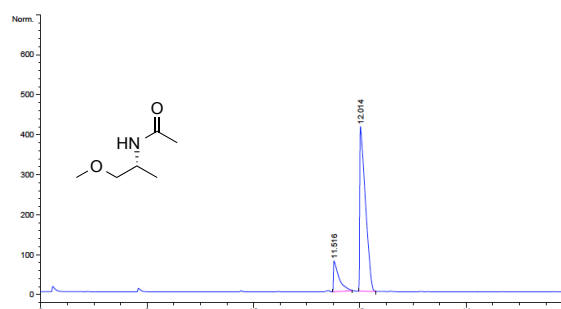
3.3.4 Determination of Absolute Configurations

Absolute configurations of chiral compounds were determined by means of the methods shown in the following table.

Table 3.1 | Methods used for the determination of the absolute configuration.

Compound[a]	Method
1	Optical rotation
2	racemic reference substance, from follow-up reactions to **1**
6	racemic reference substance, from follow-up reactions to **1**
14	known GC-FID elution order of enantiomers[36, 39, 73]
27a	known GC-FID elution order of enantiomers[36, 39]
28a	known GC-FID elution order of enantiomers[74]
29a	known GC-FID elution order of enantiomers[36, 39, 73]
30a	known GC-FID elution order of enantiomers[73]
31a	known GC-FID elution order of enantiomers[36, 39]

[a] For enantiomer GC-elution orders of **14** and **27a** through **31a** may also see Master Thesis of Desiree Pressnitz.

4 References

[1] C. Voelckel, G. Jander, *Annual Plant Reviews, Insect-Plant Interactions*, Wiley, **2014**.

[2] H. M. Garraffo, J. Caceres, J. W. Daly, T. F. Spande, N. R. Andriamaharavo, M. Andriantsiferana, *J. Nat. Prod.* **1993**, *56*, 1016-1038.

[3] E. Fattorusso, O. Taglialatela-Scafati, *Modern Alkaloids: Structure, Isolation, Synthesis, and Biology*, Wiley, **2008**.

[4] J. Robertson, K. Stevens, *Nat. Prod. Rep.* **2014**, *31*, 1721-1788.

[5] a) J. P. Michael, *Nat. Prod. Rep.* **2008**, *25*, 139-165; b) C. Bhat, S. G. Tilve, *RSC Advances* **2014**, *4*, 5405-5452; c) J. Robertson, K. Stevens, *Nat. Prod. Rep.* **2014**.

[6] M. Mori, M. Hori, Y. Sato, *J. Org. Chem.* **1998**, *63*, 4832-4833.

[7] D. J. Robins, *Nat. Prod. Rep.* **1993**, *10*, 487-496.

[8] P. Dewi-Wülfing, PhD Thesis thesis, Technische Universität Berlin (Berlin), **2005**.

[9] a) J. R. Liddell, *Nat. Prod. Rep.* **2002**, *19*, 773-781; b) J. R. Liddell, *Nat. Prod. Rep.* **2001**, *18*, 441-447; c) J. R. Liddell, *Nat. Prod. Rep.* **2000**, *17*, 455-462; d) J. R. Liddell, *Nat. Prod. Rep.* **1999**, *16*, 499-507; e) J. Richard Liddell, *Nat. Prod. Rep.* **1998**, *15*, 363-370; f) J. R. Liddell, *Nat. Prod. Rep.* **1997**, *14*, 653-660; g) J. R. Liddell, *Nat. Prod. Rep.* **1996**, *13*, 187-193; h) D. J. Robins, *Nat. Prod. Rep.* **1995**, *12*, 413-418; i) D. J. Robins, *Nat. Prod. Rep.* **1994**, *11*, 613-619; j) D. J. Robins, *Nat. Prod. Rep.* **1992**, *9*, 313-321; k) D. J. Robins, *Nat. Prod. Rep.* **1991**, *8*, 213-221; l) D. J. Robins, *Nat. Prod. Rep.* **1990**, *7*, 377-386; m) D. J. Robins, *Nat. Prod. Rep.* **1989**, *6*, 577-589; n) D. J. Robins, *Nat. Prod. Rep.* **1989**, *6*, 221-230; o) D. J. Robins, *Nat. Prod. Rep.* **1987**, *4*, 577-590; p) D. J. Robins, *Nat. Prod. Rep.* **1986**, *3*, 297-305; q) D. J. Robins, *Nat. Prod. Rep.* **1985**, *2*, 213-220; r) D. J. Robins, *Nat. Prod. Rep.* **1984**, *1*, 235-243; s) D. J. Robins, in *The Alkaloids: Volume 1, Vol. 10* (Ed.: M. F. Grundon), The Royal Society of Chemistry, **1981**, pp. 49-62; t) J. E. Saxton, in *The Alkaloids: Volume 1, Vol. 1* (Ed.: J. E. Saxton), The Royal Society of Chemistry, **1971**, pp. 59-75.

[10] L. M. Mascavage, S. Jasmin, P. E. Sonnet, M. Wilson, D. R. Dalton, in *Ullmann's Encyclopedia of Industrial Chemistry*, Wiley-VCH Verlag GmbH & Co. KGaA, **2000**.

[11]   P. M. Dewick, *Medicinal natural products: a biosynthetic approach*, Wiley, **1997**.

[12]   T. H. Jones, M. S. Blum, H. M. Fales, C. R. Thompson, *J. Org. Chem.* **1980**, *45*, 4778-4780.

[13]   H. M. Garraffo, T. F. Spande, J. W. Daly, A. Baldessari, E. G. Gros, *J. Nat. Prod.* **1993**, *56*, 357-373.

[14]   J. W. Daly, T. F. Spande, H. M. Garraffo, *J. Nat. Prod.* **2005**, *68*, 1556-1575.

[15]   A. M. Belostotskii, E. Markevich, *J. Org. Chem.* **2003**, *68*, 3055-3063.

[16]   H. Takahata, S. Takahashi, N. Azer, A. T. Eldefrawi, M. E. Eldefrawi, *Bioorg. Med. Chem. Lett.* **2000**, *10*, 1293-1295.

[17]   a) M. Vavrecka, A. Janowitz, M. Hesse, *Tetrahedron Lett.* **1991**, *32*, 5543-5546; b) A. Barthelme, D. Richards, I. R. Mellor, R. A. Stockman, *Chem. Commun.* **2013**, *49*, 10507-10509.

[18]   a) D. Lathbury, T. Gallagher, *J. Chem. Soc., Chem. Commun.* **1986**, 1017-1018; b) T. Jiang, T. Livinghouse, *Org. Lett.* **2010**, *12*, 4271-4273; c) D. C. Lathbury, R. W. Shaw, P. A. Bates, M. B. Hursthouse, T. Gallagherb, *J. Chem. Soc., Perkin 1* **1989**, 2415-2424.

[19]   a) S. Takano, S. Otaki, K. Ogasawara, *J. Chem. Soc., Chem. Commun.* **1983**, 1172-1174; b) S. Arseniyadis, P. Q. Huang, H. P. Husson, *Tetrahedron Lett.* **1988**, *29*, 1391-1394; c) O. Provot, J. P. Celerier, H. Petit, G. Lhommet, *J. Org. Chem.* **1992**, *57*, 2163-2166; d) H. Takahata, H. Bandoh, T. Momose, *J. Org. Chem.* **1992**, *57*, 4401-4404; e) G. D. Cuny, S. L. Buchwald, *Synlett* **1995**, *1995*, 519-522; f) H. Dhimane, C. Vanucci-Bacqué, L. Hamon, G. Lhommet, *Eur. J. Org. Chem.* **1998**, *1998*, 1955-1963; g) V. M. Arredondo, S. Tian, F. E. McDonald, T. J. Marks, *J. Am. Chem. Soc.* **1999**, *121*, 3633-3639; h) C. Grandjean, S. Rosset, J. P. Célérier, G. Lhommet, *Tetrahedron Lett.* **1993**, *34*, 4517-4518; i) K. Uchiyama, Y. Hayashi, K. Narasaka, *Tetrahedron* **1999**, *55*, 8915-8930; j) Y.-G. Xiang, X.-W. Wang, X. Zheng, Y.-P. Ruan, P.-Q. Huang, *Chem. Commun.* **2009**, 7045-7047.

[20]   a) W. Oppolzer, C. G. Bochet, E. Merifield, *Tetrahedron Lett.* **1994**, *35*, 7015-7018; b) X.-K. Liu, X. Zheng, Y.-P. Ruan, J. Ma, P.-Q. Huang, *Org. Biomol. Chem.* **2012**, *10*, 1275-1284.

[21]   T. C. Nugent, M. El-Shazly, *Adv. Synth. Catal.* **2010**, *352*, 753-819.

[22]   T. C. Nugent, *Chiral Amine Synthesis: Methods, Developments and Applications*, Wiley, **2010**.

[23]   K. Huang, M. Ortiz-Marciales, V. Stepanenko, M. De Jesús, W. Correa, *J. Org. Chem.* **2008**, *73*, 6928-6931.

[24]   W. Tang, X. Zhang, *Angew. Chem. Int. Ed.* **2002**, *41*, 1612-1614.

[25]   a) A. A. Desai, *Angew. Chem. Int. Ed.* **2011**, *50*, 1974-1976; b) D. Steinhuebel, Y. Sun, K. Matsumura, N. Sayo, T. Saito, *J. Am. Chem. Soc.* **2009**, *131*, 11316-11317.

[26]   A. Ricci, *Amino Group Chemistry: From Synthesis to the Life Sciences*, Wiley, **2008**.

[27]   S. G. Ouellet, A. M. Walji, D. W. C. Macmillan, *Acc. Chem. Res.* **2007**, *40*, 1327-1339.

[28]   E. Milczek, N. Boudet, S. Blakey, *Angew. Chem. Int. Ed.* **2008**, *47*, 6825-6828.

[29]   R. Wolfenden, M. J. Snider, *Acc. Chem. Res.* **2001**, *34*, 938-945.

[30]   K. Faber, *Biotransformations in Organic Chemistry: A Textbook*, Springer, **2011**.

[31]   a) E. O'Reilly, C. Iglesias, D. Ghislieri, J. Hopwood, J. L. Galman, R. C. Lloyd, N. J. Turner, *Angew. Chem. Int. Ed.* **2014**, *53*, 2447-2450; b) I. Oroz-Guinea, E. García-Junceda, *Curr. Opin. Chem. Biol.* **2013**, *17*, 236-249; c) E. Ricca, B. Brucher, J. H. Schrittwieser, *Adv. Synth. Catal.* **2011**, *353*, 2239-2262.

[32]   K. Hult, P. Berglund, *Trends Biotechnol.* **2007**, *25*, 231-238.

[33]   R. B. Silverman, *The Organic Chemistry of Enzyme-catalyzed Reactions*, Academic Press, **2002**.

[34]   A. Łyskowski, C. Gruber, G. Steinkellner, M. Schürmann, H. Schwab, K. Gruber, K. Steiner, *PLoS ONE* **2014**, *9*, e87350.

[35]   R. L. Hanson, B. L. Davis, Y. Chen, S. L. Goldberg, W. L. Parker, T. P. Tully, M. A. Montana, R. N. Patel, *Adv. Synth. Catal.* **2008**, *350*, 1367-1375.

[36]   D. Koszelewski, M. Göritzer, D. Clay, B. Seisser, W. Kroutil, *ChemCatChem* **2010**, *2*, 73-77.

[37]   K. Smithies, M. E. B. Smith, U. Kaulmann, J. L. Galman, J. M. Ward, H. C. Hailes, *Tetrahedron: Asymmetry* **2009**, *20*, 570-574.

[38]   H. Yun, B.-K. Cho, B.-G. Kim, *Biotechnol. Bioeng.* **2004**, *87*, 772-778.

[39]   F. G. Mutti, C. S. Fuchs, D. Pressnitz, J. H. Sattler, W. Kroutil, *Adv. Synth. Catal.* **2011**, *353*, 3227-3233.

[40]   R. C. Simon, F. Zepeck, W. Kroutil, *Chem. Eur. J.* **2013**, *19*, 2859-2865.

[41]   D. Koszelewski, K. Tauber, K. Faber, W. Kroutil, *Trends Biotechnol.* **2010**, *28*, 324-332.

[42]   M. Höhne, S. Kühl, K. Robins, U. T. Bornscheuer, *ChemBioChem* **2008**, *9*, 363-365.

[43]   R. C. Simon, N. Richter, E. Busto, W. Kroutil, *ACS Catal.* **2013**, *4*, 129-143.

[44]   a) P. Tufvesson, J. S. Jensen, W. Kroutil, J. M. Woodley, *Biotechnol. Bioeng.* **2012**, *109*, 2159-2162; b) K. E. Cassimjee, C. Branneby, V. Abedi, A. Wells, P. Berglund, *Chem. Commun.* **2010**, *46*, 5569-5571.

[45]   P. Tufvesson, C. Bach, J. M. Woodley, *Biotechnol. Bioeng.* **2014**, *111*, 309-319.

[46]   K. Gadamasetti, T. Braish, *Process Chemistry in the Pharmaceutical Industry: Challenges in an Ever Changing Climate*, Taylor & Francis, **2007**.

[47]   J. Farnberger, Diploma Thesis thesis, University of Graz (Graz, Austria), **2014**.

[48]   S. Kara, D. Spickermann, J. H. Schrittwieser, C. Leggewie, W. J. H. van Berkel, I. W. C. E. Arends, F. Hollmann, *Green Chem.* **2013**, *15*, 330-335.

[49]   B. Wang, H. Land, P. Berglund, *Chem. Commun.* **2013**, *49*, 161-163.

[50]   A. P. Green, N. J. Turner, E. O'Reilly, *Angew. Chem. Int. Ed.* **2014**, *53*, 10714-10717.

[51]   C. K. Savile, J. M. Janey, E. C. Mundorff, J. C. Moore, S. Tam, W. R. Jarvis, J. C. Colbeck, A. Krebber, F. J. Fleitz, J. Brands, P. N. Devine, G. W. Huisman, G. J. Hughes, *Science* **2010**, *329*, 305-309.

[52]   D. Koszelewski, I. Lavandera, D. Clay, G. M. Guebitz, D. Rozzell, W. Kroutil, *Angew. Chem. Int. Ed.* **2008**, *47*, 9337-9340.

[53]   W. Kroutil, E.-M. Fischereder, C. S. Fuchs, H. Lechner, F. G. Mutti, D. Pressnitz, A. Rajagopalan, J. H. Sattler, R. C. Simon, E. Siirola, *Org. Process Res. Dev.* **2013**, *17*, 751-759.

[54]   H. Kohls, F. Steffen-Munsberg, M. Höhne, *Curr. Opin. Chem. Biol.* **2014**, *19*, 180-192.

[55]   M. Höhne, U. T. Bornscheuer, *ChemCatChem* **2009**, *1*, 42-51.

[56]   J. H. Schrittwieser, V. Resch, *RSC Advances* **2013**, *3*, 17602-17632.

[57]   R. C. Simon, C. S. Fuchs, H. Lechner, F. Zepeck, W. Kroutil, *Eur. J. Org. Chem.* **2013**, 3397-3402.

[58]   R. C. Simon, B. Grischek, F. Zepeck, A. Steinreiber, F. Belaj, W. Kroutil, *Angew. Chem. Int. Ed.* **2012**, *51*, 6713-6716.

[59]   a) K. Maruoka, H. Yamamoto, *Angew. Chem.* **1985**, *97*, 670-683; b) H. Yamamoto, H. Nozaki, *Angewandte Chemie International Edition in English* **1978**, *17*, 169-175.

[60]   D. Bacos, J. P. Célérier, E. Marx, C. Saliou, G. Lhommet, *Tetrahedron Lett.* **1989**, *30*, 1081-1082.

[61]   a) T. Hudlicky, J. O. Frazier, G. Seoane, M. Tiedje, A. Seoane, L. D. Kwart, C. Beal, *J. Am. Chem. Soc.* **1986**, *108*, 3755-3762; b) D. J. Robins, S. Sakdarat, *J. Chem. Soc., Perkin 1* **1981**, 909-913; c) H. A. Kelly, D. J. Robins, *J. Chem. Soc., Perkin 1* **1989**, 1339-1342; d) C. W. Jefford, J. B. Wang, *Tetrahedron Lett.* **1993**, *34*, 3119-3122; e) J. C. Conrad, J. Kong, B. N. Laforteza, D. W. C. MacMillan, *J. Am. Chem. Soc.* **2009**, *131*, 11640-11641.

[62]   a) D. Gamenara, P. Dominguez de Maria, *Org. Biomol. Chem.* **2014**, *12*, 2989-2992; b) F. Leipold, S. Hussain, D. Ghislieri, N. J. Turner, *ChemCatChem* **2013**, *5*, 3505-3508.

[63]   J. E. Baldwin, *J. Chem. Soc., Chem. Commun.* **1976**, 734-736.

[64]   a) A. K. Kankaanperä, Sirkka, *Acta Chem. Scand.* **1969**, *23*, 3607-3608; b) K. Alder, C.-H. Schmidt, *Ber. Dtsch. Chem. Ges. (A and B Series)* **1943**, *76*, 183-205.

[65]   L. Huang, J. Qi, X. Wu, W. Wu, H. Jiang, *Chem. Eur. J.* **2013**, *19*, 15462-15466.

[66]   A. Kouridaki, T. Montagnon, M. Tofi, G. Vassilikogiannakis, *Org. Lett.* **2012**, *14*, 2374-2377.

[67]   B. A. Steinhoff, A. E. King, S. S. Stahl, *J. Org. Chem.* **2006**, *71*, 1861-1868.

[68]   G. Piancatelli, M. D'Auria, F. D'Onofrio, *Synthesis* **1994**, *1994*, 867-889.

[69]   L. Kurti, B. Czako, *Strategic Applications of Named Reactions in Organic Synthesis*, Elsevier Science, **2005**.

[70]   J. A. Joule, K. Mills, *Heterocyclic Chemistry*, Wiley, **2013**.

[71]   a) T. T. Shawe, C. J. Sheils, S. M. Gray, J. L. Conard, *J. Org. Chem.* **1994**, *59*, 5841-5842; b) F. J. Ritter, I. E. M. Rotgans, E. Talman, P. E. J. Verwiel, F. Stein, *Experientia* **1973**, *29*, 530-531.

[72]   N. B. McKeown, I. Chambrier, M. J. Cook, *J. Chem. Soc., Perkin 1* **1990**, 1169-1177.

[73]   F. G. Mutti, C. S. Fuchs, D. Pressnitz, N. G. Turrini, J. H. Sattler, A. Lerchner, A. Skerra, W. Kroutil, *Eur. J. Org. Chem.* **2012**, *2012*, 1003-1007.

[74]   D. Pressnitz, C. S. Fuchs, J. H. Sattler, T. Knaus, P. Macheroux, F. G. Mutti, W. Kroutil, *ACS Catal.* **2013**, *3*, 555-559.

5 Curriculum Vitae

Personal

Name and Title:

Stefan Payer, BSc.

Date and location of birth:

July 16, 1989, Leoben, Steiermark (AUT)

Address:

Schützenhofgasse 34, A-8010 Graz, Steiermark (AUT)

Phone:

0043 676 30 92 640

E-mail:

stefan.payer@gmail.com

Education

Sept. 1995 - July 1999	Primary School (Volksschule) in Turnau/ Thoerl
Sept. 1999 - July 2003	Lower Secondary school (Hauptschule) in Thoerl
Sept. 2003 - June 2008	Vocational education and training college (HTBLA) Kapfenberg; dept. for Plastics and Environmental Engineering
June 26. 2008	Matura (final exam) with honors
Oct. 2009 - July 2012	Bachelor Program for Chemistry, NAWI Graz
Sept. 2011-April 2012	Bachelor's Thesis in Prof. Frank Wiesbrock's lab at the Instititute for Chemistry of Materials, Graz University of Technology: "Ring-Opening Metathesis-Polymerization of Oxa-Aza-Norbornenes"
Since July 2012	Master Program for Chemistry, NAWI Graz
Aug. 2013 - Dec. 2014	Participation in the International Student Exchange Program (ISEP): Student at the University of Utah, Salt Lake City, UT, (USA). Work on oxidative cyclization techniques to furnish α-carbolines in the lab of Prof. Jon D. Rainier beside regular university coursework.
Since March 2014	Master's Thesis at Prof. Kroutil's lab at the institute for Bioorganic Chemistry, University of Graz: "Preparation of α-chiral tert-amines."

Aug. 2008 - Apr. 2009	Alternative Service (Zivildienst) at the LKH-Univ. Clinic Graz

Completed Internships and Trainings

Summer 2005, 2006 and 2007	Joh. Pengg AG Thörl, Sytria. Dept. for Neutralization
Summer 2009	DSM Fine Chemicals Linz, Upper Austria. Pilot Plant for Industrial Organic Synthesis: supervision of industrial scale reactions.
Summer 2011	SANDOZ GmbH Kundl, Tirol. Dept. for downstream processing: purification and analysis of proteins.
Summer 2012 and 2013	Austrian Centre for Industrial Biotechnology (ACIB) Graz, Styria. Biocatalysis under the supervision of Dr. Mandana Gruber.